

GLACIOLOGICAL
DATA

SNOW WATCH '85

World Data Center A
for
Glaciology
[Snow and Ice]



March 1986

GLACIOLOGICAL DATA

REPORT GD-18

SNOW WATCH '85

Edited by

G. Kukla

Lamont-Doherty Geological Observatory
Columbia University
Palisades, New York, U.S.A.

R.G. Barry

National Snow and Ice Data Center
Cooperative Institute for Research
in Environmental Sciences
University of Colorado
Boulder, Colorado, U.S.A.

A. Hecht

Climate Dynamics Program
National Science Foundation
Washington, D.C., U.S.A.

D. Wiesnet

Satellite Hydrology Associates
Vienna, Virginia, U.S.A.

Published by:

**WORLD DATA CENTER FOR GLACIOLOGY
[SNOW AND ICE]**

Cooperative Institute for Research in Environmental Sciences
University of Colorado
Boulder, Colorado 80309 U.S.A.

Operated for:

U.S. Department of Commerce
National Oceanic and Atmospheric Administration
National Environmental Satellite, Data, and Information Service
Boulder, Colorado 80303 U.S.A.

March 1986

DESCRIPTION OF WORLD DATA CENTERS¹

WDC-A: Glaciology (Snow and Ice) is one of three International data centers serving the field of glaciology under the guidance of the International Council of Scientific Unions Panel of World Data Centers. It is part of the World Data Center System created by the scientific community in order to promote worldwide exchange and dissemination of geophysical information and data. WDC-A endeavors to be promptly responsive to inquiries from the scientific community, and to provide data and bibliographic services in exchange for copies of publications or data by the participating scientists.

1. The addresses of the three WDCs for Glaciology and of a related Permanent Service are:

World Data Center A
University of Colorado
Campus Box 449
Boulder, Colorado, 80309 U.S.A.

World Data Center B
Molodezhnaya 3
Moscow 117 296, USSR

World Data Centre C
Scott Polar Research Institute
Lensfield Road
Cambridge, CB2 1ER, England

Permanent Service on the Fluctuations
of Glaciers
Swiss Federal Institute of Technology
CH-8092 Zurich, Switzerland

2. Subject Matter

WDCs will collect, store, and disseminate information and data on Glaciology as follows:

Studies of snow and ice, including seasonal snow, glaciers, sea, river, or lake ice, seasonal or perennial ice in the ground, extraterrestrial ice and frost.

Material dealing with the occurrence, properties, processes, and effects of snow and ice, and techniques of observing and analyzing these occurrences, processes, properties, and effects, and ice physics.

Material concerning the effects of present day and snow and ice should be limited to those in which the information on ice itself, or the effect of snow and ice on the physical environment, make up an appreciable portion of the material.

Treatment of snow and ice masses of the historic or geologic past, or paleoclimatic chronologies will be limited to those containing data or techniques which are applicable to existing snow and ice.

¹International Council of Scientific Unions. Panel on World Data Centers. (1979) Guide to International Data Exchange Through the World Data Centres. 4th ed. Washington, D.C. 113p.

[†]The lowest level of data useful to other prospective users.

This guide for Glaciology was prepared by the International Commission on Snow and Ice (ICSI) and was approved by the International Association of Hydrological Sciences (IAHS) in 1978.

3. Description and Form of Data Presentation

- 3.1 General. WDCs collect, store and are prepared to disseminate raw, analyzed, and published data, including photographs. WDCs can advise researchers and institutions on preferred formats for such data submissions. Data dealing with any subject matter listed in (2) above will be accepted. Researchers should be aware that the WDCs are prepared to organize and store data which may be too detailed or bulky for inclusion in published works. It is understood that such data which are submitted to the WDCs will be made available according to guidelines set down by the ICSU Panel on WDCs in this Guide to International Data Exchange. Such material will be available to researchers as copies from the WDC at cost, or if it is not practicable to copy the material, it can be consulted at the WDC. In all cases the person receiving the data will be expected to respect the usual rights, including acknowledgement, of the original investigator.
- 3.2 Fluctuations of Glaciers. The Permanent Service is responsible for receiving data on the fluctuations of glaciers. The types of data which should be sent to the Permanent Service are detailed in UNESCO/IASH (1969)*. These data should be sent through National Correspondents in time to be included in the regular reports of the Permanent Service every four years (1964-68, 1968-72, etc.). Publications of the Permanent Service are also available through the WDCs.
- 3.3 Inventory of Perennial Snow and Ice Masses. A Temporary Technical Secretariat (TTS) was recently established for the completion of this IHD project at the SWISS Federal Institute of Technology in Zurich. Relevant data, preferable in the desired format**, can be sent directly to the TTS or to the World Data Centers for forwarding to the TTS.
- 3.4 Other International Programs. The World Data Centers are equipped to expedite the exchange of data for ongoing projects such as those of the International Hydrological Project (especially the studies of combined heat, ice and water balances at selected glacier basins***), the International Antarctic Glaciological Project (IAGP), and Greenland Ice Sheet Project (GISP), etc., and for other developing projects in the field of snow and ice.

4. Transmission of Data to the Centers

In order that the WDCs may serve as data and information centers, researchers and institutions are encouraged:

- 4.1 To send WDCs raw or analyzed data in the form of tables, computer tapes, photographs, etc., and reprints of all published papers and public reports which contain glaciological data or data analysis as described under heading (2); one copy should be sent to each WDC or, alternatively, three copies to one WDC for distribution to the other WDCs.
- 4.2 To notify WDCs of changes in operations involving international glaciological projects, including termination of previously existing stations or major experiments, commencement of new experiments, and important changes in mode of operation.

*UNESCO/IASH (1969) Variations of Existing Glaciers. A Guide to International Practices for their Measurement.

**UNESCO/IASH (1970a) Perennial Ice and Snow Masses. A Guide for Compilation and Assemblage of Data for a World Inventory; and

***UNESCO/IASH (1970b) Combined Heat, Ice and Water Balances at Selected Glacier Basins. A Guide for Compilation and Assemblage of Data for Glacier Mass Balance Measurements; and

UNESCO/IASH (1973) Combined Heat, Ice and Water Balances at Selected Glacier Basins. Part II, Specifications, Standards and Data Exchange.

FOREWORD

This issue of Glaciological Data reports on the results of a workshop on snow cover and its role in the climate system, specifically as it may relate to potential CO₂-induced climatic changes. The workshop, held in October 1985 at the University of Maryland, College Park, was a successor to SNOW WATCH 1980 (Glaciological Data Report GD-11). Apart from the presentation of scientific papers, the 40 participants from 4 countries divided into three working groups to discuss questions of data bases, the role of snow cover in the climate system and the treatment of snow cover processes in climate models. The recommendations from these groups, included here, will be forwarded to the sponsors of the meeting - the World Meteorological Organization, the Carbon Dioxide Research Division of the U.S. Department of Energy, the Office of Climate Dynamics of the National Science Foundation, the National Environmental Satellite, Data, and Information Service of the National Ocean and Atmospheric Administration and the International Commission on Snow and Ice. The wider dissemination of these results through our mailing list will, we hope, increase awareness of the importance of these issues in the climatological and glaciological communities.

We are pleased to acknowledge the support provided through the U.S. Department of Energy, Carbon Dioxide Research Division, by agreement DE-FG02-85ER60366 to Dr. G. Kukla, for the publication costs of this issue.

R.G. Barry
Director
World Data Center-A for
Glaciology (Snow & Ice)

PREFACE

SNOWWATCH 1985: Workshop on CO₂/Snow Interaction

The growth and decay of Pleistocene ice sheets demonstrated how changeable the earth's climate is and how important is the role which snow plays in the climate system. Because rapidly increasing concentrations of many greenhouse gases in the atmosphere are expected to result in a major world wide warming, it is important to know to what degree changes in snow cover will amplify the CO₂ impact. To address this problem, researchers from several countries gathered on October 28-30, 1985, at the University of Maryland, to discuss existing knowledge on the potential role of snow in the CO₂-induced climate change and to identify problems in need of further research.

The workshop was sponsored by the World Meteorological Organization, the Carbon Dioxide Research Division of the Department of Energy, the Office of Climate Dynamics of the National Sciences Foundation, the National Environmental Satellite, Data, and Information Service of the National Oceanic and Atmospheric Administration and the International Commission on Snow and Ice of the International Association of Hydrological Sciences. Funding for the workshop was provided by the U.S. Department of Energy, Carbon Dioxide Research Division by agreement DE-FG02-85ER60366 and by grant ATM-83-18676 from the Office of Climate Dynamics of the National Science Foundation.

The workshop was a follow-up to an earlier SNOW WATCH conference held in Washington D.C. in 1980 (Glaciological Data Report GD-11, 1981). The first two days were dedicated to individual presentations which are included in this volume. On the third day the participants, divided into three working groups, discussed and drafted recommendations of actions considered to be of highest priority.

Organizing Committee

G. Kukla
R.G. Barry
D.R. Wiesnet
A.D. Hecht

CONTENTS

	Page
FOREWORD	v
PREFACE	vii
SNOW WATCH '85 (University of Maryland, 28-30 OCTOBER 1985)	
RECOMMENDATIONS	1
PARTICIPANTS	19
Climate Impact of Snow	
Snow Cover, Cyclogenesis and Cyclone Trajectories - J. Walsh	23
The Relationship between Snow Cover and Atmospheric Thermal and Circulation Anomalies - K.F. Dewey and R. Heim, Jr.	37
Relationships between Snow Cover and Temperature in the Lower Troposphere, General Circulation in East Asia and Precipitation in China - Z. Zhao and S. Wang	55
Progression of Regional Snow Melt - D.A. Robinson	63
Soot from Arctic Haze: Radiation Effects on the Arctic Snowpack - S.G. Warren and A.D. Clarke	73
Ground Station Data	
The Snow Cover Record in Eurasia - J. Foster	79
Distribution of Snow Cover in China - P. Li	89
Snow Surveying in Canada - B. Goodison	97
Satellite Data Bases	
Snow Cover in Real Time Climate Monitoring - C.F. Ropelewski	105
Northern Hemisphere Snow and Ice Chart of NOAA/NESDIS - T. Baldwin	109
NOAA Satellite-Derived Snow Cover Data Base: Past, Present and Future - M. Matson	115
Joint Ice Center Global Sea Ice Digital Data - C.E. Gross	125

Remote Sensing

Snow Cover Data: Status and Future Prospects - R.G. Barry	127
Comparison of Northern Hemisphere Snow Cover Data Sets - A. Robock and J. Scialdone	141
Influence of Snow Structure Variability on Global Snow Depth Measurement Using Microwave Radiometry - D.K. Hall	161
Retrieval of Snow Water Equivalent from Nimbus-7 SMMR Data - M. Hallikainen and P. Jolma	173
Nimbus-7 SMMR Snow Cover Data - A.T.C. Chang	181
Snow Cover Monitoring using Microwave Radiometry - N. Grody	189
Remote Sensing of Snow Properties in Mountainous Terrain - J. Dozier	193
Remote Sensing of Snow Cover over the Carpathian Watersheds - H. Grumazescu	205

Snow Cover Modeling

Effects of Snow Cover and Tropical Forcing on Mid-Latitude Monthly Mean Circulation - A. Robock and J.W. Tauss	207
Parameterization of Snow Albedo for Climate Models - S. Marshall and S.G. Warren	215
Modelling of a Seasonal Snowcover - E.M. Morris	225
Characteristics of Seasonal Snow Cover as Simulated by GFDL Climate Models - A. Broccoli	241
CO ₂ -Induced Changes in Seasonal Snow Cover Simulated by the OSU Coupled Atmosphere-Ocean General Circulation Model - M. Schlesinger	249
ACRONYMS and ABBREVIATIONS	271
NOTES	273

Kukla, G; Barry, R.G.; Hecht, A.; Wiesnet, D. eds. (1986) SNOW WATCH '85. Proceedings of the Workshop held 28-30 October 1985 at the University of Maryland, College Park, MD. Boulder, Colorado, World Data Center A for Glaciology (Snow and Ice), Glaciological Data, Report GD-18, p.1-17.

SNOW WATCH '85 RECOMMENDATIONS

The participants divided into three working groups to discuss the actions deemed to be of the highest urgency in specific areas. These groups addressed the following topics:

- I. Data bases
- II. Snow-climate interactions
- III. Modeling and simulation of snow covers

Some of the tasks were assigned high priority recommendations of more than one working group.

Data Bases: Working Group I

Edited by B.E. Goodison.

Members: R.G. Barry, A. Chang, J. Foster, J. Gavin, D. Hall, P. Li, M. Matson, D. Robinson, C. Ropelewski, D. Wiesnet.

Background

Most, if not all, snow cover data (notably extent, depth, water equivalent and albedo) are collected by agencies for purposes other than climatology. In addressing the question of CO₂/ snow interaction the snow data base is one area which requires special attention if research on CO₂-induced climate change is to progress. The working group focused on data needs, new sources of data, and recommended action required to ensure a data base useful to the climate modeling community. It is recognized that an efficient method of integrating remotely sensed data with conventional ground data must be found if sufficiently accurate information on snow is to be obtained on a global scale. Because methods of acquiring the data were addressed in the presented papers, a review will not be presented here. However, the important question of data management will be given special attention since it is crucial to successful use of the data, whatever their origin.

Satellite data are particularly suited to address this global scale of study while at the regional scale integration of ground and satellite derived snow cover data is required.

Integration of Conventional and Remotely Sensed Data

Depth of snow on the ground is measured daily at several thousand meteorological stations world-wide. Reports of several hundred of these stations are currently collected by U.S. National Weather Service/National Meteorological Center (NWS/NMC). The National Oceanic and Atmospheric Administration/National Environmental Satellite, Data and Information Service (NOAA/NESDIS) currently produces satellite derived charts of snow cover in the Northern Hemisphere. The NOAA/Navy Joint Ice Center produces charts of the sea ice extent in both hemispheres. Automated and interactive digital and chart products showing snow cover extent on land and ice in the two hemispheres based on Advanced Microwave Sounding Unit (AMSU) and 1.6 μm sensor returns are planned to be produced by NOAA starting in 1990.

Recommendations

1. Integrate conventional and remotely sensed data to create more complete snow cover data sets. Surface station data sets could be used to refine and cross-check the validity of satellite-derived products. The accuracy and completeness of merged data sets will be dependent on the quality and density of data sources (see Data Management).
2. Produce the merged data sets, for both the Northern and Southern Hemispheres, at daily (instead of current weekly) intervals. Archival of the satellite products and the conventional data could be performed separately, but in compatible formats. NOAA/NESDIS should produce the merged data set.

Regional Data Bases

Many of the CO₂-related changes of snow cover will be in middle latitudes and the effects are expected to be localized. In order to provide a base for impact assessment analysis of both practical and economic significance, regional data bases of snow cover must be created.

Recommendations

1. Identify key regions for monitoring changes based on the results of model sensitivity studies as well as on agricultural and hydrological impact studies.
2. Assemble longer term data bases (50-100 years) on snow extent, depth, duration and water equivalent on a regional scale. Such records can be used to monitor changes over time and to improve current estimates of variability.
3. Use proxy data to the fullest extent. Permafrost records could serve as a useful indicator of long-term temperature change. Other meteorological variables should be coupled with snow information to produce climate indices.

Microwave Data

On-going research indicates that passive microwave radiometry, which can image day and night through most clouds, has utility for mapping snow cover extent, depth, and water equivalent and can indicate the presence of wet snow on regional or continental scales. Dry snow can be distinguished from snow-free land, thus allowing identification of the snowline. Dry snow and melting snow have very different signals, their differentiation is possible by continuously monitoring the snow throughout the accumulation and depletion periods. It is feasible to develop algorithms to estimate snow depth in specific regions. On a global scale, it appears feasible to distinguish broad categories of snow depth which may be useful for studies which require information on the persistence of snow cover over broad regions (cf. Kunzi et al. 1982; Hall, 1986).

In order to improve existing algorithms, research must be continued to resolve the following problems which affect the snow depth/brightness temperature relationship:

- a) Effect of snow structure - further modeling is required to look at the effect of ice lenses and layers and snow metamorphism (fresh vs. old);
- b) Effect of vegetation type - the presence of dense coniferous forests is a major factor adversely affecting the snow depth/ T_B relationship;
- c) Effect of steep topography.

Snow covered area measurements have proven to be beneficial in hydrological, agricultural, and climatological applications. Satellite microwave radiometry is promising in being able to determine snow depth/water equivalent under all weather conditions and during day and night.

Recommendations:

1. Exploit all potential information from new satellite sensors, especially passive and active microwave. Routine data collection, archiving, data management and funding for such activities must be ensured. These data bases should be developed from the time operational data acquisition begins.
2. Conduct additional analysis of the effect of regional snow structure and snow depth determination, particularly in coniferous boreal forests.
3. Support continued refinement and development of snow depth/water equivalent algorithms derived from passive microwave data. The U.S. High Plains and Canadian prairies are a desirable test area. A near continuous data record, covering a wide range of snow conditions, should be compiled. The data set should include passive microwave measurements (e.g. SMMR), visible and infrared data, ground measurements of snow depth, water equivalent, snow state and structure.

4. Operate SMMR (NIMBUS-7) and SSM/I (DMSP) sensors simultaneously for a period during the first winter season to compare the calibration of the two sensors.
5. Support research programs for validation of satellite derived snow cover parameters using ground truth.
6. Combine NOAA ground station and visible data with microwave data for snow cover mapping, particularly when the snowpack is wet or less than 5 cm deep when it is difficult to resolve the snow boundary, or where the shortwave albedo is of interest.

Data Management

Data management is one of the most crucial aspects in meeting users' needs for snow data. Data management comprises the assembly, quality control, archiving, cataloging, and distribution of data. Considerable progress has been made in some areas of snow cover data management since Snow Watch 1980 was held. The following accomplishments are noted:

- a) Digitization and archival of satellite-derived Northern Hemisphere snow cover charts have been implemented and will continue.
- b) An experimental seven year set of Southern Hemisphere snow cover charts was produced, digitized, and archived.
- c) Plans for improved passive microwave and snow/cloud discrimination measurements from future operational satellites have been approved for the late 1980s-early 1990s.
- d) NOAA-NESDIS weekly snow charts now omit the previously used arbitrary reflectance categories and include dates the snowline was observed.

Areas where no progress in data management has been made include:

- a) International exchange of snow cover data collected at ground stations. The Eurasian data are particularly needed.
- b) Mandatory global exchange on the Global Telecommunications System (GTS) of precipitation and snow depth data from SYNOP reports. Global exchange of these regional data are not prohibited, and could be organized. In addition reporting procedures differ between regions and require standardization.
- c) The absence of unified archives on snow depth and water equivalent for climate model verification.
- d) The failure to address user needs for ready access to manageable data sets (ground and satellite-derived) on snow cover properties.
- e) The failure to differentiate modeled and observed input in the global snow analysis of the Air Force Global Weather Central (AFGWC).
- f) The failure to assure appropriate data quality and homogeneity checks of the operational snow charts.

While noting the progress since recommendations were first made in 1980, it is felt that there still remain key needs which should be addressed at this time.

Recommendations

1. To help clarify snow cover/atmospheric interactions, archives of daily temporal resolution are required, with area-averaged snow cover properties on scales appropriate to numerical models. These properties are the snow cover presence or absence, melting/non-melting, depth, water equivalent and short-wave albedo. Target accuracies should be to WMO standards.
2. Urge WMO, through the Commissions on Climate, Agricultural Meteorology, Hydrology, Basic Systems and Instruments and Methods of Observation to standardize the observation and reporting of precipitation and snow-depth data and to implement mandatory global exchange of these data.
3. Provide relevant terrain and land surface type information routinely with snow cover data.
4. Continue current NESDIS snow cover maps and digital archives. Automated and interactive display and analysis systems are required to facilitate the interpretation procedures.
5. Check data quality and homogeneity of the NOAA/NESDIS snow charts and apply needed corrections applied.
6. Following algorithm development and testing, routine production of snow cover products is required from the anticipated DMSP and N-Ross SSM/I sensor, NOAA AMSU sensors, and the NOAA 1.6 μm sensor. Radiance data in gridded formats should also be retained. Processing procedures and algorithms should be fully documented in the data files.
7. Initiate pilot studies for developing merged snow cover data products from different sensors and platforms, and conventional ground data.
8. Routinely extract conventional ground station reports of snow depth and new snowfall/precipitation from the GTS data streams and archived through collaboration of NMC and the National Snow and Ice Data Center (NSIDC).
9. An inventory of snow depth data sets should be made by NCDC and other national data centers. Such snow depth data sets should be archived, documented and made available to the user community through the appropriate national/world data centers.
10. Ensure adequate long-term continuing funding must be ensured for data collection, archiving and distribution.

Summary

There is a need for development of integrated climatological data bases of snow cover if questions related to CO₂/snow interaction are to be answered. Continued collection of relevant snow data from ground, airborne and satellite observations must be ensured. Conventional ground observations of daily snow depth must continue to be observed and reported at all synoptic meteorological stations. Observation of daily snow depth at designated climate stations is recommended. Automatic snow depth sensors should be developed and used at stations being automated to ensure data continuity. Tests of data compatibility with changes in methods of observation are implicitly assumed.

Current and future satellite products must be merged with conventional data on regional and global scales compatible with those used by climate modelers. Creation of snow cover data sets compiled from all existing ground, airborne, and satellite systems for validation of climate models and for use in regional impact studies in climate sensitive areas is highly recommended. The most important element is an efficient data management system that will ensure collection, archiving, quality control and distribution of snow cover data in a format that will meet user needs.

Snow-Climate Interactions: Working Group II

Edited by J. Walsh, G. Kukla.

Members: K. Dewey, G. Kukla, A. Robock, J. Walsh, Z. Zhao.

The following recommendations pertain to snow cover and its interactions with the atmosphere over timescales ranging from days to years. The longer of these timescales provides the more appropriate context for the consideration of CO₂-induced climate changes. However, the role of snow cover in CO₂-induced climate changes may be viewed as a composite result of processes involving cryosphere-atmosphere interactions over seasons, months, and even the shorter timescales of individual synoptic events.

Snow cover may also play a major role in climatic fluctuations that are independent of CO₂. Short-term climatic variability, for example, represents the major scientific challenge in seasonal and monthly forecasts. To the extent that these forecasts may be improved by consideration of the earth's lower boundary, snow cover is directly relevant to the World Climate Program (WCP) objective of extending the range and accuracy of atmospheric predictions.

Detection of Trends

Detection of significant snow trends, whether CO₂-induced or not, requires the analysis of data-derived indices of snow cover. Insofar as snow cover is quite sensitive to air temperature, snow can be a useful indicator of surface temperature changes. Because the albedo-temperature feedback may amplify perturbations of snow cover and because the areal distribution of snow in station-sparse regions is more amenable than air temperature to remote measurement, snow data may provide the earliest warning of an incipient climatic change. Trend detection is severely hampered, however, by inhomogeneities in time series of data, and by the sampling errors inherent in relatively short records and by the very high natural variability of snow occurrences. Appropriate recommendations are made in Working Group I.

Recommendations

1. Hemispheric/regional snow indices derived from satellite data provide the most representative measures of snow cover, but high priority must be given to test the compatibility of past, present and future satellite-derived products depicting snow coverage and brightness. Only then can any conclusions be made on secular variations present in the record.
2. Surface station records for longer periods (≥ 50 years) should be examined for trends and low-frequency fluctuations. The optimal strategy will likely involve the choice of a network of (<100) "benchmark" stations having homogeneous records minimally affected by urbanization and by changes of locations, instrumentation, etc. Emphasis should be placed on climatic "key regions" in the Snow Transition Zone, which undergoes a large seasonal migration. We recommend that the WMO appoint a working group of data experts to address the selection of stations (regions) and appropriate parameters to observe (snow depth, deviation, depth threshold, etc.).

Analysis of persistence

Effective utilization of snow cover in long-range forecasting requires information about the characteristics of snow persistence. It might be expected, for example, that anomalies of snow will tend to persist for longer times if the depth and water content are large. Despite the availability of a substantial data base, a thorough documentation of the regional and large scale persistence of snow cover has not been made.

Recommendation

Snow cover persistence should be evaluated quantitatively as a function of variables on which it may depend: e.g. depth, water content, radiative fluxes, other elements of energy balance, etc. Satellite imagery will provide the most appropriate data base for computations of large-scale persistence. However, an evaluation of the depth-dependence will require a consolidation of satellite data and station reports. Attention should also be given to the choice of the parameter for which the persistence is evaluated. Candidate parameters include coverage by snow of a minimum depth (e.g., 2.5 cm, 5 cm, 10 cm), a minimum areal fraction, and a minimum brightness, etc.

Snow/atmosphere interactions on synoptic scale.

Local effects of snow cover on surface air temperature have been well established (Dewey, 1977; Kukla, 1981). Through its effects on the distribution of diabatic heating, static stability and low-level baroclinicity, snow cover might also be expected to influence the intensity and locations of synoptic-scale low and high pressure systems. Suggestive results in this regard have been accumulating from data analyses over the past several decades (Lamb, 1955; Namias, 1962; Heim and Dewey, 1984; Walsh and Ross, 1986).

To the extent that snow persists and creates feedbacks, the short-range (synoptic) influences will be relevant to forecasts for the weekly, monthly or seasonal time scales.

Recommendation

The magnitude and the regional and seasonal dependences of synoptic-scale influences of snow cover need to be demonstrated more rigorously. Because snow cover is also a response to large-scale and synoptic-scale circulation features, careful analysis strategies are required for unambiguous isolation of the snow cover influences on the evolution of synoptic systems.

Snow/atmosphere interactions on global scale

In view of the relatively small levels of skill shown by current long-range forecasts (e.g., Nicholls, 1980; Gilman, 1983), even small increments of skill resulting from consideration of snow effects are potentially valuable.

Recommendations

1. The most appropriate time frame for the detection and utilization of a snow-atmosphere "signal" needs to be established. The strength of snow-atmosphere interactions should therefore be delineated in the context of the temporal resolution of the observational data. Data will have to be stratified in more detail than by calendar month.
2. Snow cover influences on atmospheric variability (and on corresponding long-range forecasts) are likely to depend strongly on the regime of the large-scale atmospheric circulation. Objective strategies are needed for extracting this regime-dependence from the available data.
3. Simple climate models incorporating anomalous diabatic heating offer economical advantages in the study of snow cover influences, especially when used in conjunction with observational data (e.g., Robock and Tauss, 1986). Application of these models to larger samples of cases should be pursued, particularly in regard to the determination of the "regime dependence" of snow influences.
4. The extent to which the skill of numerical model forecasts depends on land surface boundary conditions (e.g., snow cover) needs to be established. Model runs incorporating prescribed and/or computed snow anomalies over periods of a week to a season are needed to place snow cover into the framework of other model sensitivities (e.g., SST, sea ice, initial conditions). This task deserves high priority in view of the impending use of dynamical models as long-range forecasting tools.

Snow-hydrology link

Snow is a precipitation in solid form. The variable occurrence of snow, though temperature dependent, is mainly the result of precipitation fluctuations. To date very few studies have addressed the relationship between wet and dry weather anomalies and snow cover.

The association between snow anomalies and soil/atmosphere anomalies of the months or seasons subsequent to the snow melt has been noted in GCM model results (Yeh et al., 1984; Schlesinger, 1985) and in speculative arguments based on observed fluctuations of seasonal temperature and precipitation (Namias, 1964; Lamb, 1972, p. 390; Obukhov, et al., 1984). The potential economic impacts of the drier continental summers suggested by CO₂-sensitivity experiments has recently added to the interest in this association. However, the existence of a soil moisture "link" between winter snow cover and spring/summer temperature or precipitation has not been demonstrated conclusively with observational data. It is also unclear whether such a link, if it exists, is strong enough to be useful in the diagnosis or prediction of spring and summer climate anomalies. In the absence of observational data on soil moisture, data-based analyses have tended to rely heavily on computed soil moisture indices, none of which include snow cover in their formulation.

Recommendation

1. The dependence of snow cover anomalies on fluctuations of precipitation, changes in the source areas of moisture and on the shifts of circulation patterns should be analyzed.
2. High priority should be given to the inclusion of snow cover in the formulation of hydrological models utilizing observational data. The formulations should then be used to quantify surface-atmosphere associations through the months and seasons subsequent to the snow melt. The validity of the snow/hydrology formulations in data-based models and in GCM's should be verified by comparisons with each other, with streamflow data, and with the small amounts of available data derived from direct measurements of soil moisture.

Snow-related feedbacks

Cause-and-effect relationships involving snow cover, air temperature and the atmospheric circulation are difficult to unravel because of the complex feedbacks and because of the frequent dependences on controlling factors external to the region of investigation. Thus the association between these variables can generally not be interpreted in straightforward manner. Even in GCM model results, the contribution of snow cover to biases in the simulated temperature fields is unclear (Broccoli, 1986).

In the scenario of nuclear winter, the snow-albedo-temperature feedback is complicated by the effects of "dirty snow", i.e., the deposition of soot from smoke clouds on the snow. Recent model experiments suggest that the soot will not alter the model forecasts for the initial stages of nuclear winter, when insolation is so small that the surface albedo is relatively unimportant. However, the role of soot in reducing the snow-albedo feedback in later stages, or in less extreme cases as for Arctic haze conditions, is uncertain.

Recommendations

1. Controlled model experiments are needed to assess the relative importance of snow cover feedbacks and other factors in the associations between snow cover, air temperature, and the atmospheric circulation. Parallel simulations with prescribed and interactive snow cover can help clarify the importance of the snow cover feedback and its potential significance over time scales ranging from those of long-range forecasting to those of CO₂-induced climatic changes.
2. The parameterization of soot-induced albedo modifications merits further attention in modeling of climatic change over the seasonal, interannual or longer timescales.

Modeling and Simulation of Snow Covers: Working Group III.

Edited by M. Schlesinger, G. Kukla.

Members: A. Broccoli, L. Morris, A. Robock, M. Schlesinger, S. Warren.

Background

Snow can affect the weather on time scales of days and weeks, and can influence the climate on time scales of months, seasons, and years. On short weather time scales, snow can produce a very cold, shallow layer of air near the ground because of its high albedo and emissivity. The temperature contrast between snow-covered and snow-free surfaces can produce enhanced baroclinicity which can generate more-intense mid-latitude cyclones and more snow in a positive feedback loop. The snow boundary can also be a location for the synoptic storm track. Air travelling over an extensive snow field is cooled and can reduce temperatures downstream by cold-air advection. However, linear atmospheric models suggest that the atmosphere can react to produce warm advection and high surface pressure downstream of the snow to counteract the cooling. This can be important in short-term weather forecasting. Negative snow anomalies can produce the opposite effects and are therefore also important.

On the longer climatic time scales, changes in snow cover can influence the surface albedo producing feedbacks. Increased snow cover raises the albedo and produces less absorption of solar energy, cooler temperatures, and more snow. Decreased snow cover lowers the albedo and produces more absorption of solar energy, warmer temperatures, and less snow. In both cases the initial change in snow cover is amplified by the response of the climate system. Early climate models suggested that this positive feedback was so strong that it could result in an ice-covered earth for even a very small reduction of the solar constant. More recent climate models show that the early models overestimated the magnitude of the snow and ice surface albedo feedback. Climate model simulations of CO₂-induced climatic change have shown that changes in the areal extent of snow and sea ice amplify the global warming by a factor of 1.1 to 1.4. Perhaps of even greater impact is the influence of a CO₂-induced change in snow cover on the surface hydrology. Several general circulation model simulations (see Schlesinger and Mitchell, 1985 and Schlesinger, 1985) have shown a considerable desiccation of the soil in the mid-latitude agriculturally-productive areas in the Northern Hemisphere. This summer drying occurred in part due to the earlier spring melting of the seasonal snowpack in the CO₂-enriched world. Finally, a simulation of CO₂-induced climatic change with an atmosphere-ocean general circulation model (Schlesinger, 1986) shows an increase in the snowpack in high-altitude locations, particularly in Antarctica. Thus, a change in the accumulation rate of snow in Antarctica may be an indicator of a CO₂-induced climatic change.

The influence of snow on the weather and climate can be studied by analyzing observations of the extent and properties of snow, and by numerical simulations with mathematical weather and climate models. These combined observational and modeling approaches are considered in the next two sections along with recommendations for their improvement.

Model Development

Most GCMs predict the mass of snow on the Earth's surface from a snow mass budget equation that includes the processes of snowfall, snow melt, and sublimation. Generally, the snow layer is considered to have uniform properties over its entire depth within a model gridbox, and the surface albedo is taken to be a function of the depth of snow and the type of underlying surface. GCMs calculate snow accumulation as the result of precipitation from clouds. Snow ablation is treated as a result of above freezing temperature.

Although most of the snow cover in middle latitudes dissipates in below freezing temperatures (Kuvaeva et al., 1967), on some occasions a snowpack can survive air temperature substantially above freezing without appreciable melt. On the south facing slopes a snow layer several inches thick will disappear in a few days whereas in the nearby shaded regions of the forest floor, it will remain for several additional weeks.

The intensity of solar radiation reaching the snow/ground interface, the ground temperature and albedo, solar angle and the proportion of the direct diffuse radiation, surface roughness, redistribution of snow by wind, formation of ice crusts and the growth of surface frost, deposition of diamond dust, rain events - all these are processes which influence the properties and the duration of the snow, but which are not adequately accounted for in climate models.

The calculation of snowmelt requires solution of the surface energy budget equation. Because the largest terms are the radiative fluxes, the calculation could be improved by incorporation of a more accurate physically-based snow albedo parameterization. In addition to parameterizing the albedo of the snow itself, the albedo of a mixed field of snow and vegetation must also be represented.

On the polar ice sheets, especially Antarctica, other processes which are not represented in the GCMs may also be important. A significant fraction of the accumulation may be due to ice crystal formation in clear sky from a humid layer at the top of the temperature inversion near the surface, and also due to hoarfrost deposition directly to the surface. There is negligible snowmelt in Antarctica, but as much as half of the annual accumulation has been estimated to be lost by sublimation on the Antarctic slope, a region of persistent katabatic winds. Representation of these processes in GCMs will require finer vertical resolution near the surface.

Recommendations

1. Develop highly-detailed, physically-based (baseline) snow models. The parameterizations of surface snow in GCMs should be developed from, and compared with, the results from highly-detailed, physically-based (baseline) models of snow in which all the snow properties are predicted. Improved equations for the parameters controlling the transfer of mass and energy across the snow-atmosphere boundary, such as the turbulent transfer coefficients and albedo, should be developed in terms of these snow properties. This model development

will require detailed data from experimental sites in a range of contrasting areas such as those of high and low radiation and evaporation.

2. Develop subgrid-scale to grid-scale aggregation methods. Because a GCM gridbox generally has dimensions of a few hundred kilometers, it encompasses a wide variety of surface types and landforms. Consequently, it is necessary to develop methods to aggregate the subgrid-scale information gained from the baseline models to the grid scale. The baseline models should be developed at successively larger scales and be validated using observed streamflow and snow cover data.
3. Develop grid-scale to subgrid-scale disaggregation methods. Because a GCM obtains only a single gridbox-average value for each predicted quantity, there is no variation of a quantity such as snowfall within a gridbox. Consequently, it may be necessary to disaggregate the GCM-predicted grid-scale quantities to the subgrid-scale to provide the information required by the aggregation method described above. Furthermore, disaggregation methods are required to transform the grid-scale climatic information provided by GCMs to the smaller scales of human endeavor so that climatic impact studies can be performed.

Model Validation

Most GCMs predict snowfall and the surface snow mass. A complete validation of the models must therefore include an assessment of their ability to reproduce both the climatological mean distribution and the interannual variability of snow cover. At present, the most suitable snow cover record for validation of GCMs is the NOAA satellite-derived snow cover data base. This data base has been used to a limited extent in model validation.

Several weather forecasting models use climatological snow cover and do not, therefore, include the interaction between the snow and the atmosphere. Other forecast models predict the snow, but it is not known how well.

The observed water equivalent of snow is required to validate the surface snow mass simulated by GCMs. (See Recommendations of Working Group I). Because satellite observations of the water equivalent of snow are not yet available, a climatology can be constructed now based only on surface observations. Such observations have been made locally for Europe, North America and elsewhere, and are archived in synoptic reports.

Recommendations

1. Define the snow-identification threshold in satellite charts. The definition of the snow-identification threshold in satellite observation is needed so that the snow cover simulated by GCMs can be correctly compared with the observed snow cover. The definition of this threshold must include its dependence on the surface type such as boreal forest or tundra.

2. Evaluate weather forecasts with interactive snow. Snow cover predicted by numerical weather forecasting models on short (1 to 3 days), medium (3 to 10 days), and long (10 to 30 days) ranges should be compared with the observed snow cover.
3. Develop a climatology of the water equivalent of snow and use it for validation of climatic models. An international effort is needed to obtain these observations. The surface snow observations would also be useful for comparison with the satellite snow observations.
4. Develop an observationally-based surface albedo climatology for validation of the models. Most albedo climatologies are based on a variety of snow albedo parameterizations. Comparison of an observationally-based albedo climatology with the albedos simulated by GCMs is needed.

Model Applications

Numerical model simulations and experiments can be useful in determining the role of snow in weather and climate. Very few numerical experiments have been performed to date, and many more will be needed to arrive at a definitive understanding of the importance of snow. The importance of snow for weather and climate can be evaluated by performing sensitivity studies in which the snow cover is prescribed to be different from that of a control simulation. The response of the atmosphere to the change in snow cover on several time scales can be determined and compared with the atmosphere's natural variability to discriminate the signal from the noise. The statistically-significant component of the atmospheric response can then be analyzed to determine the influence of the snow anomaly.

The earliest GCM simulation of the annual cycle of CO₂-induced climatic change by Manabe and Stouffer (1980) showed a considerable desiccation of the soil in the mid-latitude agriculturally-productive land areas in the Northern Hemisphere. This summer drying occurred in part due to the earlier spring melting of the seasonal snowpack in the CO₂-enriched world. More recent GCM studies (Hansen et al., 1984 and Washington and Meehl, 1984) with similar fixed-depth ocean models do not simulate this summer drying, while the study of Schlesinger (1986) with a coupled atmosphere-ocean GCM does and also indicates a linkage with the seasonal snowmelt.

An analysis of the surface albedo/temperature feedback, f_{SA} , in the radiative convective model (RCM) simulation of Wang and Stone (1980) gives a value of $f_{SA} = 0.2$ to 0.3 which, acting alone, would amplify the global warming by 20 to 40 percent (Schlesinger, 1985). However, the estimate of f_{SA} in the recent GCM study of Hansen et al. (1984) yielded a value of less than 0.1.

Recommendations

1. Sensitivity studies of the atmospheric response to snow should be performed and/or continued.

2. Further analysis of the snow albedo feedback in CO₂-induced climatic simulations change should be undertaken to clarify the value of the feedback and to determine the individual contributions of snow and sea ice. These analyses should include not only the method of inserting the GCM-simulated changes into a compatible RCM, but also the utilization of the GCM evolution from the 1xCO₂ equilibrium climate to the 2xCO₂ equilibrium.
3. Since the existence of a summer drying is a CO₂-induced climatic change with potentially significant agricultural impact, it is essential that the extant GCM simulations be analyzed further to understand the hydrological changes and the contributions thereto by changes in the seasonal snowcover.
4. Because the simulation of CO₂-induced climate change with a coupled atmosphere-ocean GCM (Schlesinger, 1986) indicates a substantial increase in the permanent snowpack in the interior of Antarctica, with a corresponding decrease along the Antarctic coast, the stability of Antarctic ice shelves to CO₂ induced increases in Antarctic snow accumulation should be analyzed.

References

- Broccoli, A.J. (1986) Characteristics of seasonal snow cover as simulated by GFDL climate models. World Data Center A for Glaciology [Snow and Ice]. Glaciological Data. Report GD-18, Snow Watch '85, p.241-248.
- Dewey, K.F. (1977) Daily maximum and minimum temperature forecasts and the influence of snow cover. Monthly Weather Review, 105, p.1594-1597.
- Gilman, D.L. (1983) Predicting the weather for the long term. Weatherwise, 36, p.290-297.
- Hall, D.K. (1986) Influence of snow structure variability on global snow depth measurement using microwave radiometry. World Data Center A for Glaciology [Snow and Ice]. Glaciological Data. Report GD-18, Snow Watch '85, p.161-171.
- Hansen, J.; Lacis, A.; Rind, D; Russell, G.; Stone, P.; Fung, I.; Ruedy, R.; Lerner, J. (1984) Climate sensitivity: Analysis of feedback mechanisms. (In: Climate Processes and Climate Sensitivity, Maurice Ewing Series, 5, Hansen, J.E.; Takahashi, T., Eds., American Geophysical Union, Washington, DC, p.130-163.)
- Heim, R., Jr.; Dewey, K.F. (1984) Circulation patterns and temperature fields associated with extensive snow cover on the North American continent. Physical Geography, 4, p.66-85.
- Kukla, G.. (1981) Snow covers and climate. World Data Center A for Glaciology [Snow and Ice]. Glaciological Data. Report GD-11, Snow Watch 1980, p.27-39.

- Kunzi, K.F.; Patil, S.; Rott, H. (1982) Snow cover parameters retrieved from NIMBUS 7 scanning multichannel microwave radiometer (SMMR) data. IEEE Translation of Geoscience and Remote Sensing, GE-20, p.452-467.
- Kuvaeva, G.M.; Sulakvelidze, G.K; Chitadze, V.S.; Chotorlishvili, L.S.; El'mesov, A.M. (1967) Physical Properties of snow cover of the greater Caucasus. Moscow, Nauka. (Published for the U.S. Department of Agriculture, Forest Service and the National Science Foundation, Washington, D.C. by the Indian National Scientific Documentation Centre, New Delhi. Translated from Russian.)
- Lamb, H.H. (1955) Two-way relationship between snow or ice limit and 1000-500 mb thickness in the overlying atmosphere. Quarterly Journal Royal Meteorological Society, 81, p.172-189.
- Lamb, H.H. (1972) Climate: Present, Past and Future. Vol. 1. Methuen and Co, London, 613p.
- Manabe, S.; Stouffer, R.J. (1980) Sensitivity of a global climate model to an increase of CO₂ concentration in the atmosphere. Journal of Geophysical Research, 85, p.5529-5554.
- Namias, J. (1962) Influence of abnormal heat sources and sinks on atmospheric behavior. (In: Symposium on Numerical Weather Prediction. Proceedings. Tokyo. Meteorological Society, p.615-627.)
- Namias, J. (1964) Seasonal persistence and recurrence of blocking during 1958-1960. Tellus, 16, p.394-407.
- Nicholls, N. (1980) Extended and long range forecasting. Review of Geophysics and Space Physics, 18, p.771-788.
- Obukhov, A.M.; Kurganskii, M.V.; Tatarskaya, M.S. (1984) Dynamic conditions on the origin of droughts and other large-scale weather anomalies. Soviet Meteorology and Hydrology, 10, p.1-8.
- Robock, A.; Scialdone, J. (1986) A comparison of northern hemisphere snow cover data sets. World Data Center A for Glaciology [Snow and Ice]. Glaciological Data. Report GD-18 Snow Watch '85, p.141-160.
- Robock, A.; Tauss, J.W. (1985) Anomalous snow cover effects on the monthly mean circulation using a steady-state climate model. World Data Center A for Glaciology [Snow and Ice]. Glaciological Data. Report GD-18 Snow Watch '85, p.207-214.
- Schlesinger, M.E. (1986) Co₂-induced changes in seasonal snow cover simulated by the OSU coupled atmosphere-ocean general circulation model. World Data Center A for Glaciology [Snow and Ice]. Glaciological Data. Report GD-18, Snow Watch '85, p.249-270.

- Schlesinger, M.E. (In press) Feedback analysis of results from energy balance and radiative-convective models. (In: The Potential Climatic Effects of Increasing Carbon Dioxide, MacCracken, M.C.; Luther, F.J., eds., U.S. Department of Energy [in press])
- Schlesinger, M.E.; Mitchell, J.F.B. (In press) Model projections of equilibrium climate response to increased CO₂. (In: The Potential Climatic Effects of Increasing Carbon Dioxide, MacCracken, M.C.; Luther, F.M, eds., U.S. Department of Energy [in press].)
- Walsh, J.E.; Ross, B. (1986) Influence of snow cover on cyclonic events. World Data Center A for Glaciology [Snow and Ice]. Glaciological Data. Report GD-18, Snow Watch '85, p.23-35.
- Wang, W.-C.; Stone, P.H. (1980) Effect of ice-albedo on global sensitivity in a one-dimensional radiative-convective climate model. Journal of the Atmospheric Sciences, 37, p.545-552.
- Washington, W.M.; Meehl, G.A. (1984) Seasonal cycle experiment on the climate sensitivity due to a doubling of CO₂ with an atmospheric general circulation model coupled to a simple mixed-layer ocean model. Journal of Geophysical Research, 89, p.9475-9503.
- Yeh, T.-C.; Wetherald, R.T.; Manabe, S. (1984) The effect of soil moisture on the short-term climate and hydrology change--A numerical experiment. Monthly Weather Review, 112, p.474-490.

PARTICIPANTS

Robert Atkins
National Climate Program Office
NOAA
6020 Executive Blvd
Rockville, MD 20852

Thomas Baldwin
Satellite Analysis Branch Rm 401
World Weather Building
Camp Springs, MD 20233

Roger Barry
World Data Center A for Glaciology
CIRES
University of Colorado
Boulder, CO 80309

Anthony Broccoli
Geophysical Fluid Dynamics
Laboratory/NOAA
P.O. Box 308
Princeton, NJ 08542

Jerry Brown
Arctic Res. & Policy Staff
Division of Polar Programs
National Science Foundation
1800 G St. NW, Rm 620
Washington, DC 20550

Al Chang
NASA/Goddard Space Flight Center
Code 624
Greenbelt, MD 20771

Antony Clarke*
Hawaii Institute of Geophysics
University of Hawaii
Honolulu, HI 96822

Kenneth Dewey
311 Avery Lab
University of Nebraska
Lincoln, NE 68588-0135

Jeff Dozier
Dept. of Geography
University of California
Santa Barbara, California 93106

James Foster
NASA/Goddard Space Flight Center
Code 624
Greenbelt, MD 20771

Joyce Gavin
Lamont-Doherty Geological Obs.
Palisades, NY 10964

Barry Goodison
Canadian Climate Centre
Atmospheric Environment Service
4905 Dufferin Street
Downsview, Ontario, M3H 5T4
Canada

Norman Grody
NOAA/NESDIS
Suitland, MD 20233

Charles Gross
Navy/NOAA Joint Ice Center
4301 Suitland Rd.
Washington D.C. 20390

Horia Grumazescu *
Lab. Remote Sensing
Institute of Meteorology and Hydrology
Sos. Bucuresti-Ploiesti 97
Bucharest, Romania

Dorothy Hall
NASA/Goddard Space Flight Center
Code 624
Greenbelt, MD 20771

Martti Hallikainen *
Helsinki University of Technology
Radio Laboratory
Otakaari 5A, 02150 Espoo
Finland

William Klein
Dept. of Meteorology
University of Maryland
College Park, MD 20742

George Kukla
Lamont-Doherty Geological Obs.
Palisades, NY 10964

Helmut Landsberg
Dept. of Meteorology
University of Maryland
College Park, MD 20742

Peiji Li
Lanzhou Institute of Glaciology and
Cryopedology
Academia Sinica
Lanzhou, China

Susan Marshall
Geography Department
University of Colorado
Boulder, CO 80309

Michael Matson
NOAA/NESDIS
World Weather Building, Rm 510
Washington, DC 20233

Kingtse Mo
NASA/Goddard Space Flight Center
Code 611
Greenbelt, MD 20771

Elizabeth M. Morris
Institute of Hydrology
Crowmarsh Gifford
Wallingford
Oxfordshire, OX10 8BB, U.K.

Jerome Namias *
Scripps Institution of Oceanography
A-024 La Jolla, California 92093

Al Rango
U.S. Dept. of Agriculture
Beltsville, MD

Mike Riches
U.S. Dept. of Energy
Office of Energy Research ER 12
Washington D.C. 20545

Dave Robinson
Lamont-Doherty Geological Obs.
Palisades, NY 10964

Alan Robock
Cooperative Institute of
Climate Studies
Dept. of Meteorology
University of Maryland
College Park, MD 20742

Chester Ropelewski
Climate Analysis Center W/MNC52
Washington, D.C. 20233

Greg Scharfen
CIRES
University of Colorado
Campus Box 449
Boulder, CO 80309

John Scialdone
Cooperative Institute of Climate
Studies
Dept. of Meteorology
University of Maryland
College Park, Maryland 20742

Michael Schlesinger
Dept. of Atmospheric Sciences
Oregon State University
Corvallis, OR 97331

Mark Serreze
Lamont-Doherty Geological Obs.
Palisades, NY 10964

Jagadish Shukla
Laboratory for Atmospheric Sciences
NASA/Goddard Space Flight Center
Greenbelt, MD 20771

Honnappa Siddelingaiah
Dept. of Meteorology
University of Maryland
College Park, MD 20742

James Tauss
Cooperative Institute of Climate
Studies
Dept. of Meteorology
University of Maryland
College Park, MD 20742

Hassan Virji
Office of Climate Dynamics
National Science Foundation
1800 G Street NW
Washington, D.C. 20550

Sastri Vemury
IFAORS/STC
7474 Greenway Center Drive
Suite 580
Greenbelt, MD 20770

John Walsh
Dept. of Atmospheric Sciences
University of Illinois
1101 W. Springfield Ave.
Urbana, Illinois 61801

Shao-wu Wang*
Beijing University
Beijing, China

Stephen Warren
Dept. of Atmospheric Sciences AK-40
University of Washington
Seattle, WA 98195

Donald Wiesnet
Satellite Hydrology Associates
601 McKinley St., NE
Vienna, VA 22180

Jay Winston
Dept. of Meteorology
University of Maryland
College Park, MD 20742

Note: *Contributed by Mail

Kukla, G; Barry, R.G.; Hecht, A.; Wiesnet, D. eds. (1986) SNOW WATCH '85. Proceedings of the Workshop held 28-30 October 1985 at the University of Maryland, College Park, MD. Boulder, Colorado, World Data Center A for Glaciology (Snow and Ice), Glaciological Data, Report GD-18, p.23-35.

Snow Cover, Cyclogenesis and Cyclone Trajectories

J. E. Walsh
B. Ross
Department of Atmospheric Sciences
University of Illinois
Urbana, Illinois, U.S.A.

Abstract

Samples of 75-150 cyclogenetic events in eastern North America, the North Atlantic and the North Pacific are obtained from daily data for thirty winters (1951-1980). The large-scale distribution of snow or sea ice cover is used to composite the errors of forecasts derived from persistence, from a barotropic model, and from an analog system. The results are consistent with the notion that extensive snow/ice cover contributes to stronger cyclogenesis and to southward displacements of storm tracks along the East Coast of North America and in the marginal ice zone of the North Atlantic. The apparent signal is statistically significant in these two regions, although the significance is greater in the sea level pressure data than in 500 mb data. No corresponding signal is found in the North Pacific.

Controlled experiments with the NCAR Community Forecast Model are performed to determine the response of a more sophisticated model to extremes of snow and ice in eastern North America and the North Atlantic. While patterns similar to the data-based results are found, the response in the model pressure fields is weaker and farther north of the snow/ice edge than in the corresponding results from the barotropic model and persistence forecasts.

In discussions of the influences of snow cover and sea ice on the atmosphere, it is convenient to distinguish the local effects from potential synoptic-scale effects. The primary local effect is a suppression of the low-level air temperature over timescales of days (Dewey, 1977; Kukla, 1981) to months (Wagner, 1973; Namias, 1985). In support of non-local influences of snow cover, Namias (1962) has argued that the enhancement of baroclinicity by an unusually extensive snow cover favors stronger cyclogenesis and

more meridional storm tracks along the east coast of the United States. Dickson and Namias (1976) showed that the more northerly "Alberta Clipper" storm track is more common during winters when the eastern United States is warmer than normal, while Atlantic coastal storms are more common during cold winters. Carleton (1985) has recently shown that sea ice variability is associated with significant differences in the frequencies of various types of vortices detected in satellite imagery. Corresponding associations between vortex types and the continental snowline were not found to be significant, although Carleton's study included only two years of data from the late 1970's. The notion that sea ice fluctuations influence cyclone trajectories has been popular since the work by Wiese (1924) over a half century ago. However, a determination of the role played by snow or sea ice in synoptic-scale fluctuations is difficult because an anomalous distribution of snow or ice is largely the result of the large-scale circulation and its associated storm tracks.

In this work we attempt to evaluate quantitatively the influence of snow cover and sea ice on cyclone events over data samples much larger than the two-year periods used by Namias (1962) and Carleton (1985). Data on both surface variables (continental snow cover, sea ice) are used to evaluate the systematic errors in short-range atmospheric forecasts composited over cases of heavy and light snow or ice. The atmospheric forecasts are obtained from a simple numerical model, from persistence, and from an analog system. The use of large samples of events permits objective stratifications of cases which are otherwise similar except for the distribution of snow cover or sea ice. The procedure is an attempt to perform "controlled experiments" with observational data, thereby producing observationally-derived counterparts of conclusions obtained from large-scale model sensitivity tests.

Data

The snow cover data for the United States are the latitudinal extents of 1-inch snow coverage at seven longitudes: 100°W, 95°W, ..., 70°W. The data were digitized from the Weekly Weather and Crop Bulletin for the years 1947-82 and are described by Walsh et al. (1982). The specific index used here is the mean of the 1-inch extent over the seven longitudes.

The sea ice indices are the ice-covered areas in the North Atlantic (60-75°N, 20°E-40°W) and the North Pacific (50-65°N, 160°E-160°W). The ice-covered areas were obtained from the digital sea ice dataset described by Walsh and Johnson (1979).

Daily grids of 500 mb height and sea level pressure for the Northern Hemisphere were obtained from the National Center for Atmospheric Research (NCAR). The former were in the 47 x 51 NMC grid format, while the latter were in a 5° x 5° latitude-longitude format.

Data for each January from the 1948-1980 period were used for the North American snow cover experiments (the daily 500 mb grids for 1956-1958 were

not available, nor were the daily grids of sea level pressure for 1948-1950). Data for 17 winters (January-March, 1961-1977) were used for the sea ice experiments. The use of a shorter period for the sea ice experiments was dictated by considerations of the ice data reliability, which was considerably higher in the 1960's and 1970's than in the pre-satellite era.

Methodology

The following strategy was used to obtain ensembles of forecast errors in two categories of cases: those with large and those with small areal coverage by snow or ice in the region of interest. The forecasts were obtained by several techniques, none of which utilized information about the state of the surface. Thus the systematic differences between the errors of the forecasts in cases with heavy and light snow (ice) may be consequences of contrasting surface states.

At the core of each regional experiment is a "target" case, or a cyclonic event characterized by rapid intensification and by motion generally parallel to the snow (ice) boundary. The target case for each region contained a low pressure center which deepened by 20-40 mb in 24 hours during the appropriate month or season (January or winter). The 500 mb grid of the day prior to the rapid intensification of the target case was then used to obtain a pool of the 100 most similar cases from the collection of daily 500 mb grids for the same month or season. The selection was based on a ranking of the daily grids according to their pattern correlations with the target case. However, a grid was omitted from the ranking if it did not contain a maximum of vorticity advection within a 9 x 9 subset of NMC grid points located in the appropriate region.

For each of the 100 cases, 500 mb forecasts to 48 hours were then computed by three methods: (1) a one-level barotropic vorticity model solved on the NMC grid, (2) simple persistence (also used to obtain a corresponding forecast of sea level pressure), and (3) analog evolution. The analog was selected from all other days in the month or season under investigation and was chosen on the basis of the minimal root-mean-square difference over the appropriate region.

The 100 cases were then grouped into terciles according to the areal coverage of snow (ice), and the errors in the 24- and 48-hour forecasts were composited over each tercile of cases: heavy snow (ice), near-normal snow (ice) and light snow (ice). The differences in the errors of the heavy and light composites were then examined for physical plausibility and tested for statistical significance.

Results

Figure 1 shows the boundaries of the snow/ice data regions for the three study areas. Also shown are the sea-level intensities and 24-hour trajectories of the cyclonic systems in the respective target cases.

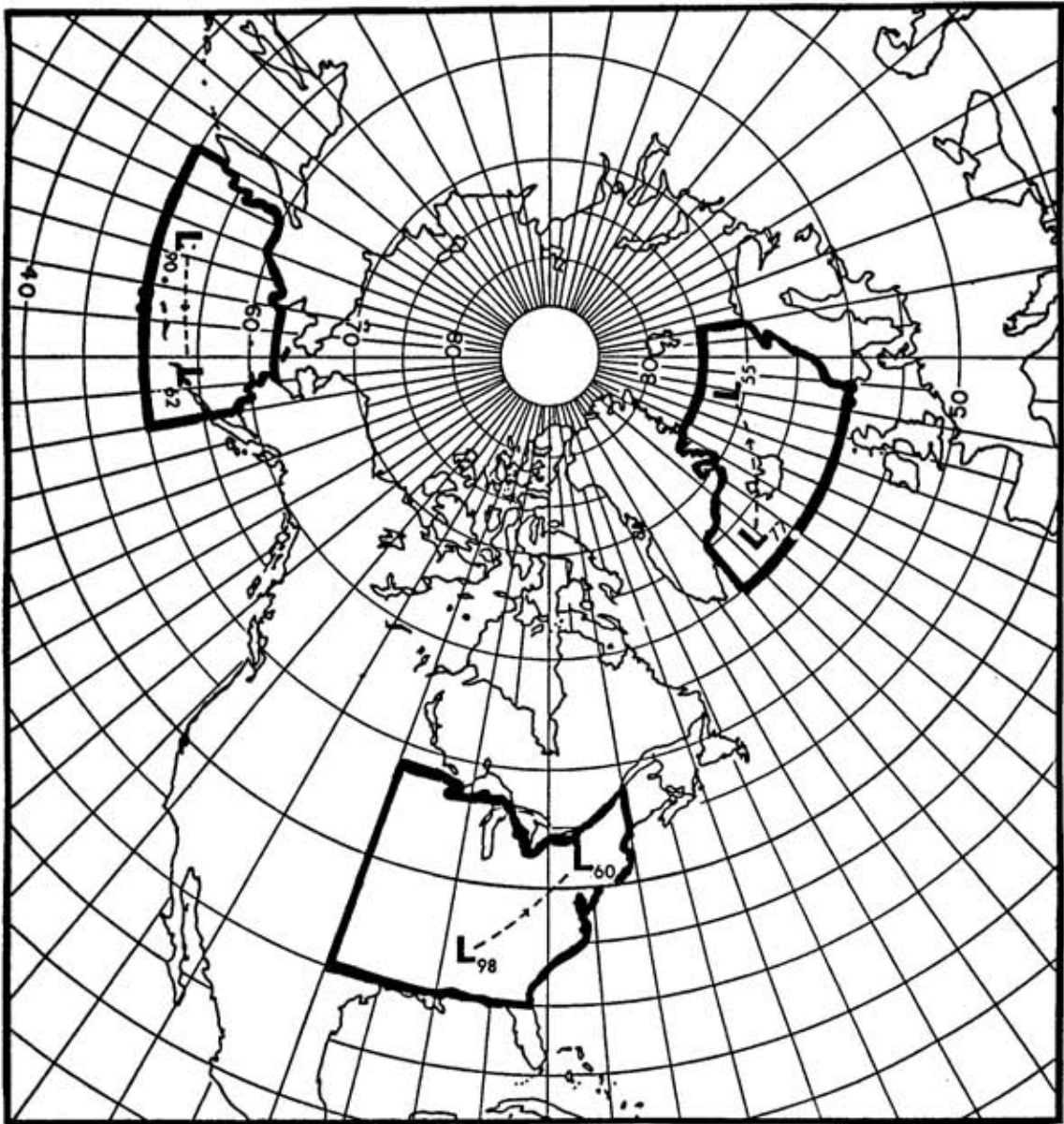


Figure 1. The boundaries of the zones for which snow and ice indices were computed. Also shown are 24-hour trajectories and intensities (mb-900) of low pressure centers in target cases.

Eastern North America

As a background for the analysis of forecast errors, Figure 2 shows the mean absolute errors of the three types of forecasts for the 100 cases based on the United States snow cover. Lower and upper "bounds" are indicated by the closeness of fit to the best 0-hour analog and by the differences between randomly selected January grids. It is apparent from Figure 2 that the forecasts of each type are nearly, but not quite, saturated with error by 48 hours, and that all three types of forecasts show comparable errors at 48 hours. At 24 hours, the errors associated with the barotropic model are slightly smaller than those associated with persistence or the analog forecasts. The similarity of the error growth rates of the three forecasts is consistent with the finding that conclusions concerning the apparent snow influence are similar no matter which type of forecast is employed.

Figure 3 shows the 500 mb maps depicting the target case for the U.S. snow cover experiment. Strong deepening and modest eastward (-15°) movement of the 500 mb trough are evident in the 24 hours following the initial time, 12Z January 25, 1978. The associated surface low pressure system deepens from 998 mb to 960 mb and moves approximately 1200 km northeastward (Figure 1).

As expected with forecasts from a one-level model, the barotropic model forecasts for both the heavy-snow and the light-snow composites contain positive errors (i.e., forecast > observed 500 mb heights) in the vicinity of the amplifying trough over eastern North America. However, in the cases with above-normal snow cover, the average errors are larger by as much as 70 m at 48 hours (Figure 4). The location of the largest differences over New England and the Canadian Maritime Provinces indicates that the intensification and/or eastward movement of the 500 mb trough is more seriously underpredicted under conditions of heavy snow. This pattern of errors is consistent with the findings of Namias (1962) for Februaries of two individual years, 1959 and 1960.

It should be noted that the differences in Figure 4 are not statistically significant at the 5% level, even at the centers of the major positive and negative lobes. The corresponding plots for the 500 mb persistence and analog forecasts were qualitatively very similar to those in Figure 4 and also failed significance tests at the 5% level.

Figure 5 shows the 24- and 48-hour composite difference errors ("heavy-light") for the persistence forecasts of sea level pressure. The 24-hour maximum of +9.8 mb over New England moves northeastward by 48 hours to the Canadian Maritime Provinces, where it has increased to +14.4 mb. The composites for the "heavy" and "light" cases show that the +14.4 mb maximum receives comparable contributions from differential intensification (stronger with heavy snow) and the systematic differences between the resultant trajectories in the heavy and light cases. As indicated in Figure 5, the sea level pressure differences are statistically significant over large areas near the maximum differences.

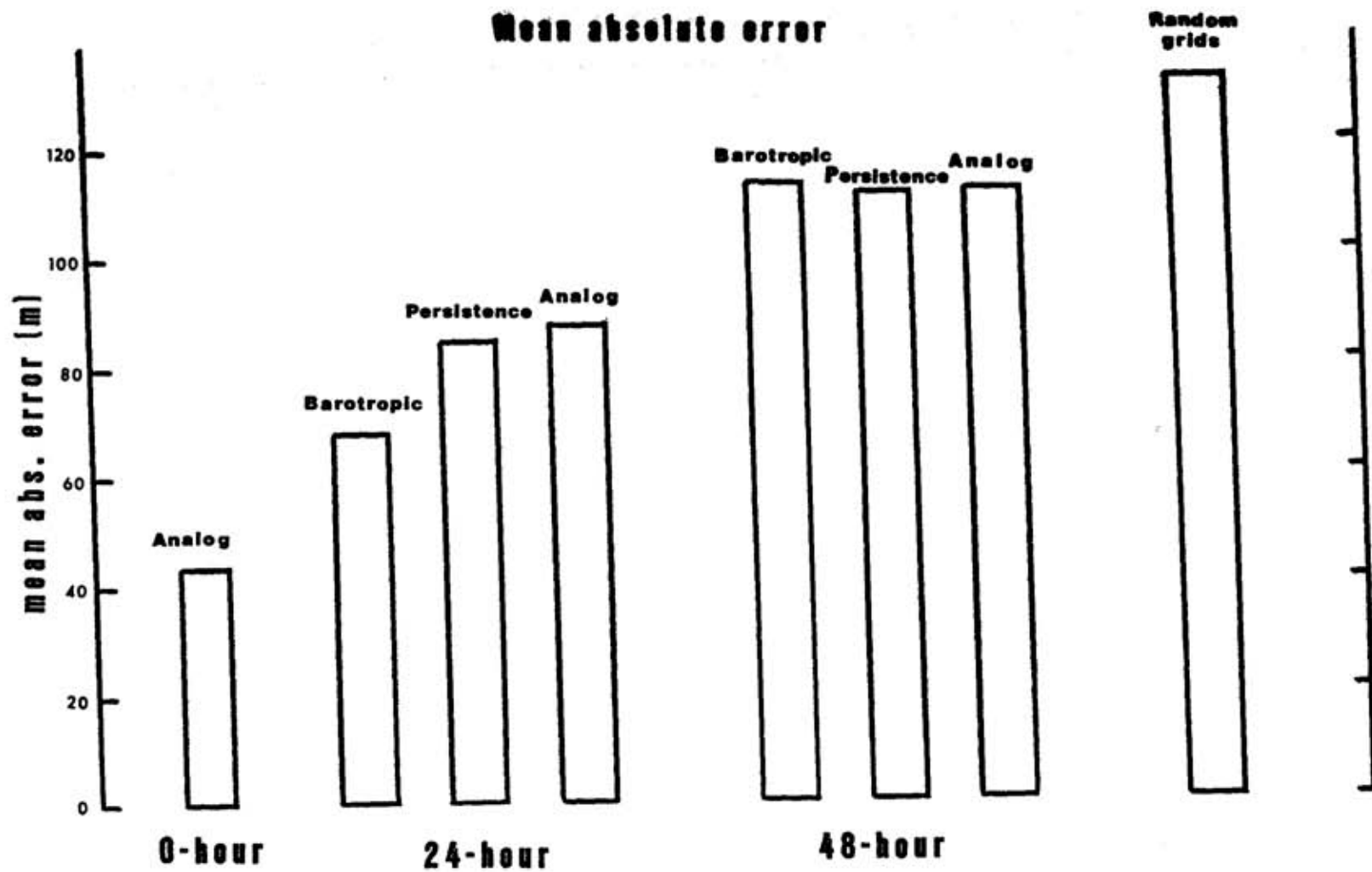
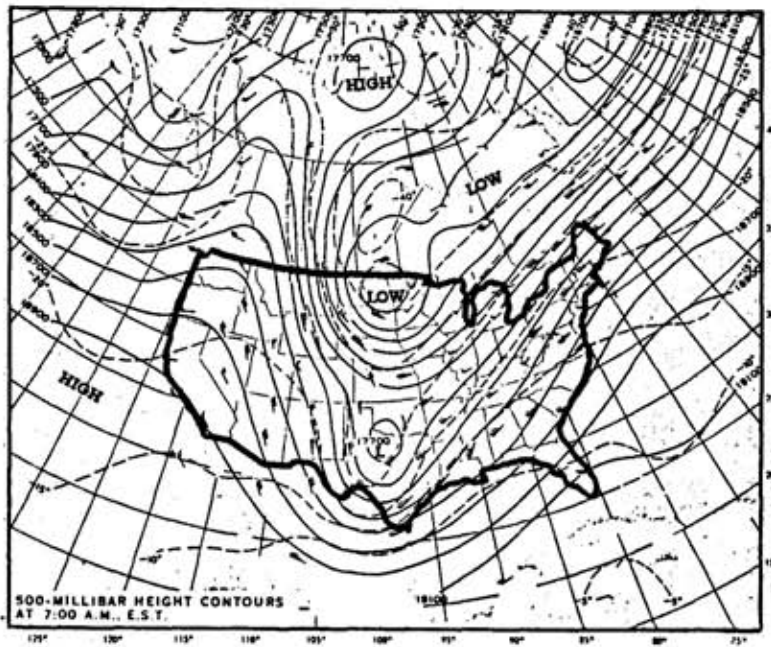
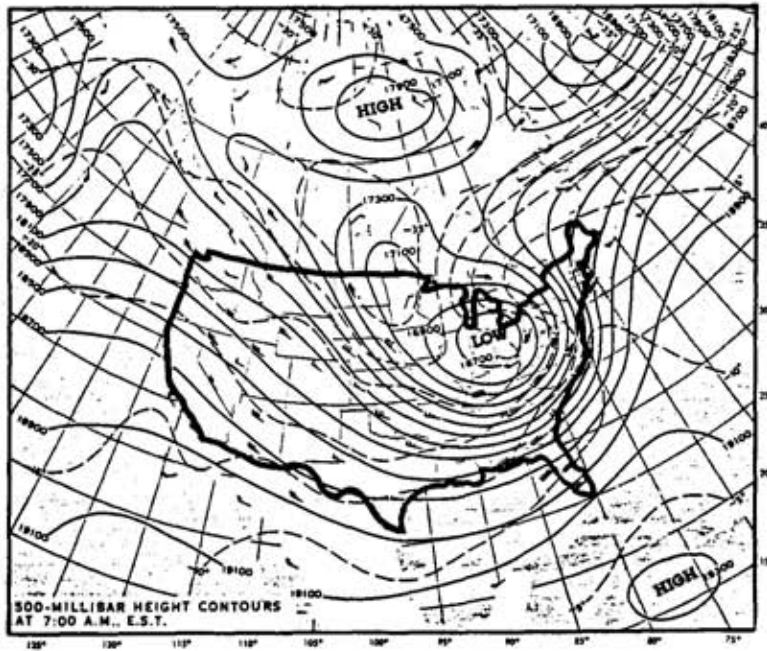


Figure 2. Mean absolute errors (m) of the various forecasts.



(a) 12Z Jan. 25, 1978



(b) 12Z Jan. 26, 1978

Figure 3. 500 mb maps for the North American "target" case of January 25-26, 1978. Solid lines are contours of 500 mb height, dashed lines are isotherms.

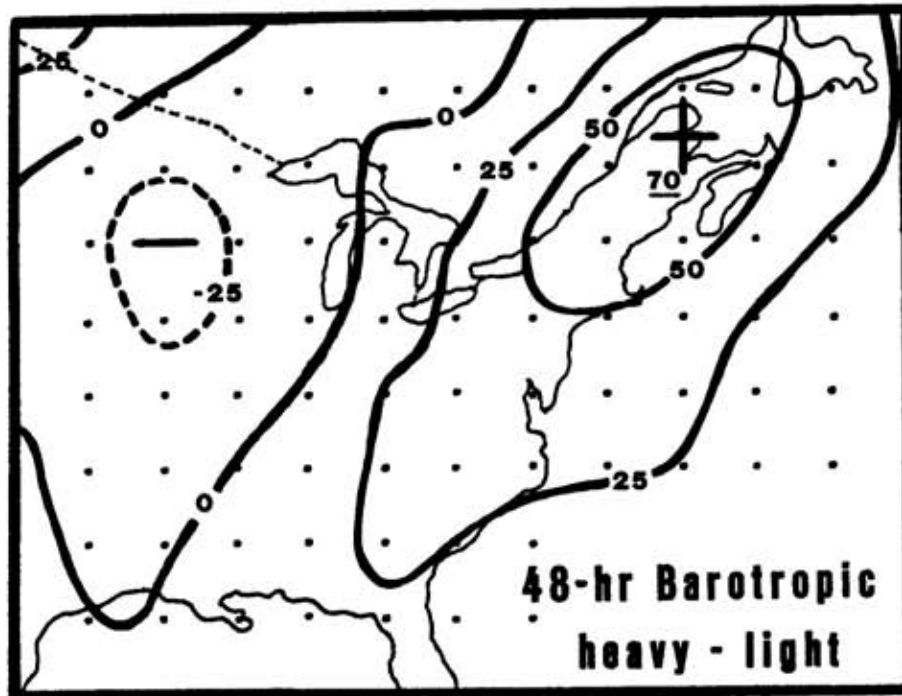


Figure 4. Composite differences of errors in 48-hour barotropic model forecasts of 500 mb geopotential height (m). Contoured values represent means for cases with "heavy" North American snow cover minus means for cases with "light" North American snow cover. Signs thus correspond to "heavy" snow cases.

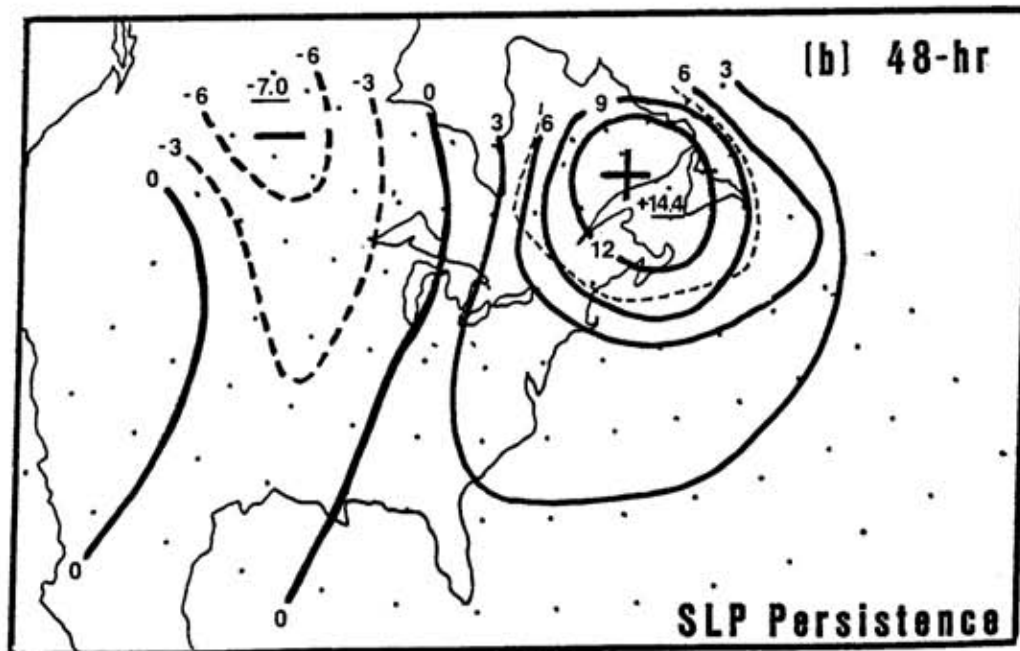
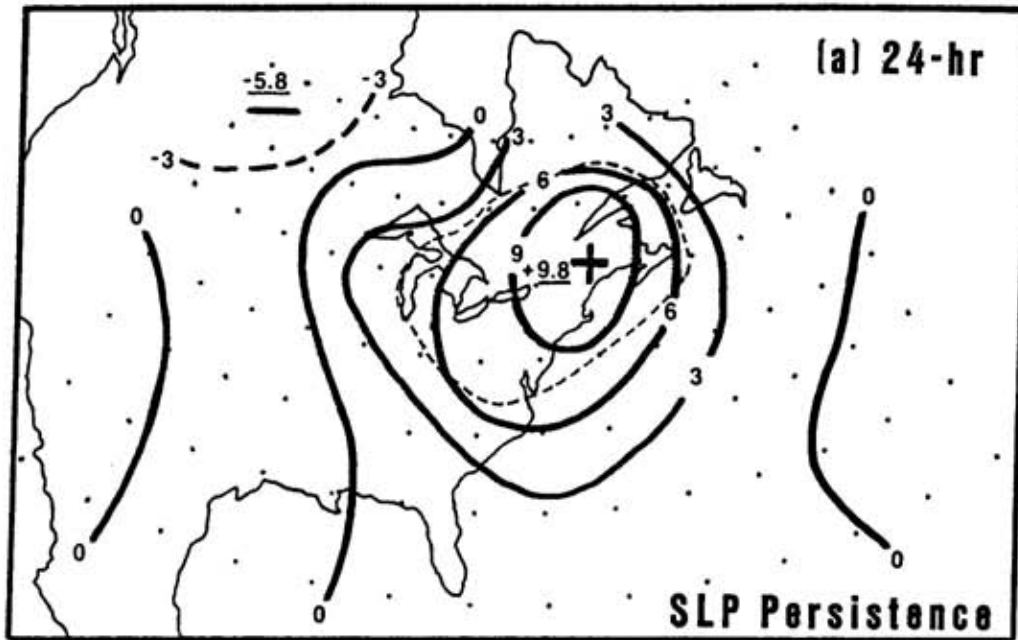


Figure 5. Composite differences of (a) 24-hour and (b) 48-hour errors in persistence forecasts of sea level pressure (mb). Contoured values represent means for cases with "heavy" North American snow cover minus means for cases with "light" North American snow cover. Signs thus correspond to "heavy" snow cases. Values inside thin dashed line are statistically significant at the 95% level.

North Atlantic and North Pacific

The North Atlantic cases were selected according to their correlation with the target case of March 18, 1967, when a surface cyclone moving north-eastward through the Denmark Strait deepened by 22 mb in the subsequent 24 hours. Figure 6 shows the persistence-derived sea level pressure difference fields corresponding to Figure 5. Maximum differences of +8.3 and +11.8 mb are found north of Great Britain. While the pattern of differences is quite similar to that in the North American case, the largest differences are somewhat farther southeast relative to the North Atlantic storm track and ice edge. Local significance (at the 5% level) is achieved over 12.1% of the total domain at 48 hours, but over only 5.8% at 24 hours.

The corresponding difference fields for the North Pacific, based on the target case of March 25-26, 1962, contained only small values (≤ 7 mb) and no areas of statistical significance near the ice edge. The apparent absence of a signal attributable to sea ice in the North Pacific is most likely a consequence of the shorter longitudinal (and latitudinal) extent of sea ice fluctuations relative to those in the North Atlantic (Walsh and Johnson, 1979).

General circulation model results

Sets of 7-day global forecast experiments were also performed with the NCAR Community Forecast Model (CFM) in order to determine the model's sensitivity to snow cover in eastern North America and sea ice in the North Atlantic. The NCAR CFM is a global spectral model and is described in detail by Williamson (1983). Forecasts with heavy and light snow (ice) were initialized with data for days in which observational data showed that strong cyclone development ensued in the respective regions: January 25, 1978 for the North American experiment and January 12, 1980 for the North Atlantic experiment. The prescribed extremes of snow (ice) corresponded to the envelope of the fluctuations observed during the length of the records used in the data-based experiments described above.

While the details of the CFM results will not be presented here, the major differences between the model-based and data-based results will be summarized. In general, there was little evidence of stronger cyclone intensification in the simulations with heavy snow (ice). The "heavy-light" differences of sea level pressure and 500 mb height were noticeably smaller than in the data-based results. The largest 48-hour pressure differences were +7.3 mb in the North Atlantic simulations but only ± 2.5 mb in the North American simulations, while the corresponding 500 mb differences were -17 and -18 m. Because these maxima occurred in regions of strong gradients in the forecast fields, they are indicative of relatively small shifts in the locations of the major centers. These shifts tended to be sufficiently small that displacements of cyclone trajectories were visually detectable only in the later portions of the 7-day period, i.e., after the skill of the forecast had largely disappeared. The model results also showed a tendency for

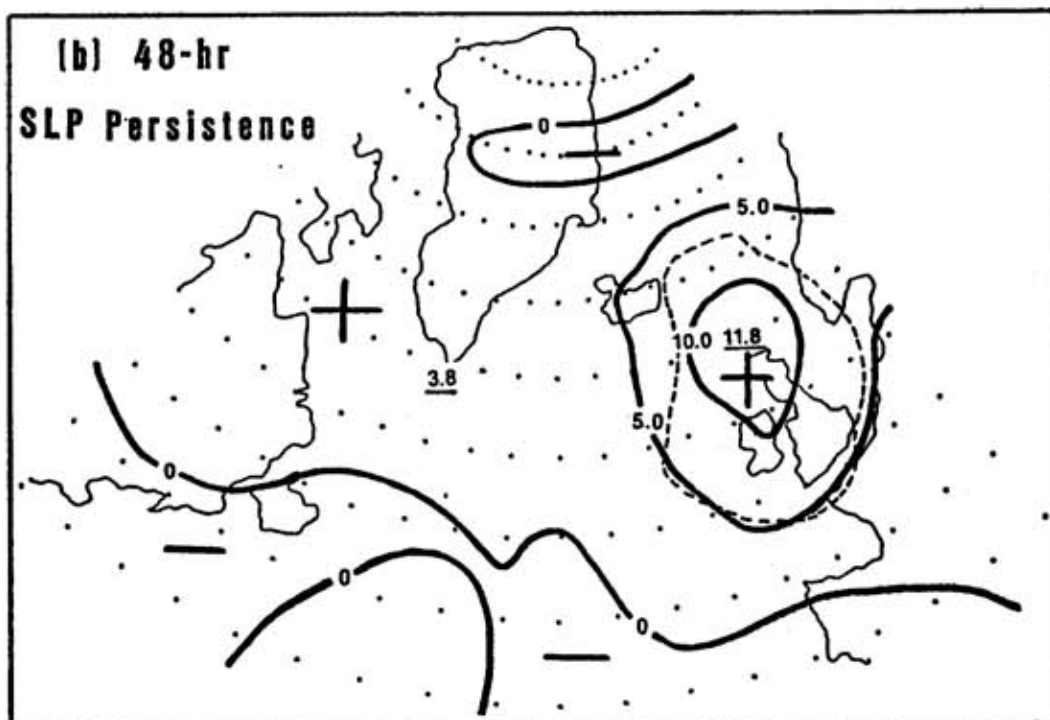
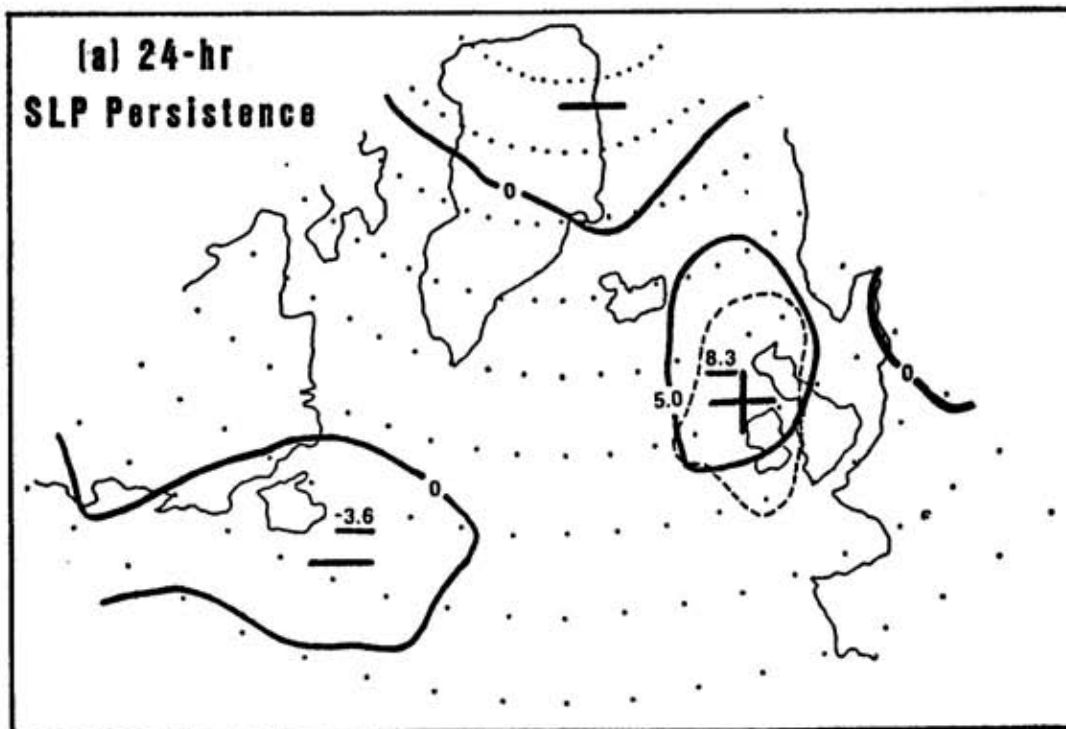


Figure 6. As in Figure 5, but for cases with "heavy" and "light" North Atlantic sea ice.

higher pressures (and heights) in the upstream ridge behind the developing cyclonic systems.

It should be noted, however, that the model results are quite sensitive to the parameters used in the surface flux formulation, e.g., the drag coefficient, the surface albedo, emissivity, etc. For this reason the model-derived conclusions are somewhat more tentative and problematic than the data-based results described earlier.

Conclusion

The results described here point to a detectable influence of North American snow cover and North Atlantic sea ice on cyclone intensification and/or trajectories in the vicinity of the snow/ice boundary. The signals are more apparent in the sea level pressure data than in the 500 mb data. No corresponding influence was detectable in the North Pacific. The most severe limitation in the experimental strategy appears to be the sensitivity of the composite difference fields to the choice of the target case. Experiments with alternative target grids produced difference fields which, in some cases, were only qualitatively similar to those obtained using the original targets. Nevertheless, the data-based conclusions for all the regions are less susceptible to the strong parametric sensitivities of the CFM simulations.

References

- Carleton, A.M. (1985) Synoptic cryosphere-atmosphere interactions in the Northern Hemisphere from DMSP image analysis. International Journal of Remote Sensing, v.6(1), p.239-261.
- Dewey, K.F. (1977) Daily maximum and minimum temperature forecasts and the influence of snow cover. Monthly Weather Review, v.105(12), p.1594-1597.
- Dickson, R.R.; Namias, J. (1976) North American influences on the circulation and climate of the North Atlantic sector. Monthly Weather Review, v.104(10), p.1255-1265.
- Kukla, G., (1981) Snow covers and climate. Snow Watch 1980, Glaciological Data, GD-11, World Data Center A for Glaciology, Boulder, CO, p.27-40.
- Namias, J.(1985) Some empirical evidence for the influence of snow cover on temperature and precipitation. Monthly Weather Review, v.113(9), p.1542-1553.
- Namias, J. (1962) Influences of abnormal heat sources and sinks on atmospheric behavior. Proceedings of an International Symposium on Numerical Weather Prediction held at Tokyo, 1960, Meteorological Society of Japan, p.615-627.

- Wagner, A.J. (1973) The influences of average snow depth on monthly mean temperature anomaly. Monthly Weather Review, v.101(8), p.624-626.
- Walsh, J.E.; Tucek, D.R.; Peterson, M.R. (1982) Seasonal snow cover and short-term climatic fluctuations over the United States. Monthly Weather Review, v.110(10), p.1474-1485.
- Walsh, J.E.; Johnson, C.M. (1979) An analysis of arctic sea ice fluctuations, 1953-1977. Journal of Physical Oceanography, v.9(3), p.580-591.
- Wiese, W. von (1924) Polareis und atmospherische schwankungen. Geographischa Annaler, v.6, p.273-299.
- Williamson, D.L. (1983) Description of NCAR Community Climate Model (CCMOB). NCAR Technical Note NCAR/TN-210+STR, National Center for Atmospheric Research, Boulder, CO, 88 pp.

Kukla, G; Barry, R.G.; Hecht, A.; Wiesnet, D. eds. (1986) SNOW WATCH '85. Proceedings of the Workshop held 28-30 October 1985 at the University of Maryland, College Park, MD. Boulder, Colorado, World Data Center A for Glaciology (Snow and Ice), Glaciological Data, Report GD-18, p.37-53.

The Relationship between Snow Cover and Atmospheric Thermal and Circulation Anomalies

Kenneth F. Dewey
Richard Heim, Jr.
Climatology Program
Department of Geography
University of Nebraska
Lincoln, Nebraska U.S.A.

Abstract

Weekly snow cover areas, derived from the NOAA/NESS Northern Hemisphere Digitized Snow and Ice Cover Data Base, were correlated with weekly temperature anomalies across the United States as well as 500-mb geopotential heights, 700-mb geopotential heights, and sea level pressure across North America. The correlations were computed for snow cover across the entire North American continent as well as the western and eastern United States for the winters 1966-67 through 1982-83. This geographic partitioning allowed for an evaluation of what influence regional snow cover might have on the larger scale circulation. Negative and positive lag correlations were also computed to determine the magnitude and direction of influence (snow cover to atmosphere or the reverse). The winter seasons were divided into two groups (8 years each) based upon the average amount of snow cover for each winter season. The cyclonic storm tracks for the winters with extensive snow cover were then compared to the winters with least snow cover.

The Climatological/Meteorological Significance of Snow Cover

The importance of snow cover goes beyond the obvious effects that it has on human day-to-day activities. Matson et al. (1979), for example, stressed that snow cover is a significant climatic index and reflects the dynamic nature of climate. Namias (1960) has indicated that, because average snowfall amounts are related to the average mid-tropospheric prevailing wind patterns, year-to-year variations in snowfall are manifestations of short-period climatic fluctuations.

In addition to the climatic significance of snow cover, there are also meteorological implications behind variations in snow cover. Wagner (1973) investigated the statistical relationship between monthly snowfall and temperature anomalies at fifteen stations located near, or just north of, the mean mid-winter snow cover limit in the United States. The results of his study indicated that average monthly snow depth or anomaly exerts a significant influence on monthly temperature anomalies. Namias (1964, 1978b) also related the influence of snow cover through a study of seasonal temperature anomalies

and western U.S. snow cover. One of the most significant results of that research effort was the suggestion that persistence of cold (or warm) springs into the following season could be associated with the lingering effects of snow (or lack of snow) in the spring. Kukla and Gavin (1981) compared departures of hemispheric total snow and ice cover with departures of zonal mean monthly temperatures. Their statistical results indicated that more extensive snow cover appears to be associated with lower temperatures in the proximity of the snow line, but with higher temperatures well north of it. They further concluded that a snow cover-temperature relationship may exist on a hemispheric scale, but they could not determine if the temperature anomaly induces the departure in snow cover or vice versa. Dewey (1977) demonstrated the significance of the inclusion of snow cover anomalies in the MOS forecasts of daily maximum/minimum temperatures.

One of the most intriguing areas of research has been the study of the interactions between snow cover and various aspects of the atmospheric circulation. Much of the premier work in this area has been conducted by Namias (1962, 1963a, 1963b, 1966, 1978a, and 1985). In his research, Namias has described the positive feedback that occurs when an extensive snow cover becomes established over portions of the North American continent. This feedback is started by some forcing mechanism (such as sea-surface temperatures in the North Pacific) which then in turn affects the upper level circulation resulting in a trough being positioned downstream over eastern North America. The Polar anticyclones continue to be directed by the airflow within this trough and draw upon the vast moisture source of the Gulf and the Atlantic Ocean. The snow cover continues to spread southward resulting in spatially increased negative thermal anomalies over the snow covered region. The increasing temperature contrast between these colder temperatures and the warmer maritime air masses to the south and east enhances the east coast baroclinicity and intensifies the polar anticyclones advecting through this region. With stronger than normal cyclonic activity, polar air advection is amplified resulting in even further southward penetration of snow cover. Namias suggests that this positive feedback loop will remain in effect until the snow cover disappears with the rising spring temperatures or until influences on the atmospheric circulation become overwhelming. Dickson and Namias (1976) further demonstrated this link between intensified cyclogenesis and increased snow cover in the southeastern U.S. It should also be pointed out that Lamb (1972) demonstrated this positive feedback with applications to Eurasia. A more recent evaluation of the interactions between snow cover and atmospheric circulation was conducted by Heim and Dewey (1984) utilizing the satellite-derived data base of snow cover.

Research Methodology

Prior to the advent of meteorological satellites, the monitoring of the areal extent of continental snow cover was limited to point measurements and extrapolations between these points (Matson *et al.*, 1979). Whereas the amount of snow cover data in the midlatitudes and surrounding population centers was sufficient, snow cover data were very limited for the higher latitude, mountainous, or sparsely populated regions. However, since 1966, a spatially and temporally continuous snow cover data archive has been growing through satellite imagery analysis under the direction of NOAA/NESDIS. This historical archive of "weekly" snow cover maps were digitized by Dewey and Heim (1982) and are being digitized on a "current time" basis now by NOAA/NESDIS. It is this

digitized snow cover data archive which was utilized in the research presented in this paper.

It is the purpose of this research effort to analyze this unique data archive in an attempt to determine the relationships that exist between snow cover and (1) atmospheric thermal anomalies and (2) atmospheric circulation anomalies. Weekly North American, as well as regional U.S. snow cover areas were spatially correlated to regional U.S. temperature anomalies (using concurrent and +1, -1 week lagged temperature data). The same North American and regional U.S. snow cover areas were statistically correlated to 500 mb and 700 mb geopotential heights as well as sea level pressure data (using concurrent and +1, -1 week lagged height and pressure data). As a last step in this research project, the frequency of North American cyclonic activity during extensive winter snow covers was compared to the cyclonic activity during those winters with less extensive snow covers.

Research Results

Snow Cover vs. Temperature

Weekly temperature anomaly data for the continental United States were obtained from the Weekly Weather and Crop Bulletin series. It is significant to note that the temperature anomaly dates corresponded exactly to the snow cover weeks. Figure 1 illustrates the grid pattern for North America and the various snow cover regions. Figure 2 illustrates the thermal anomaly regions. The correlation coefficients for snow cover and temperature anomalies at no lag are listed in table 1. All correlations that are significant at the 0.01 level are indicated with an asterisk (*).

Table 1. Correlation coefficients for snow cover vs. concurrent temperatures.

WEEKLY TEMPERATURE ANOMALY	Weekly Snow Cover Area						
	North America	NW U.S.	SW U.S.	NC U.S.	SC U.S.	NE U.S.	SE U.S.
U.S. Average	-.552*	-.152	-.302*	-.279*	-.372*	-.481*	-.221*
NW U.S.	-.350*	-.254*	-.316*	-.337*	-.284*	-.436*	-.125
SW U.S.	-.141	-.009	-.260*	-.251*	-.299*	-.403*	-.119
NC U.S.	-.545*	-.233*	-.299*	-.296*	-.338*	-.486*	-.168
SC U.S.	-.471*	-.078	-.286*	-.246*	-.402*	-.451*	-.297*
NE U.S.	-.452*	-.055	-.122	-.085	-.205*	-.229*	-.123
SE U.S.	-.329*	-.002	-.060	-.035	-.126	-.105	-.143

Significant at the 0.01 level.

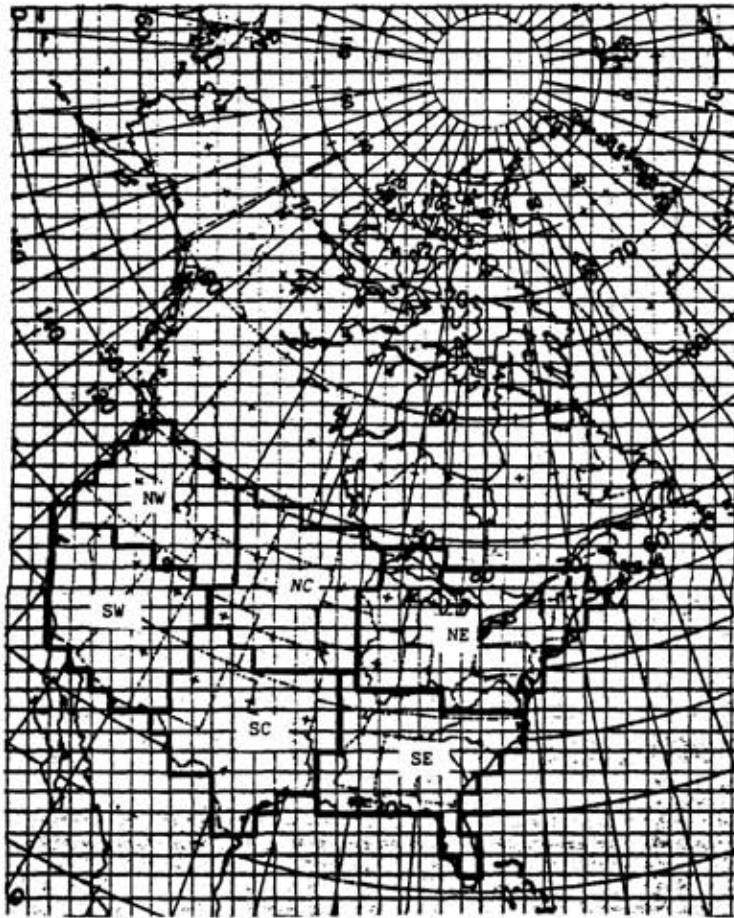


Figure 1. Grid pattern for North America with snow cover regions.

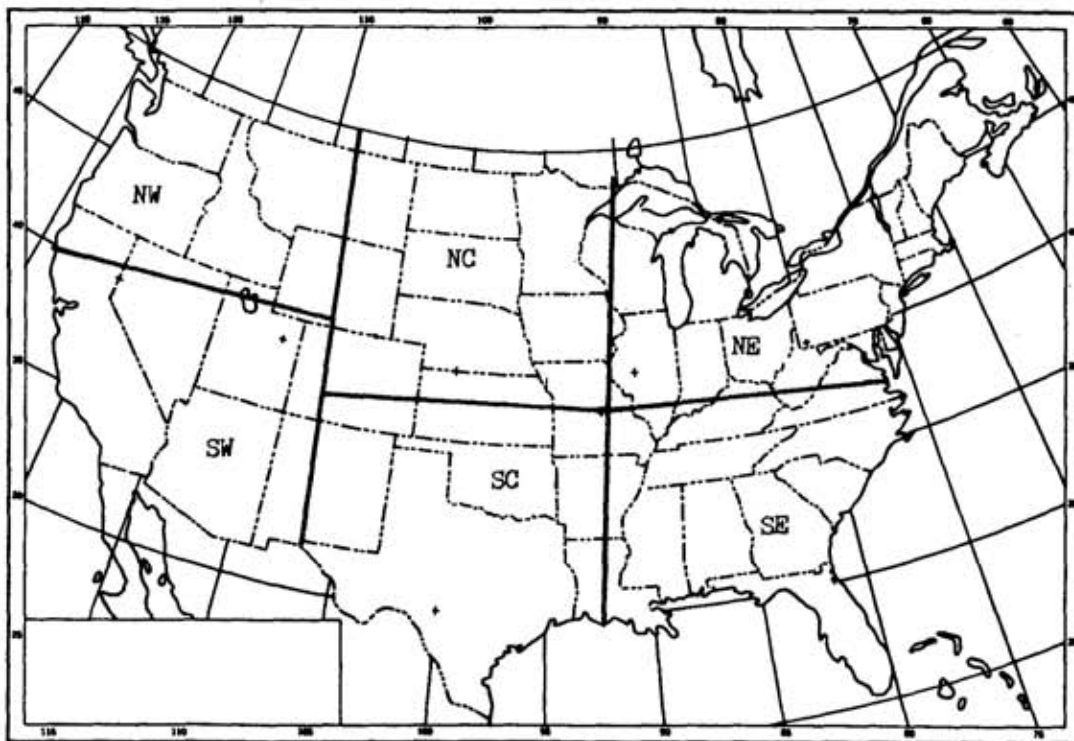


Figure 2. Thermal anomaly regions used in this study.

The highest correlations exist between North American snow cover area (as opposed to the regional snow covers) and the various thermal anomalies. The correlation between North American snow cover and the U.S. average thermal anomaly ranks the highest followed by, in decreasing order, the North Central, South Central, Northeast, Northwest, Southeast, and Southwest temperature anomalies. This hierarchy is a manifestation of the positive feedback outlined by Namias (1962, 1963a, 1963b, 1966, and 1978a). The cyclonic storms that produce extensive continental snow cover are followed by cold polar anticyclones which move out of Canada and are responsible for the negative temperature anomalies in the eastern half of the United States. The mean seasonal snow boundary passes through the NC, SC, and NE regions, hence the enlargement of the snow boundary will be most noticeable in these regions. It could be assumed that the lack of a significant relationship for the SW region is due its position upstream from the general region experiencing the Namias positive feedback. The Rocky Mountains also provide an effective barrier to these cold Canadian air masses. The highest regional snow cover correlations exist for the NE United States, again emphasizing the significant influence that the snow margin has on thermal anomalies.

The +1 and -1 week thermally lagged data which were correlated to the snow cover areas are listed in tables 2 and 3. An examination of the lagged correlations reveals that of a possible 49 correlations, there were only 9 significant positively lagged correlation coefficients, yet there were 28 significant negatively lagged correlations. The inference to be derived from these two correlation coefficient matrices is that there seems to be a larger influence of temperature on subsequent snow cover than snow cover on subsequent temperatures. It is also interesting to note that there were 32 significant concurrent correlations which is only four more than the 28 significant negatively lagged correlations. The largest significant negative and positively lagged correlation coefficients were, respectively, for the NC and NE regions. This would suggest that the largest influence of cold temperatures on subsequent snow cover occurs across the region of primary winter cold air advection and the largest influence of snow cover on subsequent temperatures occurs in the northeastern United States. The colder NE temperatures may be the result of a shifting of the polar front and cyclonic activity to a further east and south location.

Snow Cover vs. 500 mb Geopotential Heights

Weekly 500 mb geopotential height data were generated from the daily 500 mb data and correlated with the weekly snow cover area data. Concurrent and lagged correlations were computed for two geographic regions (the Southeastern states and the southern Hudson Bay region) and the gradient between those two locations. This gradient was chosen to measure the strength of the 500 mb zonal westerlies over the eastern United States. The statistical results are illustrated in tables 4, 5, and 6. Only one correlation is significant (and only marginally) indicating a lack of a relationship between snow cover and the 500 mb geopotential heights.

Table 2. Correlation coefficients for snow cover vs. temperature at +1 week.

WEEKLY TEMPERATURE ANOMALY	Weekly Snow Cover Area						
	North America	NW U.S.	SW U.S.	NC U.S.	SC U.S.	NE U.S.	SE U.S.
U.S. Average	-.262*	-.060	-.059	-.099	-.114	-.231*	-.056*
NW U.S.	-.075	-.091	-.000	-.071	-.011	-.131	+.016
SW U.S.	+.122	+.145	+.044	+.011	+.061	-.043	+.128
NC U.S.	-.257*	-.135	-.050	-.109	-.105	-.217*	-.074
SC U.S.	-.210*	-.011	-.096*	-.105*	-.132	-.213*	-.065
NE U.S.	-.333*	-.064	-.072	-.084	-.135	-.215*	-.094
SE U.S.	-.250*	-.020	-.049	-.046	-.139	-.139	-.081

*Significant at the 0.01 level.

Table 3. Correlation coefficients for snow cover vs. temperature at -1 week.

WEEKLY TEMPERATURE ANOMALY	Weekly Snow Cover Area						
	North America	NW U.S.	SW U.S.	NC U.S.	SC U.S.	NE U.S.	SE U.S.
U.S. Average	-.344*	-.078	-.290*	-.231*	-.270*	-.275*	-.175
NW U.S.	-.243*	-.164	-.310*	-.279*	-.167	-.258*	-.100
SW U.S.	-.086	+.024	-.240*	-.219*	-.144	-.252*	-.003
NC U.S.	-.351*	-.148	-.273*	-.224*	-.224*	-.273*	-.125
SC U.S.	-.251*	+.022	-.276*	-.208*	-.281*	-.248*	-.188
NE U.S.	-.272*	-.012	-.097	-.050	-.191	-.100*	-.169
SE U.S.	-.209*	+.023	-.082	-.051	-.160	-.078	-.146

*Significant at the 0.01 level.

Table 4. Correlation coefficients for snow cover vs. concurrent 500 mb data.

WEEKLY 500 MB DATA	Weekly Snow Cover Area	
	North America	Eastern U.S.
S. Hudson Bay	-0.043	+0.037
SE U.S.	-0.253*	+0.074
Gradient	-0.117	+0.013

*Significant at the 0.01 level.

Table 5. Correlation coefficients for snow cover vs. 500 mb data at +1 week lag.

WEEKLY 500 MB DATA	Weekly Snow Cover Area	
	North America	Eastern U.S.
S. Hudson Bay	-0.142	-0.149
SE U.S.	-0.185	-0.066
Gradient	+0.004	+0.085

Table 6. Correlation coefficients for snow cover vs. 500 mb data at -1 week lag.

WEEKLY 500 MB DATA	Weekly Snow Cover Area	
	North America	Eastern U.S.
S. Hudson Bay	-0.022	+0.076
SE U.S.	-0.175	+0.066
Gradient	-0.088	-0.022

North American Snow Cover vs. 700 mb Geopotential Heights

Weekly 700 mb geopotential height data were generated from the daily 700 mb data and correlated (concurrently and lagged + and - 1 week) with the weekly snow cover area data. The statistical results are presented in figures 3, 4, and 5. Snow cover area demonstrates good statistical relationships with 700 mb heights for both concurrent and negative lags. There appears to be no relationship between snow cover and subsequent (positively lagged) 700 mb heights. Significant patterns appear in the concurrent and negatively lagged correlations. In both cases, extensive snow cover is associated with higher than normal 700 mb heights across the northern portion of the continent and with lower than normal heights across the southern portion of the continent. It would appear that extensive snow cover is related to a southward shift in the location of the mean 700 mb trough and an amplified ridge shifting northward out of the Pacific and into the Arctic.

The winter of 1978-79 is an ideal example of the flow pattern associated with extensive North American snow cover. North American snow cover exceeded the mean values for every week during this season and large portions of the continental U.S. experienced below normal temperatures from December through February. The 700 mb circulation for each winter month was characterized by high latitude blocking, with the westerlies displaced south of their normal position over North America in January (Dickson, 1979; Taubensee, 1979; and Wagner, 1979).

Snow Cover area vs. Sea Level Pressure

The research of Dickson and Namias (1976) indicates that a greater frequency of cyclones occurs along the Atlantic coast of North America, and cyclone frequency decreases in the region of the Icelandic low, during winter seasons with enhanced snow cover in the eastern United States. Consequently, the greater frequency of cyclones passing a given point should result in a lower mean sea level pressure in that area. The sea level pressure data for this study were taken from the National Meteorological Center's 1200Z Northern Hemisphere synoptic map and they were then rendered into weekly averages to be statistically correlated with the weekly snow cover data. Six geographic regions were examined in order to evaluate any regional influence that might exist between snow cover and surface pressure.

Tables 7, 8, and 9 illustrate the tabular correlations for snow cover and concurrent +1 and -1 week surface pressure. Only two correlations are statistically significant: North American snow cover vs. the Icelandic low pressure index on both a concurrent and a -1 week lag basis. This direct relationship indicates that extensive North American snow cover is associated with a weaker than normal Icelandic low between Greenland and Iceland. Unfortunately, as in the evaluation of the other pressure levels, the influence seems to be one direction (pressure pattern to snow cover and not the reverse).

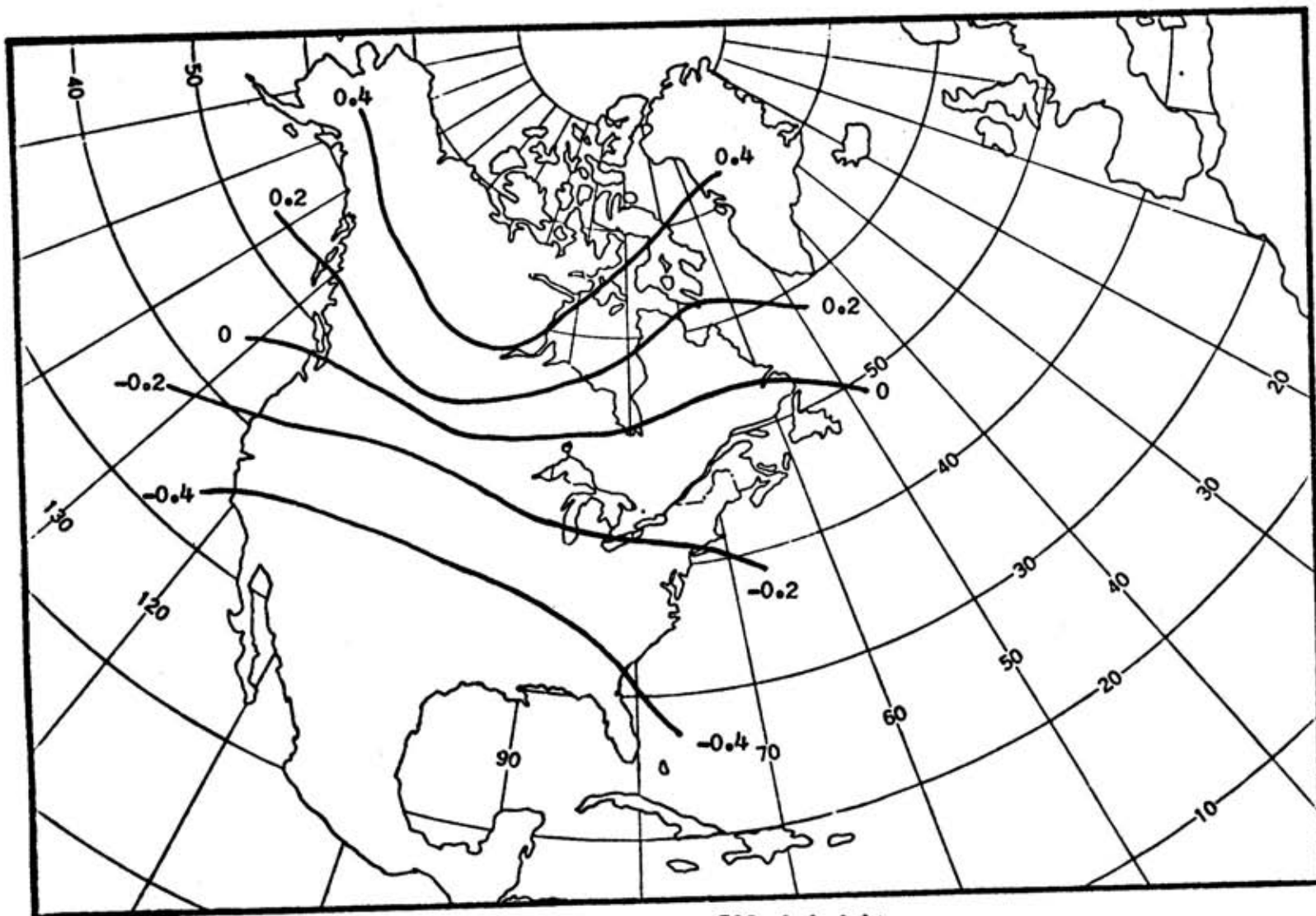


Figure 3. North American snow cover vs. concurrent 700 mb heights.

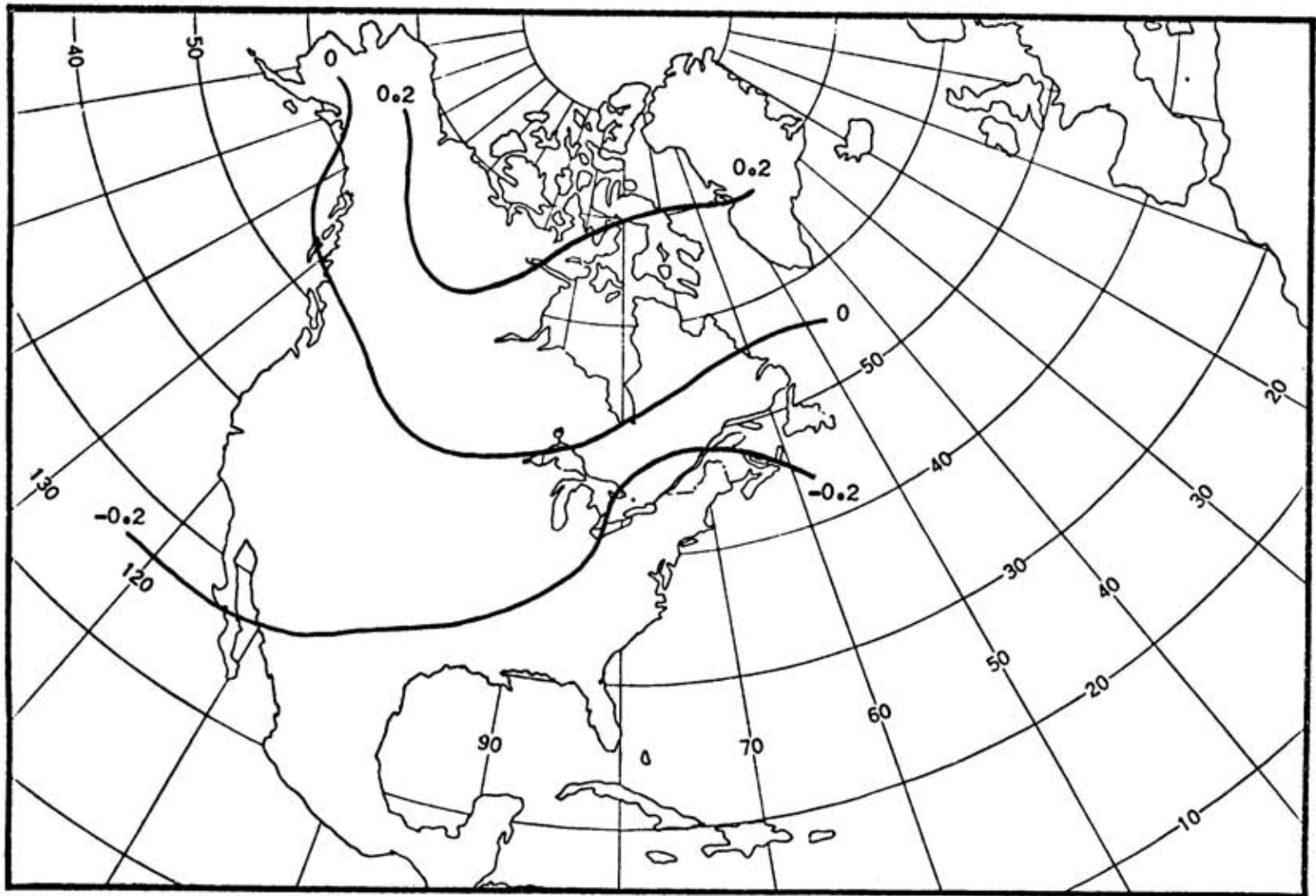


Figure 4. North American snow cover vs. 700 mb heights at +1 week lag.

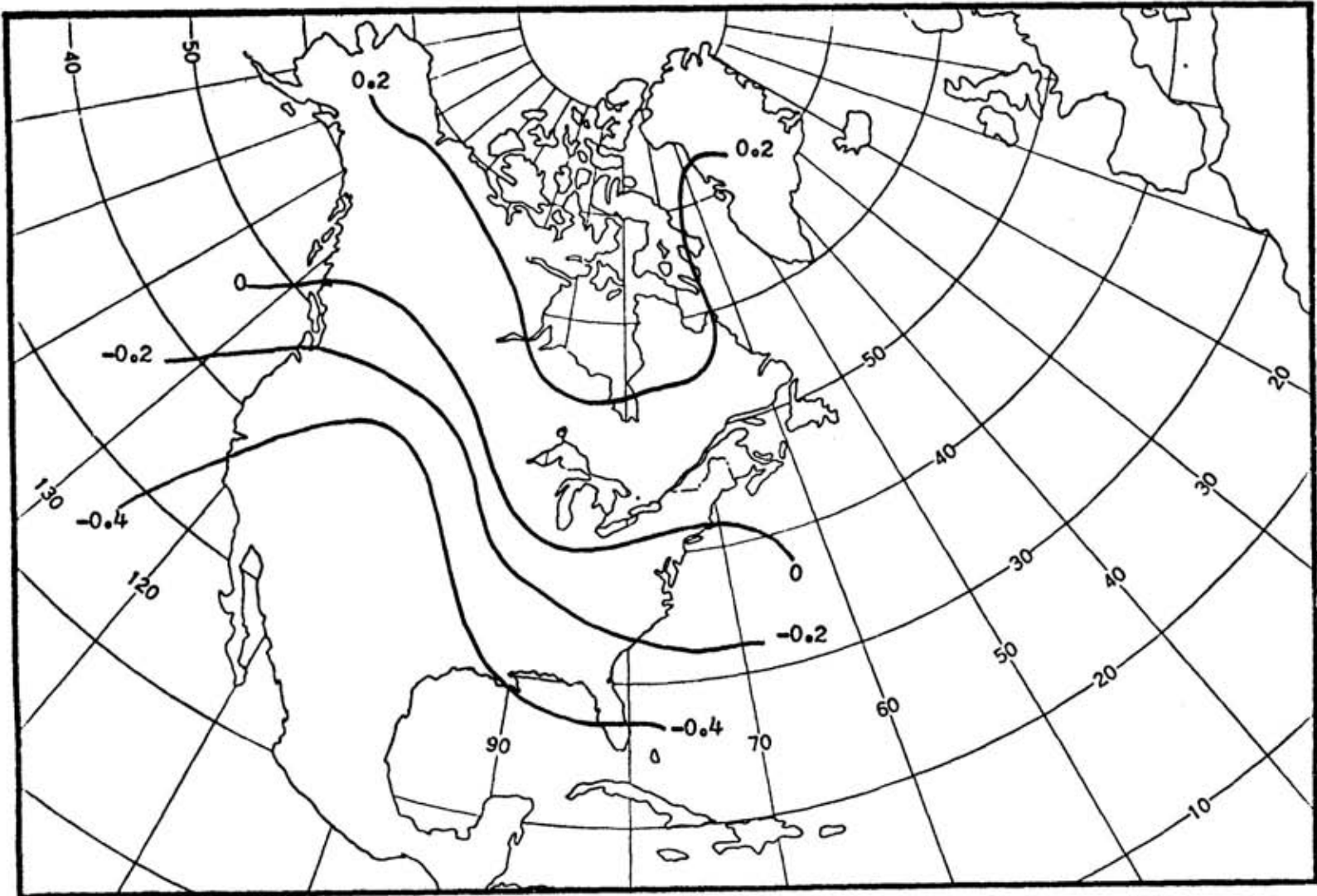


Figure 5. North American snow cover vs. 700 mb heights at -1 week lag.

Table 7. Correlation coefficients for snow cover vs. concurrent sea level pressure.

SEA LEVEL PRESSURE INDEX	Weekly Snow Cover Area		
	North America	Western U.S.	Eastern U.S.
Icelandic Low	+0.237*	+0.056	+0.059
Aleutian Low	-0.085	+0.112	+0.070
South Atl. Coast	-0.060	+0.019	-0.009
Middle Atl. Coast	-0.047	+0.062	+0.068
North Atl. Coast	-0.047	+0.028	+0.024
North Pac. Coast	+0.042	-0.125	+0.011

*Significant at the 0.01 level.

Table 8. Correlation coefficients for snow cover vs. sea level pressure at +1 week lag.

SEA LEVEL PRESSURE INDEX	Weekly Snow Cover Area		
	North America	Western U.S.	Eastern U.S.
Icelandic Low	+0.001	-0.036	-0.157
Aleutian Low	+0.018	+0.145	+0.148
South Atl. Coast	+0.009	-0.091	-0.030
Middle Atl. Coast	+0.032	+0.051	+0.054
North Atl. Coast	-0.014	+0.039	+0.024
North Pac. Coast	-0.081	-0.141	+0.062

Table 9. Correlation coefficients for snow cover vs. sea level pressure at -1 week lag.

SEA LEVEL PRESSURE INDEX	Weekly Snow Cover Area		
	North America	Western U.S.	Eastern U.S.
Icelandic Low	+0.202*	+0.121	+0.099
Aleutian Low	-0.152	-0.008	+0.056
South Atl. Coast	-0.069	-0.073	-0.060
Middle Atl. Coast	-0.092	-0.018	+0.001
North Atl. Coast	-0.083	-0.002	-0.007
North Pac. Coast	-0.050	-0.138	+0.006

*Significant at the 0.01 level.

Although caution should be exerted in inferring too much from these two significant correlations, the following scenario can be formulated. A southward shift in the location of the upper level trough normally located over eastern Canada would result in an expanded North American snow cover. The change in upper-level flow would redirect the paths taken by surface cyclones away from the Iceland-Greenland area. The more extensive snow cover over the eastern United States would enhance the surface temperature contrast along the Atlantic coast, thereby intensifying cyclogenesis along the coast, which is in agreement with the results of Dickson and Namias (1976).

An explanation can be offered as to why snow cover was poorly correlated with variations in cyclonic activity (using sea level pressure). Mean sea level pressure may be a poor index of cyclogenesis. Frequently during heavy snow cover seasons, the intense cyclones are followed by large high pressure systems. When the pressures are averaged to compute the weekly means, the presence of the cyclones would be masked by the intense highs. Barry and Perry (1973), in their discussion of mean pressure maps, have pointed out that, while deep depressions frequently tend to move, such maps should be examined with reference to charts of the frequency and tracks of cyclones and anticyclones. As a last step then, the cyclonic paths of extensive and non-extensive snow cover years were compared.

Cyclonic Activity During Extensive and Non-Extensive Snow Cover Years

The winter snow covers were averaged and divided into two equal groups, extensive (above the median) snow cover years and non-extensive (below the median) snow cover years. Using the cyclonic paths as presented in Mariners Weather Log, the frequency of cyclones passing through a 5 degree square gridded network was computed. The frequency of cyclonic activity for each grid

cell during the less extensive snow cover years was then subtracted from the frequency of cyclones during the extensive snow cover years. The results are illustrated in figure 6. It is significant to note that, as has been suggested in the literature, there is an increased amount of cyclonic activity across the southern and southeastern states during extensive snow cover years. The southward displacement of the cyclonic storm track is made even more evident with the indication of decreased cyclonic activity across the northern states during extensive snow cover years.

Summary and Conclusions

The purpose of this research project was to determine the relationships that exist between snow cover and (1) atmospheric thermal anomalies and (2) atmospheric circulation anomalies. Instead of using point observations of snow cover, which are highly clustered into the midlatitudes as well as near population centers, the newly created digitized archive of satellite-derived snow cover observations was utilized. This satellite-based data archive extends back to fall 1966 and provides a spatially and temporally continuous archive of snow cover. Weekly North American, as well as regional U.S. snow cover areas, were spatially correlated to regional U.S. temperature anomalies (using concurrent and +1, -1 week lagged temperature data). The same North American and regional U.S. snow cover areas were statistically correlated to 500 mb and 700 mb geopotential heights as well as sea level pressure data (using concurrent and +1, -1 week lagged height and pressure data). As a last step in this research project, the frequency of North American cyclonic activity during extensive winter snow covers was compared to the cyclonic activity during those winters with less extensive snow covers.

Correlating snow cover to temperature, the highest correlations exist between North American (as opposed to regional) snow cover and the regional thermal anomalies. The regional thermal anomalies of most significance were the entire United States, North and South Central, and northeast United States. The concurrent and negatively lagged statistics produced an almost equal number of significant correlations (32 and 28 of a possible 49) yet the positively lagged data produced only 9 significant correlations. Therefore, the influence of temperature on subsequent snow cover far exceeds the influence of snow cover on subsequent temperatures.

The 700 mb geopotential height field was much more significantly related to snow cover than was the 500 mb geopotential height field. It was concluded that there is no statistical or physical relationship between 500 mb height anomalies and snow cover. Significant patterns appear in the concurrent and negatively lagged correlations between 700 mb heights and snow cover, once again emphasizing that the influence is from the atmosphere to snow cover and not the reverse. It was concluded that extensive snow cover is associated with higher than normal 700 mb heights across the northern portion of the continent and with lower than normal heights across the southern portion of the continent.

The only relationship that appears to exist between sea level pressure (concurrent and -1 week lag) and snow cover is a reduced Icelandic low during extensive snow cover years. The occurrence of disappointing correlations between sea level pressure and snow cover was judged to be a function of intensified cyclonic activity being balanced by subsequent intensified advection of

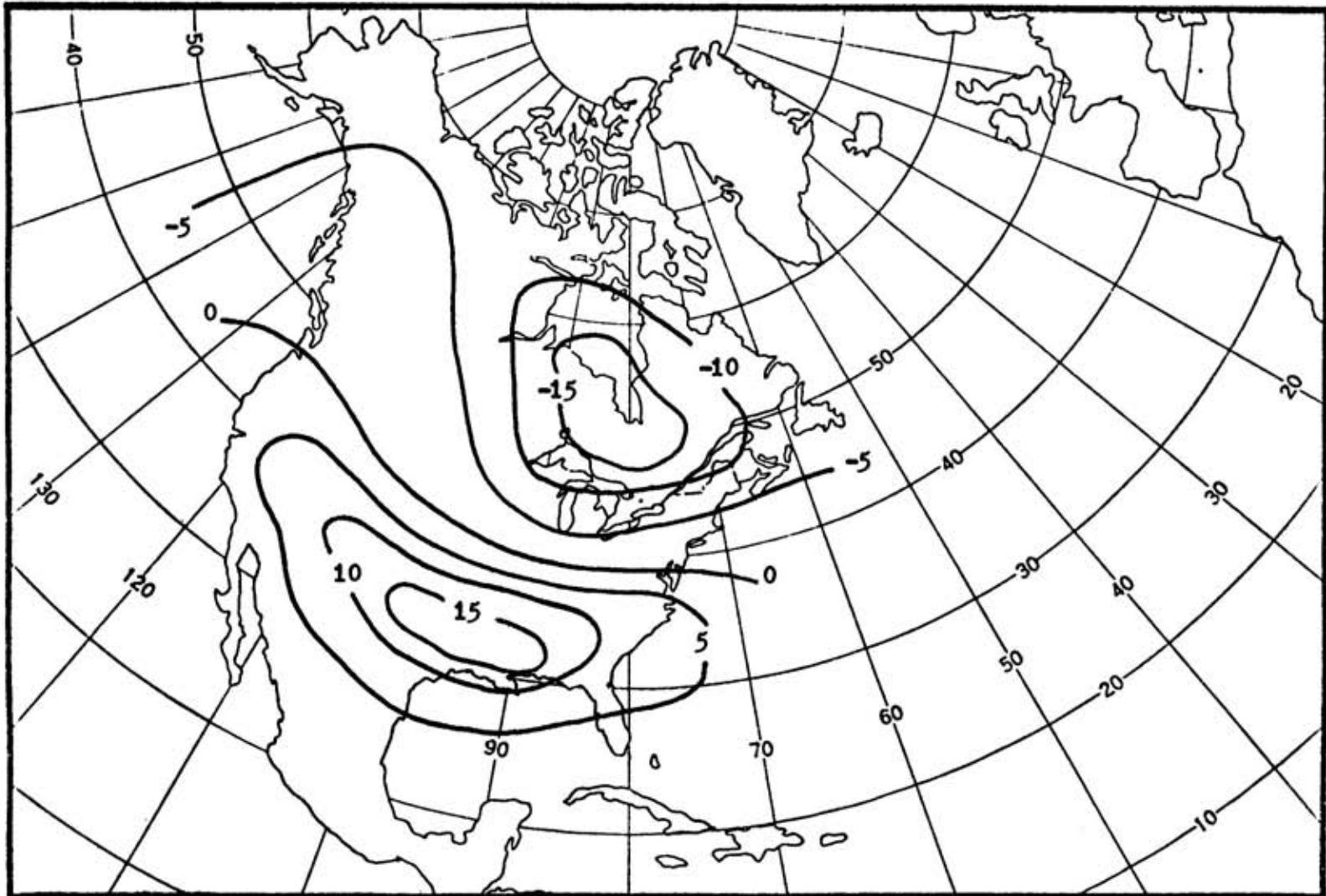


Figure 6. The difference in the total number of cyclones (as calculated for 5° squares) between winters with extensive snow cover and winters with reduced snow cover. Positive values indicate that there is a greater amount of cyclonic activity during winters with extensive snow cover.

polar high pressure. Therefore, the cyclonic paths were then mapped to determine if there was an influence or relationship between snow cover and cyclonic activity. It was demonstrated that during winters of extensive snow cover, the cyclonic storm track was displaced south and eastward resulting in increased cyclonic activity (as has been suggested in the literature) across the southeastern and east coast regions of the United States. Unfortunately, because seasonal data were utilized, it could not be determined whether extensive snow cover caused the shift in the cyclonic paths or the shift in the cyclonic activity caused the extensive snow cover.

References

- Barry, R.G.; Perry, A.H. (1973) Synoptic Climatology: Methods and Applications. London, Methuen and Co., Ltd.
- Dewey, K.F. (1977) Daily maximum and minimum temperature forecasts and the influence of snow cover. Monthly Weather Review, v.105, p.1594-1597.
- Dewey, K.F.; Heim, R. (1982) A digital archive of Northern Hemisphere snow cover, November 1966 through December 1980. Bulletin of the American Meteorological Society, v.105, p.1594-1597.
- Dickson, R.R.; Namias, J. (1976) North American influence on the circulation and climate of the North Atlantic sector. Monthly Weather Review, v.104, p.1255-1265.
- Dickson, R.R. (1979) Weather and circulation of February 1979: Near-record cold over the northeast quarter of the country. Monthly Weather Review, v.107, p.624-630.
- Heim, R.; Dewey, K.F. (1984) Circulation patterns and temperature fields associated with extensive snow cover on the North American continent. Physical Geography, v.4, p.66-85.
- Kukla, G.; Gavin, J. (1981) Cool autumns in the 1970's. Monthly Weather Review, v.109, p.903-908.
- Lamb, H.H. (1972) Climate: Present, Past and Future, vol. 1. London, Methuen and Co., Ltd.
- Matson, M.; Wiesnet, D.R.; Berg, C.P.; McClain, E.P. (1979) New data and new products: The NOAA/NESS continental snow cover data base. (In: Fourth Annual Climate Diagnostics Workshop. Proceedings. National Oceanic and Atmospheric Administration, p.351-364.)
- Namias, J. (1960) Snowfall over eastern United States: Factors leading to its monthly and seasonal variations. Weatherwise, v.13, p.238-247.
- Namias, J. (1962) Influence of abnormal surface heat sources and sinks on atmospheric behavior. (In: International Symposium on Numerical Weather Prediction, Tokyo, November 7-13, 1960. Proceedings. Meteorological Society of Japan, p.615-627.)

- Namias, J. (1963a) Large-scale air-sea interactions over the North Pacific from summer 1962 through the subsequent winter. Journal of Geophysical Research, v.68, p.6171-6186.
- Namias, J. (1963b) Surface-atmosphere interactions as fundamental causes of drought and other climatic fluctuations. (In: Arid Zone Research XX, Changes of Climate. Rome Symposium UNESCO and WMO. Proceedings, p.345-359.)
- Namias, J. (1964) A 5-year experiment in the preparation of seasonal outlooks. Monthly Weather Review, v.92, p.449-464.
- Namias, J. (1966) Large-scale air sea interactions as primary causes of fluctuations in prevailing weather. Transactions of the New York Academy of Sciences, S. II, v.29, p.183-191.
- Namias, J. (1978a) Multiple causes of the North American abnormal winter 1976-77. Monthly Weather Review, v.106, p.279-295.
- Namias, J. (1978b) Persistence of U.S. seasonal temperatures up to one year. Monthly Weather Review, v.106, p.1557-1567.
- Namias, J. (1985) Some empirical evidence for the influence of snow cover on temperature and precipitation. Monthly Weather Review, v.113, p.1542-1553.
- Taubensee, R.E. (1979) Weather and circulation of December 1978: Record and near record cold in the West. Monthly Weather Review, v.107, p.354-360.
- Wagner, A.J. (1973), Influence of average snow depth on monthly mean temperature anomaly. Monthly Weather Review, v.101, p.624-626.
- Wagner, A.J. (1979) Weather and circulation of January 1979: Widespread record cold with heavy snowfall in the Midwest. Monthly Weather Review, v.107, p.499-506.

Relationships between Snow Cover and Temperature in the Lower Troposphere, General Circulation in East Asia and Precipitation in China

Zhao Zong-ci
Wang Shao-wu
Department of Geophysics
Peking University, China

Abstract

Relationships between snow cover and temperature in the lower troposphere, general circulation at 500 mb in East Asia and precipitation in China were analyzed. It is shown that there are obvious negative correlations between snow cover in the Northern Hemisphere in winter and temperature in the following summer. Significant negative relationships between sea ice in summer and temperature in the higher latitudes are noticed. Snow cover in Eurasia in winter influences the general circulation in East Asia and rainfall in China in the following spring and summer. When there is more snow cover in Eurasia in winter, droughts appear in Northern China in the following spring and in the Yangtze River valley of China in the following summer.

Introduction

It was noticed that snow cover and sea ice are important elements when climatic changes in the earth-atmosphere system are studied.

The purpose of this paper is to investigate the relationships between snow cover and temperature in the lower troposphere, general circulation in East Asia and precipitation in China.

Data

Areas of snow cover in the Northern Hemisphere in winter (Dec.-Feb.) were from Wiesnet and Matson (1979) and Matson and Varnadore (1981). North American and Eurasian seasonal averages of snow cover in winter (Dec.-Feb.) were given by Kukla and Gavin (1979) and Kukla et al. (1982). Sea ice was from Zakalof and Stlokuna (1978).

Characteristic values of the general circulation at 500 mb in East Asia and precipitation and temperature in China were offered by the long-term forecasting office of the Chinese Meteorological Administration. Drought and flood data for China were shown by Wang and Zhao (1981) and Zhao and Wang (1984). Temperature in the lower troposphere was taken from Wang and Zhao, (1984).

Due to the limited amount of snow cover data, time series for data were taken from 1967 to 1982. Long-term averages were computed over this time interval.

Correlation between snow cover, sea ice and temperature in the lower troposphere.

Cross lag correlation coefficients between areas of snow cover in the Northern Hemisphere in winter, Wiesnet and Matson (1979) and Matson and Varnadore (1981), (Dec.-Feb.) and zonal mean air temperature along each latitude (10-90°N) in the lower parts of the troposphere (1000 mb-500 mb) from November to December of the following year were computed (figure 1). It was found that there are more obvious negative correlations with the following summer half-year (May-Oct.) than the same season (Dec.-Feb.), especially at 60°N (June-Sept.). The curves of snow cover in winter and average air temperature at 60°N in June-September are given in figure 2b. Winter of 1966-67 of figure 2 is represented by 1967. It is noticed from figure 2b that the relationship is strong. Temperature in the middle latitudes of the Northern Hemisphere in summer has a close relation to snow cover in winter. When there is more snow cover in the Northern Hemisphere in winter, lower temperature at the middle latitudes of the Northern Hemisphere in the following summer appear and vice versa.

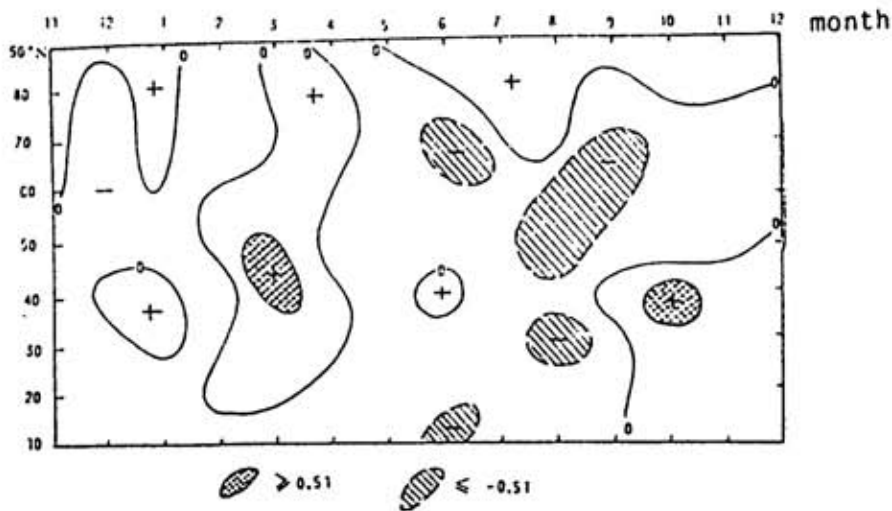




Fig. 1 Cross correlation between snow cover in the Northern Hemisphere in winter and average air temperature along each latitude. (Positive and negative correlation which received the 95% level of confidence are shown by  and  here).

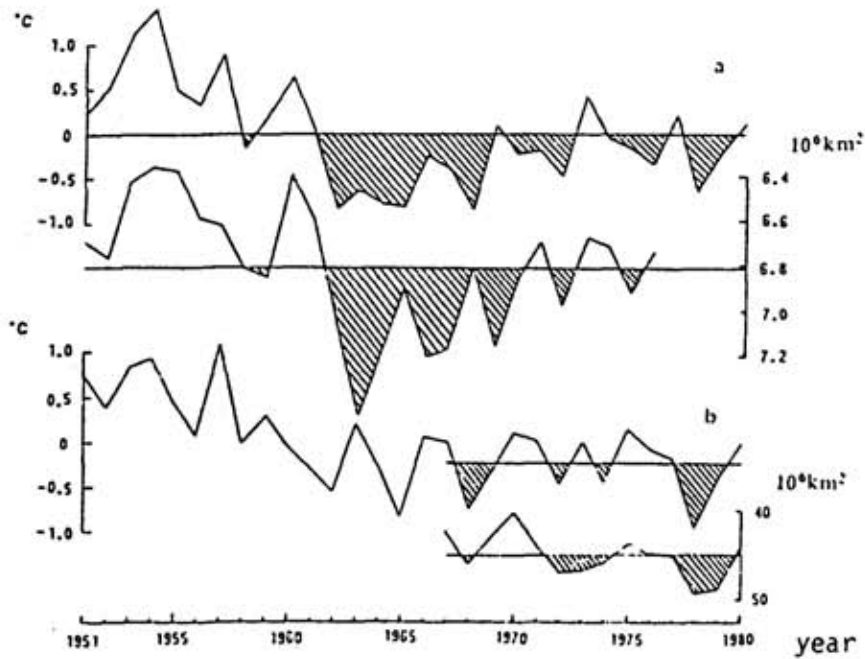


Fig. 2. Curves of Arctic ice (a), snow cover (b) in the Northern Hemisphere and air temperature in summer.

Cross lag correlation coefficients between areas of Arctic ice in July and August and zonal mean air temperature along each latitude (10°N - 90°N) in the lower parts of the troposphere (1000 mb-700 mb) from November to December of the following year for 1951-1976 were computed (figure 3). There are significant negative correlations between Arctic ice and air temperature in the higher latitudes at the same season and prior seasons. In other words, the negative correlations continue from winter, spring, to summer. Fig. 2a shows curves of areas of Arctic ice in July and August and averaged air temperature at 70°N between May and August. It is interesting to note that the trend of temperature change varies with Arctic ice. When there is more Arctic ice, there is lower temperature and vice versa.

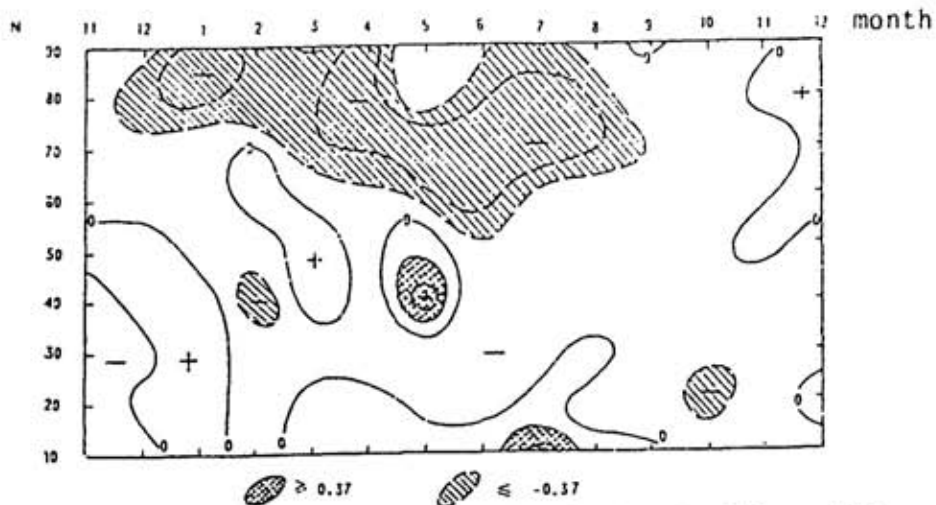


Fig. 3. Cross lag correlations between Arctic ice in July and August and zonal averaged air temperature along each latitude from the prior November to December.

Relationships between snow cover and general circulation at 500 mb in East Asia.

Major synoptic systems that influence rainfall and temperature in China are the intensity and position of the subtropical high in the western Pacific, of the trough in East Asia, intensity of the trough in India and Burma, height of Tibet Plateau and the zonal circulation index in East Asia at 500 mb. They are called "circulation characteristic values in East Asia". Relationships between snow cover in Eurasia and North American in winter (Dec.-Feb.) and the circulation characteristic values in East Asia at the same season and the following seasons were examined. It was found that there are obvious relations between snow cover in Eurasia in winter and several circulation characteristic values in East Asia in the following seasons. Several examples are shown in figure 4. It is interesting to note from figure 4 that when there is more snow cover in Eurasia in winter, there is weaker intensity of the trough in East Asia in March, and there is weaker zonal circulation (and stronger meridional circulation) in East Asia in April and the southern extreme of the subtropical high ridgeline in the western Pacific in July.

Relationships between snow cover and precipitation and temperature in China.

Relationships between snow cover in Eurasia and North America in winter and the major weather phenomena in China at the same season and the following seasons, such as droughts and floods, Bai-u, cold damage, typhoon, and so on, were analyzed. Several obvious relationships are shown in figure 5. When there is more snow cover in Eurasia in winter, there is dry weather in the North of China in spring and in the Yangtze River valley of China in summer.

Conclusion

1. There are obvious negative correlations between snow cover in the Northern Hemisphere in winter and temperature in the following summer.
2. Temperature in the higher latitudes from the prior winter to summer relates to the Arctic air in summer.
3. There are significant relationships between snow cover in Eurasia in winter and several characteristic values of circulation at 500 mb in East Asia in the following spring and summer.
4. There are obvious relationships between snow cover in Eurasia in winter and droughts and floods in China in the following spring and summer.

Due to the limited data on snow cover, these relationships will be further examined in the future.

Acknowledgements

The authors wish to acknowledge the excellent working conditions and computer time given by the Climatic Research Institute, Oregon State University. We would like to thank Mr. William McKie for improving the English in this paper, and Ms. Naomi Zielinski for typing the manuscript.

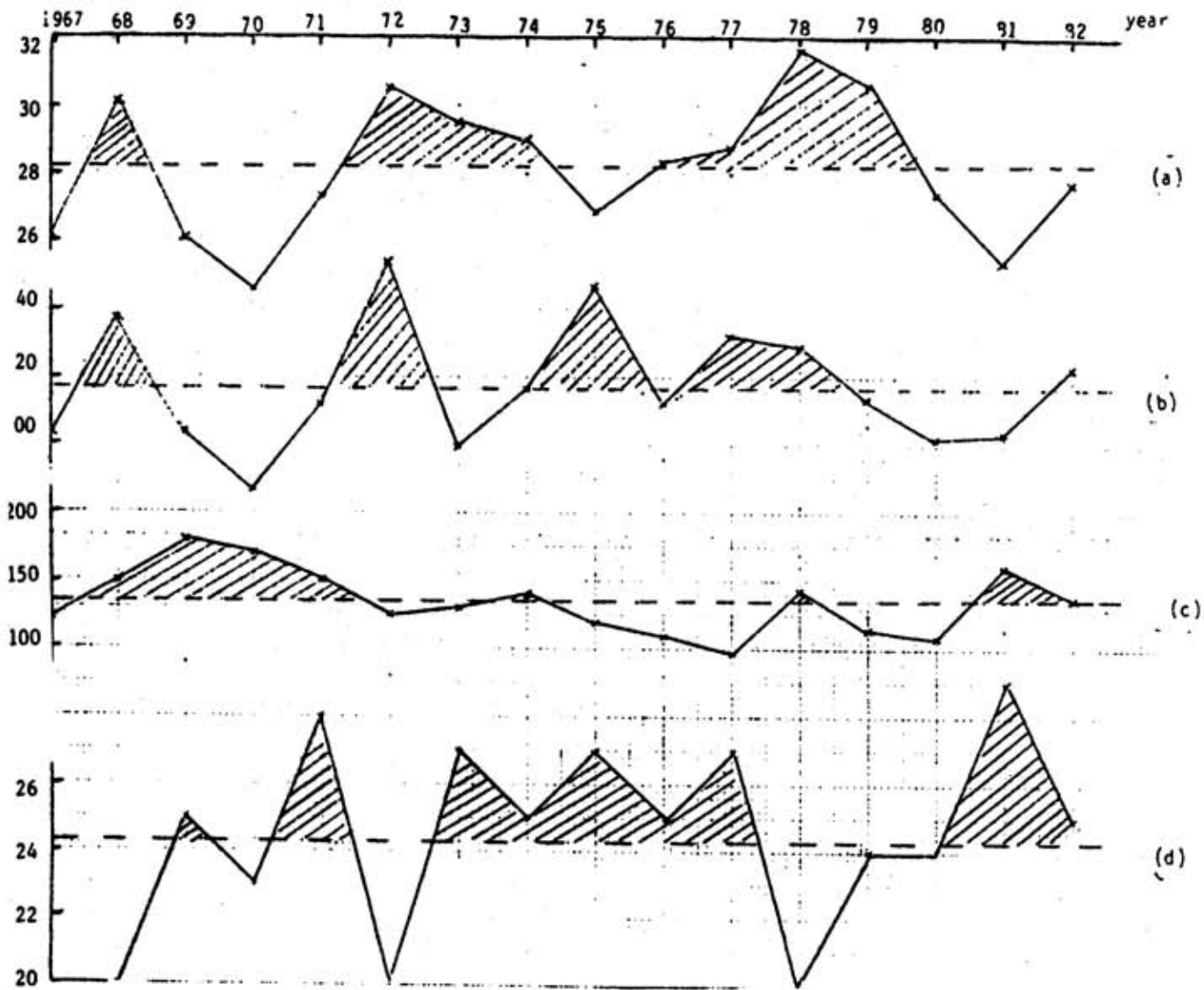


Fig. 4. Curves of snow cover in Eurasia in winter (unit: million sq. km) (a), intensity of the trough in East Asia in March (unit: 10^4 geopotential meter), zonal circulation index in East Asia in April (c) and the position of the subtropic high ridgeline in the western Pacific in July (unit: latitude) (d).

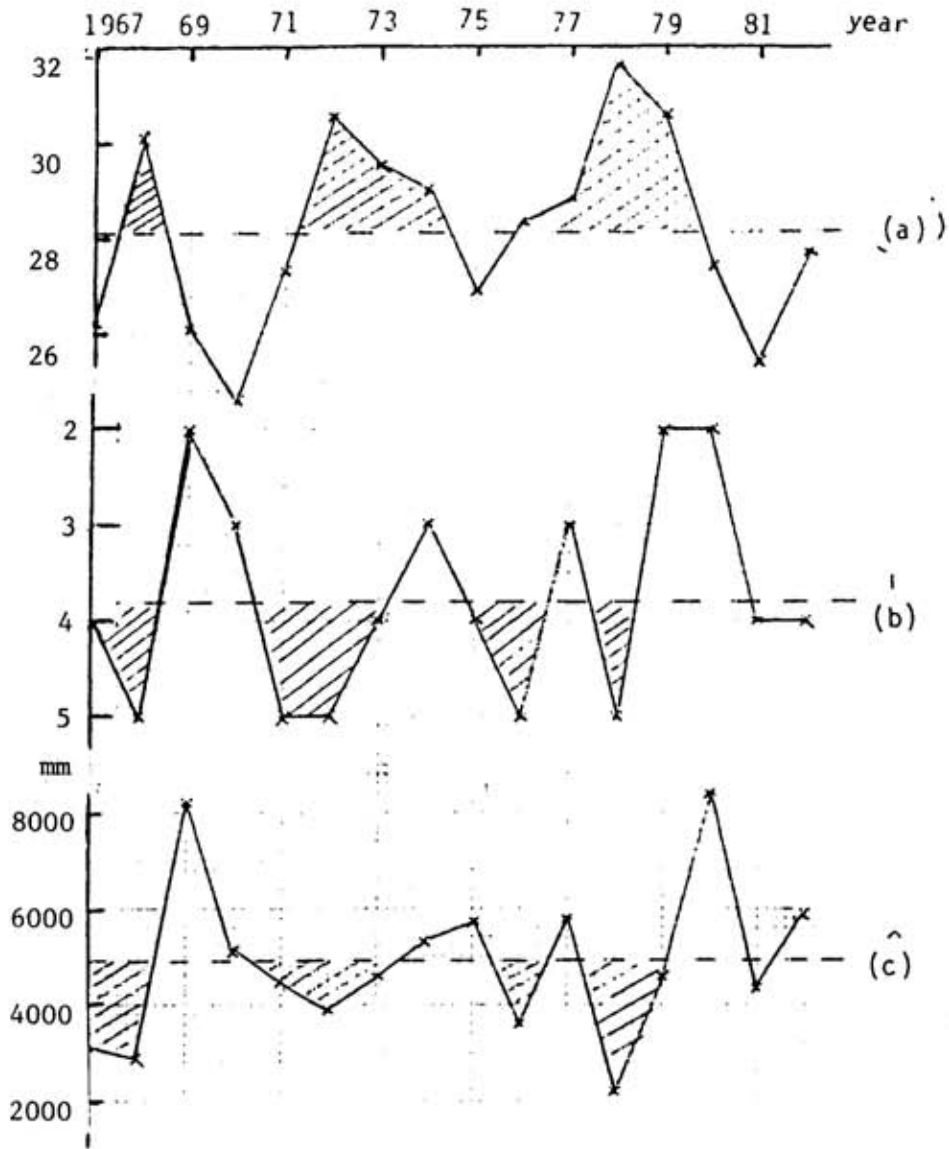


Fig. 5. Curves of (a) Eurasian seasonal averages of snow cover, Dec.-Feb. (unit: million sq. km)
 (b) Grades of rainfall in the North of China in spring (Mar.-May)
 (c) Precipitation in the Yangtze River of China in summer (Jun.-Aug.) (unit: mm).

References

- Kukla, G.; Gavin, J. (1979) Snow and sea ice in 1978-1979. Fourth Annual Climate Diagnostics Workshop. Proceedings.
- Kukla, G.; Gavin, J.; Varnadore, M.; Ropelewski, C. (1982) Snow and variations of 1981-82. Seventh Annual Climate Diagnostics Workshop. Proceedings.
- Matson, M.; Varnadore, M.S. (1981) The winter snow cover drought of 1980-81. Sixth Annual Climate Diagnostics Workshop, New York, October 14-16, 1982. Proceedings.
- Wang, S.; Zhao, Z. (1981) Droughts and Floods in China, 1470-1979, Climate and History. Cambridge University Press.
- Wang, S.; Zhao, Z. (1984) Investigation of temperature change in the lower parts of troposphere in the Northern Hemisphere. Acta Meteorologica Sinica, 42, p.283-245.
- Wiesnet, D.R.; Matson, M. (1979) The satellite-derived northern hemisphere snow cover record for the winter 1977-78. Monthly Weather Review, v.107, p.928-933.
- Zakalof, B.F.; Stlokuna, L.A. (1978) Changes in sea ice in Arctic Ocean. Meteorology and Hydrology, 7.
- Zhao, Z.; Wang, S. (1984) Spring Droughts in Huabei of China and its Development, Weather in North China. Peking University Press, 5.

Kukla, G; Barry, R.G.; Hecht, A.; Wiesnet, D. eds. (1986) SNOW WATCH '85. Proceedings of the Workshop held 28-30 October 1985 at the University of Maryland, College Park, MD. Boulder, Colorado, World Data Center A for Glaciology (Snow and Ice), Glaciological Data, Report GD-18, p.63-72.

Progression of Regional Snow Melt

David A. Robinson
Lamont-Doherty Geological Observatory
Columbia University
Palisades, New York, U.S.A.

Abstract:

Snow melt may be accurately monitored by observing time-related variations of surface albedo. When snow is present, regional surface albedo is primarily a function of 1) the physical properties of snow, 2) the fraction of the snow covered surface which is unobstructed and 3) the amount of exposed snowfree ground. The second is a function of the height and density of vegetation or other objects protruding through the pack. The most accurate means of obtaining data on regional to continental scales is through the analysis of shortwave satellite imagery in an interactive manner on an image processor by an observer familiar with the studied area.

Introduction:

As snow dissipates its strong insulating and atmospheric drying capacities diminish. Its capacity to cool the atmosphere, which stems from its high emissivity and high albedo, also decreases. This is primarily a result of changes in the physical properties of snow, including snow depth, increases in snow grain size, wetness and contaminants, and changes in the amount of exposed snowfree ground.

Presently, the most accurate means of monitoring the state of a regional snow cover is by observing its surface albedo in shortwave satellite imagery. The utility of ground station data in monitoring melt is limited because of

drifting, topography, local variations in initial snow depth and heat island effects.

Shortwave image analysis is not without its problems. Clouds may obscure the surface, particularly in the transitional zone between fully snow-covered and snowfree terrain. Albedo can not be directly measured from satellites when skies are clear, due to atmospheric attenuation of solar radiation reaching the surface and reflected from it, and due to the narrow-band bi-directional nature of the sensors. For these reasons, it is necessary to have ground-truth knowledge of different regions under a variety of snow-cover conditions. Here we present albedo data gathered on the ground and from aerial and satellite platforms to exemplify their utility in monitoring the progression of melt and, also, to show how the albedo of different surfaces varies with changing snow conditions.

Ground truth:

Measurements of broadband hemispheric albedo (0.28-2.80 microns) were made following a snowstorm in order to document melt conditions over surfaces representative of broad regions of the middle latitudes. The study was undertaken in southeastern New York and northern New Jersey following the major East Coast storm of February 11-12, 1983. Albedo was monitored on the ground and from a low-flying aircraft as a 50 cm deep snowpack dissipated. Data were collected during a three week period where daily high temperatures were above freezing and no significant rain or snow fell until March 2.

Ground measurements of the snowpack were made at midday over a short grassy field. Albedo of the pack fell by 0.29, from 0.83 to 0.54, between the 13th and 25th (fig. 1). While the snow was slushy on the 25th, and some portion of the reflected signal was from the underlying grass, no grass blades had yet protruded through the pack. Thus, significant changes in regional albedo occurred when snow continued to cover 100% of the surface. However, it was observed that over all but extremely level and smooth surfaces some bare ground began to be exposed prior to the albedo of most of the snowpack falling below 0.70 (Feb. 21).

Time series of albedo were constructed over key middle latitude surfaces as the snow dissipated (fig. 2). Data were gathered from wingtip-mounted pyranometers flown at an altitude of approximately 200m.

Forests (lines B & C) masked much of the snow, thus initial albedo values were low. They diminished in a quasi-linear fashion as the snow dissipated. Shrubland (F) albedo initially dropped rapidly, in response to snowpack settling and snow falling off of branches, and later slowed. The opposite pattern was observed over open fields and meadows (A,D,E) where albedos initially were as much as eight times their snowfree values. Initial decreases in albedo paralleled the snowpack values. Later, as bare ground became exposed, the melt accelerated and albedo decreased more rapidly. Over residential sites (H) and particularly over industrial locations (G), albedo decreased and snow disappeared more rapidly than over natural terrain.

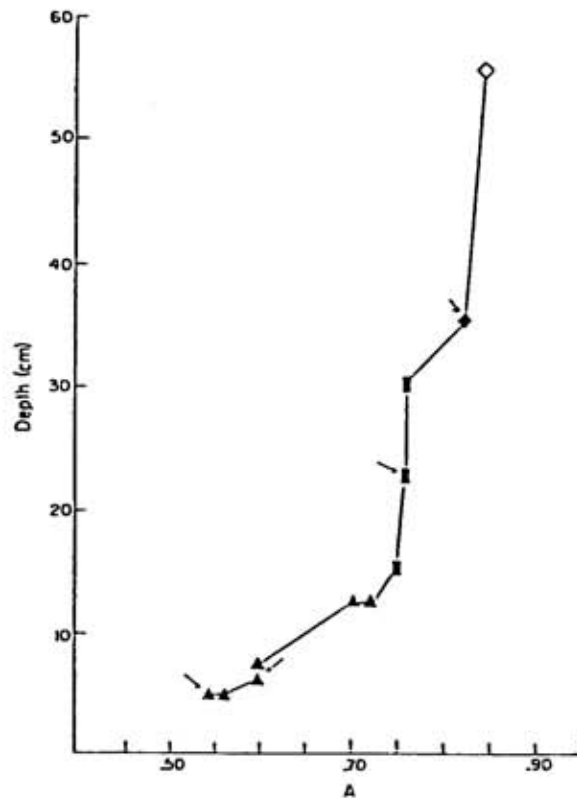


Figure 1. Midday albedo of a complete snowpack over a short grassy field at the Lamont Observatory (41°N) from Feb. 13-25, 1983. Albedo is shown with a diamond for 1-3 day old snow (open diamond: dry, Feb. 13 and 14), squares 4-6 days old, triangles 7 days or more old. Solid symbols indicate a wet snowpack. Datum for Feb. 20 is missing. Arrows point to cases where global atmospheric transmissivity was below 40%. (after Robinson, 1984)

The ground truth study also exemplified the difficulties in using station snow depth data alone, even a dense network, when monitoring regional snow dissipation. Albedos from 26 sites along the flight path on a day with 13 cm deep 3 day old snow (Feb. 10, 1983) were approximately 20% greater than the identical sites on a day with 13 cm deep 9 day old snow (Feb. 22, 1983) (fig. 3). Snow depth was averaged from a network of stations with a density of approximately 1 per 100km^2 . Skies were clear on both dates. The albedo of the snowpack was 0.78 on the 10th and 0.60 on the 22nd. Only the industrial site (cf. Figure 2 G), where snow of any depth remained for only a short time, does not fit the relationship.

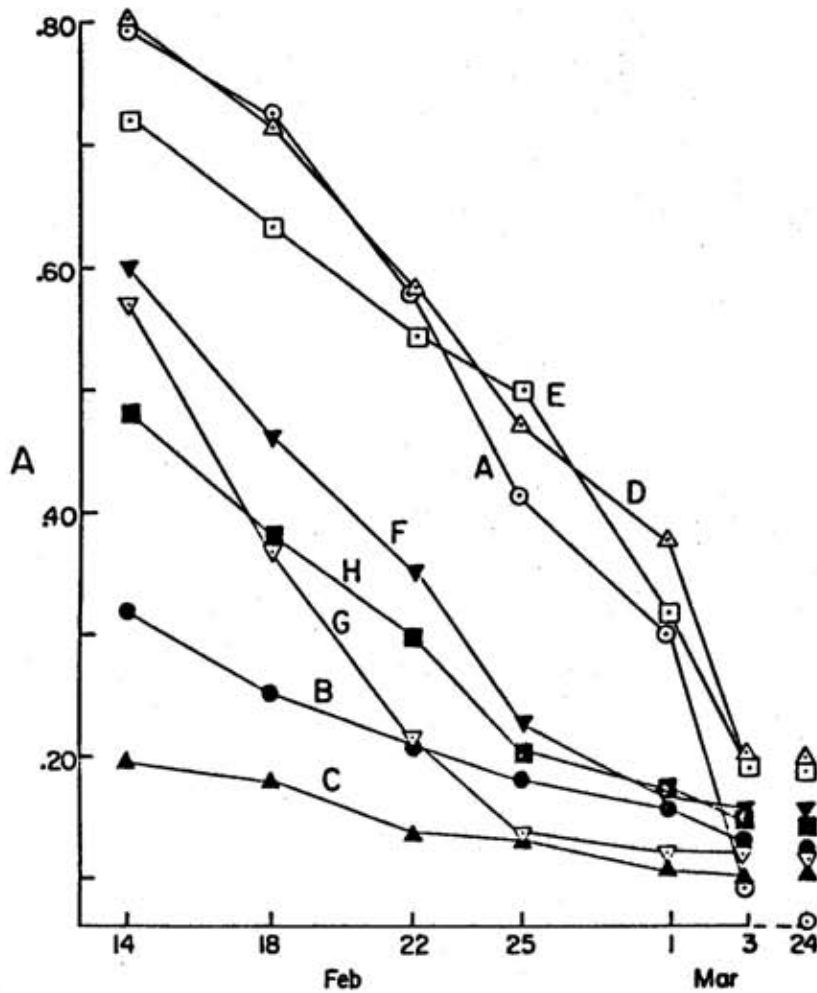


Figure 2. Albedo (A) of major surface elements in southeastern New York and northern New Jersey under winterlike snowfree (March 24, 1983) and a variety of snow-cover (Feb. 14-March 3, 1983) conditions. The lettered curves indicate locations which include: (A) dark soiled farmland, (B) deciduous forest, (C) mixed coniferous forest, (D) cultivated field, (E) grassy meadow, (F) shrubby grassland, (G) industrial and (H) residential. (from Robinson and Kukla, 1984)

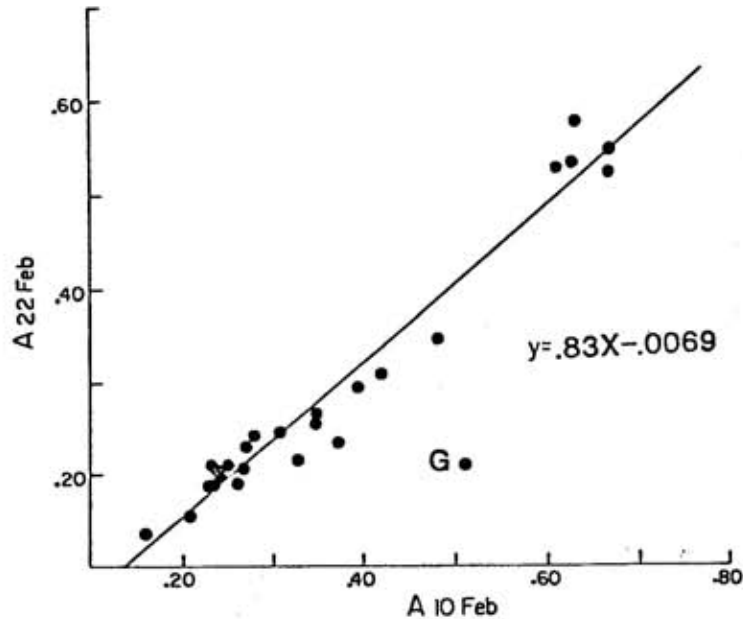


Figure 3. Snow depth-age-albedo relationships. The albedo of a site on Feb. 10, 1983 is plotted against the albedo of the identical site on Feb. 22, 1983. Both days had clear skies and identical snow depths at forest and field test sites. Snow on the 10th was 3 days old and dry with an albedo of 0.78. Snow on the 22nd was 10 days old and wet with an albedo of 0.60. The regression equation has a correlation of 0.96. It does not include point G which is an industrial site (cf. fig. 2, location G). (from Robinson and Kukla, 1984)

Satellite observations:

To permit an assessment of regional snow melt from satellite imagery it is first necessary to know the maximum regional albedo that may be expected under deep fresh snow-cover conditions. This has been done in $1^{\circ} \times 1^{\circ}$ latitude/longitude cells over Northern Hemisphere seasonally snow covered lands (fig. 4) (Robinson and Kukla, 1985). Data were obtained by image processor analyses of clear-sky Defense Meteorological Satellite Program (DMSP) imagery. Scene brightness was converted to surface albedo by linear interpolation between bright and dark snow-covered surfaces with known albedo.

A broad zonal distribution of forests masks the underlying snowpack in Eurasia and North America. For instance, in Eurasia the areally averaged albedo is 0.36 over the boreal forest zone between 60° and 65° N. It rises to 0.76 over the short grassy tundra further north.

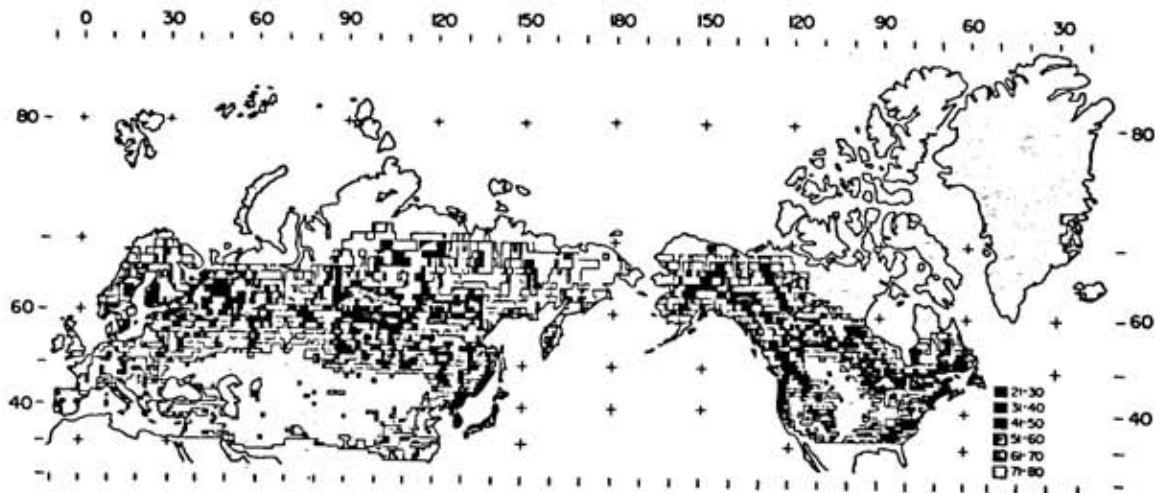


Figure 4. Maximum surface albedo of Northern Hemisphere land with the potential of developing seasonal snow cover. Cells, measuring $1^{\circ} \times 1^{\circ}$, are marked in 0.10 increments. Comparisons with Figure 5a may be made in south central Asia. (from Robinson and Kukla, 1985)

The ground truth study exemplified the fact that regional albedo with snow present is frequently below its potential maximum. This is particularly so where the climate is dry and snow cover shallow (eg. south central Asia) or in the snow transition zone. In figure 5a the fully snow-covered steppe (points 1-3) is considerably brighter than the forested hills to the northwest (point 4), where the snow cover is masked by the forest canopy. In Figure 5b the snow cover has melted over portions of the steppe and bare ground is exposed (points 1 and 2). The dark pattern of roads and rails radiating from cities (point 3) is more pronounced in b.

Thus, many of the same characteristics of snow-covered and partly snow-covered lands observed on and near the ground are recognized on clear-sky shortwave satellite images. Analysis of this imagery in an interactive manner on an image processor by an observer familiar with the studied area is quite useful in identifying and quantifying this information. Figure 6 shows brightness histograms measured from NOAA Very High Resolution Radiometer (VHRR) images over an approximately $100,000 \text{ km}^2$ portion of central U.S. farmland. Histogram 1 shows the area a year earlier, when it was covered with over 15cm of fresh snow. There is a single peak at a high brightness value.

The February 1, 1977 histogram (2) quantifies the distribution of snow over the region when an originally complete snow cover was 7 days old. Some bare ground had begun to appear, giving the histogram a slightly bimodal character. Compared to histogram 1, the bright peak is shifted towards the

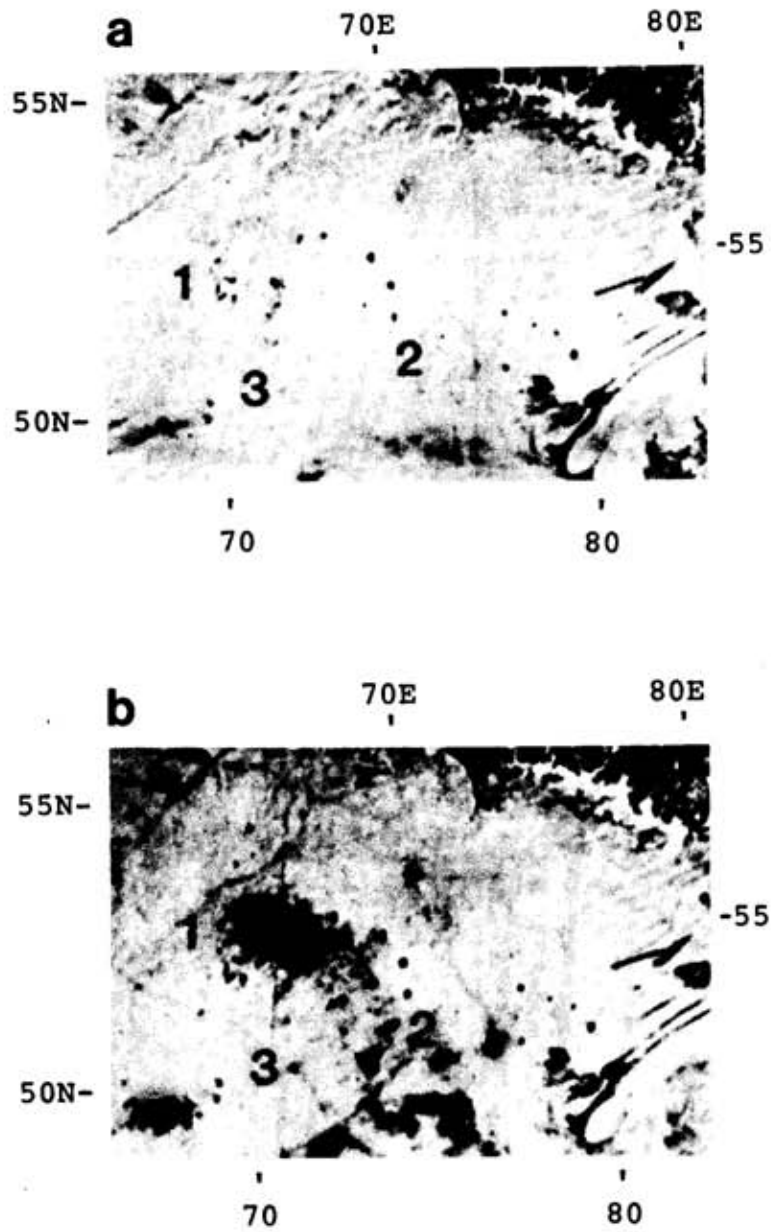


Figure 5. A portion of a DMSP image covering south-central Asia on (a) Feb. 19, 1979 and (b) March 23, 1979, showing a decrease of surface albedo due to progressing snow melt. (after Robinson and Kukla, 1985)

dark end, probably due to a combination of decreasing snow albedo and subresolution patches of bare ground. Some 80% of the stations in the region reported snow cover on the 1st. At these stations the average depth was 10 cm. In subsequent days (histograms 3-5), the amount of snowfree ground began to exceed that of snow-covered ground. By the 10th the single dark peak on the histogram (5) indicates that most surfaces were snowfree, however, some subresolution snow patches were present, which broadens the peak and skews it towards the right. On this date, 50% of the stations reported snow cover, with the depth averaging 4 cm.

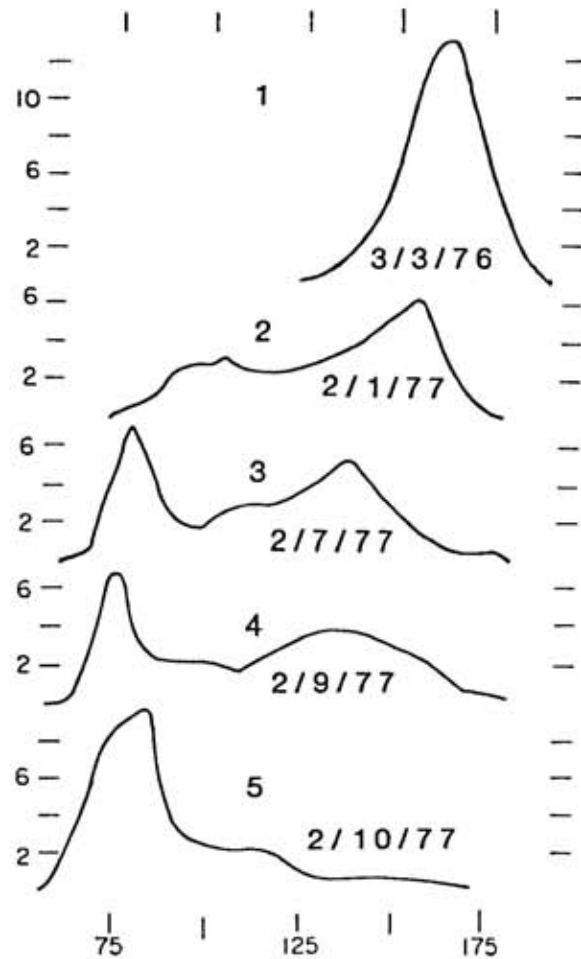


Figure 6. Brightness histograms with different snow-cover conditions over central U.S. farmland. Vertical axis shows the number of processor pixels ($\times 10^3$) with a particular brightness (horizontal axis). (after Robinson and Kukla, 1982)

Further evidence of the utility of satellite-derived time series in monitoring regional snow melt is shown in figure 7. Brightness histogram statistics from clear-sky Advanced VHRR imagery over tundra and forest in Alaska are plotted for the springs of 1981 and 1980, respectively. Mean brightness is expressed as surface albedo. Each region is approximately 50,000 km².

In both regions, decreases in brightness as snow melted were found to be accompanied by simultaneous shifts in other histogram statistics. For instance, standard deviation decreased and kurtosis and skewness rose as snow disappeared in forested areas. These shifts indicate that the open fields, lakes, rivers, etc. in this region were no longer brightly snow covered. Once both the woodlands and the openings were snowfree, skewness fell to zero. In the tundra, standard deviation rose, kurtosis fell and skewness became negative once snowfree areas began to appear. Once dark snowfree areas predominated, skewness became positive, standard deviation decreased and kurtosis increased. When snowfree conditions were reached (around June 15), relatively bright ice-covered water bodies resulted in skewness remaining positive and the standard deviation staying high.

Snow dissipation can be successfully monitored by only observing changes in skewness, kurtosis and standard deviation. This is useful in cases where image quality or thin homogeneous clouds permit the surface to be seen but prohibit accurate albedo estimates.

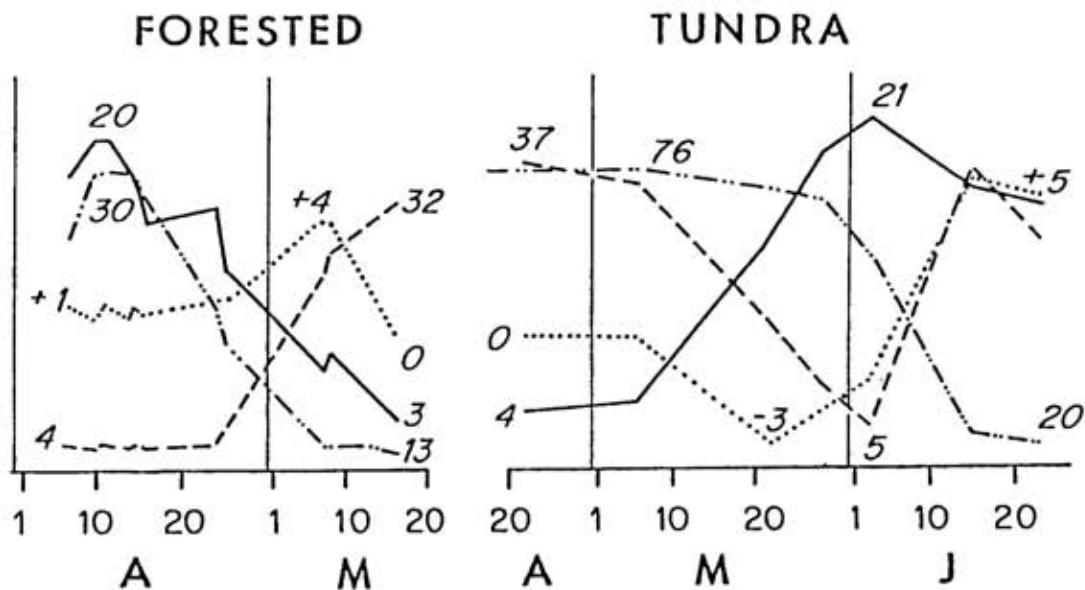


Figure 7. Response of brightness histogram standard deviation (-----), skewness (.....), kurtosis (---) and surface albedo (-.-.-) to snow melt in forest and tundra areas of Alaska in the springs of 1981 and 1980, respectively. Horizontal scale shows dates between April 1 and June 23. (from Robinson and Kukla, 1982)

Conclusions:

Accurate representation of snow cover and its impact on surface albedo is important for the realistic performance of climate models used to project climate perturbations due to increasing levels of CO₂. Continued monitoring of snow melt is needed, as model results to date indicate that the initial signs of a CO₂ climate impact may be recognized in the marginal cryosphere. Shortwave satellite imagery is the most accurate means of obtaining this data on regional to continental scales, particularly if it is analysed in an interactive manner on an image processor by an observer familiar with the studied area.

References:

- Robinson, D.A. (1984) Anthropogenic Impact On Winter Surface Albedo. Doctoral thesis, Columbia Universtiy, 384pp.
- Robinson, D.A.; Kukla, G. (1982) Remotely sensed characteristics of snow covered lands. in: (Keydel, W., ed.) 1982 IEEE International Geoscience and Remote Sensing Symposium Digest, WA-1, 2.1-2.9.
- Robinson, D.A.; Kukla, G. (1984) Albedo of a dissipating snow cover. Journal of Climate and Applied Meteorology, 23, 1626-1634.
- Robinson, D.A.; Kukla, G. (1985) Maximum surface albedo of seasonally snow-covered lands in the Northern Hemisphere. Journal of Climate and Applied Meteorology, 24, 402-411.

Kukla, G; Barry, R.G.; Hecht, A.; Wiesnet, D. eds. (1986) SNOW WATCH '85. Proceedings of the Workshop held 28-30 October 1985 at the University of Maryland, College Park, MD. Boulder, Colorado, World Data Center A for Glaciology (Snow and Ice), Glaciological Data, Report GD-18, p.73-77.

Soot from Arctic Haze: Radiative Effects on the Arctic Snowpack

Stephen G. Warren
Department of Atmospheric Sciences
University of Washington
Seattle, Washington, U.S.A.

Antony D. Clarke
Hawaii Institute of Geophysics
University of Hawaii
Honolulu, Hawaii, U.S.A.

The burning of fossil fuels adds not only CO₂ to the atmosphere but also particulates which are the products of incomplete combustion. The small soot particles, which seem to be largely responsible for the absorption of solar radiation in the Arctic haze, are eventually scavenged from the atmosphere and are incorporated in the Arctic snowpack. Here we examine the possible effects of these particulates on the snow albedo and the surface radiation budget, using a model for radiative transfer in snow.

The model (Wiscombe and Warren, 1980) was developed to explain the reasons for the large observed variability of snow albedo. It showed good agreement with available spectral measurements. The principal factor controlling snow albedo is the grain size (Figure 1a of Marshall and Warren, these proceedings), which normally increases with snow age due to metamorphism.

Small amounts of absorptive impurities in snow can reduce the albedo dramatically in spectral regions where the albedo is high (visible wavelengths). Warren and Wiscombe (1980) computed the radiative effects of graphitic carbon ('soot') distributed uniformly through a snowpack (shown in Figure 1d of Marshall and Warren, these proceedings). Subsequent experiments which measured both albedo and soot content (Grenfell et al, 1981) showed agreement with results of the radiation model to within the experimental uncertainty, which was about a factor of 2 in soot content (Sec. H1 of Warren, 1982).

Clarke and Noone (1985) collected snow samples from several locations in the Arctic (but none in the Siberian sector), shown here in Figure 1. They applied an optical method to the filter through which meltwater from these samples had been passed, to determine the concentration of soot in the snow. The mass fraction of soot ranged from about 5×10^{-9} to 5×10^{-8} (shaded area in Figure 2). Warren and Wiscombe (1985) then estimated the effect on snow albedo due to these soot concentrations. For the energy

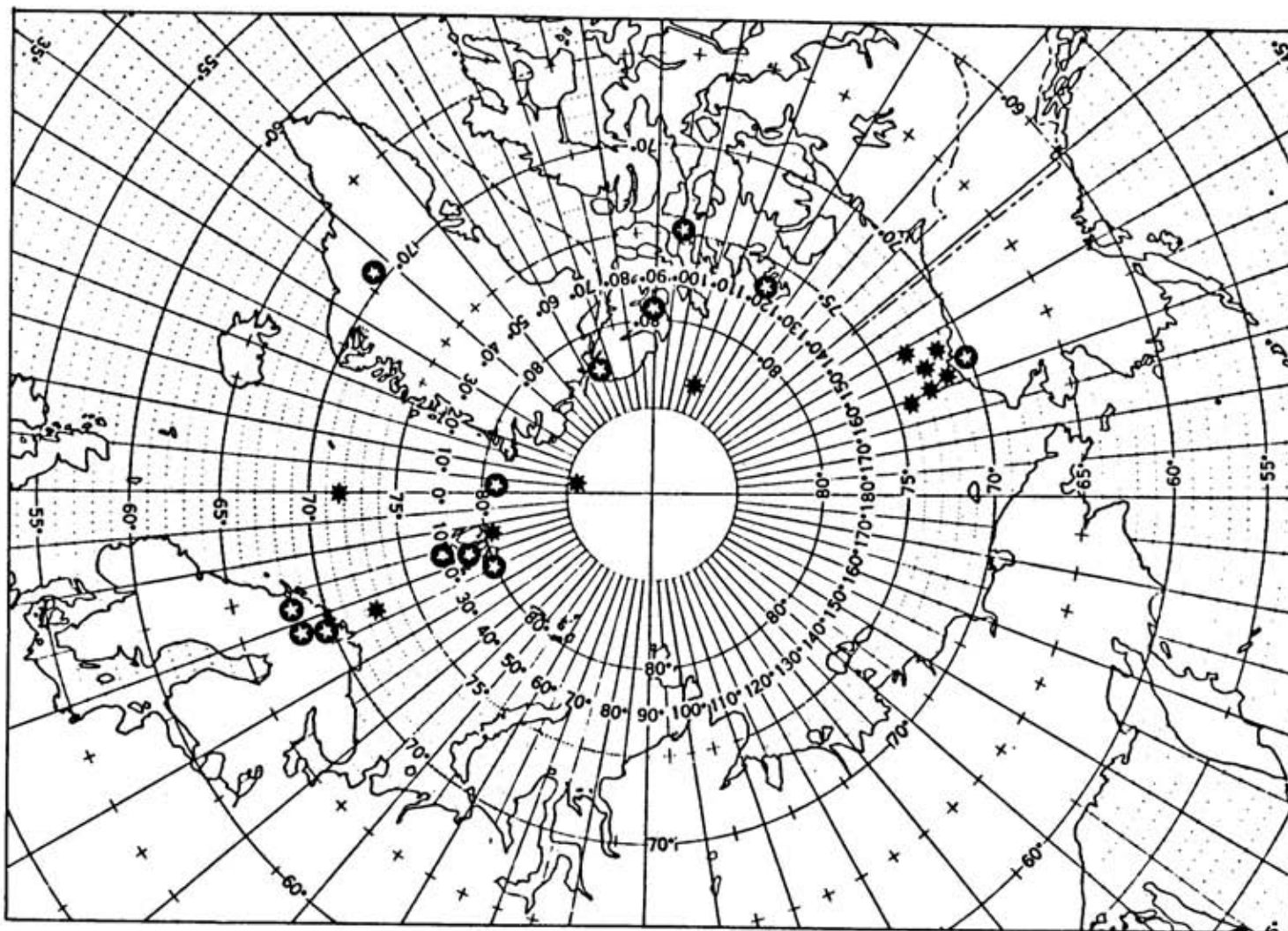


Figure 1. Map of Arctic sampling locations for the University of Washington atmospheric (★) aircraft samples and snowpack (●★) samples for 1983 - 1984. (Figure 1 of Clarke and Noone, 1985).

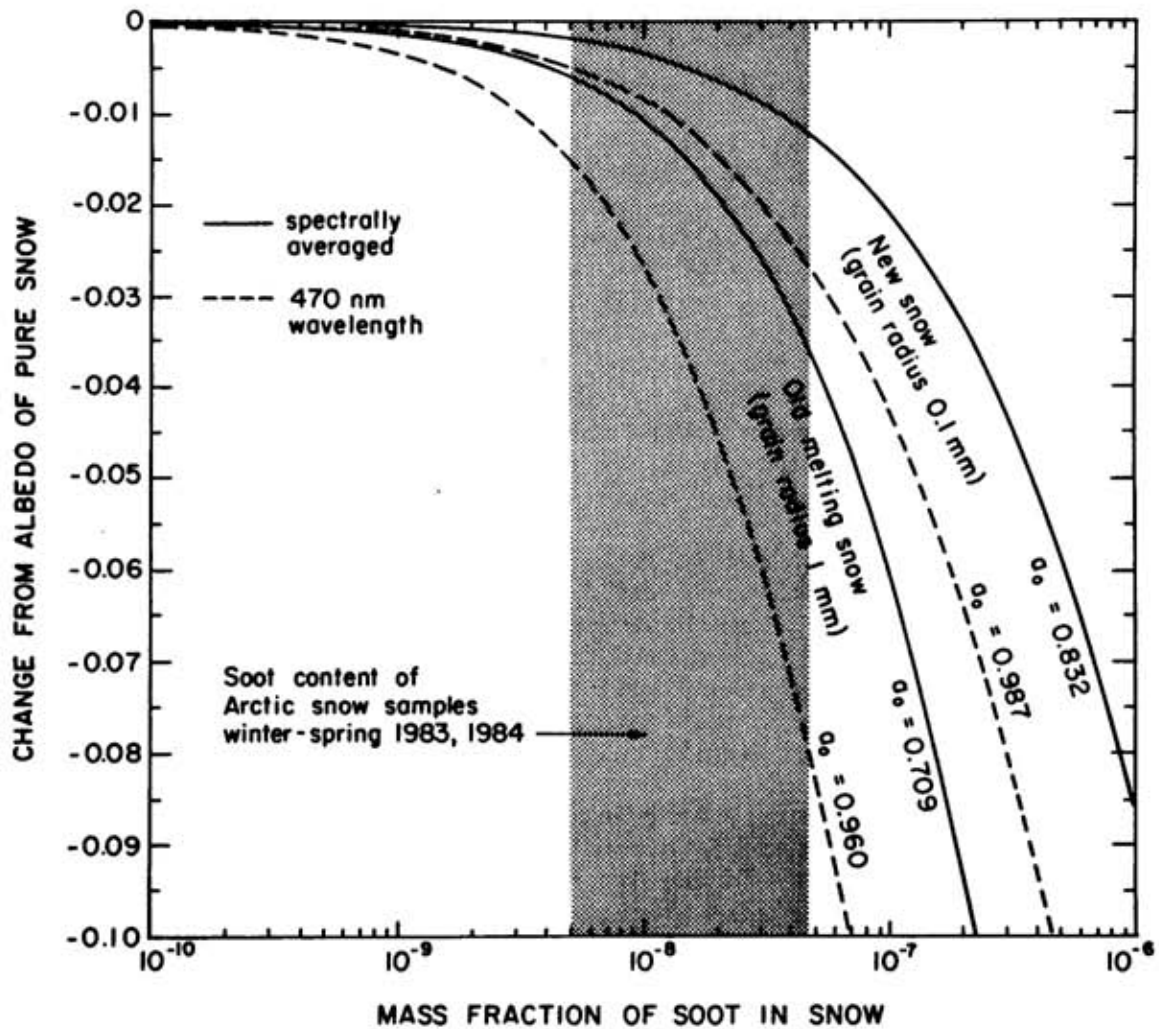


Figure 2. Computed effects on snow albedo due to small mass fractions of soot. Plotted is the change from the albedo values of pure snow, a_0 . The spectrally-averaged changes are shown as solid lines. The dashed lines are calculations at the wavelength where snow albedo is most sensitive to soot content (470 nm wavelength). The reduction in spectrally-averaged albedo is thus about half as large as the reduction at visible wavelengths. The shaded region indicates the range of soot concentrations determined by Clarke and Noone (1985) in 12 samples of snowfall collected from Arctic Canada, Alaska, Greenland and Svalbard during winter and spring 1983, 1984. To ensure consistency between soot measurement and albedo calculation they have been multiplied here by the factor 0.85 because Clarke and Noone assumed a mass absorption coefficient $k_{abs} = 8.5 \text{ m}^2\text{g}^{-1}$ for ambient soot at 525 nm wavelength, whereas the Mie calculation for the soot parameters used by Warren and Wiscombe (1985) gave $k_{abs} = 10.0 \text{ m}^2\text{g}^{-1}$. [Figure and caption from Warren and Wiscombe (1985).]

budget of the snowpack, it is the spectrally-averaged albedo which is important. The solid lines in Figure 2 show that the reduction in spectrally-averaged albedo is in the range 0 to 0.035.

Clarke and Noone (1985) took 0.02 as a representative albedo reduction from Figure 2 and computed the effect on the radiation budget in the Arctic Ocean during spring and summer, using the solar radiation climatology of Fletcher (1965). The effect on the earth-atmosphere radiation budget is estimated to be $+4.6 \times 10^7 \text{ J m}^{-2}$ for the period 1 February - 15 July for 75°N (sunlight is negligible before February, and snow is mostly gone after mid-July). The positive sign means a net gain by the earth-atmosphere system. This compares to $+8.2 \times 10^7 \text{ J m}^{-2}$ estimated by Cess (1983) for the net effect of Arctic haze in the atmosphere on absorption of solar radiation by the earth-atmosphere system at 75°N . Cess's calculations were for clear sky conditions only. If clouds were included, his estimate would be smaller.

Thus we conclude that Arctic-haze soot in the snowpack should have an effect on the earth-atmosphere radiation budget comparable to that of Arctic haze in the atmosphere. However, the effects we calculated are based on soot concentrations measured in newly-fallen snow. The effect of soot during the melting season will be greater than we calculate if the soot particles tend to concentrate at the surface of melting snow, as do micron-size dust particles (Higuchi and Nagoshi, 1977).

These effects on absorption of solar radiation do not take into account any feedbacks. There is a positive feedback which would make the effect larger, but which would require a climate model to estimate it: The lower snow albedo could cause increased melting rates in summer, and cause the snow to disappear sooner than usual, thus uncovering the lower-albedo sea ice earlier in the season.

References

- Cess, R.D. (1983) Arctic aerosols: model estimates of interactive influences upon the surface-atmosphere clear-sky radiation budget. Atmospheric Environment, v.17(12), p.2555-2564.
- Clarke, A.D.; Noone, K.J. (1985) Soot in the Arctic snowpack: a cause for perturbations in radiative transfer. Atmospheric Environment, v.19, in press.
- Fletcher, J.O. (1965) The Heat Budget of the Arctic Basin and Its Relation to Climate. RAND Report R-444-PR, RAND Corp., Santa Monica, CA.
- Grenfell, T.C.; Perovich, D.K.; Ogren, J.A. (1981) Spectral albedos of an alpine snowpack. Cold Regions Science and Technology, v.4, p.121-127.

- Higuchi, K.; Nagoshi, A. (1977) Effect of particulate matter in surface snow layers on the albedo of perennial snow patches. Isotopes and Impurities in Snow and Ice, IAHS Publ. No. 118, p.95-97.
- Marshall, S.; Warren, S. (1986) Parameterization of snow albedo for climate models. These Proceedings.
- Warren, S.G. (1982) Optical properties of snow. Reviews of Geophysics and Space Physics, v.20(1), p.67-89.
- Warren, S.G.; Wiscombe, W.J. (1980) A model for the spectral albedo of snow, II. Snow containing atmospheric aerosols. Journal of the Atmospheric Sciences, v.37(12), p.2734-2745.
- Warren, S.G.; Wiscombe, W.J. (1985) Dirty snow after nuclear war. Nature, v.313(6002), p.467-470.
- Wiscombe, W.J.; Warren, S.G. (1980) A model for the spectral albedo of snow, I. Pure snow. Journal of the Atmospheric Sciences, v.37 (12), p.2712-2733.

Kukla, G; Barry, R.G.; Hecht, A.; Wiesnet, D. eds. (1986) SNOW WATCH '85. Proceedings of the Workshop held 28-30 October 1985 at the University of Maryland, College Park, MD. Boulder, Colorado, World Data Center A for Glaciology (Snow and Ice), Glaciological Data, Report GD-18, p.79-88.

The Snow Cover Record in Eurasia

James Foster
Hydrological Sciences Branch
National Aeronautics and Space Administration
Goddard Space Flight Center
Greenbelt, Maryland, U.S.A.

Abstract

Eurasia has considerably more of its surface area in northern latitudes than does North America and so its snow cover is more extensive. Trends in the Northern Hemisphere and Eurasia are thus similar. As a result in any study of hemispheric feedback mechanisms involving snow cover, Eurasia has a greater feedback potential than North America. Satellites have been used to map and measure continental snow cover only since the mid-1960's. If snow cover data can be retrieved from pre-satellite climatological records, an historical file representing varying snow cover conditions may be used to get a longer estimate of any trend or cycles which may exist. An attempt was made in this study to lengthen the satellite snow cover record in Eurasia by reviewing past climatological records in Europe and Asia and by examining proxy indices such as Arctic sea ice data. Also, the satellite snow cover record was investigated to determine if there is a correlation between the continental snow cover extent and the number of days of snow cover at several different geographic areas in Eurasia where a winter snow cover does not always occur. Results indicate that while there is a rather weak association between sea ice extent and continental snow cover, an r^2 of .77 exists between the mean number of snow cover days for selected locations in the interior of Eurasia and the continental snow cover extent. It may be possible then to use the mean number of snow cover days at selected sites in Eurasia prior to the advent of satellite monitoring capabilities as an index of the continental snow covered area.

Introduction

The polar caps of Earth expand and contract in accordance with the distance from the sun and the amount of solar radiation received. The dramatic increase in ice and snow cover from one season to another is bound to have a considerable impact on climate (Kukla and Robinson, 1981). Prior to the mid-1960's the monitoring of the areal extent of snow cover was limited to point measurements and extrapolation between these often widely separated points. But since November of 1966, continental and hemispheric snow cover has been monitored on a weekly basis by satellites. Except for the summer months, the proportionately larger variations in Eurasian snow cover dominate

the North American variations so that trends in the Northern Hemisphere and Eurasia in autumn, winter, and spring are very similar. As a result in any study of hemispheric feedback mechanisms involving snow cover, Eurasia has a greater feedback potential than North America (Matson and Wiesnet, 1981). As the satellite snow cover record is extended temporally in years to come it should provide a new understanding of global and regional climate. Additionally, if snow cover data can be retrieved from past records, an historical file representing varying snow cover conditions may be used to get a longer look at any trends or cycles which may exist.

Snow cover data for North America collected since 1948 have been digitized using data from surface stations to extend the satellite record providing over 35 years of snow cover information (Walsh et al., 1982). In this study an effort was made to reconstruct the pre-satellite seasonal variations in Eurasia snow extent by reviewing climatological publications and by examining proxy indices such as Arctic sea ice extent and the number of snow cover days for different geographic locations in Europe and Asia.

Winter Snow Cover Regime

From December until March, Eurasia has more of its land covered by snow than any other surface feature. By early December a stable snow cover is formed in most years over all but the south central and southwestern areas of the Soviet Union. Much of northern and western China and Mongolia is snow covered at this time as are the mountain ranges of the Himalayas. In western Europe, typically only Scandinavia and the highland areas surrounding the Alps and Carpathian Mountains are snow covered during December. Generally the snow covered area reaches its greatest extent in late January or early February when as much as 30 million square kilometers of the continent may be snow covered. Almost all of Eurasia north of 40° and east of the Black Sea is beneath a veneer of snow (Lydolph, 1977). During most years coastal areas of western Europe are snow covered for only a few days at a time, but in some extreme years a snow cover will persist for several weeks even in those countries which are usually thought of as having rather mild winters such as England and France. By March the snow covered area begins its northward retreat.

Methodology

It is known that snow records gathered at stations of the climatological network are often incomplete in time and space. In Asia the network is especially sparse, making delineation of the snowline particularly difficult. But it was hoped that by assembling past records on snowfall and snow cover from locations in Europe and Asia that more information on seasonal variations in snow cover extent prior to the time of satellite observations could be derived.

Climatological data have been examined in Great Britain as well as in Scandinavia and other locations in western Europe. However, these records are of little value without data for the Soviet Union, because of its vast size, when assembling a snow cover data set for the entire continent of Eurasia.

In order to find out more about the pre-satellite snow extent in the Soviet Union, a survey of the literature was performed which identified many papers dealing with various aspects of snow. Most of these papers required translation from Russian to English. For the most part, the papers deal with seasonal dynamics of snow depth, snow density, snow cover distribution, and snow cover conditions including maximum depth and mean dates for its establishment and disappearance (Bigl, 1984), (Bilello, 1984). But articles concerned with seasonal variations in snow cover area or the annual maximum limit of the snow boundary either for the Soviet Union as a whole or for specific locales have not been found and, in fact, may not exist. The Soviet Union's tremendous size and numerous autonomous provinces would likely discourage and perhaps be prohibitive to the compilation of snow cover data on a monthly or even seasonal basis. In addition, throughout most of the Soviet Union a snow cover is an expected occurrence and so its presence is less likely to be noted in the literature than if it were a less frequently occurring phenomenon. Therefore, proxy indices have been examined to see if they can be used in place of actual snow cover data. The proxy data which have been looked at here include Arctic sea ice data and data on the number of snow cover days for selected areas in Eurasia.

Since 1966, NOAA has prepared a weekly snow and ice boundary chart for the Northern Hemisphere. This chart is prepared on a 1:50,000,000 polar-stereographic base map centered on the North Pole. Satellite images from the visible scanning radiometers on board the NOAA polar-orbiting satellites are the main source of information used in making the charts. Secondary input comes from the system of Geostationary Satellites (GOES) which even though transfixed over the equator are capable of observing areas south of about 60°N latitude. With the advent of the Very High Resolution Radiometer aboard the NOAA series' satellites since 1972, more sophisticated snow and ice charts have been produced (Smigielski, 1980).

Problems identified in the production of the charts stem from variability in orbit time, sensor differences on the different satellites, varying experience of the analysts, and lack of information on snow under persistent clouds. Also the scale of the charts limits the precision of snowline positioning to about 20-30 km (Kukla, 1976).

The snow and ice charts show three levels of increasing improvement in consistency and detail (1966-70, 1971-73, 1974-present) with the most recent charts being more reliable (Kukla and Robinson, 1981). Himalayan snow cover was not consistently mapped during the 1966-1974 period. For these reasons in this study only satellite data from 1973 were used to calculate the number of snow cover days.

Sea ice has been routinely monitored from satellites since 1972 (Kniskern, 1979), but records for sea ice extent exist back to the turn of the century (Kelly, 1979). The variable year to year positions of the snow cover and sea ice edge at their winter maxima and summer minima have often been used as indicators of changes in global climate during colder climatic periods (Lamb, 1972), such as the Little Ice Age in the eighteenth century. Ice cover data from 1972 (table 1) was plotted against snow cover for Eurasia for the same time period to determine if a reliable association between these data sets could be found. If so, then perhaps the pre-satellite ice cover data could be used as an indicator of continental snow cover.

In a similar manner the number of days with snow cover, as mapped from satellite images for selected sites in Europe and Asia where a winter snow cover does not always appear, was plotted against the continental winter snow cover area. If a strong correlation exists between these data, then the number of snow cover days might be used to estimate the continental snow cover. This would preclude the need to piece together snow cover data from hundreds of meteorological stations, if such data are available, in order to derive the pre-satellite continental snow cover area. Five different geographic areas (figure 1) were chosen and the number of days with snow lying from December through February were tallied at these sites for the years 1973-1985 (table 1). The five areas are Scotland, the Crimea area north of the Black Sea, the Turan Lowland of south central Soviet Union, the Tarim Basin of northwestern China, and the Korean Peninsula (South Korea). Each of these areas is about 30° in longitude apart in non-mountainous areas, and in areas where a snow cover exists generally for only a portion of the winter season.

The weekly snow and ice charts were used to determine the number of snow cover days at a given site for each week during the winter. This was accomplished by monitoring the position of the snowline relative to one of the selected sites. If a site was south of the continental snowline, then the number of snow cover days for that week was zero, and if the site was north of the snowline, then the number of snow cover days was seven. If the site was at the edge of the snow covered area, then the number of snow cover days was estimated to be four.

Table 1. Ice cover data plotted against snow cover data for Eurasia.

Average Dec-Feb Snow Cover Area for Eurasia (10 ⁶ km ²)	Number of Snow Cover Days for Five Geographic Sites* in Eurasia	Number of Snow Cover Days in the Turan Lowlands	Maximum Arctic Sea Ice Extent (10 ⁵ km ²)	
1973	29.5	116	54	147.9
1974	28.9	110	40	139.1
1975	26.8	79	19	146.7
1976	28.3	146	29	150.0
1977	28.8	121	55	152.0
1978	31.6	252	76	150.7
1979	30.5	164	44	157.0
1980	27.4	81	34	147.8
1981	25.3	65	7	145.2
1982	27.8	134	34	150.7
1983	28.2	105	23	151.3
1984	27.0	127	30	141.8
1985	28.4	191	48	149.6

*Five Geographic Sites are: Scotland
 Crimea area north of the Black Sea
 Turan Lowlands in the South Central USSR
 Tarim Basin in northwestern China
 South Korea

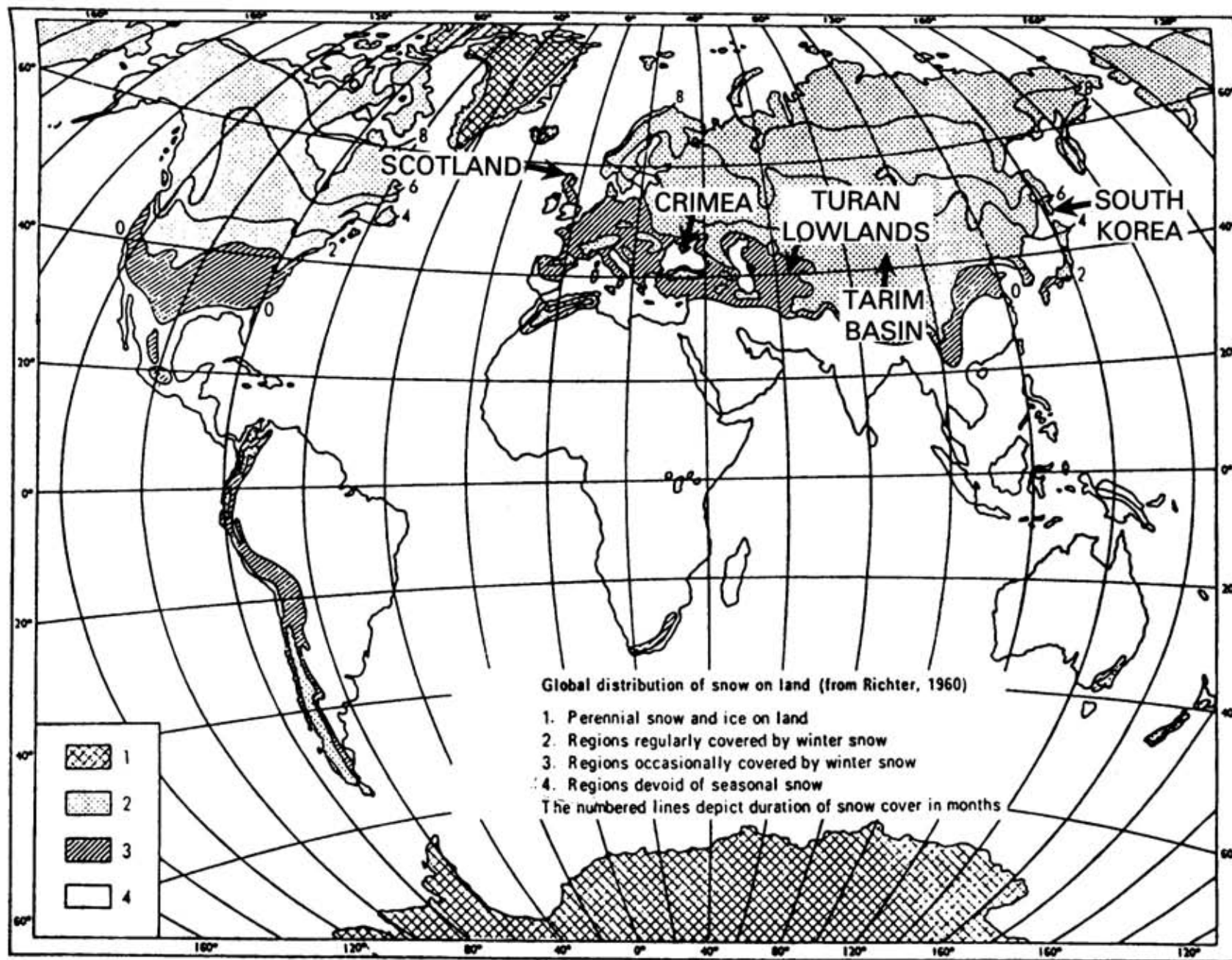


Figure 1. Location of geographic sites where the number of snow cover days was determined from satellite observations.

Results

Table 2 gives coefficient of correlation (r) and coefficient of determination (r^2) values for the data in Table 1 for the years 1973-1985. It seems that the Eurasian snow covered area is well related to the number of snow cover days. The amount of variance in the snow cover area of Eurasia explained by the number of snow cover days at five different geographic sites is fairly high ($r = .78$, $r^2 = .61$) and was found to be significant at the .02 level. For each individual site the amount of variance in the Eurasian snow cover explained by the number of snow cover days at that site ranged from a high of .77 for the Turan Lowland to a low of .01 for the Korean Peninsula. It appears that a simple linear regression using the number of snow cover days for the Turan Lowland as the predictor variable and the continental snow cover area as the criterion variable produces the best results.

Table 2. Coefficient of Correlation (r) and Determination (r^2) for snow cover in Eurasia versus number of snow cover days and Arctic sea ice maximum extent for the years 1973-1985.

		<u>r</u>	<u>r^2</u>
Average Dec-Feb Snow Cover Area in Eurasia	vs. Number of Snow Cover Days in the Turan Lowland	.88 _s	.77
Average Dec-Feb Snow Cover Area in Eurasia	vs. Number of Snow Cover Days for Five Geographic Sites	.78 _s	.61
Average Dec-Feb Snow Cover Area in Eurasia	vs. Arctic Sea Ice Maximum Extent	.47	.22
		<u>Multiple r</u>	<u>Multiple r^2</u>
Average Dec-Feb Snow Cover Area in Eurasia	vs. Number of Snow Cover Days in the Turan Lowland and Arctic Sea Ice Maximum Extent.	.90 _s	.81

s = significant at the 98% level

In relating the Arctic sea ice maximum extent to the Eurasian snow cover, the resulting r^2 value of .22 was considerably less than for the number of snow cover days. Multiple regression approaches using the number of snow cover days and the Arctic sea ice maximum extent provided no marked improvement in the relationship than when using only the number of snow cover days

(table 2). Even though some of the correlations shown in table 2 are statistically significant at a high level, the interpretation of the correlations in terms of cause and effect is by no means obvious. But it should be noted that the data sets include a wide range of values for the 13 year period. The number of snow cover days as used in this study is intended to be a simple indicator of the mean winter snow covered area for Eurasia and is not meant to reflect the snow cover extent at given locations across the continent.

The regression equation shown in figure 2 was used to estimate the Eurasian snow cover for the observed years (1973-1985). The average difference between the observed and the estimated values is about 2.2 percent and as can be seen in figure 3, the predicted values show trends comparable to the observed values. However, the limits of prediction for any given year are likely to be quite wide since so few data points were used. For example, using the data for 1975 shows that when the number of snow cover days for the December-February period is forty, then there is a 95 percent change that the estimated snow covered area for Eurasia will be between 27.1 and 30.7 million km². The observed value is 28.9 million km².

Discussion

Pronounced changes in snow cover and sea ice extent have occurred during the first half of the twentieth century which according to Kelly (1979) and Lamb and Morth (1978) is considered to be without a climatic parallel during the last few hundred years. In order to extend the existing satellite data base, the number of snow cover days at specified sites in Eurasia, where a snow cover does not always occur, was used as an indicator of the continental snow cover. As pointed out by the working group of the 1980 Snow Watch meeting (World Data Center A Glaciology, 1981) there is a need for historical series of snow cover and ice cover charts incorporating data from all available sources.

Determining if an area is actually snow covered and subsequent measurement of snow covered areas have been problems which require a degree of subjectivity not only from remote sensing platforms but from ground-based vantage points as well. Mention has already been given about the problems identified in the production of the snow and ice charts. But difficulty can also arise when trying to decide at what point the ground near a meteorological station is considered to be snow covered. For many stations, the ground is said to be snow covered when half the ground area in the vicinity of the station is observed lying in snow. In some areas, 2.5 cm of snow must cover the ground at 7:00 a.m. local time for a snow covered day to occur (Jackson, 1978). However, there is no standard or convention that has been universally accepted. Perhaps this is because the snow cover is frequently discontinuous. South facing slopes may be snow free, whereas north facing slopes may remain fully covered; drifting may expose bare ground in the lee of some obstacles and pile up snow on the windward side of others; forested areas generally retain snow longer than open areas; and snow lying over dark soil or rocks is likely to melt faster than snow lying over unplowed ground. In some areas snow measuring sites are located in areas not subject to interference by man, but in other areas snow cover determinations may be made at airports. Also the sparse network of reporting stations in much of central and eastern U.S.S.R. and western and northern China requires much interpretation of where to draw the snowline. For these reasons, determining whether or not an area is snow

**EURASIAN SNOW COVER AREA VS
NUMBER OF SNOW COVER DAYS IN
CENTRAL EURASIA (1973-1985)**

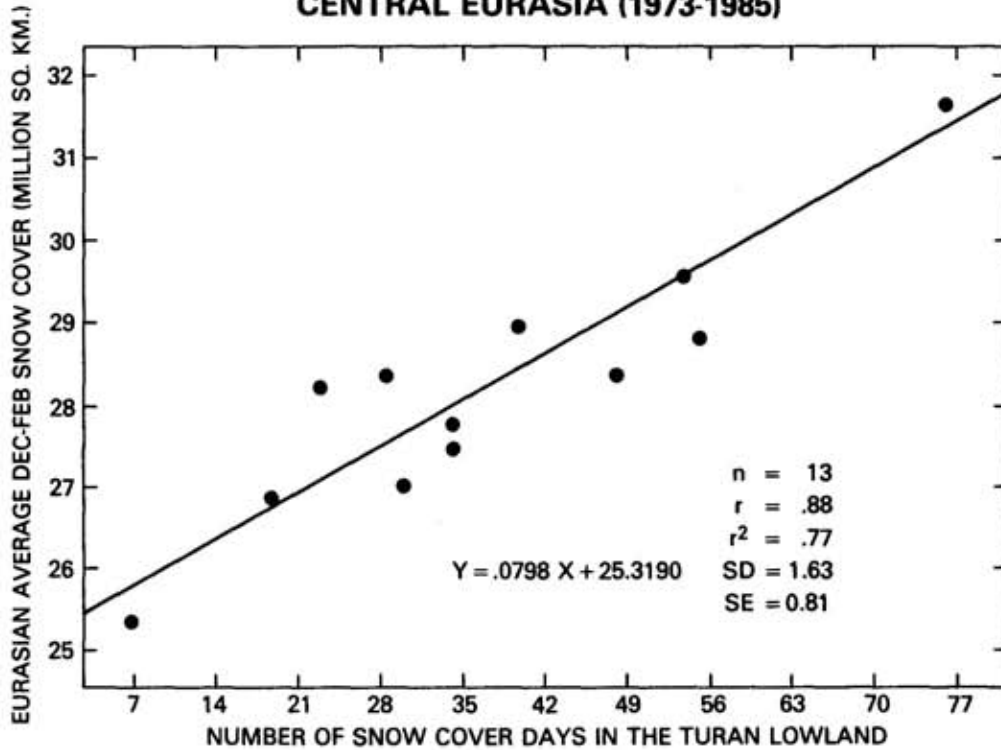


Figure 2. Relationship between number of snow cover days for the Turan lowlands and the Eurasian snow cover extent.

**EURASIAN AVERAGE WINTER SNOW COVER
(DEC.-FEB.)**

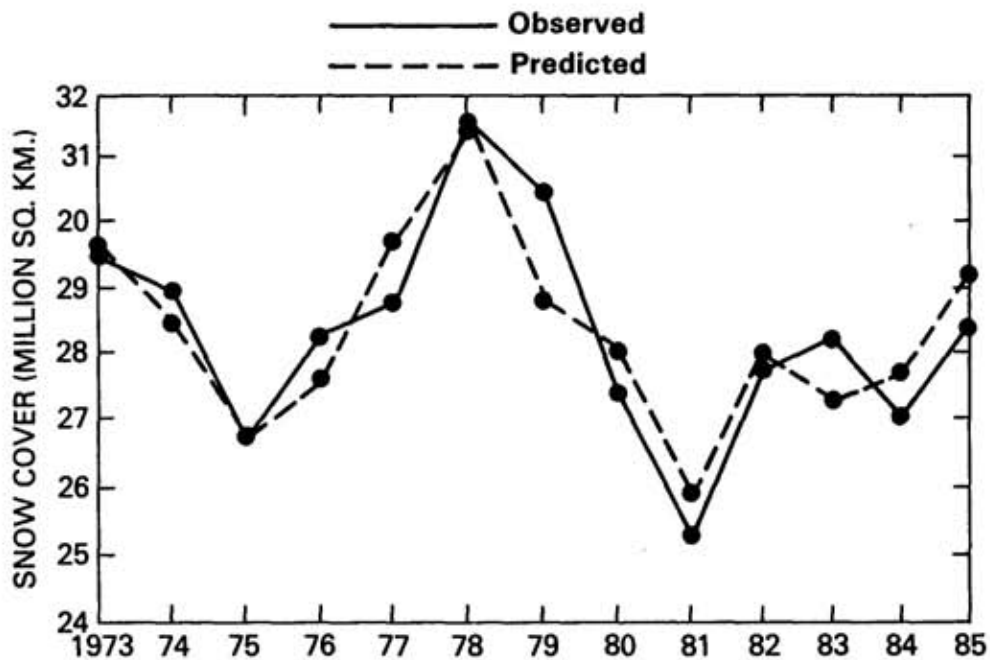


Figure 3. Relationship between the observed and predicted values for Eurasian average winter snow cover.

covered and hence the location of the snowline from ground based climatological records is probably no more accurate than mapping the snow covered area from space.

As demonstrated in this study, past records of the number of snow covered days at specified sites seem to be useful indicators of continental snow cover. The use of such an index requires much less time and resources than is required to reconstruct the snowline from the hundreds of ground-based stations across Eurasia. But it is paramount that data are available for the number of snow cover days in the interior of Eurasia, for the number of snow cover days at interior stations appears to be much more representative of continental snow cover conditions than do data from coastal areas or northern lands. This is reasonable since interior locations have a higher degree of continentality and so are more likely to reflect large scale continental patterns. During the winter months in Eurasia, the Siberian or Asiatic High has become well developed as a result of the extreme surface cooling and the constant feeding of fresh Arctic air into central Asia (Lydolph, 1977). This high in most years is large enough to effectively prevent the incursion of maritime air or air from other source regions into the continental interior.

Summary and Conclusions

The polar caps on Earth wax and wane in response to seasonal changes, and the interannual difference in the size of the polar caps is intimately linked to global energy balance. Before the advent of satellites, it was practically impossible to monitor snow cover on a continental basis. Efforts to reconstruct the pre-satellite snow cover record from data for climatological stations across Eurasia have thus far proved futile. An attempt was made in this study to utilize proxy indices in order to estimate snow cover extent. It was found that the number of snow cover days, as derived from satellite observations for selected sites in areas of the interior of Eurasia where a snow cover does not always occur, are well correlated with continental snow cover. If pre-satellite data on the number of snow cover days for these interior sites are available, then it may be possible to extend the snow cover record and therefore get a longer look at any trends or cycles which may exist. This is important because variations in snow cover extent and duration are being studied as possible indicators of large scale changes in weather patterns. As the snow cover record is extended in future years, it should help in providing a better understanding of global and regional climate.

Bibliography

- Bigl, S.R. (1984) Permafrost, seasonally frozen ground, snow cover and vegetation in the USSR. U.S. Army. Cold Regions Research and Engineering Laboratory. CRREL Special Report, 84-36, 128p.
- Bilello, M.A. (1984) Regional and seasonal variations in snow-cover density in the USSR. U.S. Army. Cold Regions Research and Engineering Laboratory. CREEL Report 84-22, 70p.
- Foster, J.L.; Owe, M.; Rango, A. (1983) Snow cover and temperature relationships in North America and Eurasia. Journal of Climate and Applied Meteorology, v.22(3), p.460-469.

- Jackson, M.C. (1978) Snow cover in Great Britain. Weather, v.33, p.298-308.
- Kelly, P.M. (1979) An Arctic sea ice data set, 1901-1956. World Data Center A for Glaciology [Snow and Ice]. Glaciological Data. Report GD-5, Workshop on Snow Cover and Sea Ice Data, p.101-106.
- Kniskern, F.E. (1979) Ice products derived from satellites at NOAA/NESS. World Data Center A for Glaciology [Snow and Ice]. Glaciological Data. Report GD-5, Workshop on Snow Cover and Sea Ice Data, p.27.
- Kukla, G. (1976) Global variation of snow and ice extent. (In: Symposium on Meteorological Observations from Space: Their Contribution to the First GARP Global Experiment, Proceedings. Boulder. National Center for Atmospheric Research, p.110-115.)
- Kukla, G.; Robinson, D. (1981) Climatic value of operational snow and ice charts. World Data Center A for Glaciology [Snow and Ice]. Glaciological Data. Report GD-11 Snow Watch 1980, p.103-120.
- Kukla, G. (1981) Snow covers and climate. World Data Center A for Glaciology [Snow and Ice]. Glaciological Data. Report GD-5, Workshop on Snow Cover and Sea Ice Data, p.27-40.
- Lamb, H.H. (1972) Climate: Present, Past, and Future. London, Methuen and Co., 613p.
- Lamb, H.H.; Morth, H.T. (1978) Arctic ice, atmospheric circulation, and world climate. Geographical Journal, v.144, p.1-22.
- Lydolph, P.E. (1977) Climates of the Soviet Union. (In: World Survey of Climatology, Vol. 7. Elsevier.
- Matson, M.; Wiesnet, D. (1981) New data base for climate studies. Nature, v.289(5797), p.1-6.
- Smigielski, F. (1980) Northern Hemisphere snow and ice charts of NOAA/NESS. World Data Center A for Glaciology [Snow and Ice]. Glaciological Data. Report GD-11, Snow Watch 1980, p.59-62.
- Walsh, J.E.; Tucek, D.R.; Peterson, M.R. (1982) Seasonal snow cover and short-term climatic fluctuations over the United States. Monthly Weather Review, v.110, p.1474-1485.
- World Data Center A for Glaciology [Snow and Ice] (1981) Snow Watch 1980. Glaciological Data. Report GD-11, p.1-7.

Kukla, G; Barry, R.G.; Hecht, A.; Wiesnet, D. eds. (1986) SNOW WATCH '85. Proceedings of the Workshop held 28-30 October 1985 at the University of Maryland, College Park, MD. Boulder, Colorado, World Data Center A for Glaciology (Snow and Ice), Glaciological Data, Report GD-18, p.89-95.

Distribution of Snow Cover in China

Li Peiji

Lanzhou Institute of Glaciology and Geocryology
Academia Sinica
Lanzhou, China

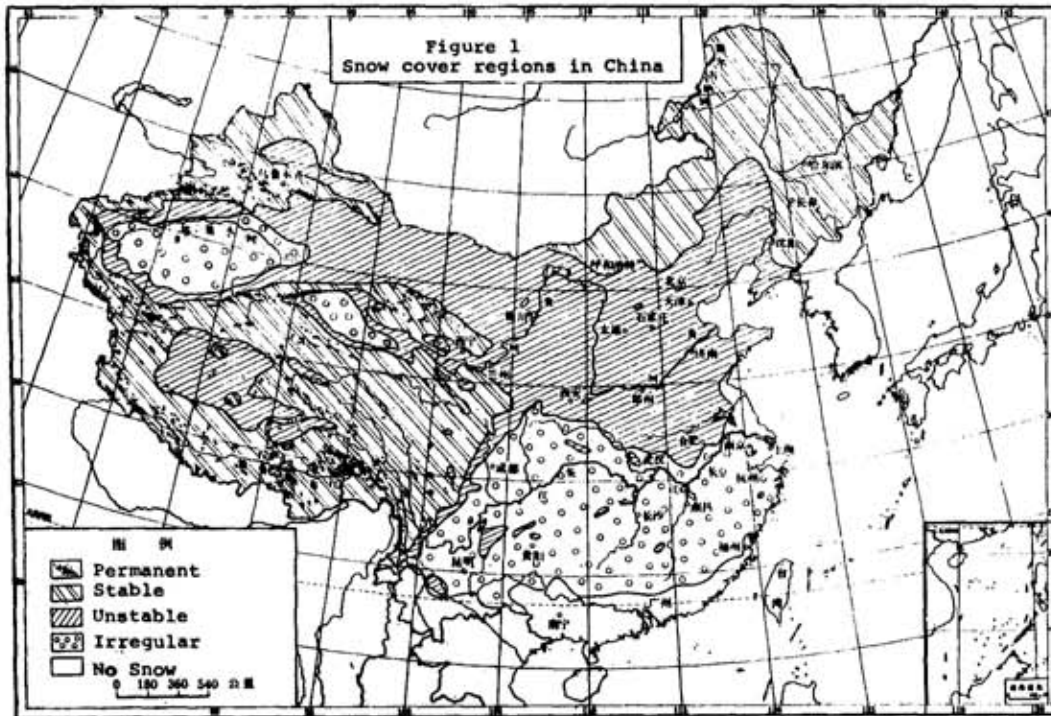
Seasonal snow cover in China is highly variable from year to year. As much as 9 million km² has been occupied by snow at some time during the past 35 years. The distribution, duration and depth of snow have a large impact on agriculture and on the supply of industrial and drinking water which is especially important in the western mountains and in the northernmost part of the country. Snow on the Tibetan Plateau is suspected of influencing the general circulation of the atmosphere and the summer precipitation in Southeast Asia.

In order to determine the recent characteristics of the snow cover, the average number of days with snow on ground and snow depth have been analysed from 1600-2300 stations from the 1951-80 interval. For the purpose of this study it is assumed that glaciers are snow covered throughout the year. Information on glacier distribution was provided by maps based on aerial surveys and ERTS satellite imagery. Based on this data the snow cover in China is divided into the following regions as shown in Figure 1.

(1) The area of permanent snow cover occupies about 50,000 km² and is limited to mountain glaciers in the west. (2) The area of stable snow cover is defined as having a mean annual number of 60 or more snow days and a standard deviation of less than 0.4. In the northernmost parts of China snow may be present for as many as 170 days. Regions of stable snow cover are important for agriculture because spring droughts are frequent in both the northern and western regions, with snow runoff being an important source for irrigation.

(3) Unstable snow cover forms almost every winter with the mean annual number of snow cover days varying between 10 and 60 and an interannual variability from 0.4-1.0. The presence or absence of snow cover during winter in this area is particularly crucial for the growing of wheat. (4) The area of irregular

snow cover generally occurs in southeast China with the mean annual number of snow days less than 10. Together these two regions occupy 4.8 million km². Only 0.55 million km² of China is not affected by snow.



Snow depth in China is generally less than in other parts of the world. The maximum snow depth in most of the country is only about 20 cm. However in the north of Xinjiang province in both Altay and the Yili Valley the maximum snow depth reaches between 80-90 cm. This is also true for the eastern part of the Tibetan Plateau. In the northeast of China the maximum depth is 40-50 cm. The average daily depth is 25-35 cm in Altay and in the Yili Valley and 10-15 cm in the northeast. Occasionally a snow cover from 30-50 cm deep is also formed in southeast China in the lower reaches of the Yangtse river valley.

In most of China precipitation falls mainly during the summer while snowfall peaks in the spring and autumn. Maximum snow depth and number of days with snow cover occurs in winter. Figure 2 shows the average monthly precipitation, snowfall, snow depth, number of days with snow cover and temperature for Harbin located in Heilongjiang province in the northeast of China. The seasonal distribution of these elements can be considered typical for most of the country. Figure 3 shows the same data for Pagri which is located on the Tibetan Plateau. The average snow depth decreases from 10 cm in October to less than 2 cm in December and increases thereafter to a second maximum during January. The number of days with snow cover decreases from

October through December and then increases reaching a maximum in March. The seasonal distribution of snow cover days at this station appears to be approximately representative of the plateau region.

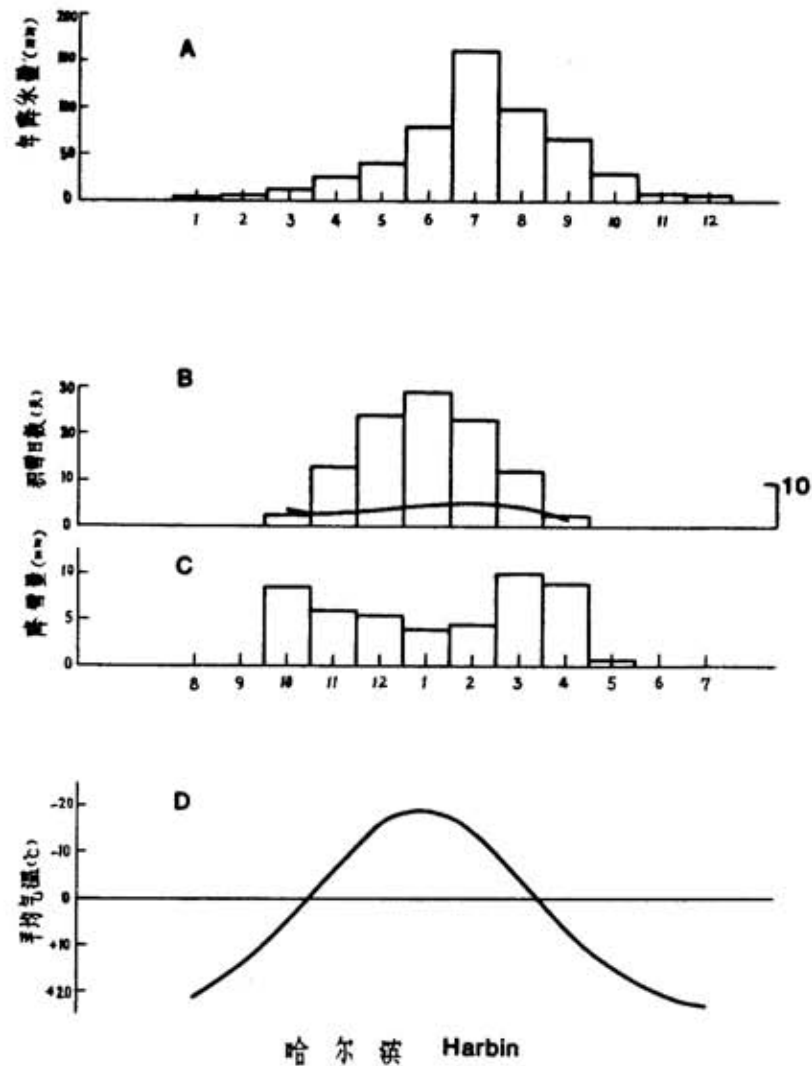


Figure 2: Mean monthly distribution of meteorological elements for Harbin based on the 1951-80 period. A = precipitation in mm; B = average number of days with snow cover (bar graph, scale on left) and average depth of snow for days with snow cover in cm (solid line, scale on right); C = snowfall in mm; D = temperature in °C

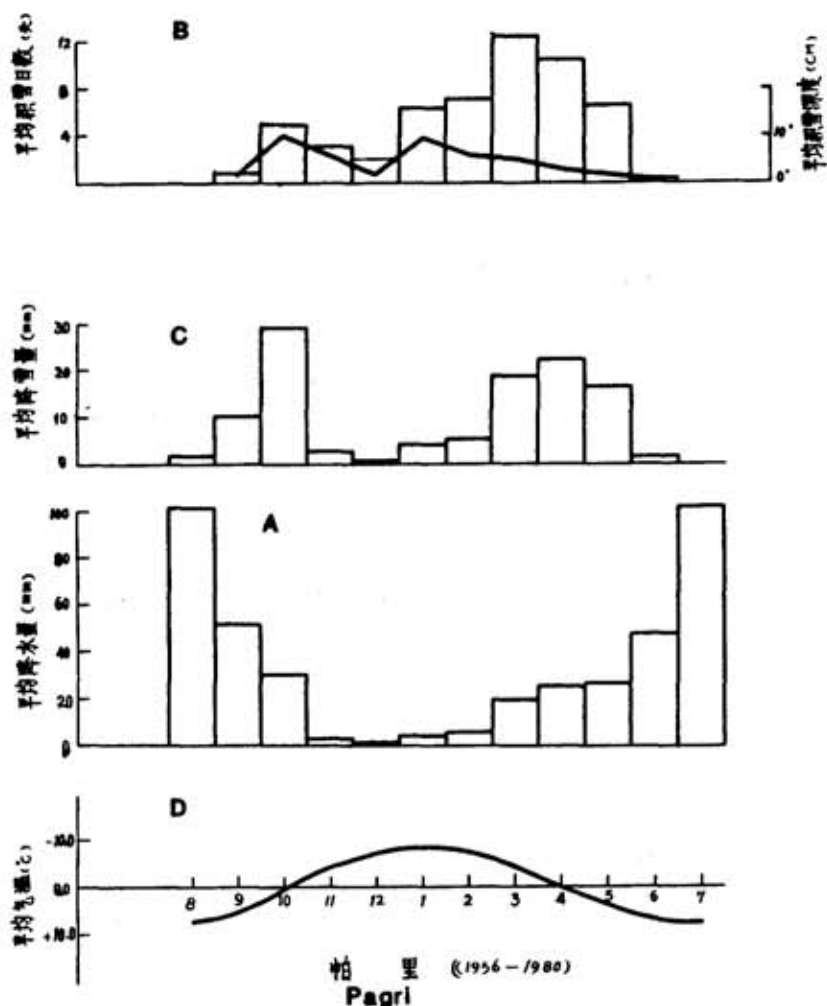


Figure 3: Mean monthly distribution of meteorological elements for Pagri based on the 1956-80 period. A-D as described for Figure 2.

The surface air temperature in the Northern Hemisphere fluctuated considerably in the last 100 years. To what degree then does the surface air temperature and the seasonal snow cover in China show any secular trend? During 106 years of instrumental records, the mean annual temperature in Shanghai oscillated within a range of 2.3°C . As in the Northern Hemisphere record, temperatures show a gradual increase from the 1920's to the 1940's followed by a cooling into the 1960's. A long term record of snow cover in Shanghai starts in 1882. It shows a greater maximum snow depth and more days with snow on the ground during the 1951-70 interval than in 1921-40. No relationship can be seen between annual precipitation and temperature (Figure 4).

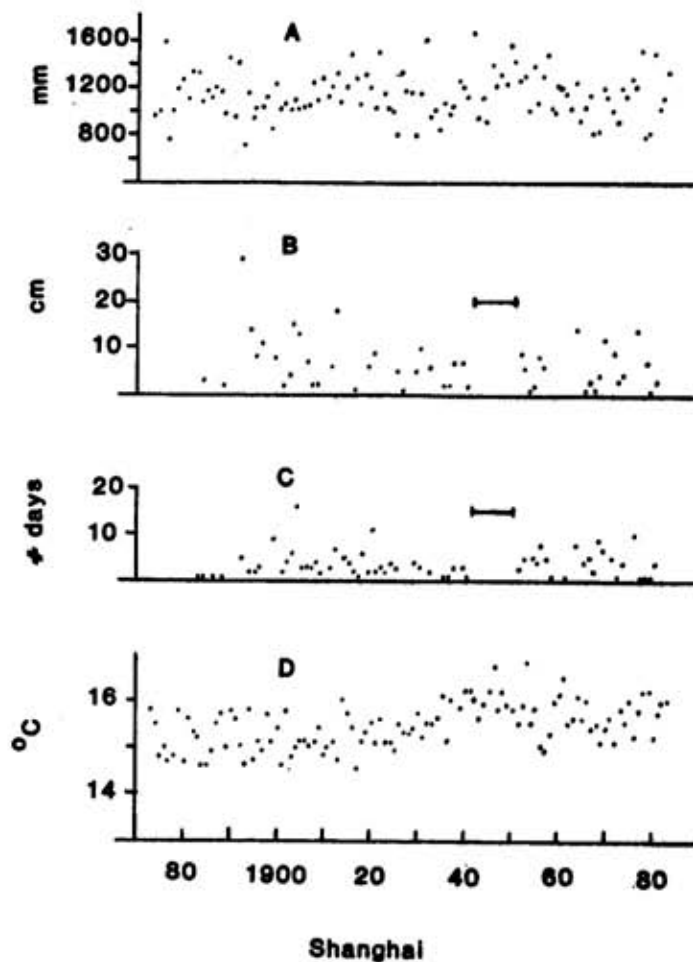


Figure 4: Annual mean values from 1873 for temperature and precipitation and from 1884 for snow cover. A = precipitation in mm; B = maximum snow cover in cm; C = number of days with snow cover; D = temperature in °C. Missing data for the 1940's for B and C.

Shorter records of snow cover and temperature from various regions are shown in Figures 5-7. Large year-to-year and regional variations are evident. For example, Altay and Pagri located in the west show abnormally heavy snow conditions and cold temperatures during the winter of 1968/69 while Shenyang situated in the northeast does not. The heaviest ice conditions in Qinghai lake, also located in the west, occurred in 1967/68 and 1969/70.

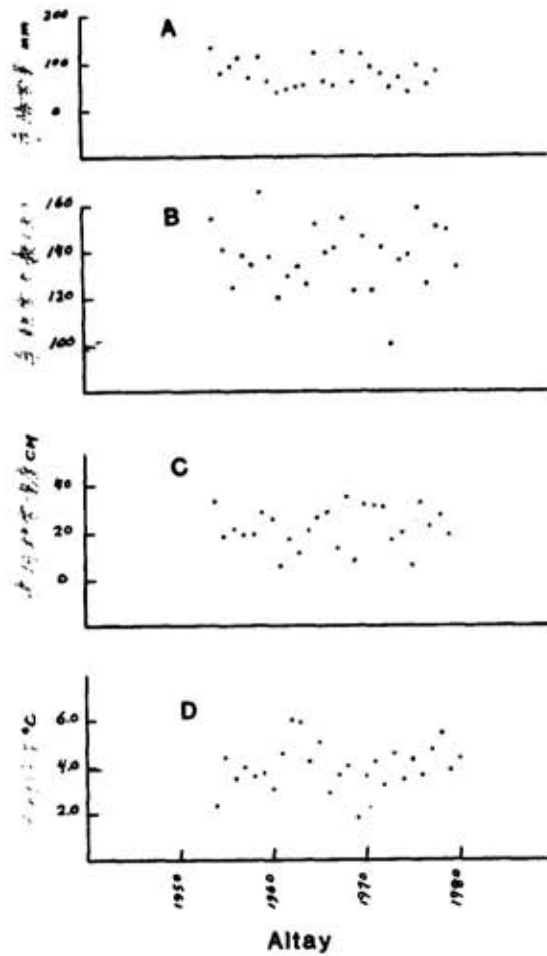


Figure 5

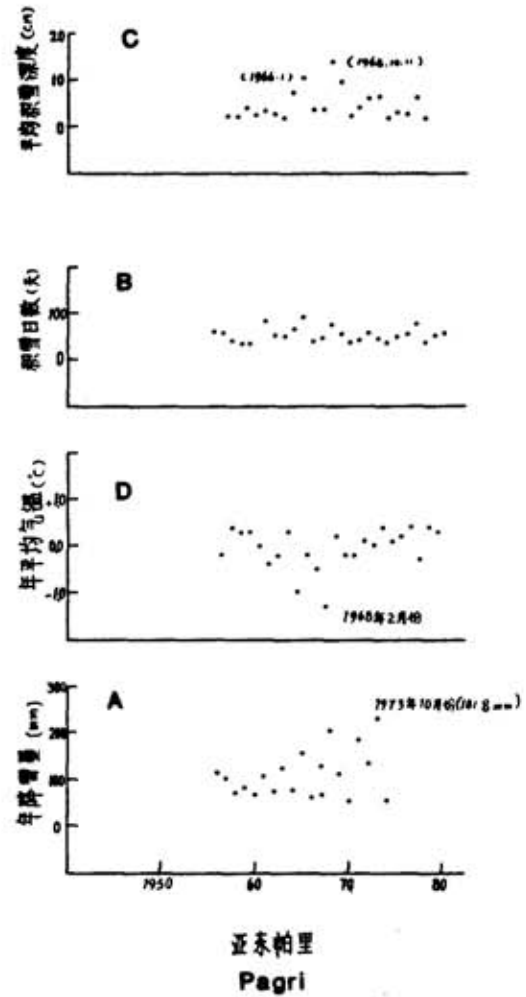


Figure 6

Figures 5, 6 and 7: Mean annual values for meteorological elements for Altay, Pagri and Shenyang from the 1950's to 1980. A = snowfall in mm; B = number of snow cover days; C = mean depth of snow for those days with snow cover in cm D = temperature in °C.

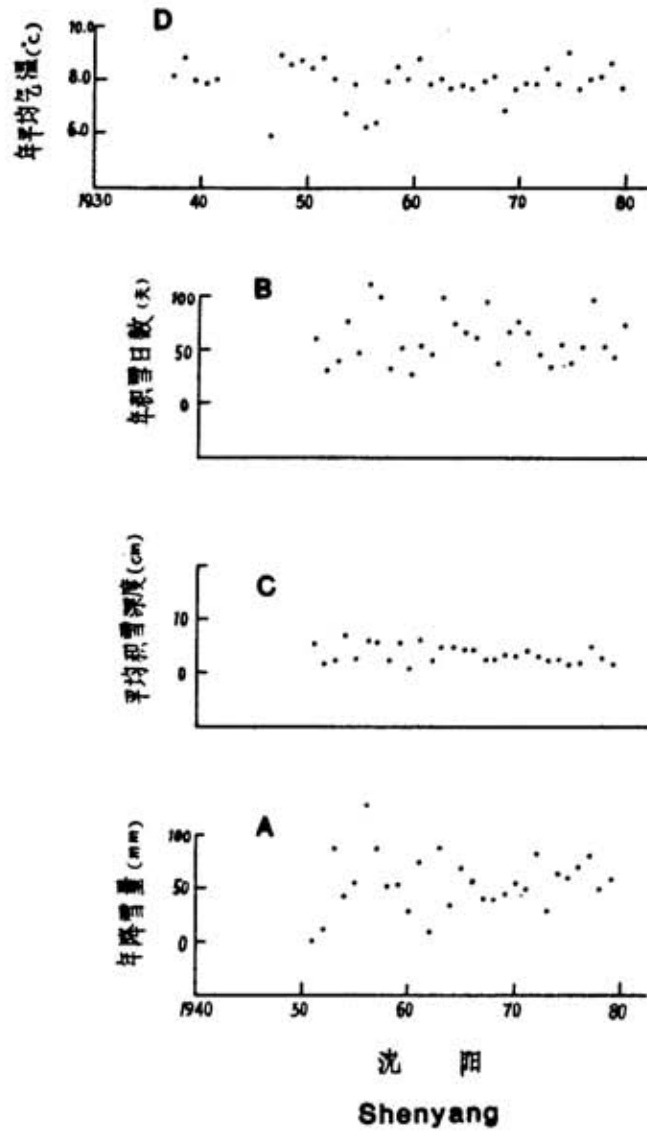


Figure 7

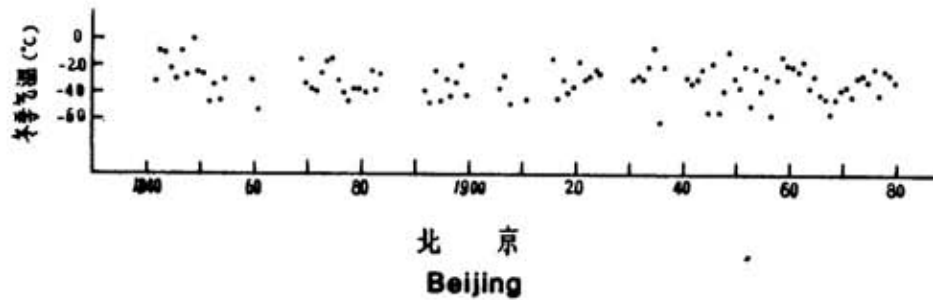


Figure 8: Mean winter temperature (D,J,F) for Beijing in °C from 1841.

Mean winter temperatures were well below normal in Beijing in 1935/36, 1944/45, 1946/47, 1956/57, and in 1967/68 (Figure 8). The heaviest sea ice in both Po Hai and Hwang Hai bays occurred in 1935/36, 1944/45 and in 1968/69.

Kukla, G; Barry, R.G.; Hecht, A.; Wiesnet, D. eds. (1986) SNOW WATCH '85. Proceedings of the Workshop held 28-30 October 1985 at the University of Maryland, College Park, MD. Boulder, Colorado, World Data Center A for Glaciology (Snow and Ice), Glaciological Data, Report GD-18, p.97-103.

Snow Surveying in Canada

B.E. Goodison
Canadian Climate Centre
Atmospheric Environmental Service
Downsview, Ontario, Canada

ABSTRACT

Snow cover data for Canada are available from ground, airborne or satellite surveys. The conventional ground observations - daily snow depth at synoptic and climate stations and weekly, bi-weekly or monthly snow surveys at over 1200 snow course sites - form the basic snow cover network. The current and future availability of these data and some of the problems in using the data are outlined. It is not unreasonable to expect the number of snow courses operating in Canada will decline in the future. Development of alternative methods, notably airborne gamma-ray surveys of water equivalent and satellite determination of areal extent, and more recently, depth and water equivalent, are necessary. The status of these methods are summarized. These data are generally collected for hydrological rather than climatological applications. Some questions related to their use in addressing the question of CO₂/snow interaction are raised for further discussion.

INTRODUCTION

Snow cover data have traditionally come from surface observations of snow depth and water equivalent, either from snow courses or meteorological observations. Although ground based measurements have formed the basis of the snow survey network, recent advances in remote sensing technology offer the potential for significant changes in snow survey procedures in Canada. A combination of ground based, airborne and satellite information, or ultimately remote sensing methods alone, may be the most effective and efficient means of snow survey data collection to meet a variety of user needs. Although snow surveys have a history in hydrology, many of the current uses of these data are in other fields, climatology and the study of climate change being one of the most notable.

It is important that all users of these data are aware of what data are available, what changes may occur in data collection and what the outlook for data continuity may be in the future. Such questions are particularly relevant in the discussion of current and future studies on climate change and particularly in the context of CO₂/snow interactions.

CANADIAN SNOW COVER NETWORK

a) Snow Depth Observations:

The most basic snow cover observations available are the daily snow depth measurements made at 12GMT at about 225 Atmospheric Environment Service (AES) synoptic weather stations. These data are available in real-time on the GTS network and later from the AES national climate archive in Downsview, Ontario. In addition, since 1980 all climate stations have been requested to measure snow depth daily, rather than just on the last day of the month as was the earlier practice. These data are also available from the digital archive.

Figure 1 is an example of a weekly national map of depth of snow on the ground at 12GMT as published in Climatic Perspectives, a weekly bilingual publication of the Canadian Climate Centre, AES, Downsview. The representativeness of these observations may be open to discussion, particularly in non-uniform topographical regions such as the Rocky Mountains and this must be considered in any analysis and subsequent use in climate models. However, its availability on a weekly basis provides a regular monitoring of the progression of the snow season.

A complement to the snow depth map is a monthly map of snow cover water equivalent for Canada which is also published in Climatic Perspectives. Water equivalent is a derived component of a water budget model which uses

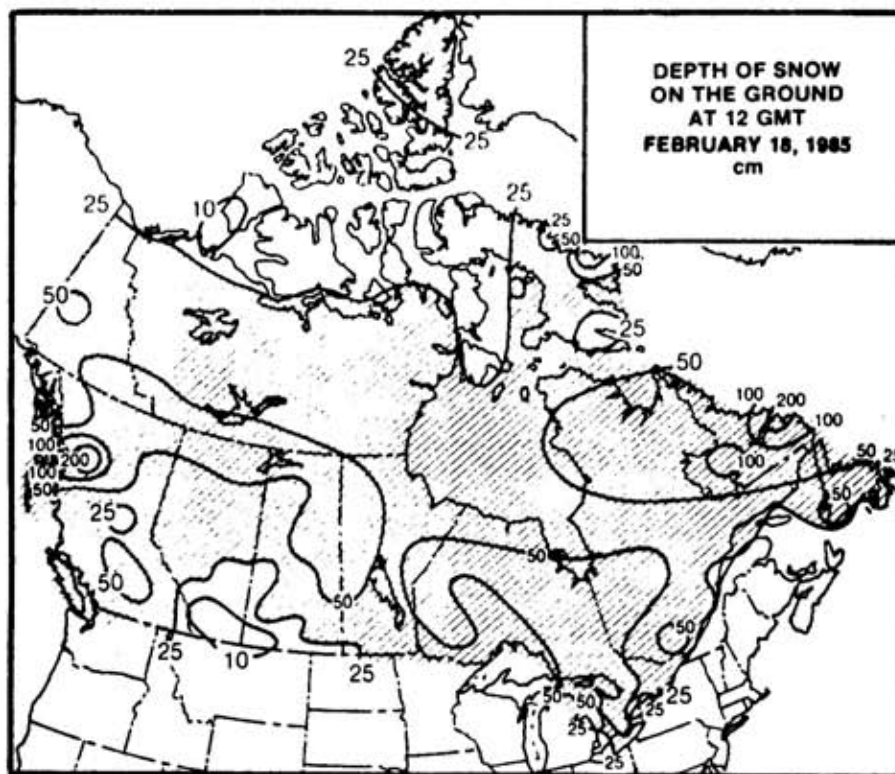


Figure 1. National map of snow depth on the ground

daily temperature and precipitation observations from synoptic stations as input (Johnstone and Louie, 1984). Like the snow depth map, it is one tool available for monitoring snow cover during the winter.

b) Snow Course Observations:

Table 1 outlines the growth of the snow course network by province from 1963-64 to 1982-83 and includes the number of courses operated by the Atmospheric Environment Service (AES) and the Water Resources Branch (WRB), the only agencies operating national snow survey programs. By 1973, 13.6% of all courses were operated by WRB. The number of WRB courses peaked in 1976, when 175 courses were surveyed out of some 1200 across Canada, but by 1982-83 the number of stations reporting had dropped to 94. In 1984-85 another substantial reduction by WRB resulted in the retirement of all but 9 snow courses in the Saint John River Basin and 13 courses in the Lake-of-the-Woods watershed. In 1985-86 the Lake-of-the-Woods network will be eliminated. AES continues to operate 130 snow courses at principal observing stations across Canada, representing about 10% of the total network. All AES stations take observations twice monthly and many make weekly observations.

Table 1. Canadian Snow Course Network

Province/Territory	Network Size		
	1963-64	1972-73	1982-83
British Columbia	139	219	265
Alberta	34	64	54
Saskatchewan & Manitoba	149	258	228
Ontario	125	201	278
Quebec	104	192	183
New Brunswick	38	52	67
Nova Scotia	30	42	32
Prince Edward Island	3	8	4
Newfoundland & Labrador	42	81	74
Yukon & Northwest Territories	10	40	106
TOTAL	674	1157	1291
Total operated by AES	11	128	130
Total operated by WRB	122	157	94

The development of a snow survey network and the frequency and accuracy of the measurements must be related to its purpose. The Canadian snow course network was established to obtain an index of snow water equivalent over an area, primarily for hydrological applications. Absolute estimates of areal water equivalent can only be obtained after allowance is made for observational, instrumental (eg. Farnes et al., 1983) and siting biases and the sampling network has been specifically designed to reflect areal snow cover variability (eg. Steppuhn and Dyck, 1974; Goodison, 1981). Unless one knows

the site characteristics of snow courses used in an analysis, it is difficult to develop climatological or synoptic maps of snow cover water equivalent.

However, by using known vegetative and physiographic parameters, objective techniques such as multiple regression, trend surface or proximity analysis can then be tested for development of basin maps of snow distribution (Trivett and Waterman, 1980). Table 2 is one example of the difficulty in making effective use of standard snow survey data for hydrological or climatological purposes. The three snow courses are at three different sites at Sioux Lookout, each with a different number of sampling points, operated by three different agencies, and possibly using different equipment. Is there a "right" or "wrong"? Each may, in fact, be correct for the land cover and terrain characteristics that it represents. This example is one of the practical problems which must be considered when preparing a snow cover data base for climatological analyses related to the CO₂ question.

Table 2. Comparison of Snow Course Water Equivalent Measurements (mm) Sioux Lookout 1975-1979

March (first week)	AES ¹ (mm)	% Change	Ontario Hydro (mm)	% Change	WRB (mm)	% Change
1975	183		102		130	
1976	134	-26%	84	-18%	97	-25%
1977	117	-13%	99	+17%	112	+15%
1978	154	+32%	106	+ 7%	112	0
1979	108	-30%	76	-28%	99	-12%

¹ Means of surveys on March 1 and 8

Atmospheric Environment Service publishes Snow Cover Data, which is an annual summary of snow course observations made by 19 agencies. No national digital archive of these data currently exists, although individual agencies may have their own data archived for their specific uses. The lack of an easily accessible national digital archive has often hindered spatial and temporal analyses of snow data. AES is currently investigating a change in the method and format of publication in line with the proposal of Findlay and Goodison (1979). A readily accessible digital archive is necessary if snow course data are to be used in any climatic change analysis.

c) Future of the Snow Cover Network

Snow depth observations at synoptic stations should continue. Since it is a manual observation, there is expected to be a requirement for an inexpensive automatic snow depth sensor for use at stations being automated. Such a sensor is currently being tested in Canada (Goodison et al., 1985).

In view of recent trends, it is not unreasonable to expect that the number of snow courses operating in Canada will decline in the future. WRB has almost eliminated its network of snow courses for a variety of reasons. Agencies independently continue to operate snow courses across Canada, usually to meet their own needs.

Networks are susceptible to the pressure of resource constraints; uses and users of the data must be clearly identified in an effort to show the value of snow cover data. Even though snow courses are primarily intended for hydrological applications, if the data would be useful in addressing the CO₂/snow interaction question, then this should be clearly indicated to the operating agencies. One of the most important uses will be in the "ground truthing" of new airborne or satellite methods of snow survey. The accuracy of snow data derived from satellite remote sensing will very much be a function of the accuracy of the "ground truth" data against which it is calibrated.

ALTERNATIVE SURVEY METHODS

One very viable alternate snow survey procedure is the airborne gamma ray method. This technique has been used in Canada on an experimental basis since 1972. In the last three years extensive surveys have been performed in southern Saskatchewan, around the north shore of Lake Superior and in the Saint John River Basin. An operational airborne snow survey program in Canada is not yet available. If one were to be implemented and operated regularly for many seasons over the same flight line network, the data might be very useful for climatological analyses, particularly in climate sensitive areas such as the Canadian prairies and the Great Lakes. Development of a reliable data base would be required for the data to be useful in the context of climate impact assessment.

Satellite remote sensing of snow cover is another method of snow survey which would complement the existing ground and airborne systems. Currently in Canada, only the areal extent of snow cover is operationally derived from satellite data, and only for selected basins (eg. Waterman et al., 1980). There is no centralized system for mapping every basin that might be required by user agencies. On a continent-wide basis, Canadian users could use snow cover products of NOAA/NESDIS.

A major challenge in the remote sensing of snow cover is to develop algorithms to determine snow depth, water equivalent, areal extent and liquid water content using sensors having all-weather capabilities. At the moment, passive microwave data offer the greatest prospect for the determination of snow cover. Recent investigations (eg. Kunzi et al., 1982; Chang et al., 1982) have shown that there is a potential for using passive microwave sensors to monitor snow cover, notably areal extent, depth, water equivalent and melt.

One of the objectives of the Canada/US Prairie Snow Cover Runoff Study was to assess the applicability of passive microwave data for mapping snow cover on the Canadian prairies. Details of the study are given in Goodison et al. (1984). Initial results have been very encouraging. Maps of snow

cover water equivalent derived from NIMBUS-7 SMMR data are now being prepared for selected dates using test algorithms derived from airborne data collected during the experiment.

Since passive microwave resolution from space is currently 30 km, the technique is best suited to large, relatively homogeneous regions such as the Prairies and the North. The spatial resolution provides a snow water equivalent or depth distribution already "smoothed"; the siting problems associated with conventional surveys are minimized. It must be considered as a technique deserving further research and development. It offers what could be a very useful method for collecting snow cover over large areas, often lacking data from conventional networks. Such a data source would be extremely useful in future analyses of snow cover/climate change linkages.

DISCUSSION

The question of CO₂/snow interactions might be viewed as a two-fold one. First, there is the impact that snow cover has on the climate system; secondly, there is the effect or impact that the climate system has on snow cover. The data needs may be different for each question. For example, to address the first question, climate models would be a viable approach. Does the Canadian data base meet the needs of the climate modellers? Are grid-square averages of snow depth adequate or would water equivalent estimates and percent snow cover also be useful? What temporal and spatial resolutions would be required? Are near real-time or archive data necessary? In practical terms, what accuracy levels of snow measurement would be considered satisfactory to validate the output of a model or to test a climatic change hypothesis? It would seem that a snow cover data set compiled from integration of conventional ground, airborne and satellite information would be one method of meeting the potential needs of modellers.

The study of the impact of changes in climate on snow cover would require regional data of a higher resolution than that needed for analysis of continental scale changes. Conventional ground and airborne data sets would currently be most useful for this task, although satellite data may provide additional information in the future. Compilation of regional data sets on different scales is a requirement if changes in regional snow cover are to be identified and analyzed. Finally, how important is data continuity in a region? Can we reduce our snow survey networks without affecting our climate data base?

Answers to some of these questions could lead one to the argument that there is a need for a more comprehensive and co-ordinated national snow survey program in Canada. It should ensure the standardization of data collection, analysis and dissemination procedures, while ensuring the introduction and integration of modern techniques. Such a program should be responsive to the needs of the hydrological and climatological communities. It should promote the development of the necessary expertise to apply knowledge, gained from basic research, to the analysis and interpretation of snow data. Ultimately, however, users of snow data must clearly identify their requirements.

REFERENCES

- Chang, A.T.C., J.L. Foster, D.K. Hall, A. Rango and B.K. Hartline, 1982: Snow Water Equivalent Estimation by Microwave Radiometry. Cold Regions Science and Technology. Vol. 5, 259-267.
- Farnes, P.E., B.E. Goodison, N.R. Peterson and R.P. Richards, 1983: Final Report. Metrication of Manual Snow Sampling Equipment. Western Snow Conference, Spokane, Washington, 106 pp.
- Findlay, B.F.; Goodison, B.E. 1979: Archiving and mapping of Canadian snow cover data. World Data Center A for Glaciology (Snow and Ice). Glaciological Data. Report GD-5, 71-87.
- Goodison, B.E., 1981: Compatibility of Canadian snowfall and snow cover data. Water Resources Research, 17, 4, 893-900.
- Goodison, B.E., A. Banga and R.A. Halliday, 1984: Canada - United States Prairie snow cover runoff study. Can. Water Res. J., 9, 1, 99-107.
- Goodison, B.E., B. Wilson and J. Metcalfe, 1985: An inexpensive remote snow depth gauge. Proc. TECIMO-III. WMO Technical Conference on Instruments and Methods of Observation, Ottawa. July 8-12, 1985, 111-116.
- Kunzi, K.F., S. Patil and H. Rott, 1982: Snow Cover Parameters Retrieved from NIMBUS-7 Scanning Multi-Channel Microwave Radiometer (SMMR) Data. IEEE Trans. Geosc. Rem. Sens. GE-20(4), 453-467.
- Johnstone, K.J. and P.Y.T. Louie, 1984: An operational water budget for climate monitoring. Atmospheric Environment Service CCC Report No. 84-3. 52 pp.
- Steppuhn, H. and G.E. Dyck, 1974: Estimating true basin snowcover. In, Advanced Concepts and Techniques in the Study of Snow and ice Resources, National Academy of Sciences, Washington, D.C., 314-324.
- Trivett, N.B.A. and S.E. Waterman, 1980: Evaluation of the spatial and temporal distribution of snowpack parameters in the Saint John River Basin. Proc. Eastern Snow Conf., 19-35.
- Waterman, S.E., W.D. Hogg, A.J. Hanssen and V.L. Polavarapu, 1980: Computer analysis of TIROS-N/NOAA-6 satellite data for operational snowcover mapping. Proc. 6th Can. Symp. on Remote Sensing, Halifax, N.S. May 21-23, 1980, 435-442.

Snow Cover in Real Time Climate Monitoring

Chester F. Ropelewski
Climate Analysis Center
National Meteorological Center
National Oceanic and Atmospheric Administration
Washington, D.C., U.S.A.

A number of empirical studies and numerical climate models have indicated that the large scale areal extent of snow cover is a potentially important parameter of the global climate system. Fluctuations in monthly and seasonal continental scale snow cover, monitored both with surface station data and remote satellite observations, have been linked to temperature and atmospheric circulation anomalies. In light of these studies the Climate Analysis Center has developed a program to monitor snow cover extent in real time. The results of this analysis and other products are used qualitatively as aides to the interpretation and diagnosis of anomalies in the monthly temperature, precipitation, and circulation features. Time series of Northern Hemispheric and continental scale snow cover extent and standardized anomaly are also produced monthly. These plots, e. g., Figs 1, 2, and 3, provide useful tools for: placing current snow cover fluctuations into historical context, estimating the magnitude of typical snow cover fluctuations, and identifying longer term trends in the data.

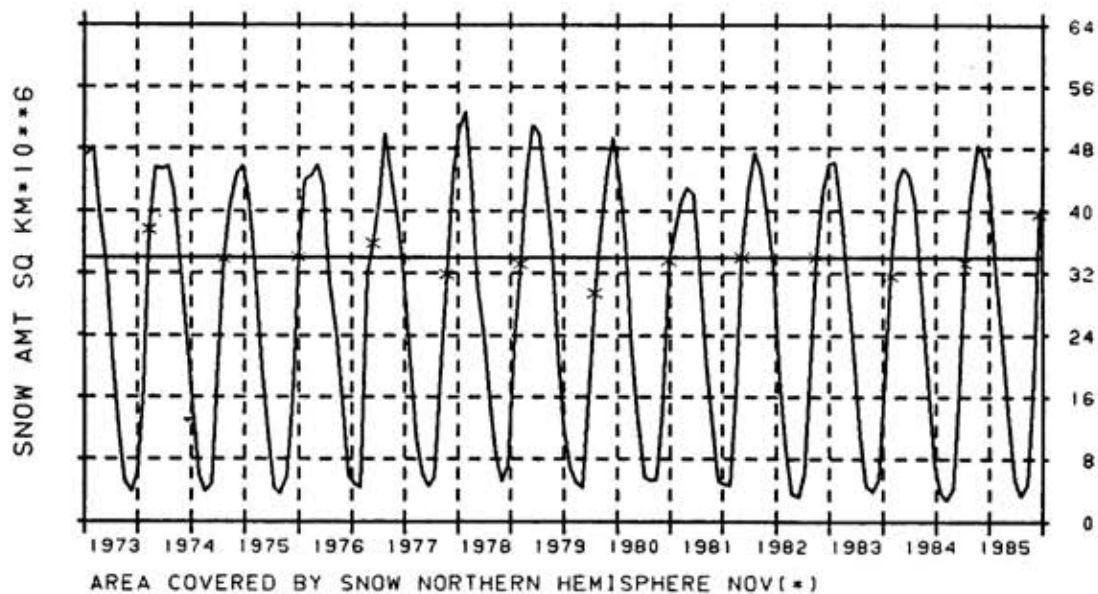


Fig 1a. Time series of Northern Hemisphere snow cover area (10^6 km^2). The heavy horizontal line corresponds to the period mean (1973-1985) November snow cover area. The (*) designates the November snow cover area for each year. Snow cover area was underestimated before 1973 and thus not plotted. Operational time series are produced and updated monthly.

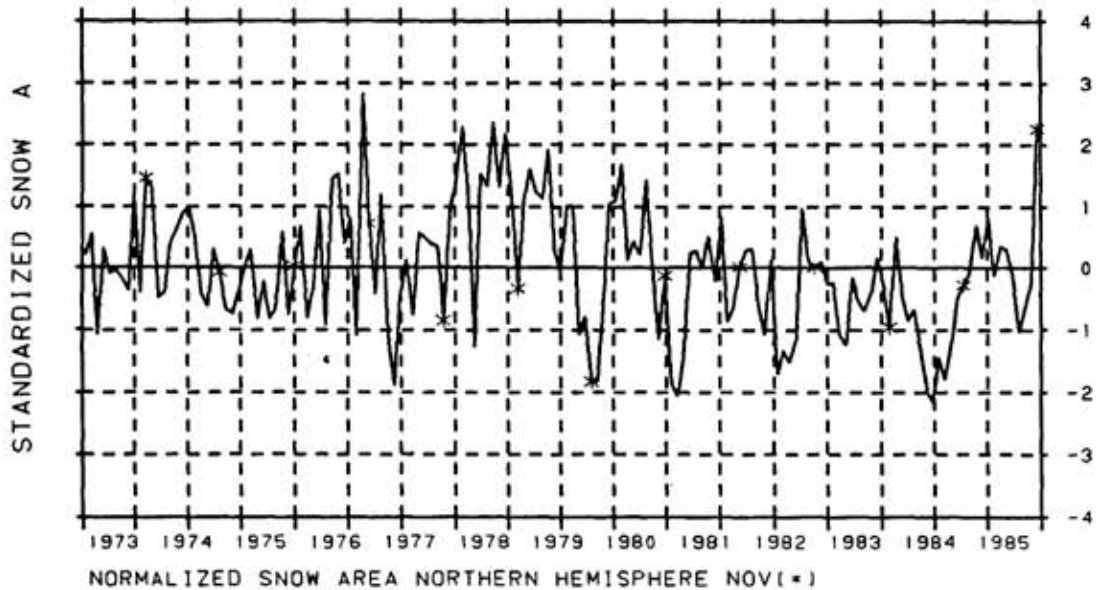


Fig 1b. Time series of standardized Northern Hemisphere snow cover area. The means and standard deviations for the normalization are computed over the 1973-present-month period. The (*) designates the standardized departures for November of each year. Operational time series are produced and updated monthly.

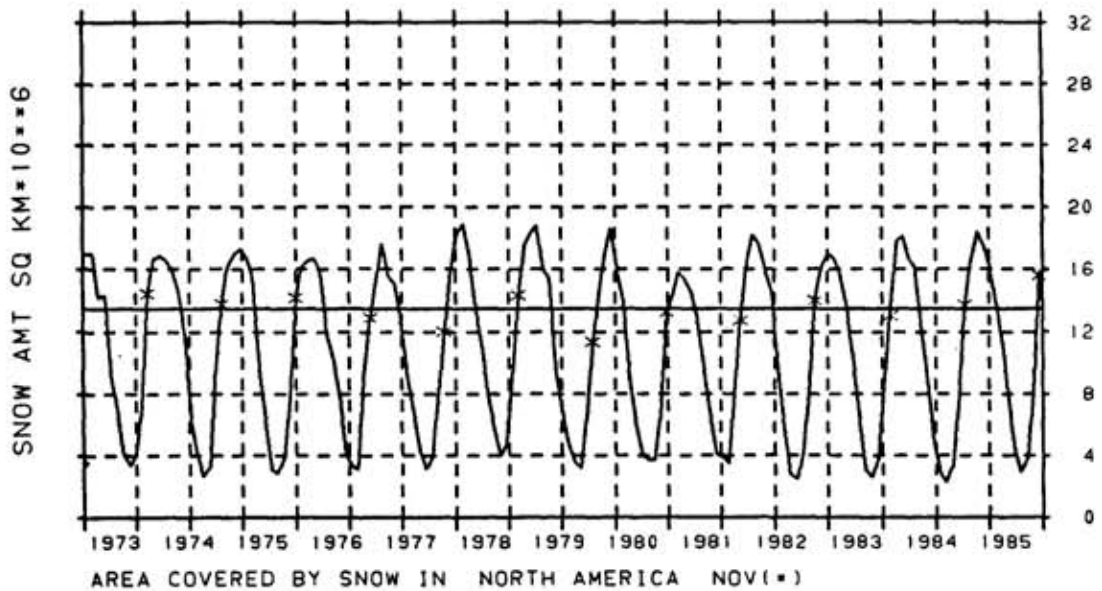


Fig 2a. Same as 1a except for North America.

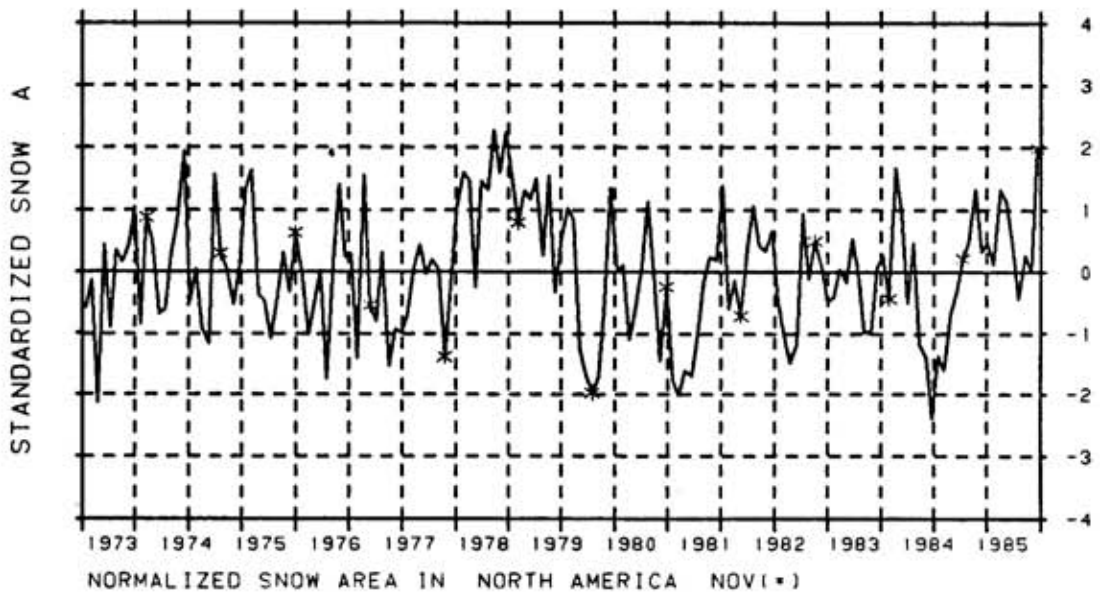


Fig 2b. Same as 1b except for North America.

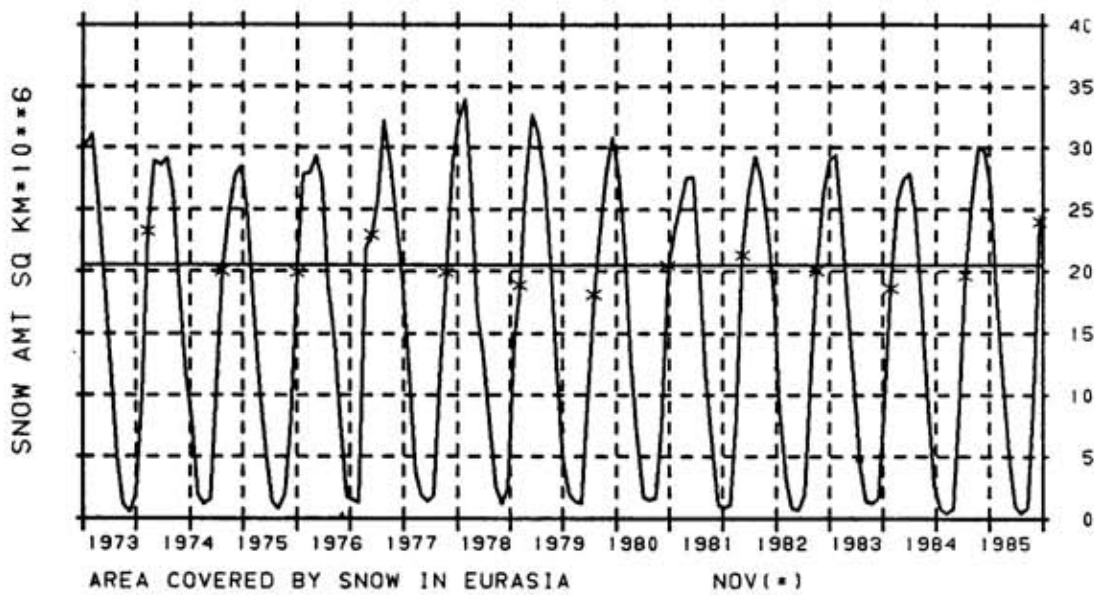


Fig 3a. Same as 1a except for Eurasia.

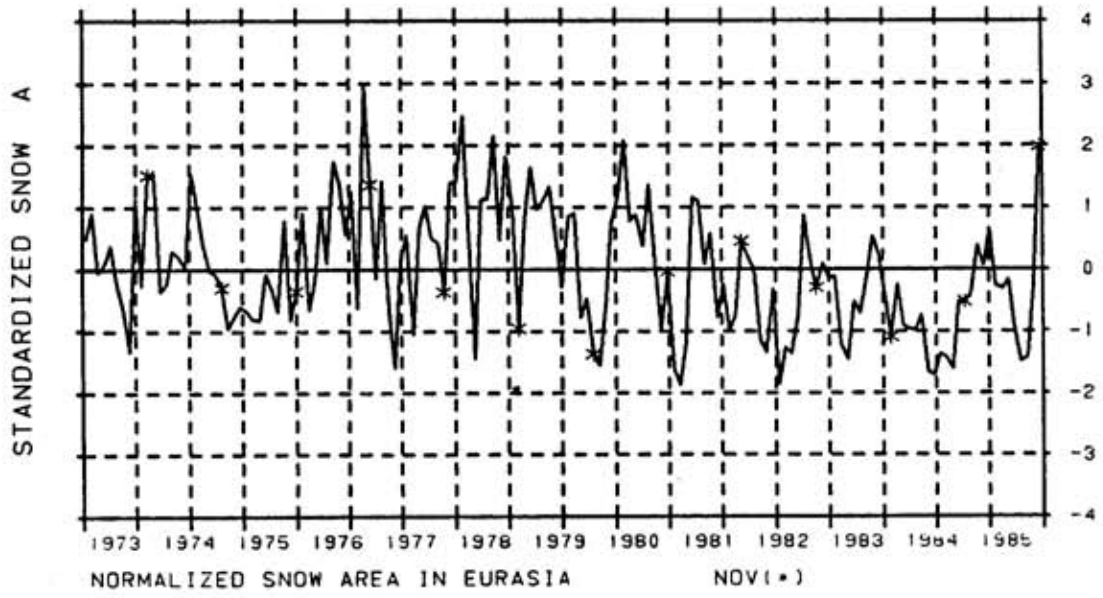


Fig 3b. Same as 1b except for Eurasia.

Kukla, G; Barry, R.G.; Hecht, A.; Wiesnet, D. eds. (1986) SNOW WATCH '85. Proceedings of the Workshop held 28-30 October 1985 at the University of Maryland, College Park, MD. Boulder, Colorado, World Data Center A for Glaciology (Snow and Ice), Glaciological Data, Report GD-18, p.109-113.

Northern Hemisphere Snow and Ice Chart of NOAA/NESDIS

Thomas E. Baldwin
National Environmental Satellite, Data, and Information Service
National Oceanic and Atmospheric Administration
Camp Springs, Maryland, U.S.A.

Abstract

Since 1966, the Satellite Analysis Branch (SAB) of the National Environmental Satellite, Data, and Information Service (NESDIS) has prepared a weekly snow and ice boundary chart for the Northern Hemisphere. This chart is prepared on a 1:50,000,000 polar stereographic base map centered on the North Pole.

Data Sources

The primary sources of information used in the preparation of this chart (figure 1) are satellite images from the visible scanning radiometers of the National Oceanic and Atmospheric Administration (NOAA) polar-orbiting satellite systems. Secondary input comes from the visible scanning radiometers of the Geostationary Satellite (GOES) systems over the North American continent south of 60°N, and occasionally from the Meteorological Satellite (METEOSAT) system.

The specifications of currently used sensors are shown below:

Satellite	Camera and Sensor	Resolution (km)	Wavelength (mm)
NOAA-9	VHRR*	1.0 - 4.0	0.58 - 0.68
GOES-6	VISSR**	1.0 - 7.4	0.55 - 0.75

*VHRR - Very High Resolution Radiometer

**VISSR - Visible Scanning Radiometer

Presently the polar-orbiting satellite crosses the equator northbound at approximately 1500 local standard time.

Philosophy and Purpose

Polar-orbiting satellites are the only source of a complete look at the polar areas of the earth, since their orbits cross near the poles approximately every two hours with 12 or 13 orbits a day of useful visible data. This visible imagery can then be analyzed to detect the snow and ice fields and the difference in reflectivity of the snow and ice. By analyzing these areas over a one week period, areas of cloud cover over any particular area of snow and ice cover can be kept to a minimum to allow a cloud free look at these regions. This chart can then be useful as a measure of the extent of snow and ice for any weekly period during the year and it can also be compared to previous years for climatic studies.

Procedure

Each Monday the analyst, a satellite meteorologist, collects all the NOAA visible data received in the past week (12 or 13 orbits per day) and deciphers snow and ice cover on the pictures and makes appropriate updates to the previous week's chart. Over North America, additional higher resolution data from GOES are used. Therefore, each segment of the chart shows the latest cloud-free satellite observation of the world. If an area is cloud covered for several days, the analysis of snow cover for that area will be several days old. If the area remains cloudy for an entire week, the previous week's analysis is used. The chart is then finalized and sent out.

Guidelines and Suggestions

To distinguish snow or ice from cloud cover, the analyst looks for geographical features, such as forested areas or rivers and lakes (figure 2,3). Valley fog on morning Polar-orbiter passes and mountain top clouds or cumulus clouds on afternoon passes are obstacles to a clear view of snowcover (figure 4). Areas of uniform brightness that persist for several days can aid in distinguishing snow from clouds.

A solid line indicates a definite snow boundary while a dotted line indicates an icy boundary. A dashed line indicates "patchy" snowcover, for example, mountain top snow in late spring. Snow or ice free areas enclosed by a snow or ice field are labeled 0, for open, snow and ice areas are then stippled.

Digitizing the Snow and Ice Chart for Archives

An 89 x 89 square polar stereographic map is placed on top of the finalized weekly snow and ice chart. Along the southern border of the snow line, each square is looked at to determine if at least 50 percent of the square is covered by snow according to the analysis. This includes squares with more than 50 percent coverage if it is snow/patchy snow mixed. Oceans and lakes are automatically eliminated in the program. The purpose is to show the area of snow cover, so a box is included if the immediate area totals one box, even if no individual box equals 50 percent coverage.

The chart is then digitized and a program is run to put data on a permanently mounted dist. A second program is run to produce a microfilm record of the analysis.

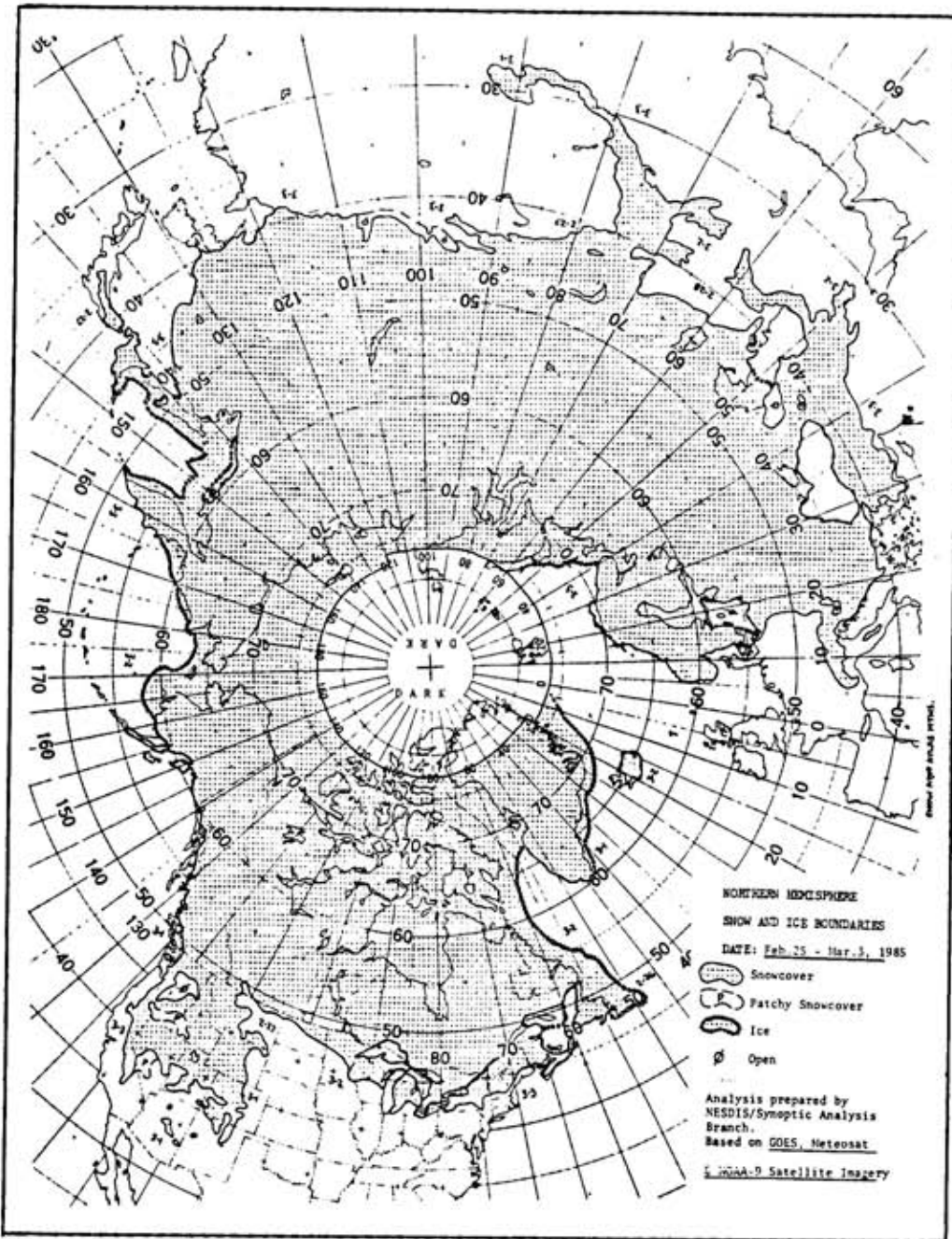


Figure 1: An example of the NESDIS Northern Hemisphere weekly Snow and Ice boundary chart.



Figure 2: Dendritic pattern of snow-cover on mountains.



Figure 3: Snowcover appears brighter in unforested areas.

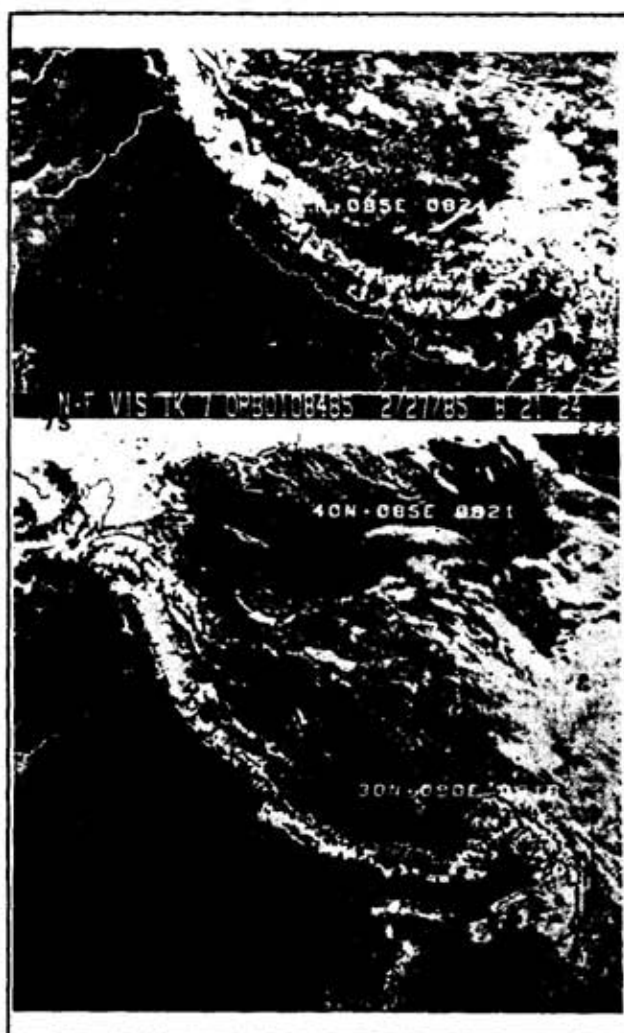


Figure 4: Cumulus clouds obscure mountain tops.

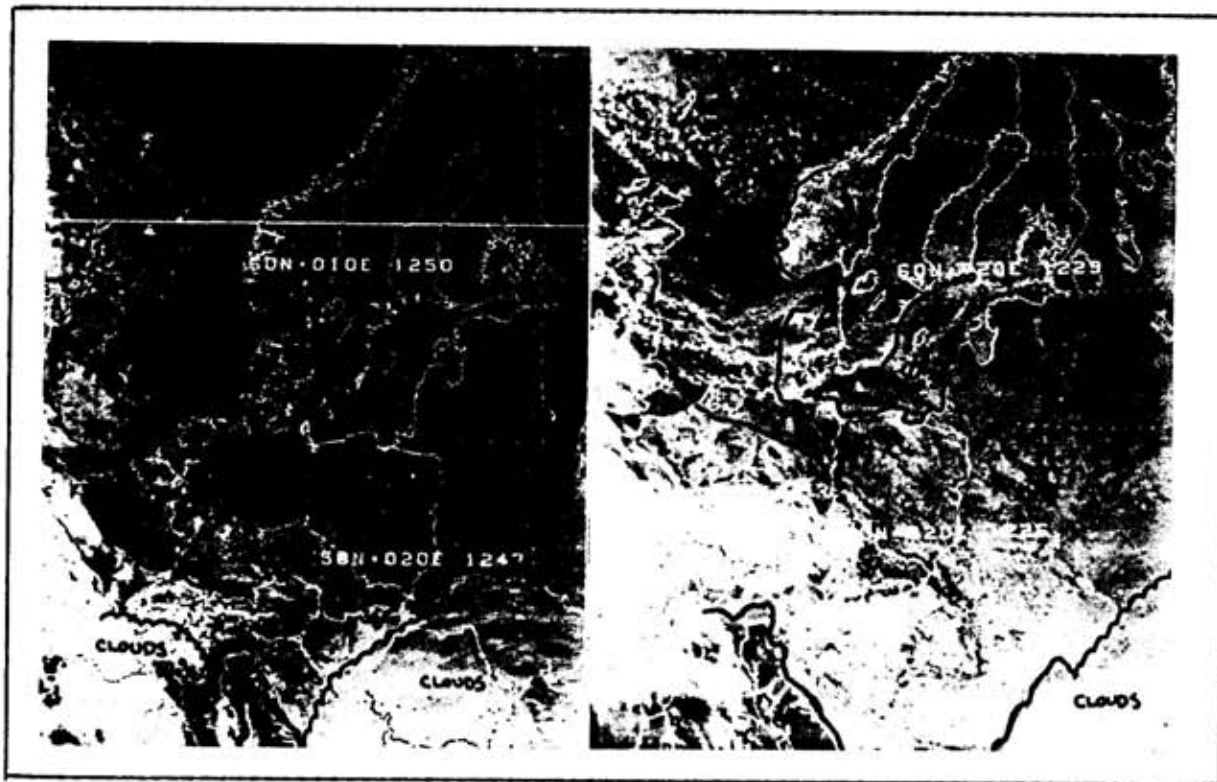


Figure 5: Using two days' data for a complete analysis.

Kukla, G; Barry, R.G.; Hecht, A.; Wiesnet, D. eds. (1986) SNOW WATCH '85. Proceedings of the Workshop held 28-30 October 1985 at the University of Maryland, College Park, MD. Boulder, Colorado, World Data Center A for Glaciology (Snow and Ice), Glaciological Data, Report GD-18, p.115-124.

The NOAA Satellite-Derived Snow Cover Data Base: Past, Present, and Future

Michael Matson

National Environmental Satellite, Data, and Information Service
National Oceanic and Atmospheric Administration
Washington, D.C., U.S.A.

The NOAA Northern Hemisphere satellite-derived snow cover data base now includes 20 years of data from 1966-1985. A time line of the history, use, and future of this data base can be divided into four periods: the Age of Darkness, the Age of Discovery, the Age of Enlightenment, and the Age of Advancement. This paper reviews the highlights of each of these periods with the goal of providing the reader a perspective on the evolution of the NOAA snow cover data base.

The Age of Darkness occurred prior to 1974, the year Kukla and Kukla (1974) published the first paper about the NOAA satellite snow cover data. Although the satellite-derived snow cover maps had been in existence since 1966, they were not used as a data set until the publication of the Kukla and Kukla paper. Before 1974, Northern Hemisphere snow cover data sets were derived from point measurements taken at reporting stations. These data sets suffer from a lack of spatial and temporal continuity, especially in remote and mountainous areas. One of the better attempts at assimilating this ground data into a Northern Hemisphere snow cover data set was done by Dickson and Posey (1967). They prepared maps depicting the probability of snow cover of one inch or more in depth at the end of each month from September through May for the Northern Hemisphere. An example of one of these maps is shown in figure 1.

The Age of Discovery began in 1974 with the publication of the previously mentioned paper by Kukla and Kukla. This paper brought to the attention of the scientific community the existence of the NOAA Northern Hemisphere Weekly Snow and Ice Cover Chart produced since 1966 (figure 2). For the first time, a snow cover data set existed having spatial and temporal continuity. The Age of Discovery was marked by manual analysis of the data set and the creation of climatologies and time series based on the data set. Few, if any quality control checks were done on the data set during this period, although the Himalayan area was recognized as an area of unreliable analysis.

The year 1980 marked the beginning of the Age of Enlightenment. The highlight of this period was the creation of a digitized data set of the NOAA Northern Hemisphere Weekly Snow and Ice Cover Chart (Dewey and Heim, 1981). The charts have been operationally digitized since the creation of the original digitized data set. The digitized data has been used to create monthly mean maps (figure 3), monthly frequency maps (figure 4), and monthly anomaly maps (figure 5). Climatologies of monthly snow cover frequency have also been created for the 1967-1981 period (figure 6). A Southern Hemisphere digitized snow cover data set was also created for the 1974-1980 period (Dewey and Heim, 1983). Although the data set showed variability in South American snow cover (figure 7), the data set was not continued because of the small snow covered areas involved when compared to the Northern Hemisphere snow cover. The Age of Enlightenment is also marked by a careful examination of the limits of the data base. Kukla and Robinson (1979, 1981), Dickson (1984), and Kukla and Gavin (1983) have shown problems in the analyses of the charts with persistent clouds, low quality in the early satellite imagery, and poor snow recognition in heavily forested and low illumination scenes. These problems must be considered when using the digitized data base.

Starting in 1990, NOAA will launch the NOAA-K,L,M series of polar-orbiting satellites which will include a 1.6 micrometer channel on the Advanced Very High Resolution Radiometer (AVHRR), and the Advanced Microwave Sounding Unit (AMSU), which will have several channels suitable for snow cover detection. The AVHRR 1.6 micrometer channel will enable users to discriminate snow from clouds and the AMSU data will allow snow cover detection through clouds. These new developments in snow cover detection mark the beginning of the Age of Advancement. Using these new instruments, NOAA plans to create automated snow cover analyses for the Northern and Southern Hemisphere. Hopefully, this will finally eliminate the biases inherent in the manual analysis of continental snow cover.

References

- Dewey, K.F.; Heim, R., Jr. (1981) Satellite observations of variations in Northern Hemisphere seasonal snow cover. NOAA Technical Report NESS 87, U.S. Department of Commerce, Washington, D.C., 83pp.
- Dewey, K.F.; Heim, R., Jr. (1983) Satellite observations of variations in Southern Hemisphere snow cover. NOAA Technical Report NESDIS 1, U.S. Department of Commerce, Washington, D.C., 20pp.
- Dickson, R.R. (1984) Eurasian snow cover versus Indian monsoon rainfall. Journal of Climate and Applied Meteorology, v.23, p.171-173.

- Dickson, R.R.; Posey, J. (1967) Maps of snow-cover probability for the Northern Hemisphere, Monthly Weather Review, v.95, p.347-353.
- Kukla, G.; Gavin, J. (1983) Recent fluctuations of Northern Hemisphere snow cover in autumn. (In: Eighth Annual Climate Diagnostics Workshop, Proceedings held at Downsview, Ontario, Canada, p.289-296).
- Kukla, G.; Kukla, H.J. (1974) Increased surface albedo in the Northern Hemisphere, Science, v.18, p.239-253.
- Kukla, G; Robinson, D. (1979) Accuracy of snow and ice monitoring. (In: Crane, R.G., ed. Glaciological Data Report GD-5. University of Colorado, Boulder, Colorado, p.91-98).
- Kukla, G; Robinson, D. (1981) Climatic value of operational snow and ice monitoring. (In: Kukla, G; Hecht, A; Wiesnet, D., eds. Glaciological Data Report GD-11. University of Colorado, Boulder, Colorado, p.103-119).

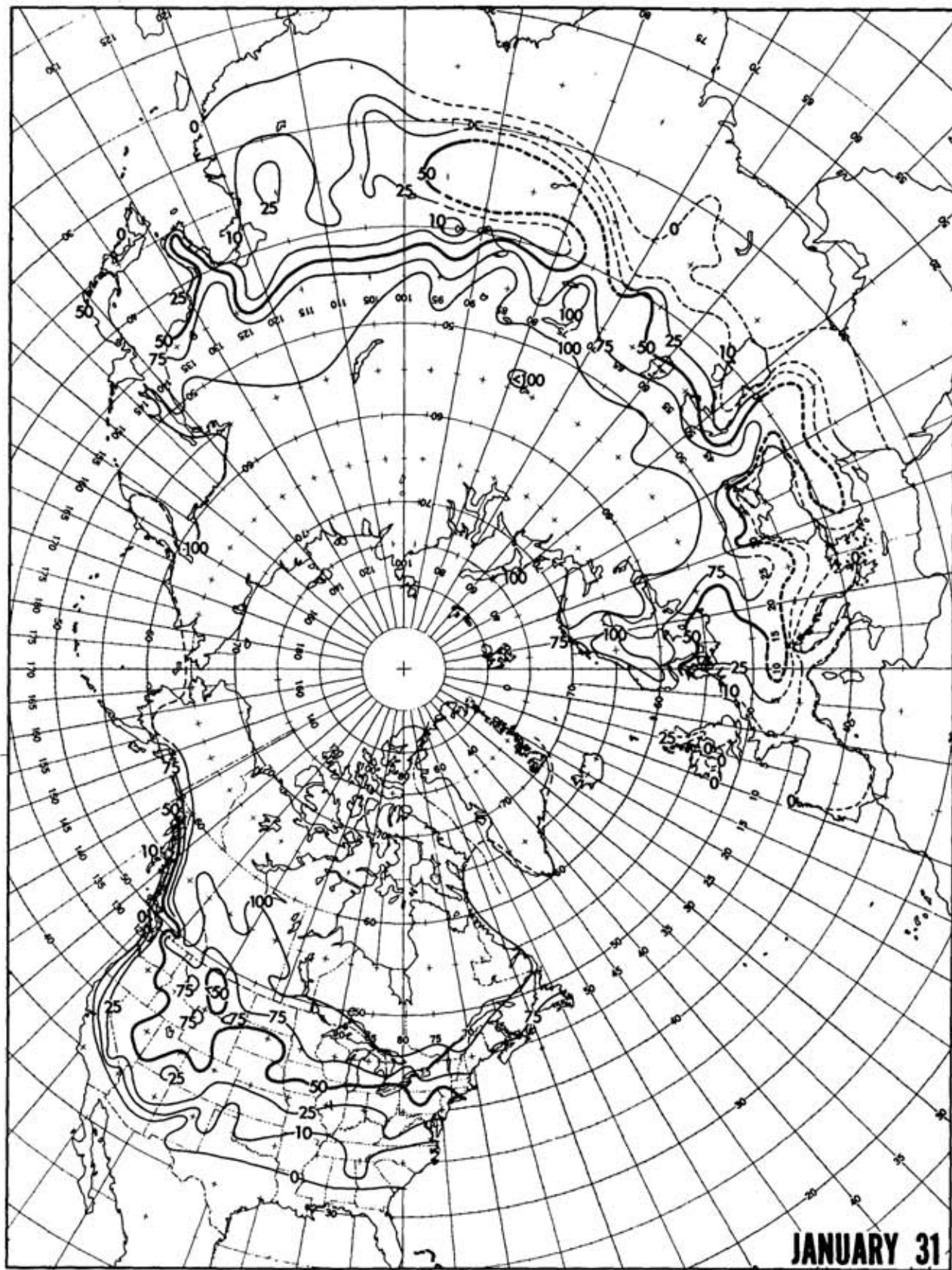


Figure 1. Northern Hemisphere snow cover probability map for January 31 based on ground data. From Dickson and Posey (1967).

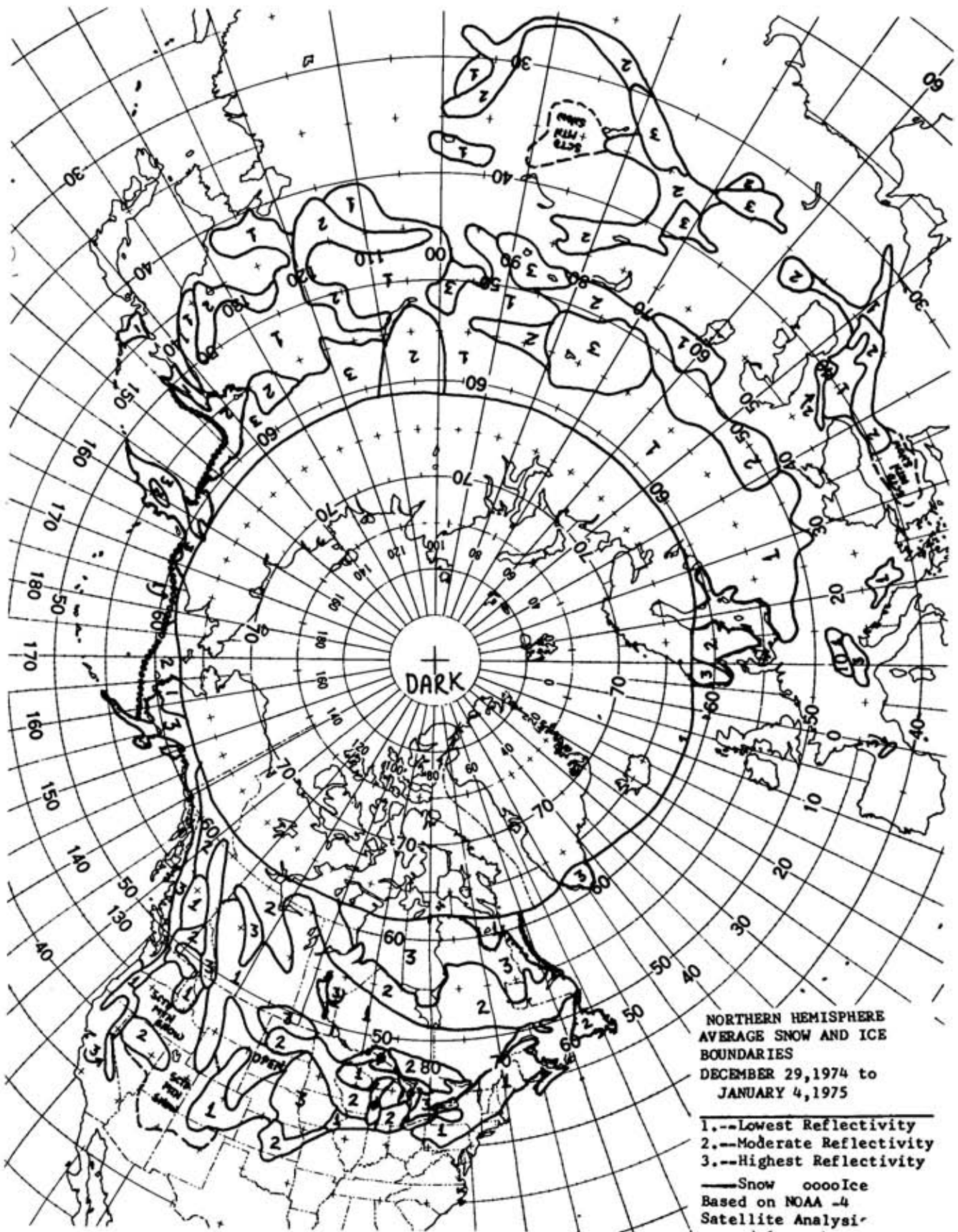
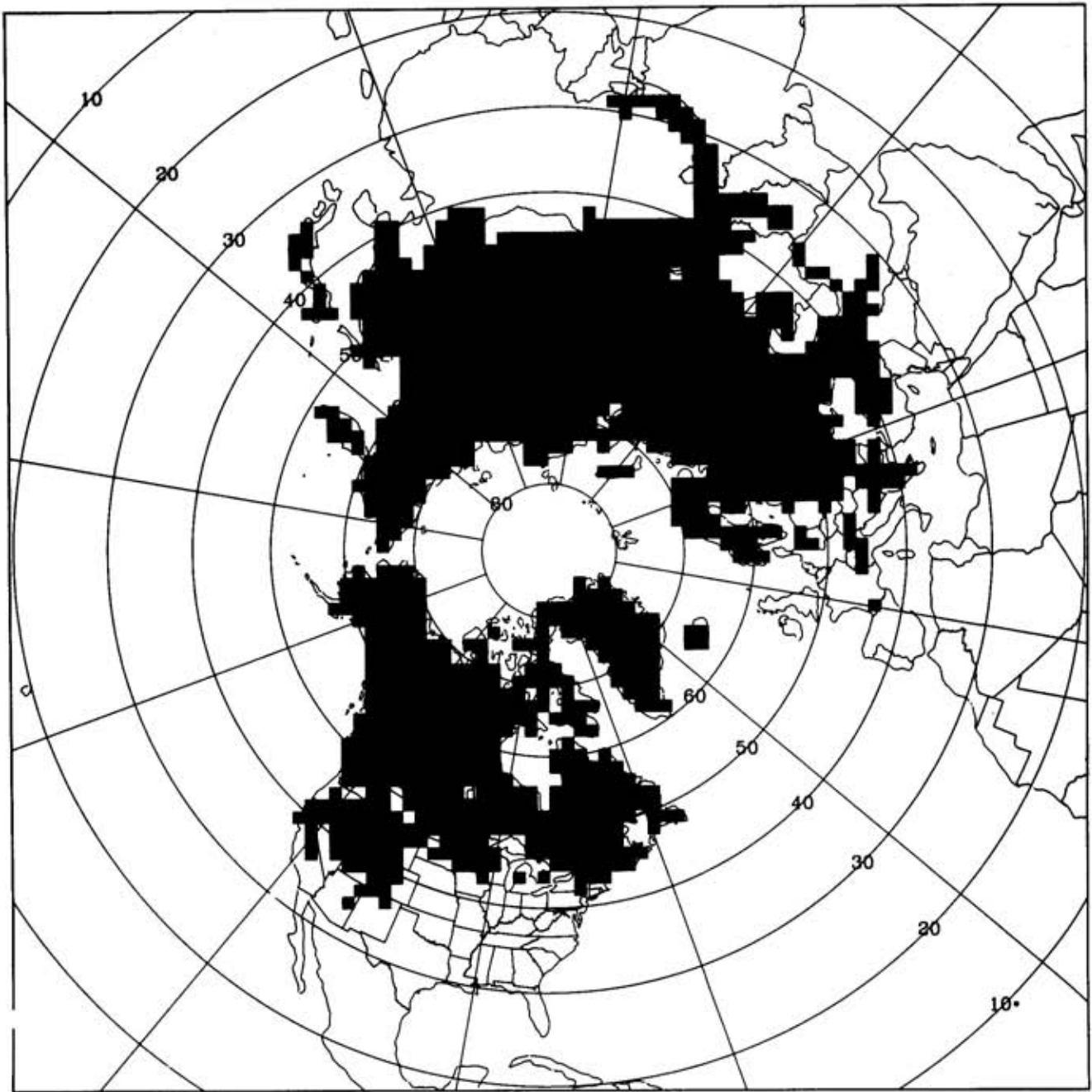


Figure 2. NOAA Northern Hemisphere Weekly Snow and Ice Cover Chart for the period December 19, 1974 to January 4, 1975.

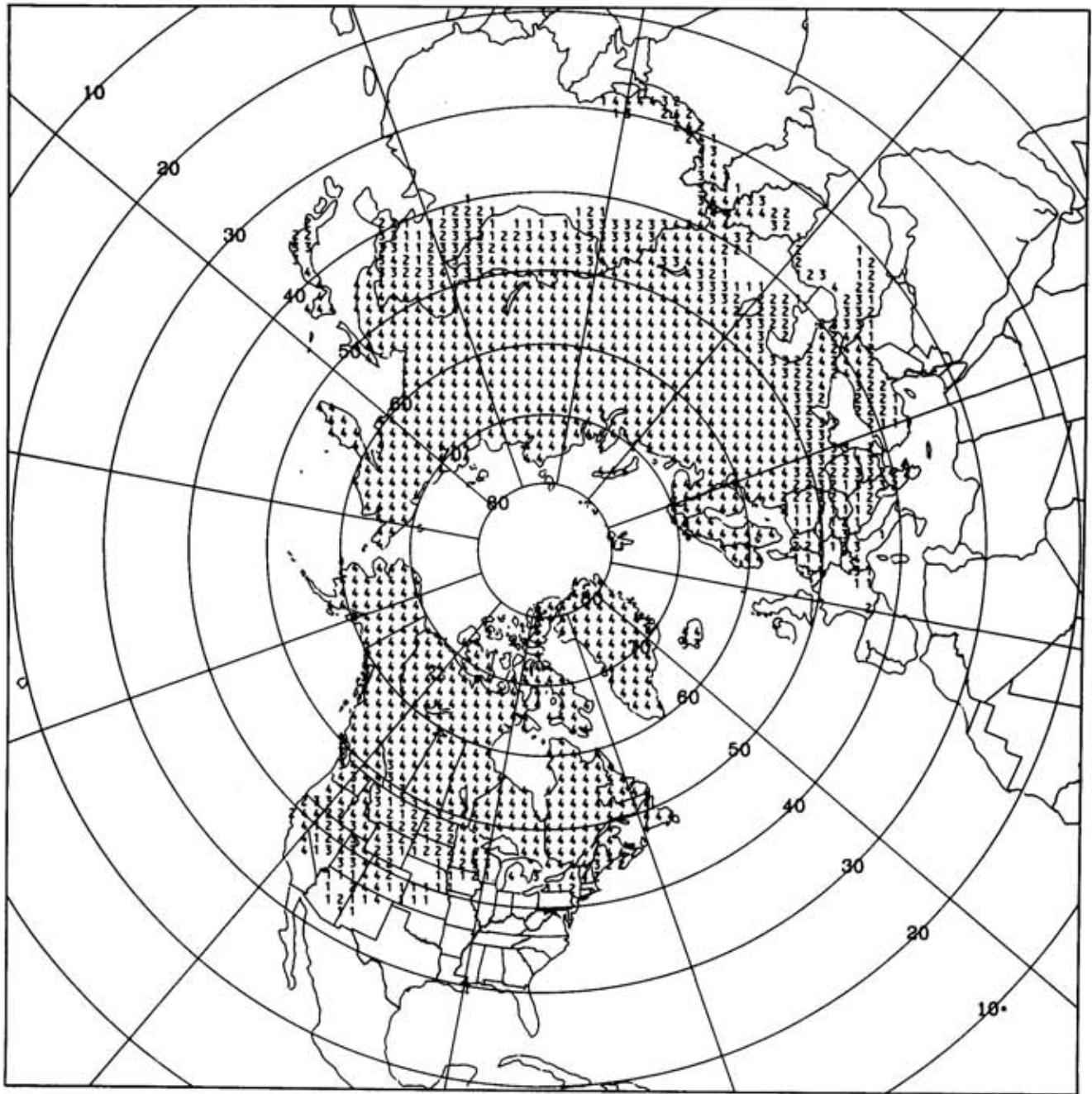


NOAA/NESS

MARCH 1985

MONTHLY MEAN SNOW COVER

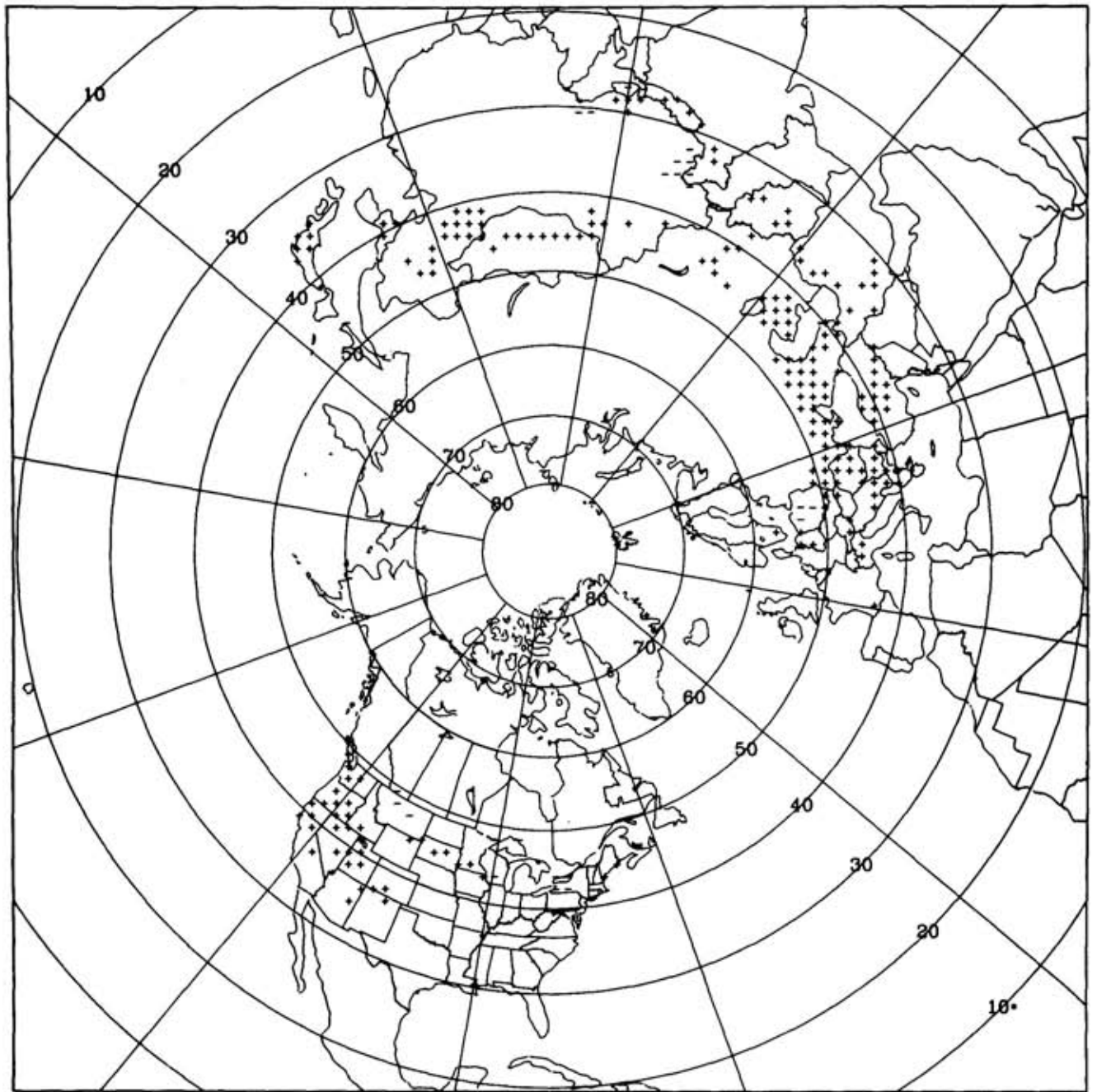
Figure 3. Digitized monthly mean Northern Hemisphere snow cover map for March 1985.



NOAA/NESS

MARCH 1985 FREQUENCY OF SNOW COVER

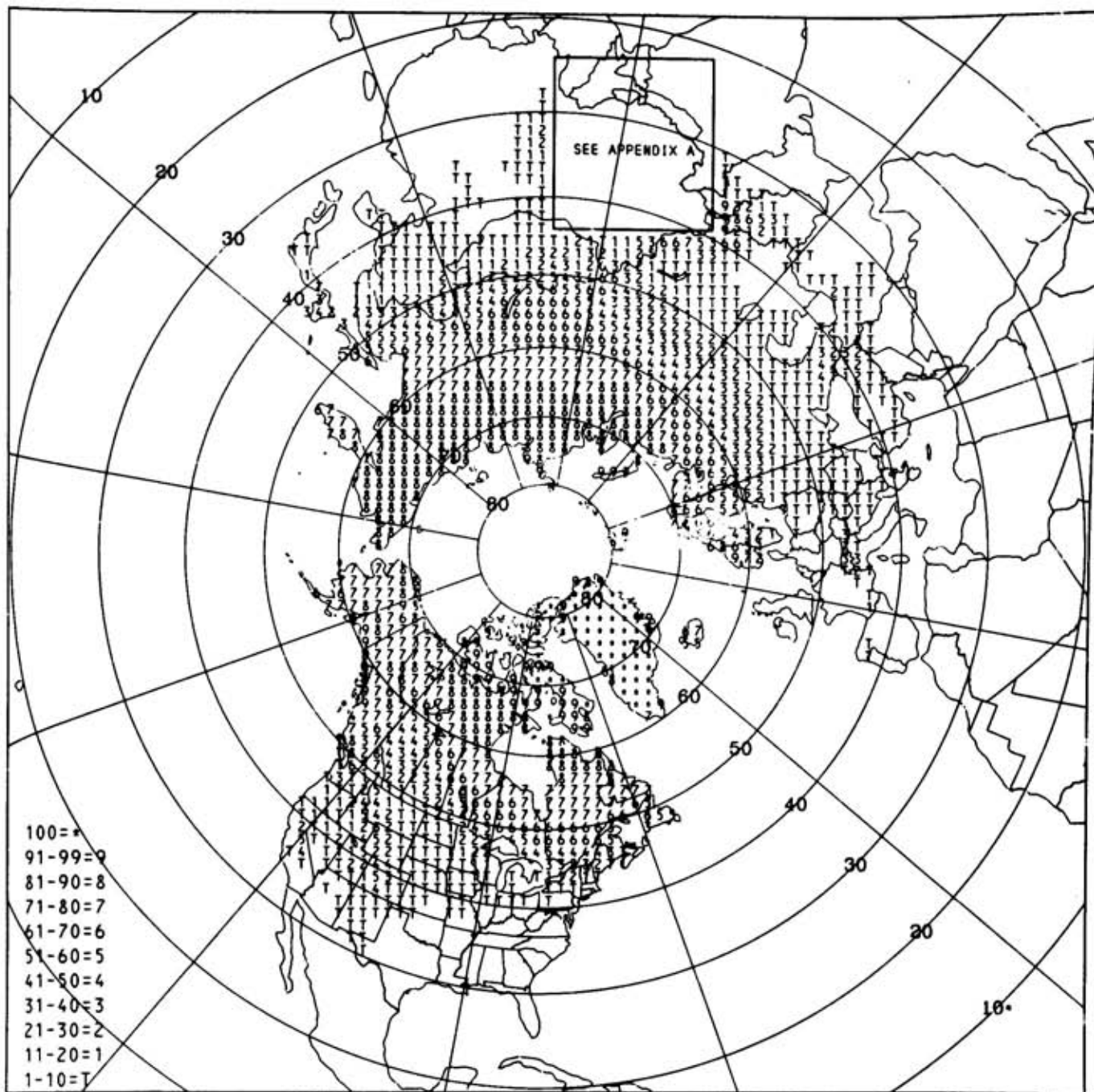
Figure 4. Digitized monthly Northern Hemisphere snow cover frequency map for March 1985. The numbers represent how many weeks snow cover was on the ground for the area.



NOAA/NESS

MARCH 1985 MONTHLY MEAN SNOW ANOMALY

Figure 5. Digitized monthly Northern Hemisphere snow cover anomaly map for March 1985. A comparison is made between the monthly 50% snow cover line and a satellite-based 15-year 50% snow cover line. Areas of excess snow cover are shown by a "+" and areas of deficit snow cover are shown by a "-".



15 YEAR APRIL SNOW COVER FREQUENCY MAP

Figure 6. A digitized satellite-based 15-year snow cover frequency map for April. The alphanumeric coding represents snow cover frequency expressed as a percentage of 100. The boxed area is calculated as a separate map due to bad data in the early years of the data set.

1977 SNOW SEASON
SOUTH AMERICA

— 7-YEAR MEAN

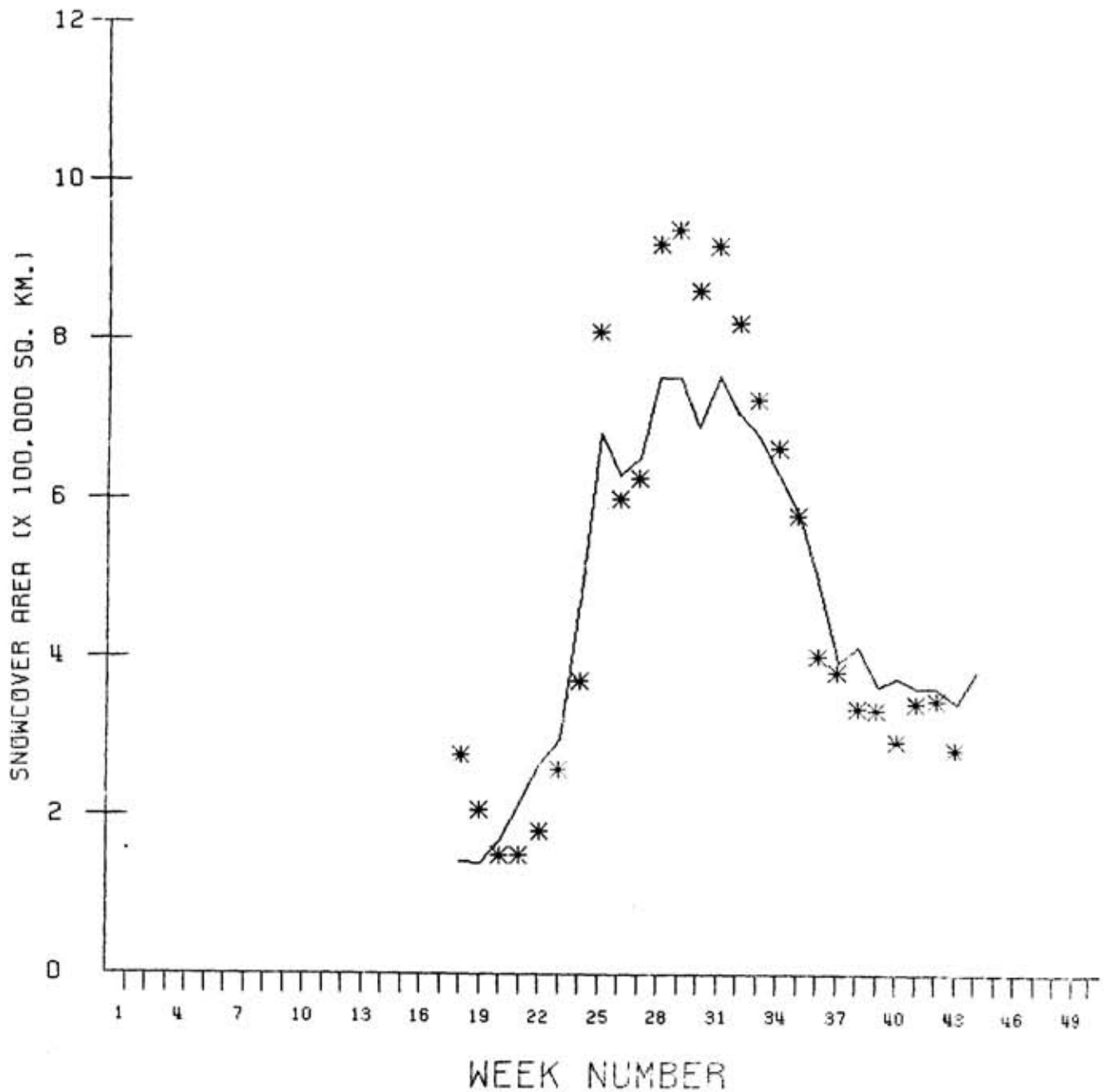


Figure 7. Satellite-based snow cover areas for South America during 1977 compared to a 7-year satellite-based climatology. The week numbers begin with the first week in January.

Kukla, G; Barry, R.G.; Hecht, A.; Wiesnet, D. eds. (1986) SNOW WATCH '85. Proceedings of the Workshop held 28-30 October 1985 at the University of Maryland, College Park, MD. Boulder, Colorado, World Data Center A for Glaciology (Snow and Ice), Glaciological Data, Report GD-18, p.125.

Joint Ice Center Global Sea Ice Digital Data

Charles E. Gross
U.S. Navy/National Oceanic and Atmospheric Administration
Joint Ice Center
Suitland, Maryland, U.S.A.

Digital sea ice data for Arctic and Antarctic regions are now being distributed through the National Snow and Ice Data Center, Boulder, Colorado. These data were digitized and gridded from the weekly sea ice charts produced by the U.S. Navy-National Oceanic and Atmospheric Administration Joint Ice Center (JIC). The gridded data are spaced at no greater than 15 nm intervals on an evenly divisible latitude-longitude geographic grid. Sea ice concentrations, ice type, surface features and other related information are coded using the proposed WMO standard SIGRID (sea ice grid) system.

The weekly gridded sea ice data were digitized from weekly operational ice charts produced by the JIC and its predecessor, the U.S. Navy Fleet Weather Facility. The original charts were produced on a scale of 1:11.6 million for the Arctic and 1:16 million for the Antarctic. Charts were plotted on an azimuthal equidistant projection with the point of tangency at the poles. The smallest homogeneous area resolved by the mapping system is less than 4 km under typical conditions and 40 km under the worst. Boundries are accurate to less than 20 km under typical conditions.

Data sets available include Antarctic data for January 1973 through December 1982, Eastern Arctic data (90 W-90 E) and Arctic West (90 E-90 W) for January 1972 through through December 1982. Annual updates for each data set are anticipated, normally in mid-summer for the previous calender year. Details of the digital format may be found in Proposed Format for Gridded Sea Ice Information, T.Thompson,1981, 27p; report prepared for the World Climate Program,WMO. Copies are available from the National Snow and Ice Data Center.

Kukla, G; Barry, R.G.; Hecht, A.; Wiesnet, D. eds. (1986) SNOW WATCH '85. Proceedings of the Workshop held 28-30 October 1985 at the University of Maryland, College Park, MD. Boulder, Colorado, World Data Center A for Glaciology (Snow and Ice), Glaciological Data, Report GD-18, p.127-139.

Snow Cover Data: Status and Future Prospects

Roger G. Barry
National Snow and Ice Data Center
Cooperative Institute for Research in Environmental Sciences
University of Colorado
Boulder, Colorado, U.S.A.

Abstract

Snow cover data are collected by a range of national meteorological and hydrological agencies and globally since the mid-1960s by satellite remote sensing. There are major problems of incompatibility between the various types of ground measurement even within a single country. Satellite information up to now refers only to snow cover extent and it is limited by cloudiness and resolution. There is also uncertainty as to what parameter (snow depth, effective integrated short-wave reflectivity, etc.) is of most relevance for climate studies as compared with hydrological prediction. A survey is given of the present status of snow cover data and its availability for North America and European countries.

New satellite systems will bring rapid changes and opportunities. The feasibility of snow cover mapping with multifrequency passive microwave radiometer data can be exploited with NASA, NOAA, and DMSP sensors by the late 1980s. In addition, NOAA polar orbiters will carry a 1.5-1.6 micrometer sensor capable of snow-cloud discrimination. Coordinated planning to ensure maximum use of these systems is urgently needed.

Introduction

Snow cover data are collected in different countries by a wide range of national agencies to serve a variety of purposes. Meteorological and hydrological services are most commonly responsible for ground measurements of snow cover, but in the United States certain data are also collected by the Soil Conservation Service and the Forest Service of the U.S. Department of Agriculture. There are, consequently, many problems of incompatibility between the various types of measurement even within a single country.

This paper reviews the requirements for snow cover data and the availability of data sets for selected European countries and for North America. Following this assessment of ground observations, the present status of, and future prospects for, satellite-based data on snow cover are discussed.

Data Requirements

Information on snow is required by several types of user. For example, near-real time (operational) information is needed for hydrological forecasts of runoff and flood risk, avalanche warnings, and for urban highway, and airport snow clearance agencies. Retrospective data are required for climate research and for design studies including questions such as snow loads on structures, snow cover frequency for development of ski centers, and risk statistics for insurance companies, etc. The data requirements for each use category differ considerably with respect to the specific variable and the needed space - time coverage.

The variables that are important for meteorological and hydrological research are listed in Table 1. They are defined with respect to the study of the global hydrological cycle from space (National Research Council, 1985). Earlier, more restrictive definitions were proposed for purposes of snow and ice research (NASA, 1979). For example, area coverage for operational needs was specified with a minimum accuracy of 5 percent (desired accuracy 1 percent) with a spatial resolution of 10 km (desired 1 km) and time interval of 7 days (desired 3 days). Even for climate purposes, the accuracy required was 5 percent. Water equivalent was requested for climate and operational purposes with an accuracy of 3 cm/cm² (1 cm/cm² desired). Simpler requirements for snow cover monitoring, identified by working groups of the World Climate Programme (World Meteorological Organization, 1981), are shown in Table 2. At present, only snow cover extent is mapped routinely, at weekly intervals, and this is limited to the northern hemisphere.

Table 1. Minimum observational requirements for snow cover.
(After National Research Council, 1985)

<u>Variable</u>	<u>Observation</u>	<u>Accuracy</u> (Percent)	<u>Resolution</u> (km)	<u>Frequency</u> (weeks)
Extent	Percent of area	10%	50	1
Thickness	Area coverage	10%	50	2
Density	Area coverage	10%	50	2
Water equivalent	Area coverage	10%	50	2
Grain size	Area coverage	10%	50	2
Albedo	Area coverage	4%	100	2

Table 2. World Climate Program requirements for global snow cover monitoring. (Modified from World Meteorological Organization, 1981)

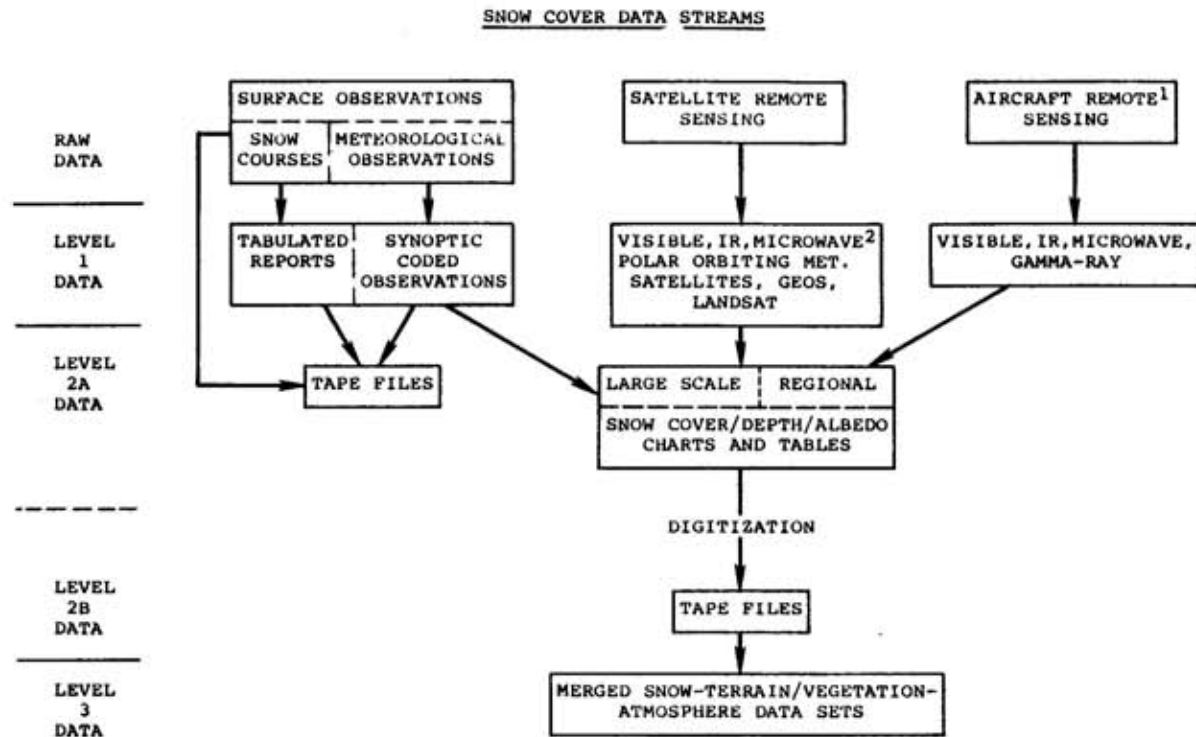
Snow Cover Variable	Type of Observation	Resolution		Accuracy	Duration*	Priority	Observational Methods
		Time	Space				
Extent	Tenths of area covered	3d	100 km square	10%	permanent	1	Visible & IR; passive microwave
Albedo	Average of area	3d	100 km square	+0.03	several years	2	Multispectral radiometry
Water equivalent	Average over area	Winter maximum	100 km square	10%	several years	2	Passive microwave?

* "Permanent" indicates the need for indefinite monitoring. "Several years" indicates that, after a period of research, a reduced monitoring effort may suffice.

Existing Modes of Data Collection

Data on snow cover are collected in a number of ways. Figure 1 identifies the separate data streams for satellite and aircraft remote sensing measurements which provide regional information on snow extent and to a lower level of accuracy on the snow water equivalent. Surface observations fall into two broad categories: meteorological reports of snow depth and snowfall, and snow course or related site measurements of snow water equivalent. The international synoptic weather code has provision for daily reports of depth of snow on the ground whenever at least half of the ground in the vicinity of the station is snow covered. These data, as well as 6- and 24- hourly reports of precipitation are collected through the Global Telecommunications System (GTS) by the three World Meteorological Centers (Washington, D.C., Moscow and Melbourne). Unfortunately, these reports are archived in high volume synoptic data files. At the present time, convenient accessible sets of these global records do not exist.

There are differences in national practices concerning snow data collected for hydrological purposes. In Canada and the United States, various agencies (see Table 3) collect data on snowpack water equivalent from measurements of depth and density at snow courses (Goodison, 1981). Typically, these observations are made at the end of each month, sometimes twice-monthly, through the winter. For the western states, snowpack data and meteorological variables are now collected from more than 500 remote automatic sites, through the snow telemetry (SNOTEL) network. Data are retrieved via ionospheric meteor burst telemetry on a daily, or more frequent basis by interrogation of the stations (Barton and Burke, 1979).



¹ Primarily in a research mode, or operational at the local/regional scale.

² The microwave is used primarily in a research mode.

Figure 1. Snow cover data streams.

In Canada, snow courses are operated by provincial and federal governments. The network has been reduced considerably in recent years, due to costs. Similarly, many meteorological stations, in northern Canada especially, are being converted to automatic stations necessitating changes in measurement procedures and introducing inhomogeneities into station records (see Goodison, this volume).

Data for North America

For both Canada (Canada, Atmospheric Environment Service, 1961 onwards) and the United States (by state), snow course data are published in full. However, these data are not currently available in computer-compatible format. The representativeness of snow course observations is dependent on the land use characteristics, but such effects are not routinely incorporated into spatial analyses (Goodison, 1981). Goodison also showed that if precipitation gauge measurements are corrected, especially for wind effects on catch, these records are then generally compatible with stick observations for seasonal and storm totals.

Table 3 shows that, in addition to the synoptic and snow course data, there are various other data sets with regional coverage in the United States, as well as the map of snow cover prepared for the Weekly Weather and Crop Bulletin (U.S. Department of Agriculture). This map product has been published weekly since 1935 based on station reports for 0900 Local Standard Time on Monday. Until recently it showed station reports as well as selected depth contours; since December 1983, only station reports of snow depth have been shown on the map.

In the western United States, the U.S. Forest Service collected snow cover and climate data as part of its former research and forecasting program on avalanches. Data for between 10 and 30 years for up to 60 stations are now available at the National Snow and Ice Data Center (NSIDC). The extensive data collected for operational purposes since 1979 by the SNOTEL network of the Soil Conservation Service, U.S. Department of Agriculture (Table 3) have not yet been made available for climate and other research by secondary users.

The National Weather Service has carried out an operational program using aircraft measurements of surface gamma radiation emissions to assess snow water equivalent since 1980 (Peck et al., 1980). Data are now available in the NSIDC for five seasons from 800 flight lines over 16 states and three Canadian provinces. They include location, percent snow cover, snow water equivalent, soil moisture and normalized over-snow gamma radiation. Ground-based observations to calibrate the aircraft data and assess the accuracy of the technique continue to be collected in various locations with surface cover types ranging from bare soil or grassland to heavily forested areas.

Table 3. Snow data for North America.

Source	Area	Stations	Variables	Frequency	Period
SCS/USDA	11 W'n States	1600	Depth, Water Content	Monthly (Winter/Spring)	1910s/30s →
Calif. Dept. Water Res.	California	> 400 (Snow Courses)			1930→
SCS/USDA SNOTEL	W'n States	>500	Water Content Precip., Temp.	> Day	(1979) →
USFS Westwide Network	W'n States (Mountains)	50-60	Depth, Snowfall	Daily	1950s/60s →
NOAA Weather and Corp Bulletin	USA	Map	Depth Contours, Point Values	Weekly (Monday)	1935 → (1949-81 digitized by Walsh et al. 1982)
Minnesota State Climatology Office	Minnesota	Map	Depth Contours	Weekly	1977/78 →
NOAA NWS (Gamma Radiation)	USA/Canada	800 flight- lines	Cover, Water Content	> 1/mo.	1980-1985
NOAA Co- operative Observers	USA	5,000	Depth (some precip.)	Daily	1890-1982
AES. (and Provinces)	Canada	1800 (snow courses)	Depth Water Content	Monthly	1955-79
J. Walsh	Canada	140	Depth, Snowfall	Monthly	1950s/60s→

Data for Some European Countries

There are extensive snow cover records for stations in many European countries (Table 4). In some cases these date back to the beginning of the century or earlier. The agencies responsible for these data differ between countries. In Austria, for example, it is the Hydrographic Bureau. In many others it is the national meteorological service. In Switzerland, the Swiss Meteorological Agency maintains one network and the Snow and Avalanche Research Institute (EISLF), Davos, collects supplementary mountain snow data from mountain stations.

Table 4. Snow cover data for some European countries.

Source	Area	Stations	Variables	Frequency	Period
Osterr. Hydrograph Dienst.	Austria	760	Depth Snowfall	Daily	1901 →
Deutscher Wetterdienst	Fed. Rep. Germany	75	Depth Snowfall, Water Content (3/week)	Daily	1961 →
Meteorol. Office	Gt. Britain	200	Days with Snow Cover, Snow Fall	Monthly	1947 →
Meteorol. Office	Gt. Britain	20	Depth	Daily	1947 →
SMHI	Sweden	412	Depth	Daily	1931→
SMA	Switzerland	52	Depth New Snow	Daily	1959/60 →
EISLF	Swiss Alps	45	Depth New Snow	Daily	1949/59 →

Most national agencies publish statistical summaries on a station basis. An example for Austria is given in table 5. This shows annual values of the dates of first and last snow cover as well as dates of stable snow cover, the number of days of snow cover so defined, days of new snowfall, the total seasonal snowfall, the amounts and dates of maximum snow depth and of maximum new snowfall. In addition to station summary data, there are also maps of average snow depths on a monthly basis and average number of days of snow cover (e.g. Pershagen, 1969, for Sweden; Simojoki, 1967, and Lavila, 1972, for Finland).

Although such statistics and maps are widely available (Caspar, 1962; Schuepp *et al.*, 1980, for example), there have been few detailed assessments of their usefulness for climatological purposes. There are obvious limitations to the value of indices such as the duration of snow cover due to the problem of definition. Figure 2 for Sodankyla, Finland, illustrates the interannual variability of snow cover duration. Duration, as defined by earliest and latest snow cover, is influenced greatly by isolated weather events; likewise, in some cases (1936, 1938 and 1942) so would be a measure of the "stable" snow cover. For Zurich, Uttinger (1963) analyzed temperature, precipitation, snowfall and snowcover data for winters 1880/81 - 1960/61. On a yearly basis, days with snowcover were only weakly correlated with snowfall frequency and air temperature, although a general relationship was more apparent for decadal averages of snowcover duration. Differences were also found in the monthly temperature-snowfall frequency-snow cover relationships between early and late winter months at Zurich. Uttinger showed also that there was considerable variability at central European stations in the timing of maxima and minima of snow cover duration from the 1880s to 1950s with quite different trends at several of the stations in this region with long records. These few isolated results point to the need for further investigation of snow cover as a climate variable.

Table 5. An example of snow cover data from Austria, mean and extreme values. (Beitraege zur Hydrographie Oesterreichs, Nr. 46, 1983)

Schneeverhältnisse mit Normalzahlen und Extremwerten													
Zeit- raum	Schnee- bedeckung (a)		Winter- decke (b)		Zahl der Tage mit			Summe der Neu- schnee- höhen		Größte Schnee- höhe		Größte Neuschnee- höhe	
	Beginn - Ende		Beginn - Ende		a	b	Neu- schnee	cm	cm	Datum	cm	Datum	
Nr.: 73		OBERLEUTASCH						Höhe: 1130 m ü. A.					
Mst. Nr.: 101303		LEUTASCHER ACHE						NZ.: 485 cm					
1970/71	03 10 28 04	22 11 12 04	166	142	53	459	125	27 02	51	23 10			
1971/72	10 11 13 05	20 11 24 03	142	125	37	281	64	15 02	27	27 04			
1972/73	21 10 09 05	12 11 09 05	193	179	66	715	136	10 03	39	22 10			
1973/74	19 10 13 06	22 10 13 04	187	174	59	534	134	08 02	54	29 11			
1974/75	29 09 02 06	21 10 30 04	205	192	79	742	126	30 01	45	30 12			
1975/76	11 10 23 05	16 11 13 04	163	149	51	287	71	25 01	32	22 11			
1976/77	08 11 27 04	20 11 27 04	162	159	63	550	96	18 01	48	15 04			
1977/78	03 10 24 06	14 11 29 04	172	167	70	554	113	20 02	35	20 03			
1978/79	18 10 18 06	26 11 09 05	168	165	67	453	98	08 04	25	06 04			
1979/80	22 09 12 05	03 11 12 05	193	191	81	790	124	05 04	40	03 02			
Mittelwerte													
1970/71													
-1979/80	15 10 23 05	11 11 24 04	175	164	63	537	109		40				
1930/31													
-1959/60	24 10 01 05	22 11 11 04	155	140	53	485	126						
1900/01													
-1979/80	26 10 06 05	23 11 14 04	156	143	54	485	118						
Extremwerte													
frühester Eintritt bzw. Minimalwerte													
1970/71	22 09 27 04	21 10 24 03	142	125	37	281	64	15 02	25	06 04			
1979 1977	1979 1977	1974 1972	1972	1972	1972	1972	1972	1972	1979	1979			
-1979/80	10 11 24 06	26 11 12 05	205	192	81	790	136	10 03	54	29 11			
spätester Eintritt bzw. Maximalwerte													

Future Products

For climate research and monitoring there is a clear need for consistent global snow cover data on a daily basis. At present, the weekly satellite-derived products are limited by problems of persistent cloud cover in some areas, and by interpretation difficulties in mountains and in areas where vegetation or land use cause small-scale heterogeneity and masking effects. The surface data are limited in terms of uncertain spatial representativeness and the difficulty and cost of data access.

New satellite sensor systems that are planned to be launched over the 1986-1990 time frame will provide opportunities for significant improvements in snow cover data products. Analysis of data from an experimental 1.5 - 1.6 micrometer sensor on the Defense Meteorological Program Satellite, flown in 1979, shows that this channel allows useful discrimination of snow cover and cloud (Scharfen and Anderson, 1982; Crane and Anderson, 1984). A similar AVHRR sensor will be flown on the NOAA polar orbiters in 1989 and daytime data

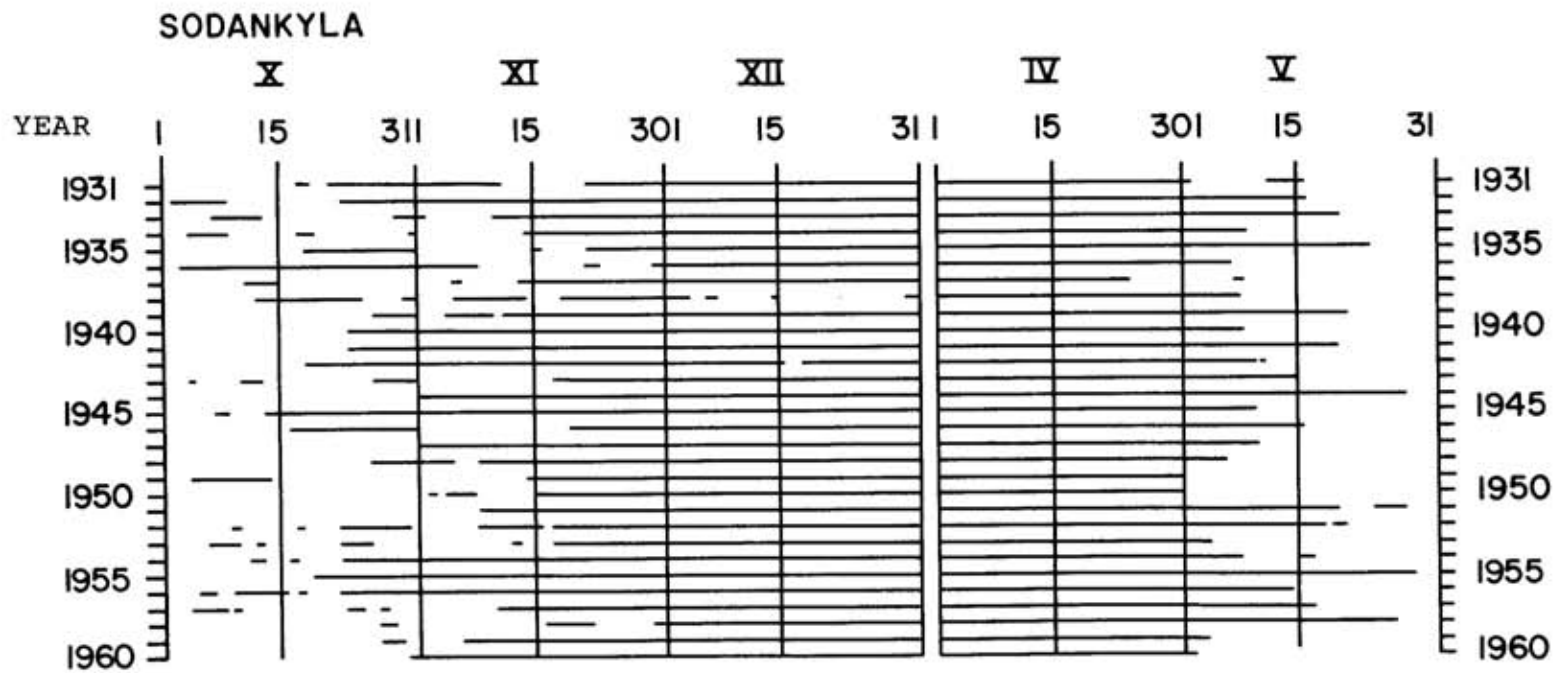


Figure 2. Time plot of seasonal snow cover, 1931-60 at Sodankyla, Finland (after Lavila, 1972).

from this channel can be combined with visible and infrared channel data to differentiate cloud from snow cover in mountain areas or wherever cloud cover exhibits persistence, especially over snow covered ground.

Research with multifrequency passive microwave data from the Nimbus 7 SMMR has demonstrated a valuable capability to map snow cover with 25 km resolution even in the presence of cloud (unless it has a high liquid water content). Some information on snow pack water equivalent can be obtained, and discrimination of thawing and dry snow is also feasible (Kunzi *et al.*, 1982; Foster *et al.*, 1984; Chang, this volume). Further work to validate the algorithms is needed, although the possibility of this is still limited by the meager data base of surface observations. Nevertheless, it is anticipated that the routine availability of such satellite-derived products will itself stimulate verification assessments for a range of geographical environments and "snow cover climates" (e.g. Hall, this volume).

Multifrequency passive microwave data will be collected by the Special Sensor Microwave Imager (SSM/I) on a DMSP satellite due to be launched in mid-1986. The National Snow and Ice Data Center has been supported by NASA Ocean Sciences program to develop a Cryospheric Data Management System (CDMS) for sea ice products on a VAX (VMS)-750 computer system, employing software specially developed by the Pilot Ocean Data System (PODS) at the Jet Propulsion Laboratory, Pasadena. The Navy-NOAA Joint Ice Center will use operational sea ice products, produced by the Fleet Numerical Oceanographic Center using an interim algorithm whereas the NSIDC products will employ the NASA Science Working Group algorithm (Weaver and Barry, 1985). It is anticipated that separate funding may be secured to incorporate snow cover algorithms into the software in order to demonstrate prototype snow cover products.

The SSM/I snow and ice products will fill the gap between the data from SMMR, which was launched on Nimbus 7 in 1978 and has already far exceeded its design life time, and the data expected from NOAA polar orbiters to be equipped with an Advanced Microwave Sounding Unit (AMSU) in 1990 (Yates, 1985; Grody, this volume).

A question remaining to be addressed is how the various new data sets (visible, infrared and passive microwave) will be integrated into consistent snow cover products. In the near term, it may be preferable to provide all of the independently-derived products. Determination of the optimal procedures for combining them into conventional snow cover variables (cf. Table 1) will be a task for future research. It is, for example, unclear whether/how to integrate surface point observations with spatially-averaged satellite pixel data. Ultimately, however, the preparation of a selected range of variables for permanent archiving may be decided through a working group. The raw scientific data (radiances, brightness temperatures etc.) should also be archived in suitable gridded formats.

Summary

The researcher requiring snow cover data for global climate or hydrological studies is considerably hampered at present. The meteorological data on snow cover have been summarized by national agencies in most countries for average monthly conditions at individual stations and in map form, but the variables provided differ from country-to-country. Archives of daily/weekly

station or gridded data are largely non-existent in conveniently accessible form. Data availability is also seriously proscribed by cost considerations.

Weekly snow cover maps have been produced for the Northern Hemisphere from satellite data by manual techniques since 1966 and are now available in digital form. Some discrepancies exist between these products and station data, particularly as a result of the compositing of weekly information. Microwave data products, demonstrated as a research capability, will eventually provide a valuable all-weather information source, although their resolution is only about 25 km (12.5 km for the snow boundary). The advent of new sensor systems over the 1986-1990 time frame offers new opportunities, provided that adequate financial resources are available for production and archiving of the data sets and for research to test and validate the algorithms and products. Snow cover data and research have been largely neglected by various funding agencies because, outside of the polar regions, the topic does not fall centrally within the purview of any single discipline or agency. Moreover, the accessibility of much satellite and other data is a major hindrance to researchers. The importance of resolving this problem has recently been recognized by the Space Science Board, Committee on Earth Sciences (National Research Council, 1985, p.142).

Acknowledgement

This paper was supported in part by the Department of Energy, Carbon Dioxide Research Division under contract DE-AC02-83ER60106.

References

- Barton, M; Burke, M. (1979) SNOTEL: An operational data acquisition system using meteor burst technology. World Data Center A for Glaciology [Snow and Ice]. Glaciological Data. Report GD-6, Snow Cover, p.59-69.
- Canada, Atmospheric Environment Service (1961) Snow Cover Data. Environment Canada, Downsview, Ontario (Annual)
- Caspar, W. (1962) Die Schneedecke in der Bundesrepublik Deutschland. Deutsche Wetterdienst, Zentralamt, Offenbach am Main, 456p.
- Chang, A.T.C. (1986) Nimbus-7 SMMR snow cover data. World Data Center A for Glaciology [Snow and Ice]. Glaciological Data. Report GD-18, Snow Watch '85, p.181-187.
- Crane, R.G.; Anderson, M.R. (1984) Satellite discrimination of snow/cloud surfaces. International Journal of Remote Sensing, 5, p.213-223.
- Foster, J.L.; Hall, K.K.; Chang, A.T.C. (1984) An overview of passive microwave snow research and results. Reviews of Geophysics and Space Physics, 22, p.195-208.
- Goodison, B.E. (1981) Compatibility of Canadian snowfall and snow course data. Water Resources Research, 17, p.893-900.

- Grody, N.C. (1986) Snow cover monitoring using microwave radiometry. World Data Center A for Glaciology [Snow and Ice]. Glaciological Data. Report GD-18, Snow Watch '85, p.189-192.
- Hall, D.K. (1986) Influence of snow structure variability on global snow depth measurement using microwave radiometry. World Data Center A for Glaciology [Snow and Ice]. Glaciological Data. Report GD-18, Snow Watch '85, p.161-171.
- Hydrographischer Dienst in Osterreich (1962) Der Schnee in Osterreich im Zeitraum 1901-1950. Beitrage zur Hydrographie Osterreichs, nr.34, Hydrographischer Dienst in Osterreich, Vienna, 174p.
- Kunzi, K.F.; Patil, S.; Rott, H. (1982) Snow-cover parameters retrieved from Nimbus-7 scanning multichannel microwave radiometer (SMMR) data. IEEE Transactions, Geosciences and Remote Sensing, GE-20, p.452-467.
- Lavila, T.O. (1972) Die Schneedeckenzeit in nordlichen Kalottengebiet in der Normalperiode 1931-1960. Publ. Inst. Geogr. Univ. Oulu., 40, 47p.
- National Aeronautics and Space Administration (1979) Ice and Climate Experiment (ICEX). Report of Science and Applications Working Group, Goddard Space Flight Center, Greenbelt, MD.
- National Research Council (1985) A Strategy for Earth Science from Space in the 1980's and 1990's. Part II. Atmosphere and Interactions with the Solid Earth, Oceans, and Biota. Committee on Earth Sciences, Space Science Board. National Academy Press, Washington, DC, 149p.
- Peck, E.L.; Carroll, T.R.; Vandemark, S.C. (1980) Operational aerial snow surveying in the United States. Hydrological Sciences Bulletin, 25, p.51-62.
- Pershagen, H. (1969) Snotacket i Sverige 1931-60. Meddel. Ser. A, No. 5, Sveriges Met. Hydrol. Inst., Norrkopping, 45p.
- Scharfen, G.; Anderson, M.R. (1982) Climatic applications of a snow/cloud discrimination sensor. (In: Western Snow Conference, 50th, Reno, Nevada, April 19-23, 1982. Proceedings, p.92-101.)
- Schuepp, M.; Gensler, G.; Bouet, M. (1980) Schneedecke und Neuschnee Klimatologie der Schweiz, 24/F. Schweiz. Met. Anstalt, Zurich, 63p.
- Simojoki, H. (1947) Uber dem Zeitpunkt des Entstehens und des Verschwinden der dauernden Schneedecke in Finland. Fennia, v.70, 31p.
- Uttinger, H. (1963) Die Dauer der Schneedecke in Zurich. Archiv fur Meteorologie, Geophysik und Bioklimatologie, B12, p404-421.
- Weaver, R.L.; Barry, R.G. (1985) Cryospheric Data Management System for Special Sensor Microwave Image DMSP Data. (In: Ocean Engineering and the Environment. Oceans '85 Conference Report. Marine Technology Society, Washington, D.C., p.411-415.)

World Meteorological Organization (1981) Report of the Informal Planning Meeting on WCP Data Management. WCP-17, World Meteorological Organization, Geneva.

Yates, H.W. (1985) U.S. operational space program for climate observations. (In: Space Observations for Climate Studies, Ohring, G.; Bolle, H.-J., eds. Advances in Space Research, 5(6), p.31-38.)

Kukla, G; Barry, R.G.; Hecht, A.; Wiesnet, D. eds. (1986) SNOW WATCH '85. Proceedings of the Workshop held 28-30 October 1985 at the University of Maryland, College Park, MD. Boulder, Colorado, World Data Center A for Glaciology (Snow and Ice), Glaciological Data, Report GD-18, p.141-160.

Comparison of Northern Hemisphere Snow Cover Data Sets

Alan Robock
John Scialdone
Cooperative Institute for Climate Studies
Department of Meteorology
University of Maryland
College Park, Maryland, U.S.A.

ABSTRACT

Four Northern Hemisphere snow cover data sets are compared on a weekly basis for the 25-month period, July 1981 through July 1983. The data sets are the NOAA/NESDIS Weekly Snow and Ice Chart, the Composite Minimum Brightness (CMB) Chart, the United States Weekly Weather and Crop Bulletin (data only for North America), and Air Force data. The NOAA/NESDIS Chart is produced through the use of photo-interpretation of visible satellite imagery and ground observations. The United States Crop Bulletin is also done manually, using only ground observations. The CMB Chart and the Air Force data are both produced using automated processes, the first by way of visible satellite imagery and the second by way of ground observations, climatology, satellite observations, and persistence. Since the NOAA/NESDIS Chart is the only standard and complete data set dating back to the mid-1960's, it is used as the basis for the study. The main emphasis of this paper is a comparison of the CMB and the NOAA/NESDIS Chart.

The CMB frequently overestimated snow cover, especially the southward extent of the main Arctic snow boundary and areas far from the snow boundary which were not present on the NOAA/NESDIS Chart. On numerous occasions, the outline of mountain ranges was either distorted or totally missed by the CMB. The CMB also underestimated snow cover, especially in densely populated forested areas. Other regions of underestimation by the CMB can be attributed to the bias factor of the NOAA/NESDIS Chart (the NOAA/NESDIS Chart uses the latest snow cover information while the CMB is composited over a week). The United States Crop Bulletin agreed fairly well with the NOAA/NESDIS Chart east of the Rockies, but differed to the west due to the sparse network of ground observation stations. The Air Force data also overestimated snow cover when compared to the NOAA/NESDIS Chart.

1. Introduction

Snow cover is an important climate parameter. In this paper we compare four snow cover data sets to see how well they portray the weekly average Northern Hemisphere snow cover. The data sets include input from both satellite and ground based observations. A primary emphasis is on the evaluation of the Composite Minimum Brightness (CMB) technique.

In this paper, four Northern Hemisphere snow cover data sets are compared on a weekly basis over a 25-month period from July 1981 through July 1983. These include the NOAA/NESDIS Weekly Snow and Ice Chart, the Composite Minimum Brightness Chart, the U.S. Weekly Weather and Crop Bulletin (CROP), and Air Force data. The NOAA/NESDIS Chart is produced through the use of photo-interpretation of visible satellite imagery and ground observations. The U.S. Crop Bulletin is also done manually, using only ground observations. The CMB Chart and the Air Force data are both produced using automated processes, the first using visible satellite imagery and the second using ground observations, climatology, satellite observations, and persistence. The main emphasis of this project focuses on the evaluation of the CMB chart for use as an "automatic snow cover detection" system. Since the NOAA/NESDIS Chart is the only standard and complete data set, it was used as verification.

2. Data

Figs. 1-4 display examples of each data set for the same weekly period. Fig. 1 is a NOAA/NESDIS Weekly Snow and Ice Chart representing the week of Jan. 11 to Jan. 17, 1982. It reveals the areal extent of the snow cover as well as three categories of brightness determined by the human analyst. Fig. 2 is an actual CMB chart for Jan. 11 to Jan. 18, 1982. This finalized chart shows bright areas representing snow or clouds that persisted during the entire 7-day period. Fig. 3 is a snow cover map taken from the U.S. Weekly Weather and Crop Bulletin for Jan. 18, 1982. This map only covers the United States and southern Canada while showing the actual snow depth values at 1200 GMT, Monday, extent of the snow cover, as well as the boundary for the previous week. An Air Force snow cover map for Jan. 17, 1982 can be seen in Fig. 4. The NCAR graphics package allowed us to display the extent of the snow cover in digital form. Since our only concern was the southern most extent of the snow fields, it was not necessary to access grid points in the northern latitudes.

3. Results

Over the 2-year study period, 108 weekly maps were produced

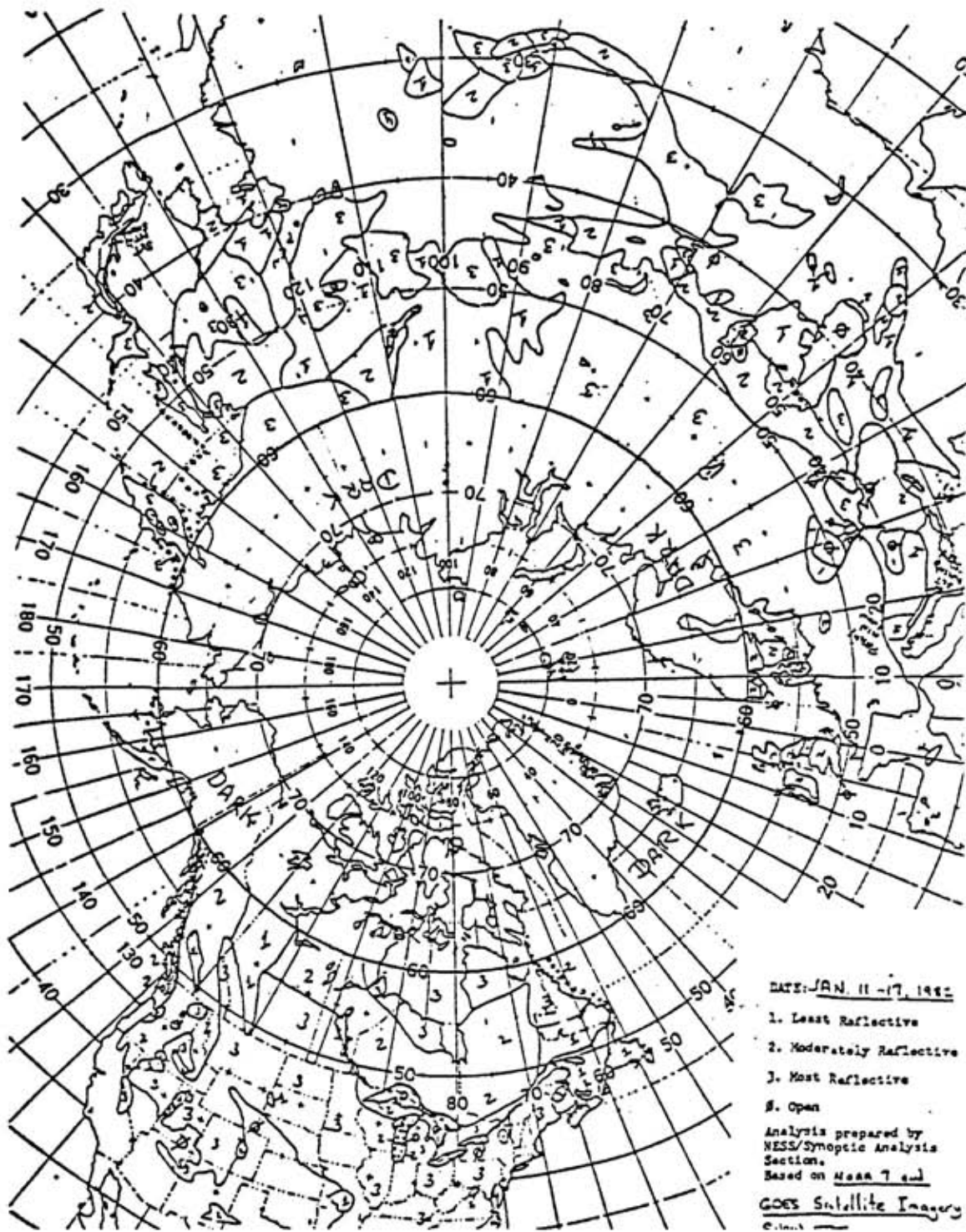


Figure 1. NOAA/NESDIS Weekly Snow and Ice Chart for Jan. 11-17, 1982.



Figure 2. Composite Minimum Brightness Chart for Jan. 11-18, 1982

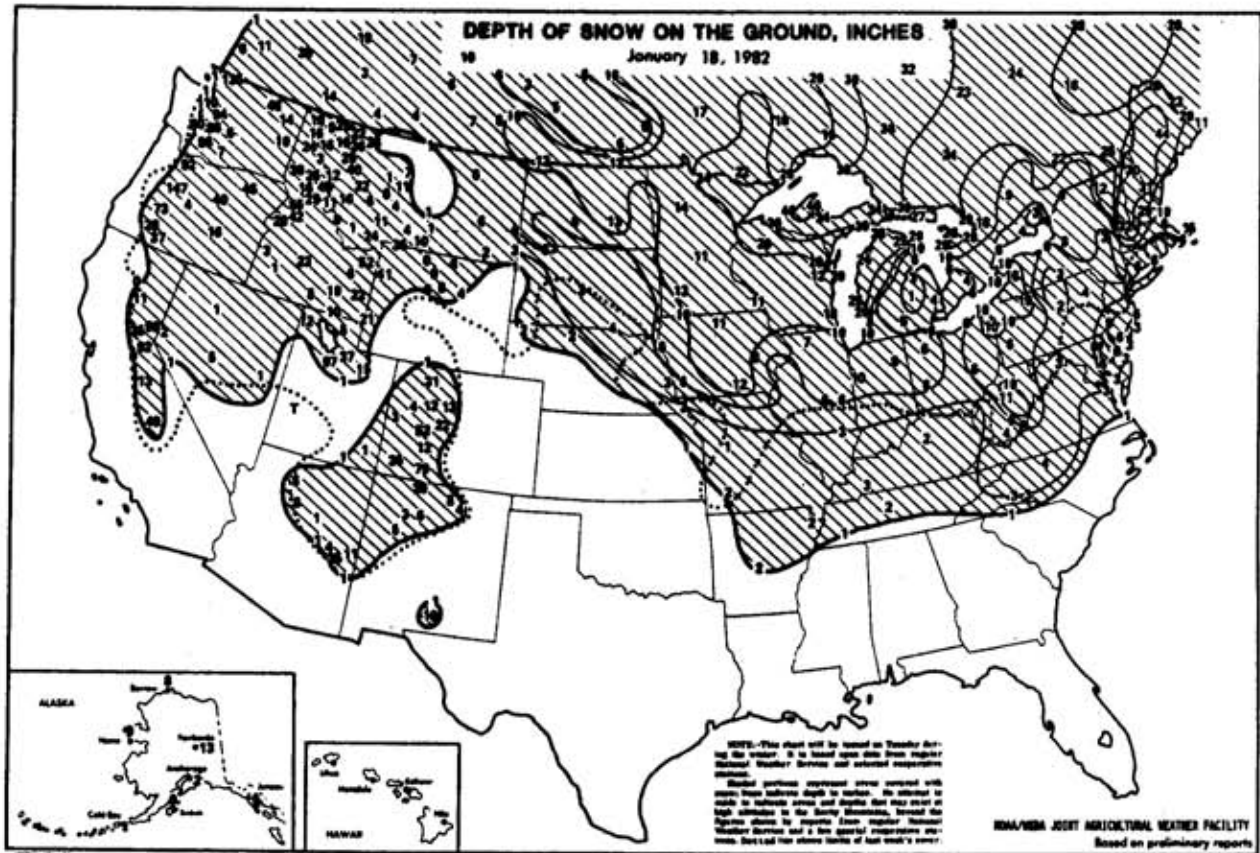


Figure 3. U.S. Weekly Weather and Crop Bulletin Snow Cover Map for Jan. 18, 1982.

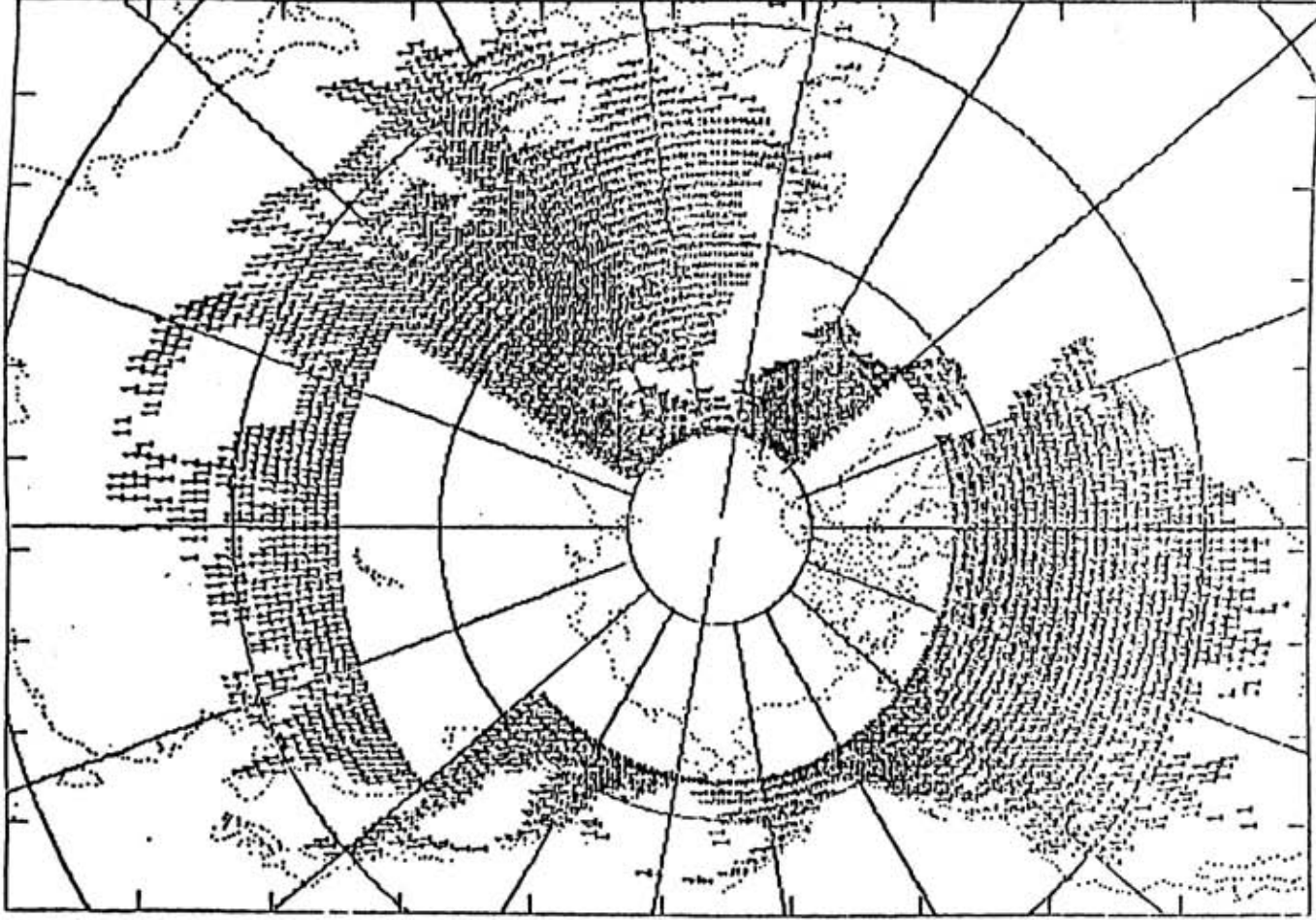


Figure 4. Air Force Snow Cover Chart for Jan. 17, 1982.

to compare the four data sets. In this report, six comparison maps are shown as examples of the similarities and differences (Figs. 5-10). Five problems became apparent when the NOAA snow cover was compared to the CMB snow cover: 1) The CMB extended the main Arctic snow boundary farther south than the NOAA Arctic snow line; This condition appeared in the north Atlantic and Pacific Oceans as well as the Arctic, and land areas in Asia and Europe; 2) Persistent bright areas far from the main Arctic snow boundary occurred quite frequently in southeast and west Asia; 3) The CMB also had trouble with most major mountain regions in the Northern Hemisphere, especially the Himalayas in central Asia. Often the southern part was missed, the whole range was shifted to the east or persistent white areas covered the entire outline. The Rockies of North America posed problems for the CMB except in the winter months, along with the Pyrenees of Spain which went constantly undetected. The CMB handled the Caucasus and Elburz mountains of west Asia fairly well and the Alps were picked up repeatedly; 4) Forested areas of Asia and Japan appeared very dark when snow covered, resulting in underestimation of the snow fields by the CMB; 5) In some areas which were not forested, the CMB still underestimated snow cover with respect to NOAA due to the fact that the CMB shows the minimum for the week while NOAA uses the most recent data with a bias toward the end of the week. CROP agreed fairly well with NOAA east of the Rockies but underestimated snow cover to the west. The AF data overestimated when compared to NOAA, especially in North America, Asia and Europe.

4. Discussion of Results

The bright areas associated with the first two problems are interpreted to be persistent cloudiness. The dominant storm track apparently coincided with the snow boundary. This may have been due to a feedback, where the snow/no snow delineation induced storm formation or paths and the storms produced the snow, but cannot be determined here. Persistent cloudiness also existed frequently in southeast Asia and both oceans where, climatologically, snow cannot occur, while other areas of Asia and Europe were apparently detected as being snow covered by the CMB.

The detection of snow cover in mountain regimes proved to be very difficult using the CMB technique. This problem was produced by positioning errors. Each day, the polar orbiting satellites cover different strips of the earth's surface and the location that they cover must be calculated from imperfect knowledge of the orbits. Furthermore, grid points have a finite size and do not cover exactly the same location on each day, shifting about as orbits vary. The result is that a grid point which includes a mountain and is bright on one day, may be

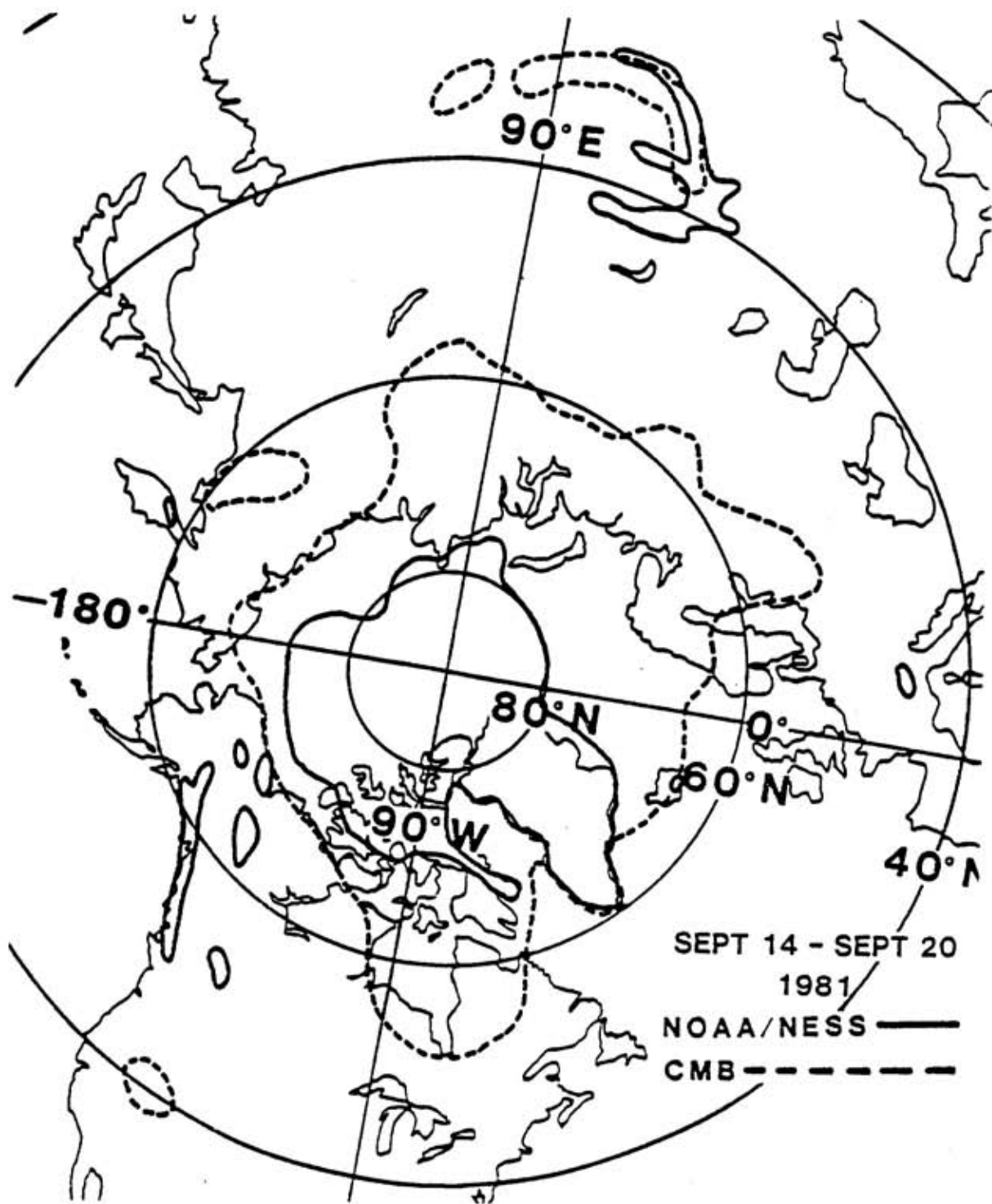


Figure 5. Weekly Comparison Map for Sept. 14-20, 1981.

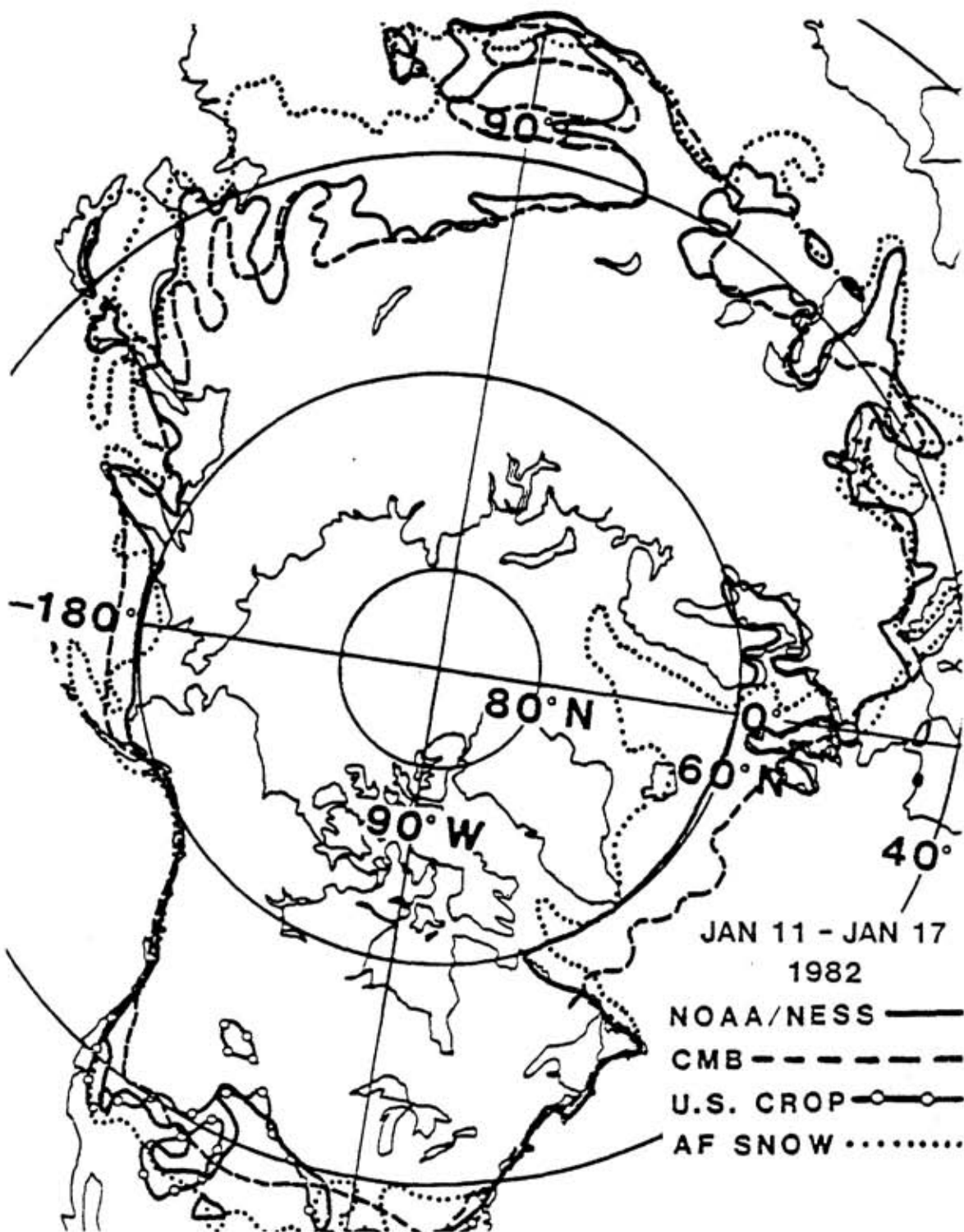


Figure 6. Weekly Comparison Map for Jan. 11-17, 1982.

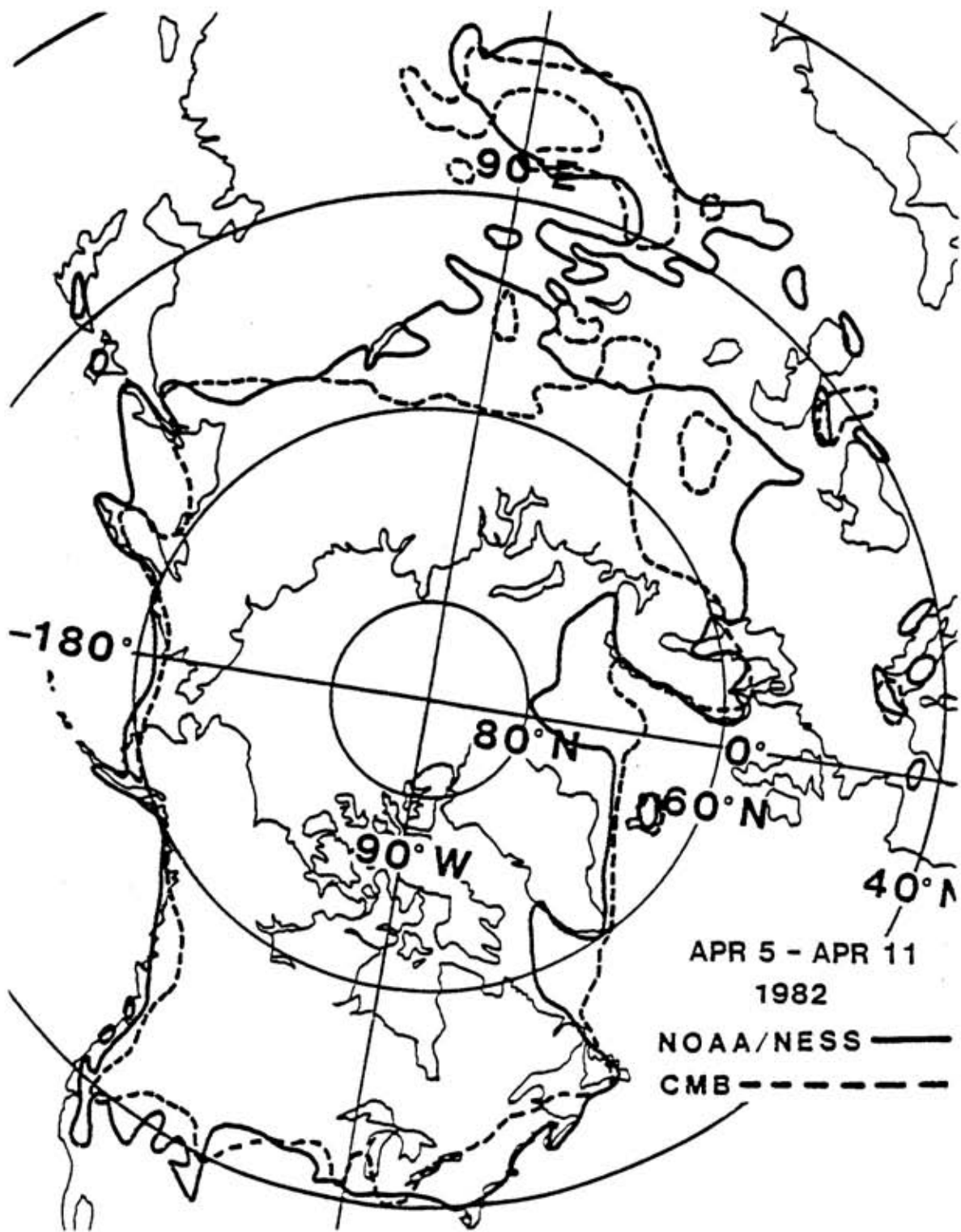


Figure 7. Weekly Comparison Map for Apr. 5-11, 1982.

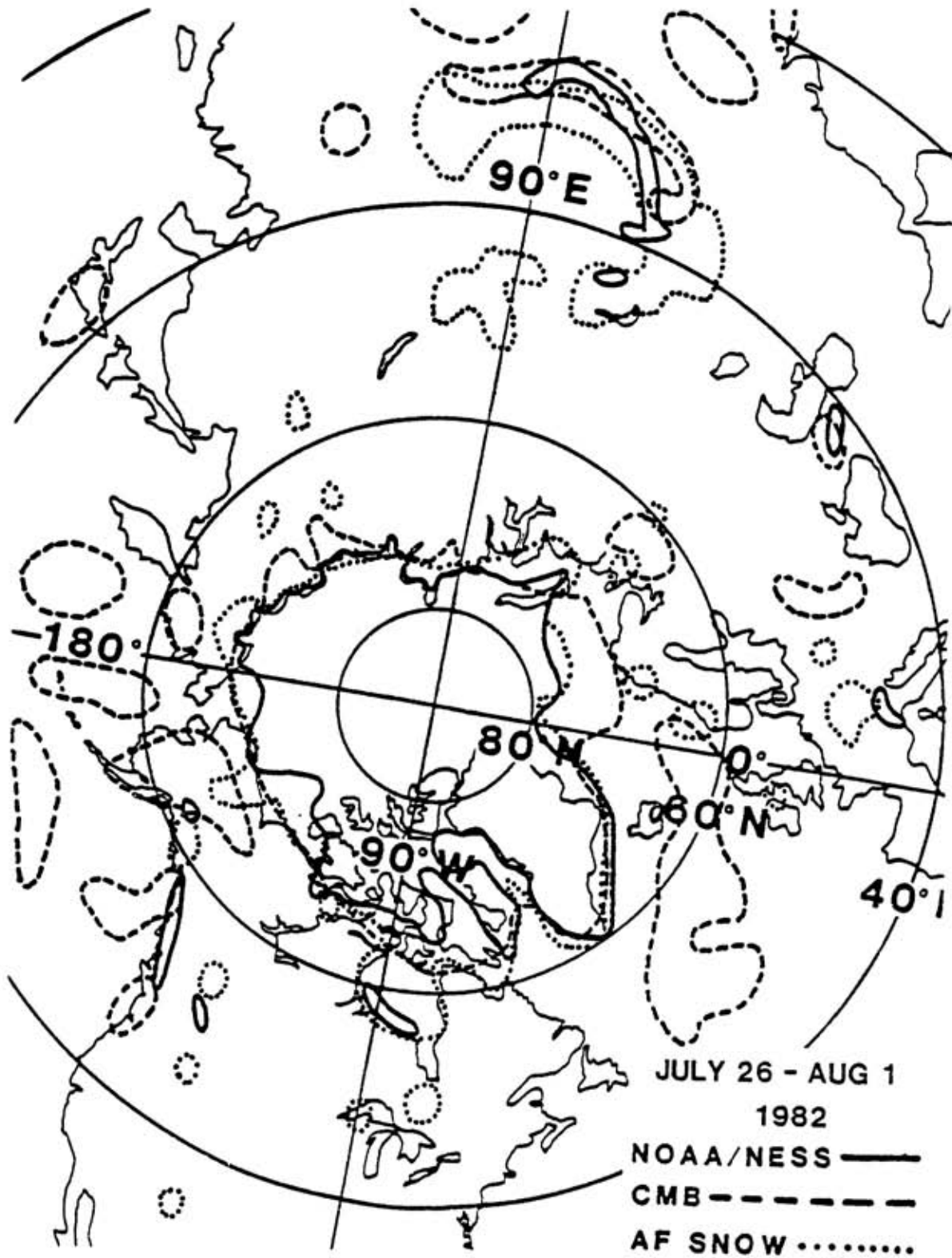


Figure 8. Weekly Comparison Map for July 26-Aug. 1, 1982.

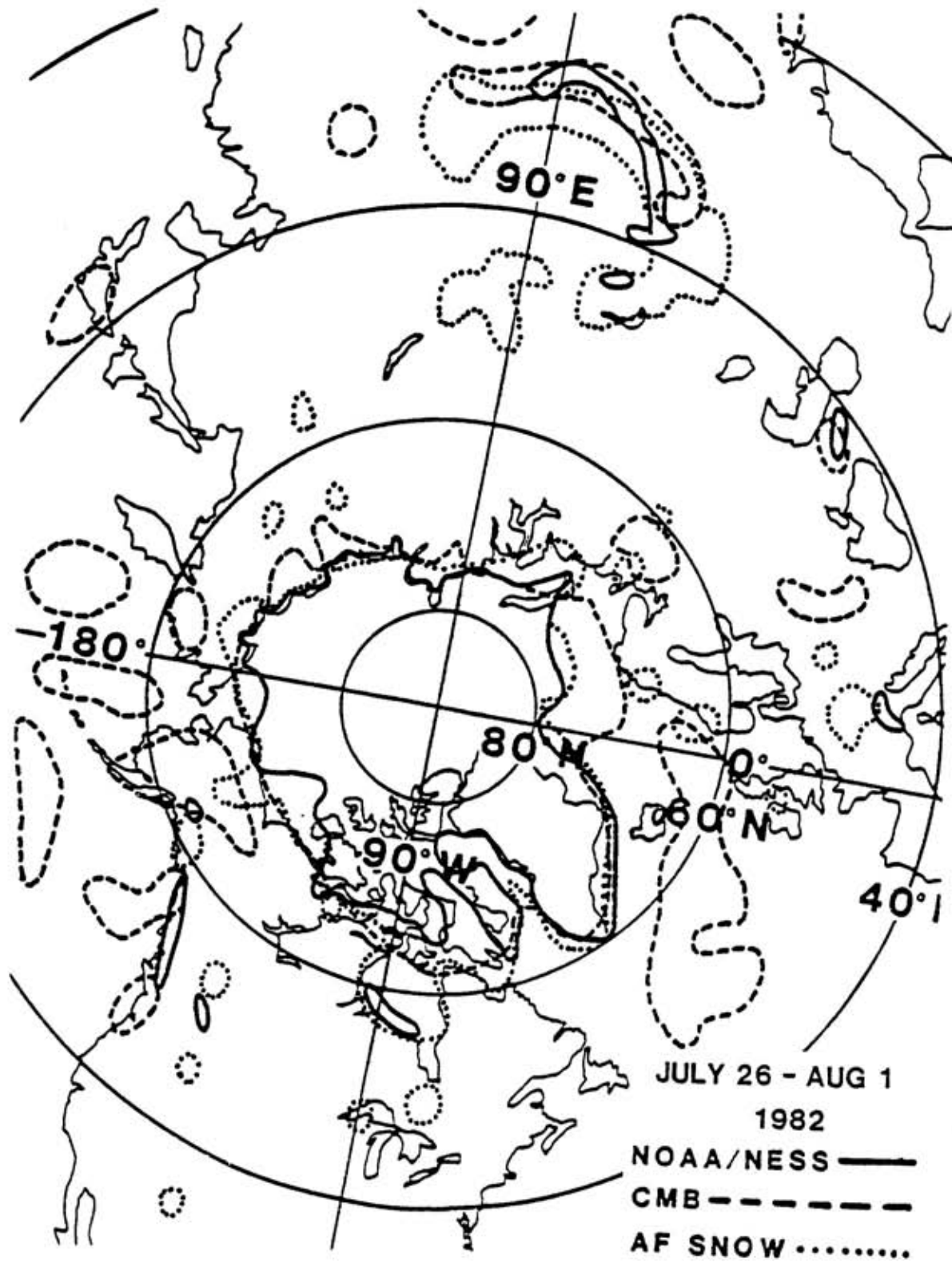


Figure 8. Weekly Comparison Map for July 26-Aug. 1, 1982.

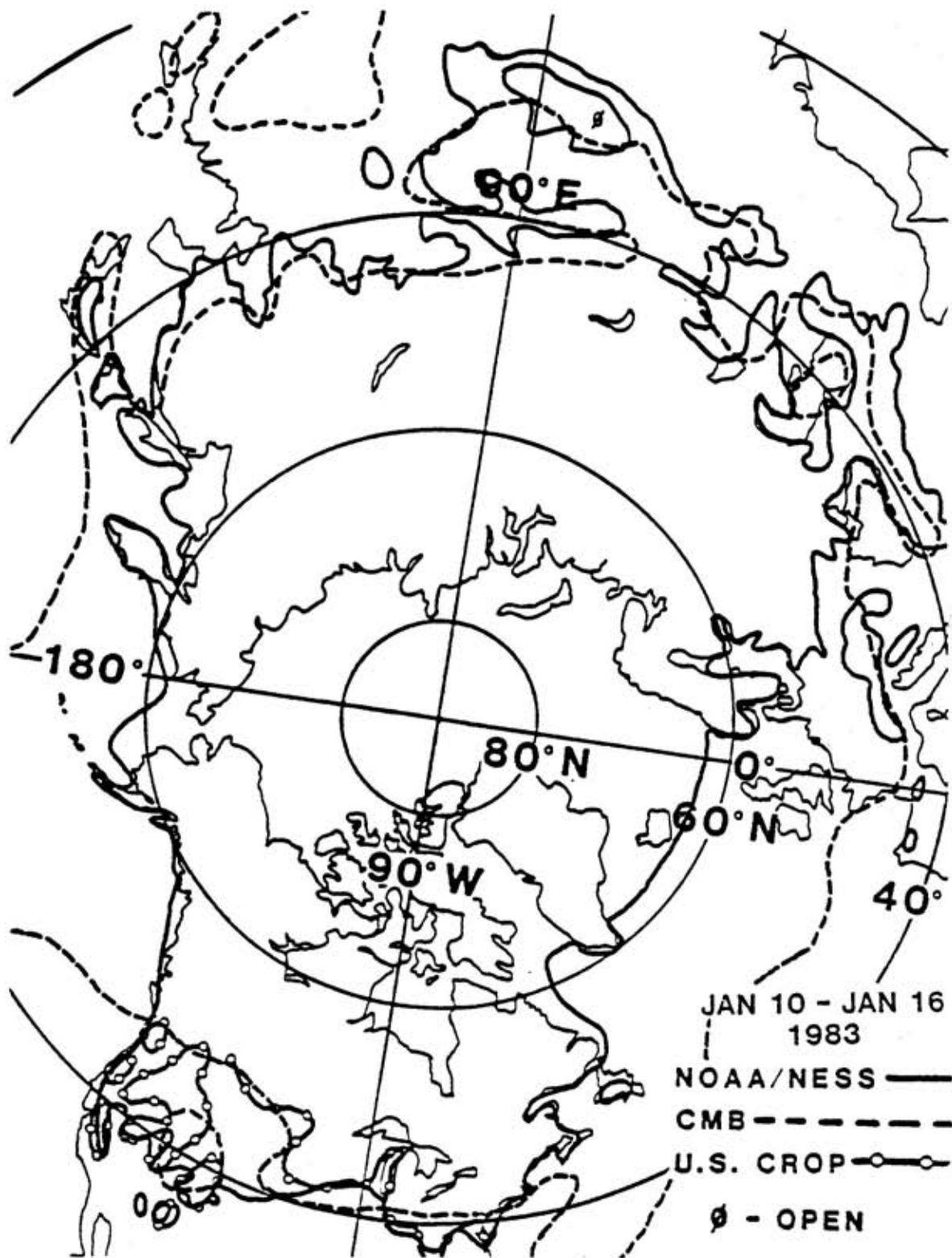


Figure 9. Weekly Comparison Map for Jan. 10-16, 1983.

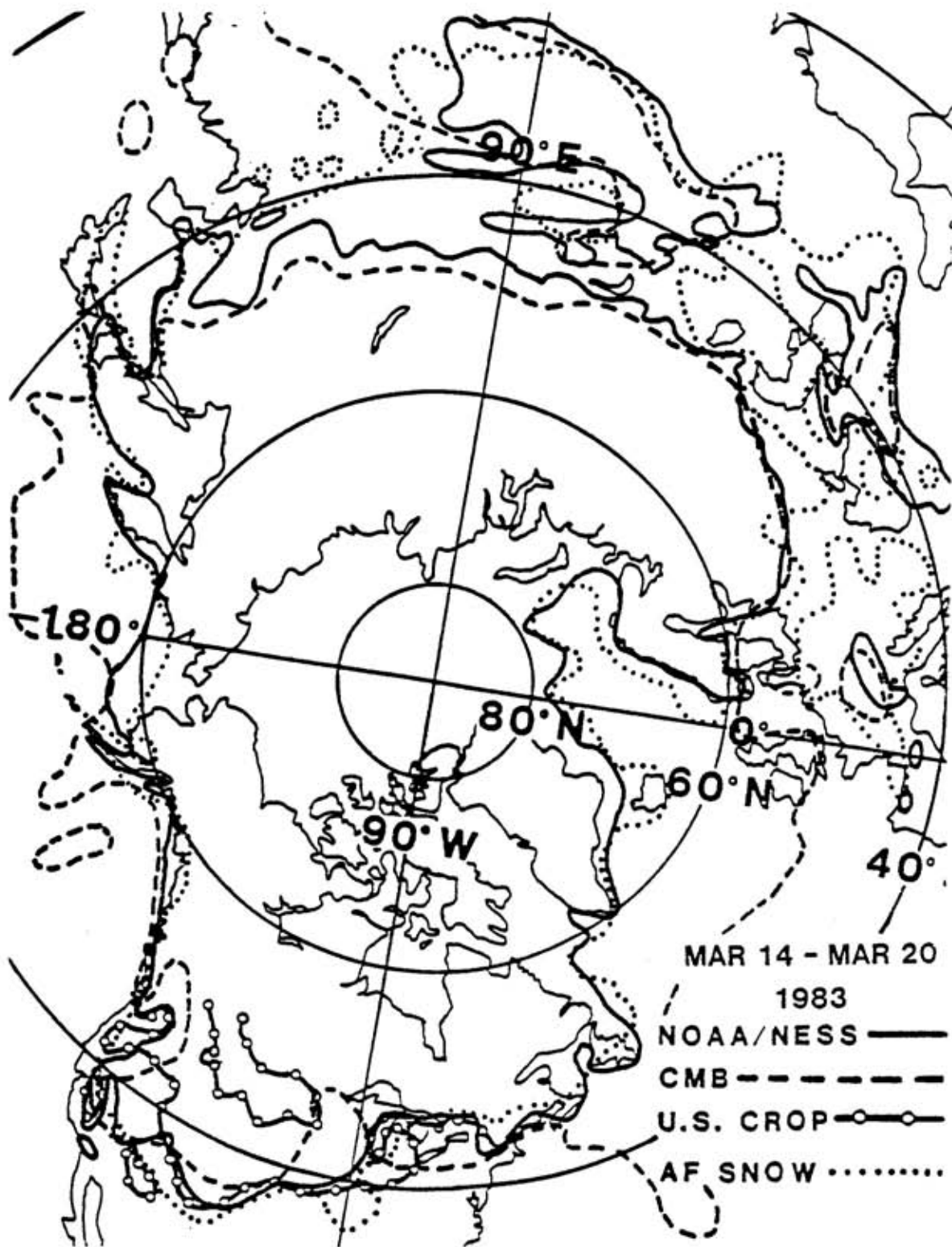


Figure 10. Weekly Comparison Map for Mar. 14-20, 1983.

slightly to the side of the mountain on the following day and appear dark. If this only happens on one day during the compositing period, the minimum brightness will be low and the snow will not appear on the chart. Except for the Himalayas, the other mountain ranges mentioned have locally dense forests below their crests which decreases the surface brightness when snow covered. Also, circulation surrounding the mountainous area may be oriented in such a way to produce orographic cloudiness for an extended period of time, and this was quite evident in the Himalayas.

The CMB technique also experienced difficulties in perceiving snow cover in heavily forested landscapes. McClain and Baker (1969) found very low surface brightness associated with snow-covered forested regions of North America. Robock and Kaiser (1985) found planetary albedos of forested areas were significantly lower than farming and grazing lands when snow-covered. Kukla and Brown (1982) found similar results observing surface brightness of various surface types. Robinson and Kukla (1985) computed zonal averages of surface albedo of Northern Hemisphere lands under maximum snow cover and found low values in Eurasia and North America between 45°N and 65°N .

The last problem deals with NOAA's bias toward the end of the week. The NOAA/NESDIS Weekly Snow and Ice Chart is compounded over a week's period from Monday thru Sunday, however, it incorporates only the most up-to-date information in its final outline, i.e. only data from the end the week are used. In the CMB technique only minimum values of surface brightness are retained. Essentially, each technique serves a different purpose, The CMB technique displays the minimum amount of snow cover while NOAA reveals more than the minimum, especially if snow is increasing toward the end of the week.

CROP agreed fairly well with NOAA east of the Rockies but underestimated snow cover to the west due to the sparse network of ground observation stations. The AF data, like the CMB, overestimated snow cover when compared to NOAA but did however, reveal the probable sea ice/open water delineation in the Arctic Ocean during the winter. This is made possible thru the use of the joint NOAA/NAVY ice charts.

Table 1 displays a quantitative comparison between NOAA and the other data sets as a function of area difference. Each category represents a problem that was found on the weekly comparison maps and is rated separately on a scale of 0 (No Difference) to 5 (Maximum Difference). Occasionally, CMB data were not available during the 2-year period so that the corresponding week was labeled as "MISSING". After each weekly map from July 1981 to July 1983 was rated, several quantities were calculated. We first computed the average difference for

Table 1.

Area Difference for NOAA vs. Other Data Sets

values: 0-No Difference
5-Maximum Difference

(Each category is rated separately)

CMB(1): Persistent clouds obstructing the main snow boundary
CMB(2): Persistent clouds far from the main snow boundary
CMB(3): Inconsistent detection in mountain regions
CMB(4): Underestimation in forested landscapes
CMB(5): Underestimation due to NOAA's end of the week bias
CROP(EAST): NOAA vs. CROP agreement east of the Rockies
CROP(WEST): NOAA vs. CROP agreement in the west
AF: Overestimation of AF vs. NOAA

DATE	C M B					C R O P		AF	
	1	2	3	4	5	EAST	WEST		
<u>1981</u>									
7/6-7/12	3	2	3	3	2			4	
7/13-7/19	3	0	2	3	2				
7/20-7/26	1	2	4	3	1				
7/27-8/2	2	2	4	3	2				
8/3-8/9		M I S S I N G							
8/10-8/16	2	2	4	3	2				
8/17-8/23	3	3	4	3	1			4	
8/24-8/30	4	2	3	2	1				
8/31-9/6	4	3	2	2	0				
9/7-9/13	4	3	2	5	1			4	
9/14-9/20	5	3	2	1	1				
9/21-9/27	5	4	3	1	0				
9/28-10/4	5	4	3	1	1				
10/5-10/11	4	3	2	1	0			5	
10/12-10/18	4	3	3	2	0				
10/19-10/25	3	3	3	3	2				
10/26-11/1	4	2	4	2	2				
11/2-11/8	4	1	5	2	2			5	
11/9-11/15	3	1	3	2	2				
11/16-11/22	3	1	2	3	2				
11/23-11/29	4	2	3	3	3				
11/30-12/6	3	2	3	2	2	2	3		
12/7-12/13	2	1	4	3	3	1	3	3	
12/14-12/20	3	2	2	2	2	1	3		
12/21-12/27	2	1	2	2	3	2	2		
<u>1982</u>									
12/28-1/3		M I S S I N G					3	2	

DATE	C M B					C R O P		AF
	1	2	3	4	5	EAST	WEST	
1/4-1/10	2	1	2	1	3	2	2	
1/11-1/17	2	0	2	2	2	2	3	3
1/18-1/24	2	1	2	2	4	1	4	
1/25-1/31	2	1	3	2	2	2	3	
2/1-2/7	2	1	2	3	2	2	2	
2/8-2/14	2	2	2	2	2	5	4	3
2/15-2/21	3	1	2	2	3	3	3	
2/22-2/28	2	1	2	2	3	2	4	
3/1-3/7	2	1	2	2	3	4	3	
3/8-3/14	2	1	3	2	2	3	5	4
3/15-3/21	2	1	3	2	3	3	4	
3/22-3/28	2	0	2	2	2	2	3	
3/29-4/4	2	1	3	2	2			
4/5-4/11	2	1	3	4	3			
4/12-4/18	2	2	3	3	3			
4/19-4/25	2	2	3	3	4			5
4/26-5/2	1	0	3	3	2			
5/3-5/9	1	0	3	2	1			
5/10-5/16	1	3	3	2	2			4
5/17-5/23	1	4	3	2	1			4
5/24-5/30	1	2	2	3	0			
5/31-6/6	2	2	3	3	2			
6/7-6/13	1	3	2	2	4			
6/14-6/20	1	4	3	2	2			5
6/21-6/27		M	I	S	S	I	N	G
6/28-7/4	1	5	4	1	1			
7/5-7/11	2	4	2	1	2			
7/12-7/18	2	5	3	1	2			
7/19-7/25		M	I	S	S	I	N	G
7/26-8/1	2	1	2	2	1			4
8/2-8/8	2	5	3	1	2			
8/9-8/15	2	5	3	1	2			
8/16-8/22	4	5	3	1	1			
8/23-8/29	3	5	2	1	3			
8/30-9/5		M	I	S	S	I	N	G
9/6-9/12	4	5	2	2	1			
9/13-9/19	3	4	4	2	3			
9/20-9/26		M	I	S	S	I	N	G
9/27-10/3	4	4	3	3	2			
10/4-10/10	4	5	4	3	1			
10/11-10/17	3	5	4	2	2			
10/18-10/24	5	5	4	2	3			
10/25-10/31	3	5	3	2	3			
11/1-11/7	4	5	4	2	3			
11/8-11/14	3	5	2	2	2			
11/15-11/21	4	4	5	3	3			5
11/22-11/28	4	2	3	1	2			
11/28-12/5	3	3	3	1	2			3

DATE	C M B					C R O P		AF
	1	2	3	4	5	EAST	WEST	
12/6-12/12	5	3	3	2	3	5	3	
12/13-12/19	5	3	3	2	2	3	4	4
12/20-12/26	4	0	2	1	3	2	1	
1983								
12/27-1/2	4	2	2	1	1	2	2	
1/3-1/9	4	3	2	1	1	2	3	4
1/10-1/16	5	4	3	1	3	5	3	
1/17-1/23	3	0	2	1	2	2	2	
1/24-1/30	5	1	3	2	2	3	3	3
1/31-2/6	4	0	3	1	2	3	4	
2/7-2/13	4	2	4	2	3	1	3	
2/14-2/20	3	1	2	1	3	1	3	
2/21-2/27	5	1	4	2	3	3	3	3
2/28-3/6	3	2	3	1	2	2	3	
3/7-3/13	3	3	4	3	2	3	4	
3/14-3/20	4	3	3	2	2	2	4	3
3/21-3/27	4	2	2	2	3	3	3	
3/28-4/3	3	2	3	1	2			
4/4-4/10	5	3	3	2	2			4
4/11-4/17	2	5	3	2	1			
4/18-4/24	3	5	4	4	2			
4/25-5/1	2	5	4	3	1			
5/2-5/8	2	4	3	3	3			
5/9-5/15	5	4	4	4	2			5
5/16-5/22	4	4	3	4	2			
5/23-5/29	2	5	4	4	2			
5/30-6/5	3	4	3	2	2			
6/6-6/12	2	5	3	2	3			
6/13-6/19	2	5	4	4	3			5
6/20-6/26	2	5	3	4	4			
6/27-7/3	2	5	3	3	2			
7/4-7/10	2	4	3	3	2			5
7/11-7/17	1	5	3	3	2			
7/18-7/24	2	5	2	3	2			
7/25-7/31	2	5	3	3	2			

DATE	1	2	C M B			5	C R O P		AF
			3	4		EAST	WEST		
AVG DIFF	2.9	2.8	2.9	2.2	2.1	2.5	3.1	4.0	
AVG DIFF (%)	58	56	58	44	42	50	62	80	
RELATIVE AREA OF LEVEL 5 DIFF (%)	80	40	10	30	5	10*	5*	100	
RELATIVE AREA OF LEVEL 5 DIFF (10 km)	8.8	4.4	1.1	3.3	.55	1.1	.55	11	
AVG AREA DIFF (10 km)	5.1	2.5	.64	1.5	.23	.55	.34	8.8	

*note that differences are zero in Eurasia because data set only covers North America.

each category, then we converted the average difference to percent values. The Air Force data showed the largest average difference, 80% of the maximum difference while CROP in the west was next highest at 62%. The CMB problems of clouds and mountains ranged from 56% to 58%. Then we compared the area of level 5 difference for each category to level 5 areas for the Air Force data. We calculated a typical level 5 area difference for the Air Force data and proceeded to calculate area difference values for the other categories in millions of square kilometers. The CMB's cloud problem showed the largest area difference next to the Air Force data. After computing the average area difference for each category, the Air Force displayed the highest value at 8.8 million sq. km. while cloud problems 1 and 2 followed at 5.1 million sq. km. and 2.5 million sq. km., respectively. If we add up the CMB average area differences (categories 1-5), the CMB area difference is larger than the Air Force area difference, 10 million sq. km. to 8.8 million sq. km.

5. Conclusions

Several differences arose between CMB and NOAA in analyzing two consecutive years of data. On many occasions, the CMB Arctic snow boundary stretched farther south than the NOAA Arctic snow boundary, leading us to interpret this as persistent cloudiness. This condition also occurred quite often far from the snow boundary. Snow cover in mountainous regions throughout the Northern Hemisphere went undetected or partially detected many times while forested regions caused underestimation by the CMB. Due to the nature of their techniques, the CMB occasionally showed less snow cover than NOAA. The U.S. Crop Bulletin and NOAA showed significant differences which should be expected since CROP does not use satellite imagery. The Air Force data overestimated snow cover, like the CMB, but did however reveal the probable sea ice/open water delineation in the Arctic during the winter months.

For research purposes, we can recommend only the weekly NOAA data set for a consistent indication of snow cover. Although this data set also has its problems, including effects of persistent cloudiness, forests and broken satellites, and hence missing data, it is still by far the best source. The CMB process introduces too many errors to be used without additional information from surface observations or human interpretation of individual high-resolution imagery. The CROP data set does provide accurate coverage in regions with a dense surface observing network and without mountains. The AF data set, although daily incorporating large amounts of surface data, is an undocumented operational product. It contains large errors and is unsuitable for research purposes.

The ideal snow cover data set of the future will include the best aspects of each of the current data sets. Surface observations will supplement satellite images with the CMB technique perhaps helping to remove clouds. New technologies, including near-infrared snow detection channels on future DMSP and NOAA satellites and microwave techniques (Robinson, et al., 1984), also show promise in producing better snow cover data sets.

Acknowledgements: We are grateful to the following people: Mike Matson and Tom Baldwin for supplying the NOAA/NESDIS data and advising us where necessary, Bruce H. Needham of the Satellite Data Service Division of NOAA for providing us access to the CMB data, John Walsh for providing copies of the U.S. Weekly Weather and Crop Bulletin, David Lee for the Air Force data, Joyce Gavin for comments and advice on snow cover information in general, Max Woods for drafting all snow cover comparison maps, and Robert G. Ellingson for continued support and encouragement. We are also much obliged for computer time supplied by NASA/GLA. This study was supported by NOAA Grant NA84AA-H-00026 and NSF Grant ATM-8213184.

REFERENCES

- Kukla, G., and J. Brown, 1982: Impact of snow on surface brightness. EOS, 63, 576-578.
- McClain, E. P., and D. R. Baker, 1969: Experimental large-scale snow and ice mapping with composite minimum brightness charts. ESSA Technical Memorandum NESCTM-12, U.S. Dept. of Commerce, 25pp.
- Robinson, D., and G. Kukla, 1985: Maximum surface albedo of seasonally snow-covered lands in the northern hemisphere. J. Climate Appl. Meteor., 24, 402-411.
- Robinson, D., K. Kunzi, G. Kukla, and H. Rott, 1984: Comparative utility of microwave and shortwave satellite data for all-weather charting of snow cover. Nature, 312, 434-435.
- Robock, A., and D. Kaiser, 1985: Satellite-observed reflectance of snow and clouds. Mon. Wea. Rev., 113, 2023-2029.

Kukla, G; Barry, R.G.; Hecht, A.; Wiesnet, D. eds. (1986) SNOW WATCH '85. Proceedings of the Workshop held 28-30 October 1985 at the University of Maryland, College Park, MD. Boulder, Colorado, World Data Center A for Glaciology (Snow and Ice), Glaciological Data, Report GD-18, p.161-171.

Influence of Snow Structure Variability on Global Snow Depth Measurement using Microwave Radiometry

Dorothy K. Hall
Hydrological Sciences Branch
National Aeronautics and Space Administration
Goddard Space Flight Center
Greenbelt, Maryland, U.S.A.

ABSTRACT

The high albedo of snow and its sometimes transient nature can have a large impact on the receipt of solar energy and thus on global circulation. In addition, snow depth and liquid water content of snow must be known for assessment of the global water balance. Passive microwave sensors are useful for measuring the snow extent through cloudcover and darkness, and snow depth can be estimated under certain snow and terrain conditions. However, the ability to measure snow depth using microwave radiometry on a global scale, in part, depends upon knowledge of the effects of snow structure on the microwave emission from snow. It has been observed that, even with no increase in snow depth, the microwave emissivity decreases throughout the winter in many snowcovered areas. This appears to be related to increasing depth hoar thickness through time. Utilization of a two layer radiative transfer model which is used to simulate the microwave emission from a snowpack has enabled a comparison of calculated data points with observations. The observational data consist of a time series of Scanning Multichannel Microwave Radiometer (SMMR) data of the Arctic Coastal Plain of Alaska during the period from January through March 1980. The snowpack on the Arctic Coastal Plain of Alaska is known to develop a depth hoar layer each year as a result of a large temperature gradient in the snowpack which causes crystal sizes at the base of the snowpack to

increase through time. Crystals can grow up to 10 mm in size although the average crystal size in the lower or depth hoar layer is considerably less than 10 mm. Using the model, the crystal diameters in the upper and lower layers of the snowpack were set at 0.50 and 1.40 mm respectively. These sizes were determined from a previous study. In the first simulation, the depth hoar layer thickness was assumed to be a constant 10 cm from January through March 1980 with the total snow depth varying as determined from climatological data. When the model results were correlated with the SMMR data, using 15 data points, the coefficient of correlation was $R = 0.30$. For the second simulation, all parameters remained the same as in the first simulation except that the depth hoar layer thickness was increased by 0.50 cm per week to simulate the reported increasing thickness of the depth hoar layer as the winter progresses. In this case, the simulated and observed data points matched quite well with a coefficient of correlation of $R = 0.85$ significant at the 0.01 level. Results thus show that the presence and variability of the depth hoar layer can have a significant effect on the microwave emission and that changing snow structure must be considered when measuring snow depth using a time series of data.

Introduction

The high albedo of snow and its sometimes transient nature can have a large impact on the receipt of solar energy and thus on global circulation. In addition, the depth and liquid water content of snow must be known for assessment of the global water balance. Passive microwave sensors are useful for measuring the snow extent through cloudcover and darkness, and snow depth can be estimated under certain snow and terrain conditions. However, the ability to measure snow depth using microwave radiometry on a global scale, in part, depends upon knowledge of the effects of snow structure on the microwave emission from snow. In this paper, the effect of changing snow structure through time is addressed for the snowpack on the Arctic Coastal Plain of Alaska.

Snow Structure on the Arctic Coastal Plain of Alaska

Local and regional energy balance processes influence the structure of a snowpack. Snowpack structure can change through time as a result of air temperature changes, wind, precipitation type and quantity and length of time that snow is on the ground. When snow remains on the ground for a substantial portion of the winter, metamorphism at the base of the snowpack can result in the formation of a layer comprised of large, loosely-bonded crystals. This is known as the depth hoar layer. Depth hoar is common in snowpacks throughout the world and is well developed in portions of Alaska.

A steep, negative temperature gradient occurs in the snowpack of the Arctic Coastal Plain. Early snow accumulation reduces upward soil heat flux (Santeford, 1979). Even though the air temperatures can be lower than -45°C , snow/soil interface temperatures may be as high as -5°C producing a 40°C difference in temperature between the snow/air and snow/soil interfaces. This temperature gradient produces inequalities in the degree

of air saturation and the diffusion rate of water vapor in the snowpack (Marbouty, 1980). Associated pressure gradients cause water vapor to diffuse from warmer to colder parts of a snowpack (Langham, 1981). This leads to constructive metamorphism in which snow crystal size increases through time as crystals grow from one side of existing snow crystals in a direction that is opposite to the vapor pressure gradient. Faster crystal growth occurs in the warmer (lower) layers of a snowpack (Colbeck, 1982). Depth hoar crystals can grow up to 10 mm in diameter (Benson et al., 1975).

On the Arctic Coastal Plain of Alaska, low snow accumulation, very cold air temperatures and strong winds contribute to the snowpack structure. A relatively thin, continuous snow cover forms each year. High average snowpack densities result from re-distribution of the snow by wind causing the crystals in the upper layers of the snowpack to be closely-packed, rounded and abraded.

Recently, a two-layer radiative transfer model developed by Chang et al., (1976), was employed to study the effect of the depth hoar layer on microwave emission from snow (Hall et al., in press). It was found that the microwave brightness temperature (T_B) decreased with increasing depth hoar layer thickness (Figure 1). The rate of increase in T_B was shown to lower with increasing thickness of the depth hoar layer. In other words, when the depth hoar layer was first formed, there was the greatest decrease in T_B (Figure 1).

In this paper, we employ the same basic model to calculate a time series of T_B s to compare with observed T_B s from the Arctic Coastal Plain of Alaska using the 37 GHz sensor on the Scanning Multichannel Microwave Radiometer (SMMR). Results show that the observed and modeled T_B s correlate well when the depth hoar layer thickness is increased through time in the model snowpack.

Previous Work

Satellite data are useful for analyzing snow conditions on regional and global scales, and microwave sensors are able to acquire data through cloudcover and darkness. Previous studies have shown that there is an inverse relationship between snow depth and microwave T_B as measured by passive microwave sensors at specified wavelengths in dry snow (Foster et al., 1984). The 37 GHz (0.81 cm wavelength) sensor on the Nimbus-7 SMMR has been shown to be particularly useful for analyzing internal properties of snowpacks especially when the horizontally polarized data are used (Hall et al., 1984). Some characteristics of the Nimbus-7 SMMR are shown in Table 1.

For temperatures generally encountered on Earth, the emitted intensity of microwave radiation is expressed as T_B in degrees Kelvin and follows the Rayleigh-Jeans approximation which shows that the radiance from a blackbody

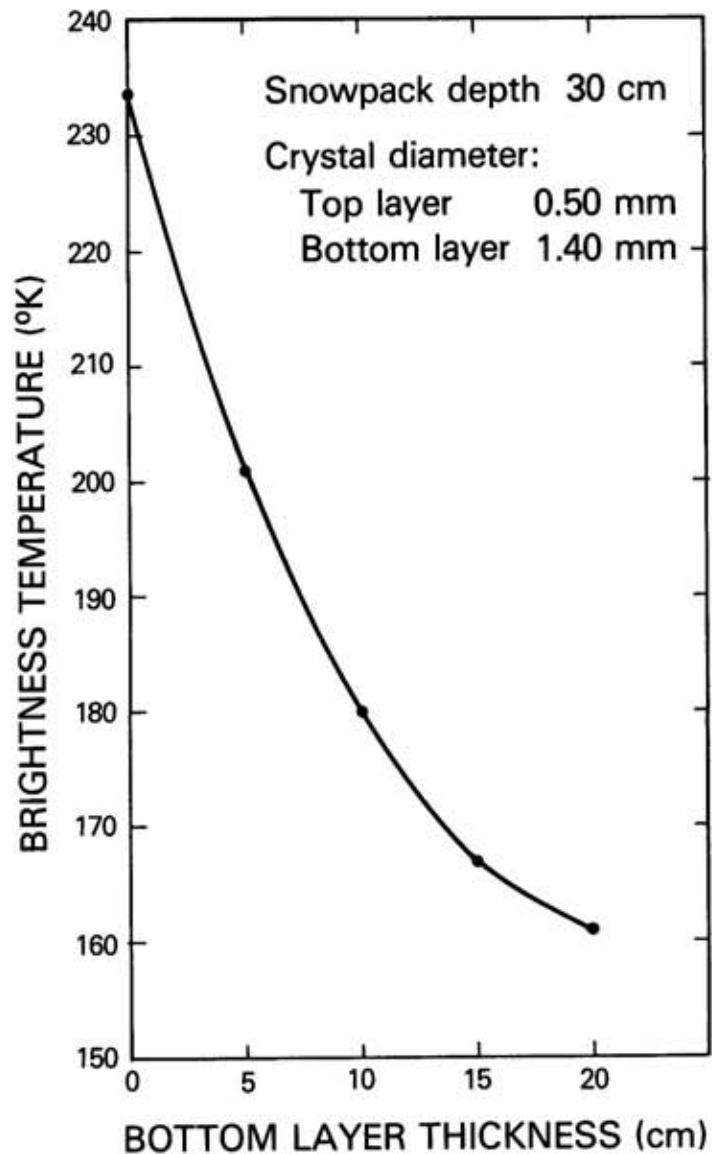


Figure 1. Calculated 37 GHz (horizontal polarization) brightness temperatures for dry snow cover over frozen ground showing the effect of changing the thickness of the depth hoar layer (from Hall et al., in press).

is proportional to its temperature:

$$T_B = \epsilon T_s e^{-\tau} + T_1 + (1 - \epsilon) T_2 e^{-\tau} + (1 - \epsilon) T_{sp} e^{-2\tau} \quad (1)$$

where ϵ is the emissivity of the surface, T_s is the sensible temperature of the surface, τ is the total atmospheric opacity, T_1 is the upward emitted radiance contribution of the atmosphere, T_2 is the total downward (emitted and reflected) atmospheric brightness temperature, and T_{sp} is the average temperature of free space (Gloersen and Barath, 1977).

Table 1. Some Characteristics of the SMMR (after Gloersen and Barath, 1977)

Wavelength (cm)	0.81	1.43	1.66	2.80	4.54
Frequency (GHz)	37.00	21.00	18.00	10.69	6.60
Spatial resolution (km)	30	60	60	97.5	156
Temperature resolution τ_{rms} ($^{\circ}$ K) (per IFOV)	1.5	1.5	1.2	0.9	0.9
Antenna beam width (degree)	0.8	1.4	1.6	2.6	4.2

Calculations have shown that the grain or crystal size is a dominant factor influencing the microwave emission of dry snow and polar firn. Additional calculations using a microscopic scattering model for snow have shown that the scattering of 37 GHz radiation from a snowpack is dependent strongly upon the grain size of the snow particles (Chang et al., 1982; Hall et al., in press). Larger grain sizes within the snowpack allow greater incidence of scattering of microwave radiation as the grain size approaches or surpasses the size of the wavelength. The relatively large crystals characterizing the depth hoar layer would tend to increase scattering of the upwelling radiation relative to scattering through a snowpack (with a similar thickness) which is lacking a depth hoar layer.

Radiative Transfer Model

The intensity of microwave radiation emitted from a snowpack depends on the physical temperature, grain size, density and the underlying surface conditions of the snowpack. By knowing these parameters, the radiation emerging from a snowpack can be calculated by solving the radiative transfer equation. The radiative transfer equation for an axially symmetric inhomogeneous medium can be written in the form of an integro-differential equation

$$\mu \frac{dI(x,\mu)}{dx} = -\sigma(x)I(x,\mu) + \sigma(x)\{[1-\omega(x)]B(x) + 1/2\omega(x) \int_{-1}^1 P(x,\mu,\mu')I(x,\mu')d\mu'\}$$
(2)

where the radiation intensity $I(x,\mu)$ is at a depth x and traveling in the direction towards increasing x , making an angle whose cosine is μ with the normal (Chang et al., 1982). The functions $\sigma(x)$, $\omega(x)$, $B(x)$ and $P(x, \mu, \mu')$ are prescribed functions of their arguments. They are the extinction per unit length, the single scattering albedo, and the source and phase functions, respectively. Instead of working with depth x , one generally works with a dimensionless depth variable called optical depth τ (Chang and Choudhury, 1978):

$$d\tau = \sigma(x)dx$$
(3)

For the snowpack on the Arctic Coastal Plain of Alaska, the air temperature as determined from the meteorological station located at Umiat, Alaska is used as a guide to infer the snow temperature, and the crystal sizes in the upper and lower layers of the model snowpack were determined from previous work by Hall et al. (in press) in which the crystal size in the upper layer was assumed to be 0.50 mm and in the lower layer 1.40 mm in diameter. The thickness of the depth hoar or lower layer was assumed to be 10 cm during the period 5-10 January 1980 which was the period during which T_B s were averaged to determine the average T_B from SMMR data. Snow depth in the model varied with reported snow depths from the meteorological station at Umiat, Alaska.

The average snowpack temperature is obviously higher than the reported air temperature. However, without in-situ measurements the average snowpack temperature is not known. Thus, for the purpose of this study, the first point shown on Figure 2 was fitted to the observed T_B by adjusting the average snow temperature until the simulated T_B matched the observed T_B . A 25°K increase (relative to reported average air temperature for each 5 day study period) was added in each case and used as an average snow temperature of the model snowpack.

Results of the Model as Compared to Observations

Brightness temperatures were calculated for 15 data points corresponding to the 15 time periods for which SMMR data were averaged in 5 day periods between 1 January and 30 March 1980 (Julian days 1-89).

When the depth hoar thickness remained at 10 cm for the study period, the correlation between modeled and observed T_B s was low, $R = 0.30$. However, when the thickness of the depth hoar or lower layer of the model

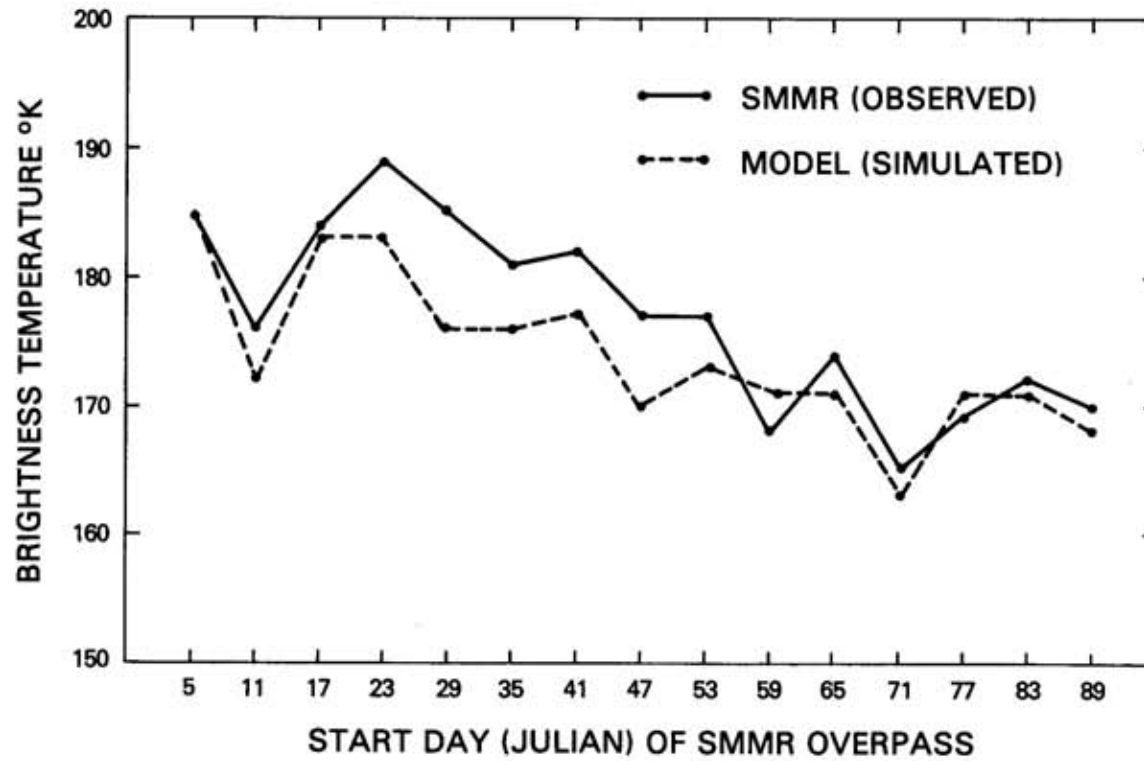


Figure 2. Observed and simulated brightness temperatures for the snowpack on the Arctic Coastal Plain of Alaska - January through March 1980.

snowpack was allowed to increase by 0.50 cm per week, the correlation between modeled and observed T_B was quite high, where $R = 0.85$ significant at the 0.01 level.

The T_B for the period beginning on day 41 that was originally determined from the model was anomalously high - 186°K. This period was unusually warm where air temperatures (which were used to infer snow temperatures in the model snowpack) averaged -8.5°C for the 5 day period. This was well above the average of the previous (-26.50°C) and subsequent (-30.88°C) SMMR overpass periods. Because it is unlikely that this unusually high air temperature caused an equivalent warming of the average temperature of the snowpack, that case was re-calculated by changing the average snowpack temperature to a value determined from averaging the air temperatures of that period, the previous period and the subsequent period. The adjusted air temperature then becomes -22.0°C and the T_B becomes 177°K (Figure 2). The correlation between the modeled and observed T_B s increases to $R = 0.88$, significant at the 0.01 level, as seen in Figure 3.

Discussion

It has been observed that the thickness of the depth hoar layer may increase through time as long as a strong negative temperature gradient is maintained in a snowpack (Giddings and LaChappelle, 1962). For example, in central Alaska, Trabant and Benson (1972) reported that the depth hoar layer increased in thickness throughout the winter and comprised almost the entire snowpack by the end of the winter. Thus it is reasonable to include an increase in depth hoar thickness through time in the present study, as it is known from meteorological records that a strong negative temperature gradient was maintained in the snowpack during the winter of 1980 on the Arctic Coastal Plain of Alaska.

Conclusion

Many of the snow covered areas on the Earth have depth hoar. It is especially common in areas where the snowpack lasts long enough to allow depth hoar crystals to grow. Thus depth hoar is an important type of snowpack structure that has to be taken into account when estimating global snow depth from microwave data because the large crystals which characterize a depth hoar layer cause increased scattering of microwave radiation and thus a lower T_B than would be expected for a snowpack of similar depth without depth hoar. Furthermore, it appears that this type of snow structure can be modeled quite successfully using radiative transfer modeling.

However, it is important to understand that, before the microwave emission from snow can be successfully modeled, one must have prior knowledge about the snowpack structure. This is necessary for a reliable estimate of snow depth to be possible.

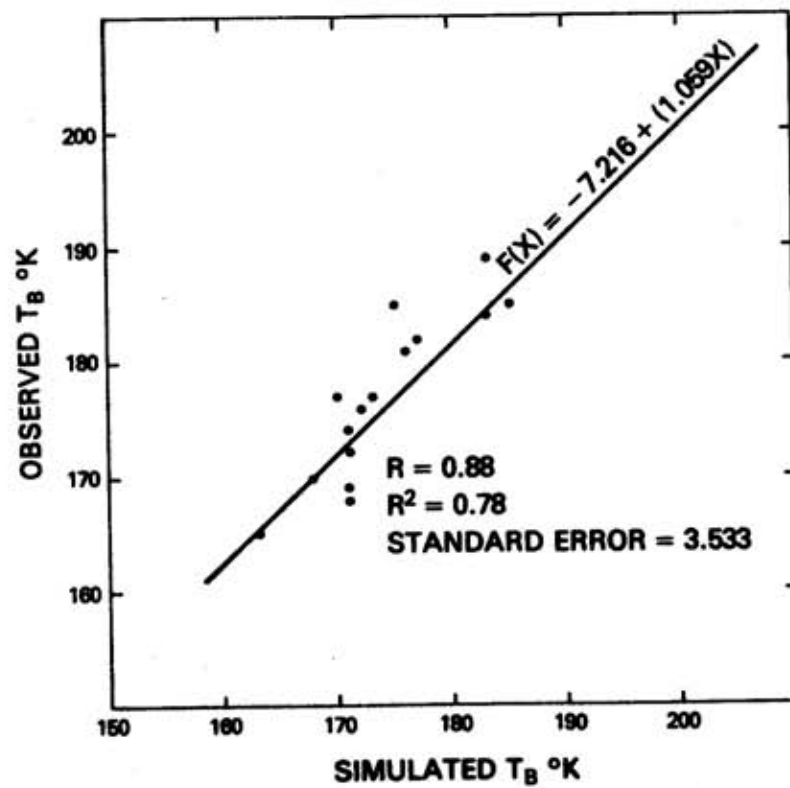


Figure 3. Correlation of model (simulated) T_Bs and SMMR T_Bs using an adjustment for day 41 as explained in text.

References

- Benson, C. S. and D. C. Trabant (1973) Field measurements on the flux of water vapor through dry snow. The Role of Snow and Ice in Hydrology, UNESCO WMO-IASH, p. 291-298.
- Benson, C., B. Holmgren, R. Timmer, G. Weller and S. Parrish (1975) Observations on the Seasonal Snow Cover and Radiation Climate at Prudhoe Bay, Alaska, during 1972. In Ecological Investigations of the Tundra Biome in the Prudhoe Bay Region, Alaska (J. Brown, ed.), Biological Papers of the University of Alaska Special Report Number 2, October, 1975, p. 13-50.
- Chang, A. T. C. and B. J. Choudhury (1978) Microwave Emission from Polar Firn. NASA Technical Paper 1212.
- Chang, A. T. C., P. Gloersen, T. Schmugge, T. T. Wilheit and H. J. Zwally, (1976) Microwave emission from snow and glacier ice. Journal of Glaciology, V. 16, p. 23-39.
- Chang, A. T. C., J. L. Foster, D. K. Hall, A. Rango and B. K. Hartline, (1982) Snow water equivalent estimation by microwave radiometry. Cold Regions Science and Technology, V. 5, p. 259-267.
- Colbeck, S. C. (1982) An overview of seasonal snow metamorphism. Reviews of Geophysics and Space Physics, V. 20, p. 45-61.
- Foster, J. L., D. K. Hall, A. T. C. Chang and A. Rango (1984) An overview of passive microwave snow research and results. Reviews of Geophysics and Space Physics, V. 22, p. 195-208.
- Giddings, J. C. and E. LaChapelle (1962) The formation rate of depth hoar. Journal of Geophysical Research, V. 67, p. 2377-2383.
- Gloersen, P. and F. Barath (1977) A Scanning Multichannel Microwave Radiometer for Nimbus-G and Seasat-A. IEEE Journal of Oceanic Engineering, V. OE-2, p. 172-178.
- Hall, D. K., J. L. Foster and A. T. C. Chang (1984) Nimbus-7 SMMR polarization responses to snow depth in the mid-western U.S. Nordic Hydrology, V.15, p. 1-8.
- Hall, D. K., A. T. C. Chang and J. L. Foster (in press): Detection of the Depth Hoar Layer in the Snowpack of the Arctic Coastal Plain of Alaska using Satellite data.
- Langham, E. J. (1981) Physics and properties of snowcover. (In: D. M. Gray and D. H. Male, eds., Handbook of Snow, Pergamon Press, New York, p. 275-337.)

- Marbouty, D. (1980) An experimental study of temperature-gradient metamorphism. Journal of Glaciology, V. 23, p. 303-312.
- NOAA (1979-1983) Climatological Data of Alaska. National Oceanic and Atmospheric Administration, National Climatic Data Center, Asheville, NC.
- Santeford, H. S. (1979) Snow soil interactions in interior Alaska. Proceedings of the Workshop on Modeling of Snow Cover Runoff, (S. C. Colbeck and M. Ray, editors), 26-28 September 1978, Hanover, NH, p. 311-318.
- Trabant, D. and C.S. Benson (1972) Field Experiments on the Development of Depth Hoar. Geological Society of America Memoir 135, p. 309-322.

Kukla, G; Barry, R.G.; Hecht, A.; Wiesnet, D. eds. (1986) SNOW WATCH '85. Proceedings of the Workshop held 28-30 October 1985 at the University of Maryland, College Park, MD. Boulder, Colorado, World Data Center A for Glaciology (Snow and Ice), Glaciological Data, Report GD-18, p.173-179.

Retrieval of Snow Water Equivalent from Nimbus-7 SMMR Data

M. Hallikainen

P. Jolma

Department of Electrical Engineering
Helsinki University of Technology
Espoo, Finland

1. Introduction

In microwave radiometry of snow cover, the intensity of microwave radiation emitted by snow and the underlying ground is measured. The result is expressed as a brightness temperature. The effect of snow cover to the brightness temperature depends on several snow parameters. Even a small amount of liquid water makes the snow a high-loss material. In that case, no radiation from the bottom of the snow cover reaches the air, and the brightness temperature does not depend on the thickness and the water equivalent of the snow cover. If the snow is dry, the microwave radiation from the ground is scattered by snow particles, while the snow itself emits practically no radiation. At frequencies above 20 GHz, the scattering is so strong that it tends to decrease the brightness temperature, depending on the average snow particle size. Since the amount of scatterers increases with increasing snow thickness, the brightness temperature of snow-covered ground can be used to retrieve the water equivalent of dry snow cover (Rango et al., 1979).

Satellite microwave radiometer data have been used to develop algorithms to retrieve the water equivalent of snow cover both on a global basis (Kunzi et al., 1982) and on a regional basis (Hallikainen, 1984a). In this paper, several factors that have an effect to the retrieval accuracy, are examined.

2. Water equivalent algorithms

Since scattering by dry snow particles tends to decrease the brightness temperature from the value observed before the first snowfall, a simple quantity related to the snow water equivalent is of the form

$$\Delta T(W_{eq}) = F(W_{eq}) - F(W_{eq}=0) \quad (1)$$

where $F(W_{eq})$ = observed quantity for water equivalent W_{eq} ,
and $F(W_{eq}=0)$ = observed quantity for water equivalent $W_{eq} = 0$ (snow-free terrain).

F may be either a brightness temperature at a single frequency, the difference between the brightness temperatures at two frequencies, or a more complicated function derived from the observed brightness temperatures. In studies employing data from the Nimbus-7 satellite (measurement angle 50 degrees from vertical), the brightness temperature difference between 18 GHz and 37 GHz, horizontal polarization, has been used. For that case, ΔT is

$$\Delta T(W_{eq}) = (T_{18H}(W_{eq}) - T_{37H}(W_{eq})) - (T_{18H}(W_{eq}=0) - T_{37H}(W_{eq}=0)) \quad (2)$$

where T_{18H} = brightness temperature at 18 GHz, horizontal polarization,
and T_{37H} = brightness temperature at 37 GHz, horizontal polarization.

Using a brightness temperature difference or a more complicated function for F has been found to give a higher retrieval accuracy than using a single-frequency value. An obvious reason for this is that the second frequency helps to partly eliminate the effects of snow and ground temperature.

The value of $F(W_{eq}=0)$ for each antenna footprint should be defined in winter-like conditions. The state (frozen or thawed) and the temperature of ground should be the same as in winter beneath the snow cover. The use of $F(W_{eq}=0)$ is necessary in areas where several land-cover categories (farmlands, forests, etc.) exist. In homogeneous areas where the brightness temperature is practically a constant before the first snowfall, the use of $F(W_{eq}=0)$ may not be necessary.

The relation between the observed ΔT and the snow water equivalent can be established experimentally for the area under examination. The relation depends on the measurement frequencies and polarization (definition of ΔT) and on the properties of snow cover and the underlying ground. Theoretical brightness temperature calculations may be used to determine suitable frequencies for the algorithm. However, the effect of vegetation canopies to the microwave temperature of snow-covered terrain cannot yet be solved theoretically.

Figure 1 shows the change of the brightness temperature due to snow cover in a 100 km x 100 km test area in Southern Finland for Winter 1979-80. Nimbus-7 data at 10.7 GHz, 18 GHz, and 37 GHz are shown along with some functions derived from those brightness temperatures. Also shown are the daily minimum and maximum air temperatures, precipitation, and manually measured snow water equivalent (compiled by the National Board of Waters). The surface type composition of the test area is: coniferous forests 84 %, lakes 14 %, and bogs 1 %. It is obvious from Figure 1 that any water equivalent algorithm for Finland should include the 37 GHz channel.

Figure 2 shows the correlation between the manually measured water equivalent values (from water equivalent maps, compiled by the National Board of Waters) and Nimbus-7-derived brightness temperature functions for Winter 1979-80. Data for Southern Finland (77 % coniferous forests, 10 % lakes, 10 % bogs, and 3 % farmland, area approximately 200,000 square kilometers) were used, including the results for both dry and wet snow. The results show that the brightness temperature difference between 18 GHz and 37 GHz gives the best correlation.

The vertical polarization is slightly better than the horizontal polarization.

At present, the accuracy of the retrieved water equivalent values does not meet the value of 10 mm, specified in the NASA climate plan. In order to increase the accuracy, several factors have to be considered, including the effects of snow particle size, snow and ground temperature, and land-cover categories.

3. Effect of snow particle size

The results from both measurements and theoretical calculations suggest that, in addition to the water equivalent, the brightness temperature of snow-covered ground depends substantially on the average snow particle size. The theoretical results in Figure 3 show that the brightness temperature difference between 18 GHz and 37 GHz saturates around $W_{eq} = 100$ mm for a grain size of 1 mm. Since both the snow particle size and the water equivalent of snow cover usually increase with time, the microwave response to snow does not follow any of the curves with a fixed snow particle diameter d in Figure 3. Rather, it may start by following the curve for $d = 0.5$ mm for small values of W_{eq} and finally reach the curve for $d = 1.25$ mm after several melt-freeze cycles.

Figure 3 suggests that for fine-grained snow, another channel with a frequency higher than 37 GHz is needed. For snow with an average particle size above 1.25 mm, the use of the brightness temperature difference between 18 GHz and 10 GHz may be a good choice.

4. Effect of snow and ground temperature

Due to the low dielectric loss of dry snow, radiometers operating below approximately 20 GHz detect the changes in the temperature of ground. This is shown in Figure 1, where the brightness temperatures at 10.7 GHz and 18 GHz follow the pattern of the air temperature. The air temperature pattern can be seen even in the 37 GHz results. Of course, the changes in the brightness temperatures are much smaller than those in the air temperature.

Since dry snow acts as an efficient thermal insulator, the changes in the temperature of ground surface are small, depending on the thickness of the snow cover. The variation of the brightness temperature is larger than expected from the variations of the soil temperature alone. This is explained by the dielectric behavior of soils as a function of temperature. In the temperature range of 0 °C to -5 °C, the amount of liquid water in soils depends strongly on the temperature. If the temperature decreases even by one degree centigrade, the fraction of liquid water decreases substantially and the dielectric properties of soils change correspondingly (Hallikainen et al., 1984b). The dependence of the soil dielectric properties on the liquid water content increases with decreasing frequency. Hence, even the use of the brightness temperature difference between 18 GHz and 37 GHz cannot totally remove the effects of the air temperature. This is illustrated in Figure 4, where the brightness temperature difference increases with decreasing air temperature. In order to remove the effect of snow water equivalent to the

results in Figure 4, only the resolution cells with W_{eq} between 50 mm and 75 mm were considered.

5. Effect of melt-freeze cycles

When the seasonal snow cover starts to melt, days are often warm and nights are cold. This causes melt-freeze cycles to occur in the topmost snow layers, resulting in a larger average snow particle size and, consequently, in a lower brightness temperature at frequencies above approximately 20 GHz. Hence, the brightness temperature may be very low at night (dry snow) and high in the daytime (wet snow surface). These variations can be interpreted as being due to the start of the melting period.

The low brightness temperature due to melt-freeze cycles may erroneously be interpreted as an increase of the water equivalent value. As illustrated in Figure 5, the microwave response to dry snow at night may increase even when W_{eq} is decreasing day by day.

6. Effect of annual variations

The stratigraphy of seasonal snow cover may vary from winter to winter, due to the local weather conditions of each winter. This causes the microwave response to snow water equivalent to vary correspondingly. Figure 5 shows that this is indeed the case for Winters 1978-79 through 1981-82. Winters 1978-79 and 1979-80 were "normal" winters, while in Winters 1980-81 and 1981-82 the maximum snow water equivalent in Finland was exceptionally high. Especially in 1980-81, frequent snowfalls kept the average snow particle size small in the topmost snow layers, resulting in a low microwave response.

7. Effect of land-cover categories

Since more than two thirds of Finland is forested, the average microwave response to snow water equivalent can be expected to be fairly small. However, in open areas (farmlands, etc.) the response should be substantially larger. In a previous study, the microwave response to snow water equivalent was indeed observed to depend considerably on the surface type (Hallikainen, 1984a). Hence, in order to use the water equivalent algorithm given in Equations (1) and (2) in Finland, the effect of land-cover categories must be included. This can be done by assuming the microwave response within each antenna footprint to be a linear combination of individual responses, weighted by the fraction of each land-cover category,

$$\Delta T(W_{eq}) = \sum f_i \Delta T_i(W_{eq}) \quad (3)$$

where f_i = fraction of surface type i
 ΔT_i = response to water equivalent for surface type i .

By accounting for various surface types within each antenna footprint, the accuracy of snow water equivalent retrieval from satellite microwave radiometer measurements was found to increase substantially (Hallikainen, 1984a).

8. References

- Hallikainen, M. (1984a) Retrieval of snow water equivalent from Nimbus-7 SMMR data: effect of land-cover categories and weather conditions. IEEE Journal of Oceanic Engineering, v. OE-9(5), p.372-376.
- Hallikainen, M.; Ulaby, F.T.; Dobson, M.C.; El-Rayes, M. (1984b) Dielectric measurements of soils in the 3- to 37-GHz band between -50 C and 23 C. (In: IGARSS '84 Symposium, Proceedings, held at Strasbourg, 27-30 August 1984, ESA SP-215, p. 163-168.)
- Kunzi, K.; Patil, H.; Rott, H. (1982) Snow-cover parameters retrieved from Nimbus-7 scanning multichannel microwave radiometer (SMMR) data. IEEE Transactions on Geoscience and Remote Sensing, v. GE-20(4), p. 452-468.
- Rango, A. et al. (1979) The utilization of spaceborne microwave radiometers for monitoring snowpack properties. Nordic Hydrology, v. 10, p. 25-40.

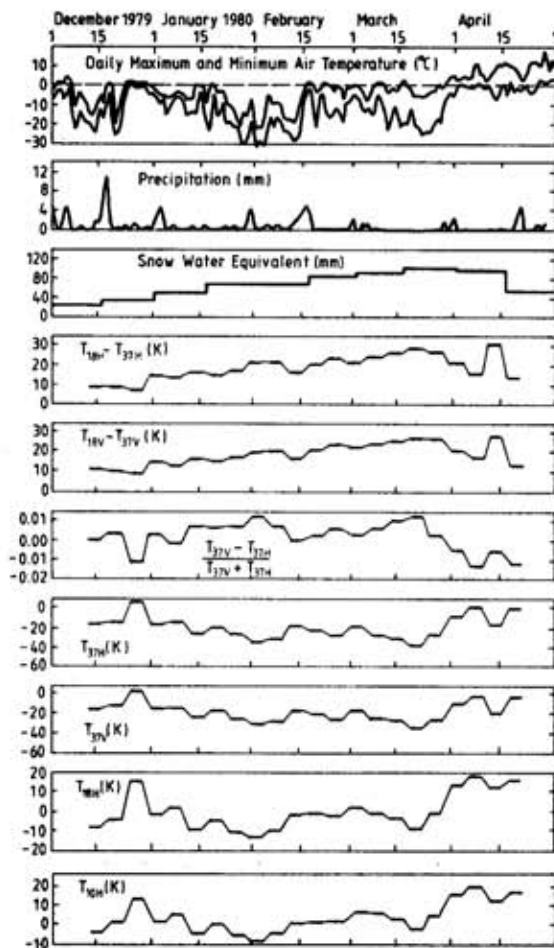


Figure 1. Comparison of ΔT (Equation 1) with meteorological data in a 100 km x 100 km test area in Southern Finland for Winter 1979-80 (Nimbus-7).

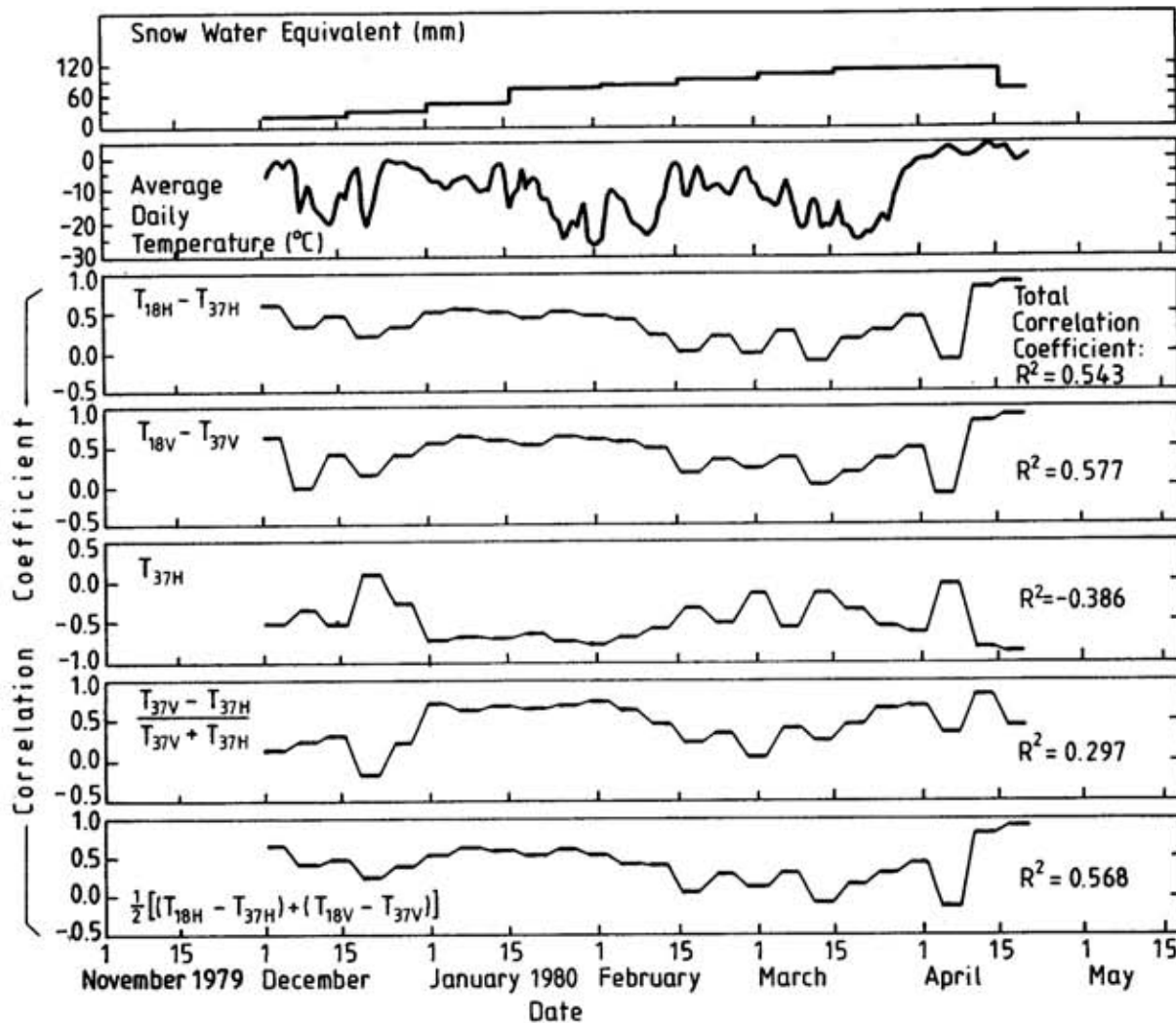


Figure 2. Correlation coefficient between brightness temperature functions (Nimbus-7, Equation 1) and snow water equivalent in Southern Finland (200,000 sq. km) for Winter 1979-80. Correlation coefficients for each 5-day period and the whole Winter are shown.

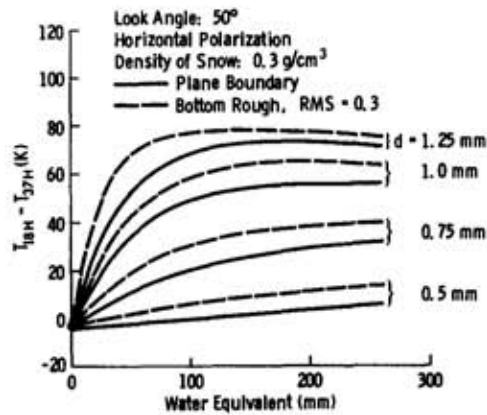


Figure 3. Theoretical brightness temperature difference between 18 GHz and 37 GHz for snow-covered terrain as a function of snow water equivalent, with snow particle diameter d as a parameter.

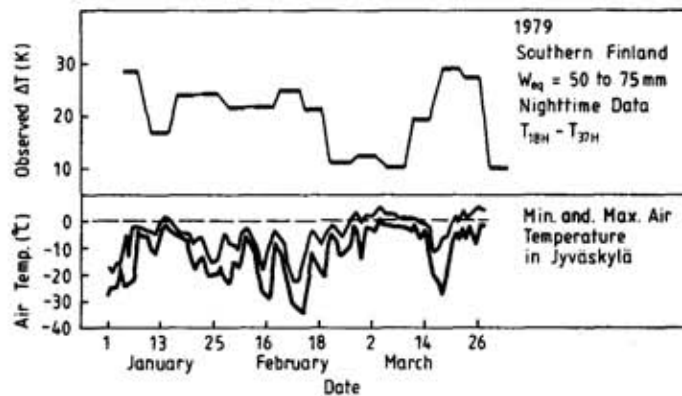


Figure 4. Comparison of average ΔT (Equation 2) in Southern Finland with daily air temperatures in Jyväskylä for Winter 1978-79 (Nimbus-7).

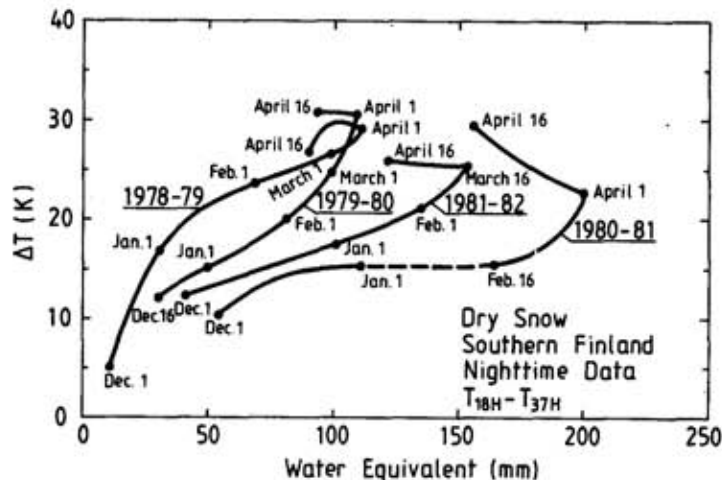


Figure 5. Average ΔT response (Equation 2) to snow water equivalent in Southern Finland for Winters 1978-79 through 1981-82 (Nimbus-7).

Kukla, G; Barry, R.G.; Hecht, A.; Wiesnet, D. eds. (1986) SNOW WATCH '85. Proceedings of the Workshop held 28-30 October 1985 at the University of Maryland, College Park, MD. Boulder, Colorado, World Data Center A for Glaciology (Snow and Ice), Glaciological Data, Report GD-18, p.181-187.

Nimbus-7 SMMR Snow Cover Data

A.T.C. Chang
Hydrological Sciences Branch
National Aeronautics and Space Administration
Goddard Space Flight Center
Greenbelt, Maryland, U.S.A.

ABSTRACT

Snow cover maps are presently produced routinely by NOAA/NESDIS and by USAFGWC. Studies concluded that the gross features of the snow cover are well represented; however the fine structure of the snow boundary is greatly generalized. The NESDIS maps which rely on data from spaceborne visible and infrared sensors sometimes miss large snow fields due to persistent cloudiness, particularly in the fall when the snow areal extent is rapidly changing. Microwave radiation penetrating through clouds and snowpacks could provide additional information of snow fields. The Nimbus-7 spacecraft which was launched on October 24, 1978, carried onboard a five channel dual polarized Scanning Multichannel Microwave Radiometer (SMMR). Based on theoretical calculations, a snow covered area retrieval algorithm was developed. Global snow cover maps for the northern hemisphere were derived from SMMR data for a period of five years (1979-1983). Comparisons with NOAA/NESDIS and USAFGWC products were conducted to evaluate and assess the accuracy of SMMR derived snow maps. In general, these data sets compared well: the total snow covered area derived from SMMR is usually about 5 percent less than for the other two products. This is because passive microwave sensors cannot detect snow less than 2.5 cm depth due to the fact that the emission from the underlying snow is not modified very much by emission or scattering by the snowpack for a shallow snow cover.

INTRODUCTION

The use of remotely-acquired microwave data, in conjunction with essential ground measurements, will most likely lead to improved information extraction regarding snowpack properties beyond that available by conventional techniques. Visible and near-infrared data have recently come into operational use for performing snowcovered area measurements. However, the data acquisition is hampered by cloudcover, sometimes at critical

times when a snowpack is ripe. Furthermore, information on water equivalent, free water content, and other snowpack properties germane to accurate runoff predictions is not currently obtainable using visible and near-infrared data alone because only surface and very near-surface reflectance are detected.

Microwaves are mostly unaffected by clouds and can penetrate through various snow depths depending on the wavelength. Hence, microwave sensors are potentially capable of determining the internal snowpack properties such as snow depth and snow water equivalent (Hall et al., 1978; Rango, et al., 1979). However, operational use of remotely-collected microwave data for snowpack analysis is not imminent because of complexities involved in the data analysis. Snowpack and soil properties are highly variable and their effects on microwave emission are still being explored. Nevertheless, much work is being done to develop passive microwave techniques (Edgerton et al., 1973; Schmugge et al., 1974; Chang et al., 1976; Kong et al., 1979; Chang and Shiue, 1980; Matzler et al., 1980 and Stiles and Ulaby, 1980) for analysis of snowpack properties. In this paper, an attempt to retrieve snow parameters by using Nimbus-7 SMMR data is reported.

MICROWAVE EMISSION FROM SNOW

Snow particles act as scattering centers for microwave radiation. Computational results indicate that scattering from individual snow particles within a snowpack can be the dominant modification factor of upwelling emission in the case of dry snow (Figure 1). This type of radiation upwelling through snow is governed by Mie scattering theories for which a good description can be found in Chang et al. (1976). Microwave radiation emanating from snow originates from a depth of ~ 10-100 times the wavelength used (Chang et al., 1976). However, when the snowpack thickness is less than the microwave penetration, the underlying surface will contribute to the brightness temperature (T_b) (Chang and Gloersen, 1975).

Using the multifrequency analysis approach, one can make inferences regarding not only the thickness of the snowpack, but the moisture conditions and the condition of the underlying soil (wet versus dry). The shorter wavelengths, such as 0.8 cm, sense near-surface temperature and emissivity, and surface roughness. At the intermediate wavelengths, 1.4 and 1.7 cm, the radiation is less affected by the surface and more information is obtained on the characteristics of the mid-pack. All of the above generalizations apply to the snow conditions encountered by the various satellite observations for different regions of the world.

The presence of liquid water content in the snowpack completely changes the observed microwave signatures (Chang and Shiue, 1980; Matzler et al., 1980; and Stiles and Ulaby, 1980). A few percent of liquid water in snow will cause a sharp increase in the brightness temperature (Chang and

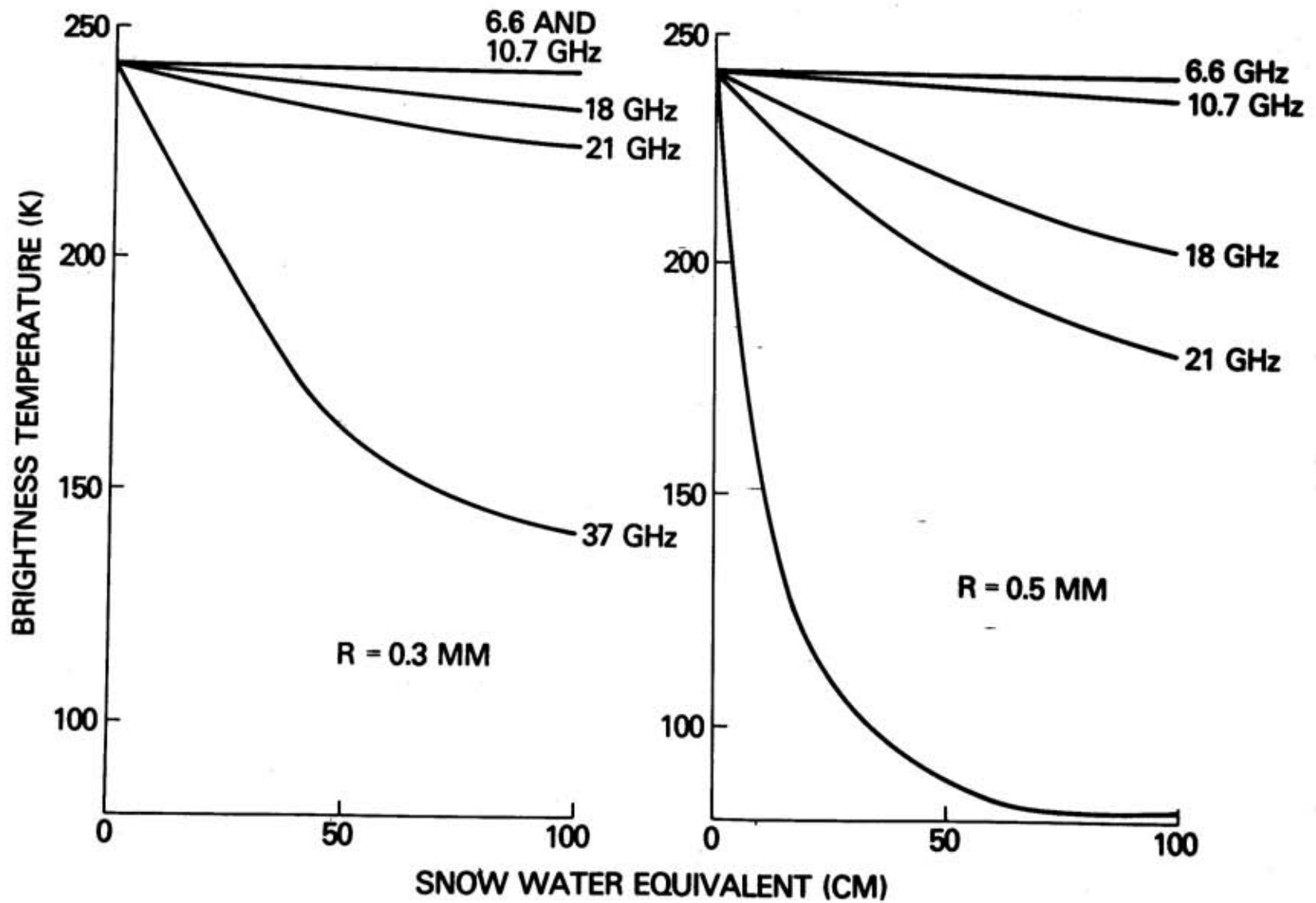


Figure 1. Computed brightness temperature vs. snow water equivalent for SMMR frequencies.

Gloersen, 1975). This is because the emission of individual snow particles are increased when liquid water coats the crystal.

The condition of the ground beneath the snow will determine the intensity of the radiation incident from below. Dry or frozen ground has a high emissivity (~ 0.90-0.95) whereas unfrozen wet ground has a much lower emissivity (~ 0.7). Knowledge of the condition of the ground underlying the snow is important for the interpretation of observed brightness temperatures and can generally be determined from the longer wavelength observations. However, due to the small penetration depth of microwave radiation into wet soil, typically 1/4 wavelength, a wavelength of the order of 20 cm will be required.

SNOW RETRIEVAL ALGORITHM AND PRELIMINARY RESULTS

SMMR is a five frequency, dual polarized microwave radiometer which measures the upwelling microwave radiation at 6.6, 10.7, 18.0, 21.0, and 37.0 GHz while scanning 25° to either side of the spacecraft (approximately 780 km swath width) with a constant incidence angle of approximately 50° with respect to the Earth's surface. The spatial resolution varies from 25 km for the 37 GHz to 150 km for the 6.6 GHz. Detailed descriptions of this instrument can be found in Gloersen and Barath (1977). It was launched on October 24, 1978, into a sun synchronous polar orbit with local noon/midnight equator crossing.

Kunzi et al. (1982) reported an algorithm to retrieve snow-cover parameters using Nimbus-7 SMMR data. The brightness temperature gradient of 37 GHz and 18 GHz were used to discriminate snow parameters. Based on the SMMR data for 1978-1979 winter season, encouraging results were derived. Chang et al. (1982) reported the snow parameter retrieval results based on a theoretically derived algorithm.

After experimenting with SMMR data over several large open areas, the Canadian Height Plains, U.S. Great Plains, Alaska and central Russia, the algorithm has been refined. Since the brightness temperature decreases with depth due to snow scattering, 37 GHz wavelength data which is sensitive to scattering are used. However, the variation of the 37 GHz brightness temperature is also affected by the snowpack temperature. By using 18 GHz channel data, which is usually less affected by scattering, in the retrieval algorithm the temperature effect is normalized. Figure 2 shows the relationship between the snow depth and brightness temperature difference of 37 GHz and 18 GHz. Due to the inhomogeneity within the large SMMR footprint (25 km x 25 km), derived snow depth less than 2.5 cm was assigned as no snow. The equation used to derive snow depth information is

$$SD = 1.59 * (T_{18H} - T_{37H}) \text{ cm} \quad (1)$$

The snow covered area is defined when retrieval snow depth is larger than 2.5 cm. By using this algorithm, a five year data set derived for Nimbus-7

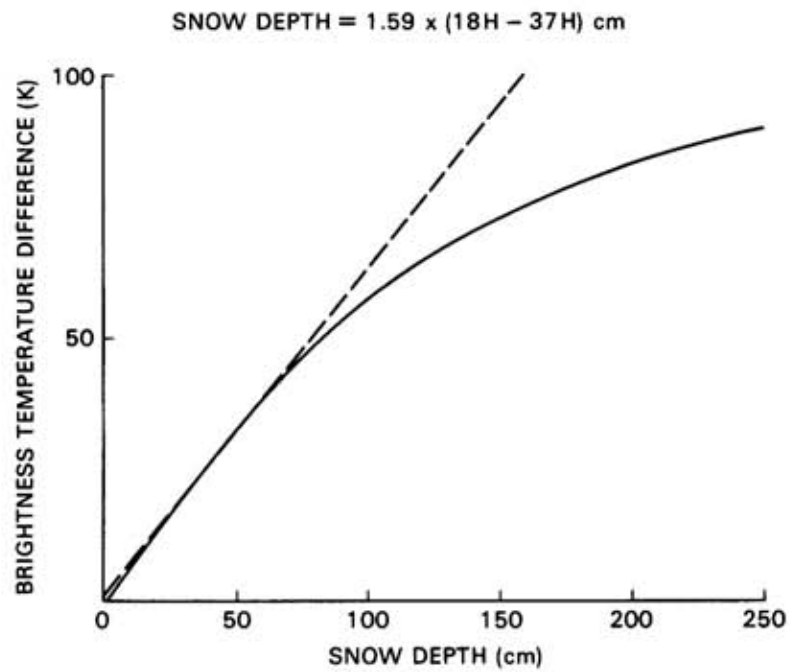


Figure 2. Brightness differences ($T_{18H} - T_{37H}$) vs. snow depth.

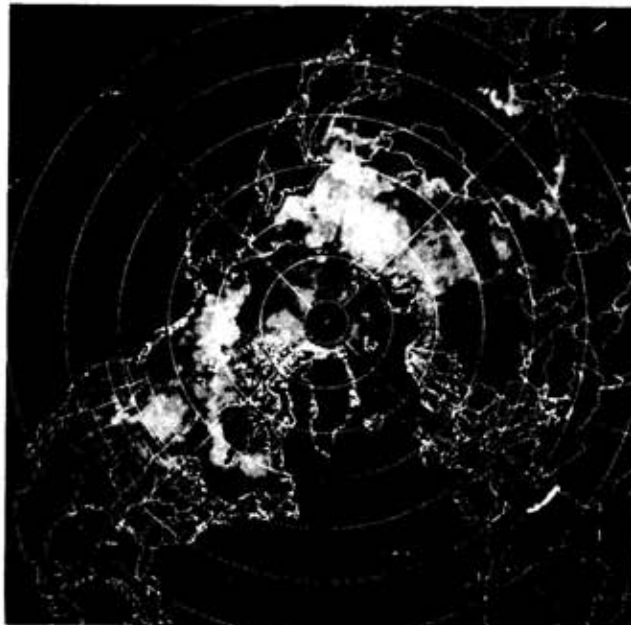


Figure 3. Nimbus-7 SMMR derived northern hemisphere snow depth map February, 1982.

SMMR brightness has been produced. It covered the period of October, 1978 to October, 1983. Figure 3 shows a sample snow map of northern hemisphere for February, 1982. In this map, the deep snow cover areas were shown with brighter tone while shallow snow were shown with darker tone.

DISCUSSION

5 year SMMR derived northern hemisphere snow parameter maps have been produced using one simple algorithm. In order to evaluate the quality of this product, several steps were taken. First, the snow boundary lines of SMMR products and NOAA products were compared. Normally, the SMMR derived snow boundary line fell behind the NOAA snow line. This is because microwave can penetrate through a shallow snowpack without registering snow effect. However, because of this characteristic, when the microwave signature indicates snow, the entire field of view is probably snow covered. Over the mountainous area, the slope tends to modify the microwave signatures. Although the sensitivity of microwave radiation with respect to snow depth has changed, the snow boundary can still be delineated. For 1979 to 1983, the boundary lines in the Great Plains and Rockies of U.S. compared favorably (within 100 km) between SMMR and NOAA products for the months of January to March. For the same time period, for eastern, mid-west and western regions of the U.S., the differences were about 200 km. In the western China and central Asia area, the comparisons gave large differences in the result. Due to limited "ground truth" data, the relative accuracies are still being assessed.

To evaluate the quality of snow water equivalent, several areas were chosen for comparison. The results from the Canadian Height Plains and the Russia steppe area, which are uniform and homogeneous, are usually good with correlation coefficients $R = 0.85$. The results from forested area and mountainous area are different. Since the surface features masked out the microwave snow signatures, a different algorithm will be required to retrieve the snow parameters. An ongoing project which studies the Colorado River basin area will suggest what algorithm is required to retrieve useful information.

References

- Chang, A.T.C.; Shiue, J.C. (1980) A comparative study of microwave radiometer observations over snowfields with radiative transfer model calculations. Remote Sensing of Environment, v.10, p.215-229.
- Chang, A.T.C.; Foster, J.L.; Hall, D.K.; Rango, A; Hartline, B.K. (1982) Snow water equivalent determination by microwave radiometry. Cold Regions Science and Technology, v.5, p.259-267.

- Chang, T.C.; Gloersen, P. (1975) Microwave emission from dry and wet snow. (In: Operational Applications of Satellite Snowcover Observations, NASA SP-391, Washington, D.C., p.399-407.)
- Chang, T.C.; Gloersen, P.; Schmugge, T.; Wilheit, T.T.; Zwally, H.J. (1976) Microwave emission from snow and glacier ice. Journal Glaciology, v.16(74), p.23-39.
- Edgerton, A.T.; Ruskey, F.; Williams, D.; Stogryn, A.; Poe, G.; Meeks, D.; Russell, O. (1973) Microwave emission characteristics of natural materials and the environment. Final Technical Report 9016R-8, Microwave Systems, Aerojet-General Corporation, Azusa, California.
- Gloersen, P.; Barath, F.T. (1977) A Scanning Multichannel Microwave Radiometer for Nimbus-G and Seasat-A. IEEE Journal of Oceanic Engineering, v.2, p.172-178.
- Hall, D.K.; Chang, A.; Foster, J.L.; Rango, A.; Schmugge, T. (1978) Passive microwave studies of snowpack properties. Proceedings of the 46th Annual Western Snow Conference, Otter Rock, OR, p.33-39.
- Kong, J.A.; Shin, R.; Shiue, J.C.; Tsang, L. (1979) Theory and experiment for passive microwave remote sensing of snowpacks. Journal of Geophysical Research, v.84, p.5669-5673.
- Kunzi, K.F.; Patil, S.; Rott, H. (1982) Snow-cover parameters retrieved from Nimbus-7 Scanning Multichannel Microwave Radiometer (SMMR) Data. IEEE Transactions of Geoscience and Remote Sensing, v.20, p.452-467.
- Matzler, C.; Schanda, E.; Hofer, R.; Good, W. (1980) Microwave signatures of the natural snow cover at Weissfluhjoch. NASA CP-2153, p.203-223, available from NTIS, Springfield, Virginia.
- Rango, A.; Chang, A.T.C.; Foster, J.L. (1979) The utilization of spaceborne microwave radiometers for monitoring snowpack properties. Nordic Hydrology, v.10, p.25-40.
- Schmugge, T.; Wilheit, T.T.; Gloersen, P.; Meier, M.F.; Frank, D.; Dirmhirn, I. (1974) Microwave signatures of snow and fresh water ice. (In: Advanced Concepts and Techniques in the Study of Snow and Ice Resources, National Academy of Sciences, Washington, D.C., p.551-562.
- Stiles, W.H.; Ulaby, F.T. (1980) Microwave remote sensing of snowpacks. NASA Contractor Report No. 3263, 404 p., available from NTIS, Springfield, Virginia.

Kukla, G; Barry, R.G.; Hecht, A.; Wiesnet, D. eds. (1986) SNOW WATCH '85. Proceedings of the Workshop held 28-30 October 1985 at the University of Maryland, College Park, MD. Boulder, Colorado, World Data Center A for Glaciology (Snow and Ice), Glaciological Data, Report GD-18, p.189-192.

Snow Cover Monitoring Using Microwave Radiometry

Norman C. Grody

National Environmental Satellite, Data, and Information Service
National Oceanic and Atmospheric Administration
Washington, D.C., U.S.A.

Abstract

Multispectral satellite observations of the earth's surface and atmosphere have provided information on geophysical parameters which are important in meteorology, hydrology, agriculture, and oceanography. The primary advantage of passive microwave measurements over those in the visible and infrared is their ability to probe through clouds, with rain being the major source of attenuation, allowing for all-weather observations. A technique is presented to identify snow cover and discriminate among a number of other surface and atmospheric parameters based on measurements by the Nimbus-7 Scanning Multichannel Microwave Radiometer.

Snowmelt is the major component of the total annual water supply in large parts of the world. Also, the amount of water stored as snow is important in forecasting its effect on the water supply, flooding, irrigation and management of agricultural commodities. As such, the major parameters required are areal extent, water equivalent or depth, and liquid water content. Repetitive coverage of the observations is required every 3-5 days with an all weather measurement capability.

Visible and infrared satellite data have recently come into operational use for snow area determinations. However, the data acquisition is hampered by cloud cover, sometimes at critical times when a snowpack is ripe. Furthermore, information on water equivalent, free water content, and other properties pertinent to accurate runoff predictions are not currently available using visible and infrared techniques. More complete information on snow properties is available from microwave radiometers whose measurements are nearly independent of clouds. The microwave emission from within a snow layer can penetrate through various depths depending on the frequency and changes dramatically between dry, refrozen snow, and melting snow (Hoffer and Matzler, 1980). The use of microwave data can therefore lead to an analysis of the internal snowpack properties with an all weather capability.

Passive microwave imagery from space has been available since December 1972, when Nimbus-5 was launched carrying a 19.35 GHz microwave radiometer. Additional data became available in June 1975 with the launch of Nimbus-6 with a 37 GHz dual polarization radiometer. This instrument was succeeded by a five-frequency, dual polarization Scanning Multichannel Microwave Radiometer (SMMR) flown on Nimbus-7 in November 1978. The SMMR frequencies are at 6.6, 10.7, 18.0, 21.0 and 37.0 GHz. Studies have been and are currently being conducted to utilize microwave radiometers for the determination of snow properties. The major drawback of these satellite sensors for snow hydrology is the relatively poor spatial resolution of about 25 km. However, results from various studies (e.g., Kunzi et al., 1984) indicate that qualitative monitoring of snowpack buildup and disappearance during the winter appears feasible. Studies have also shown the use of microwave data for deriving information on snow water equivalent for certain areas (Foster et al., 1984).

Snow produces a somewhat unusual microwave emissivity characteristic. This is illustrated in Figure 1 which summarizes the frequency dependence of emissivity for snow as well as other surfaces. A snowpack contains a collection of ice crystals or melting ice particles depending on the snow temperature. The emissivity of snow depends on the absorption and scattering due to the particles. For dry snow the ice crystals scatter some of the upwelling radiation out of the sensor's field of view. The scattering effect increases with frequency so that the emissivity decreases as the frequency increases. As shown in Figure 1, the emissivity characteristic of dry snow is different from most other surfaces. The opposite slope of emissivity with frequency can be used in distinguishing dry snow from other surfaces. A more general classification technique has been developed which utilizes both the magnitude as well as the variation of emissivity with frequency to separate the different surface types. These two quantities, the emissivity and its slope with frequency, can be inferred using dual frequency microwave measurements. The brightness temperature "difference" is proportional to the slope while the "average" of the two measurements is related to the emissivity itself.

To illustrate the classification method, Figure 2 shows a scatter plot of the average brightness temperature versus the brightness temperature difference using the 18 and 37 GHz (vertical polarization) SMMR channels. These data were obtained from a January 1979 SMMR pass over the central U.S. and contains areas of open water, wet and dry land, lake ice, rainfall and snow cover. For details on the data set see the papers by Grody (1984) and Ferraro et al., (1985). The diagram shows six "clusters" corresponding to the various surface and atmospheric parameters. Note that both the average and difference measurements are needed to separate the different geophysical parameters. Dry snow is readily distinguished from all other features where the scatter within the cluster is associated with variations in snow depth as well as other factors. Those observations which do not fall into a specific cluster are "mixed pixels" and correspond to more than one geophysical parameter in the field of view. An example of a mixed pixel is a SMMR observation which occurs along a coastline. In this case, part of the field of view contains land, part contains open water. Thus, the brightness temperatures do not correspond to a unique surface or atmospheric parameter.

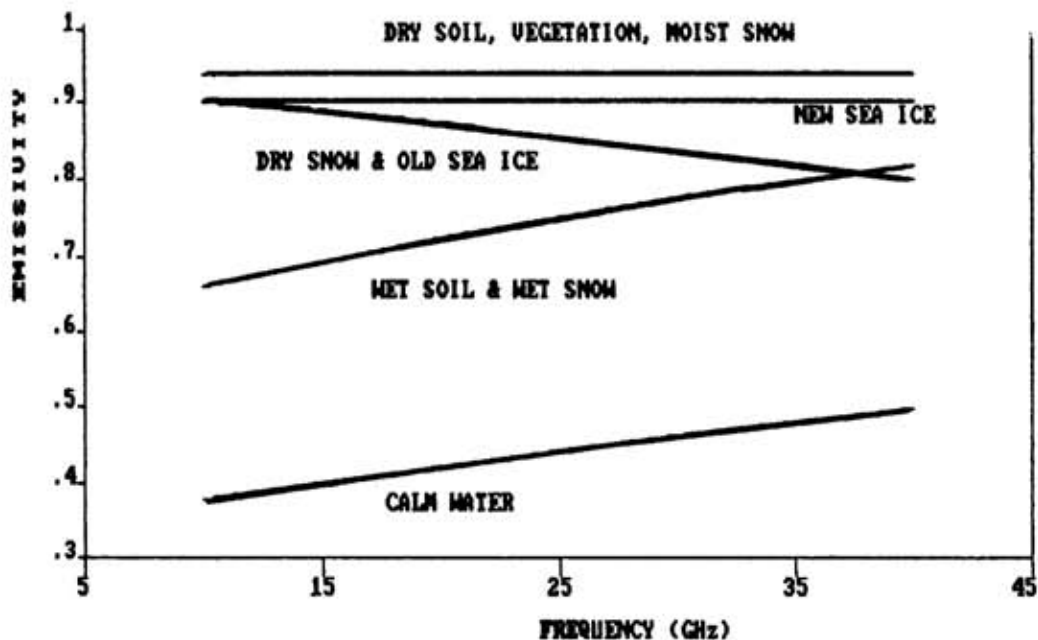


Fig. 1. Emissivity as a function of frequency for different surface types.

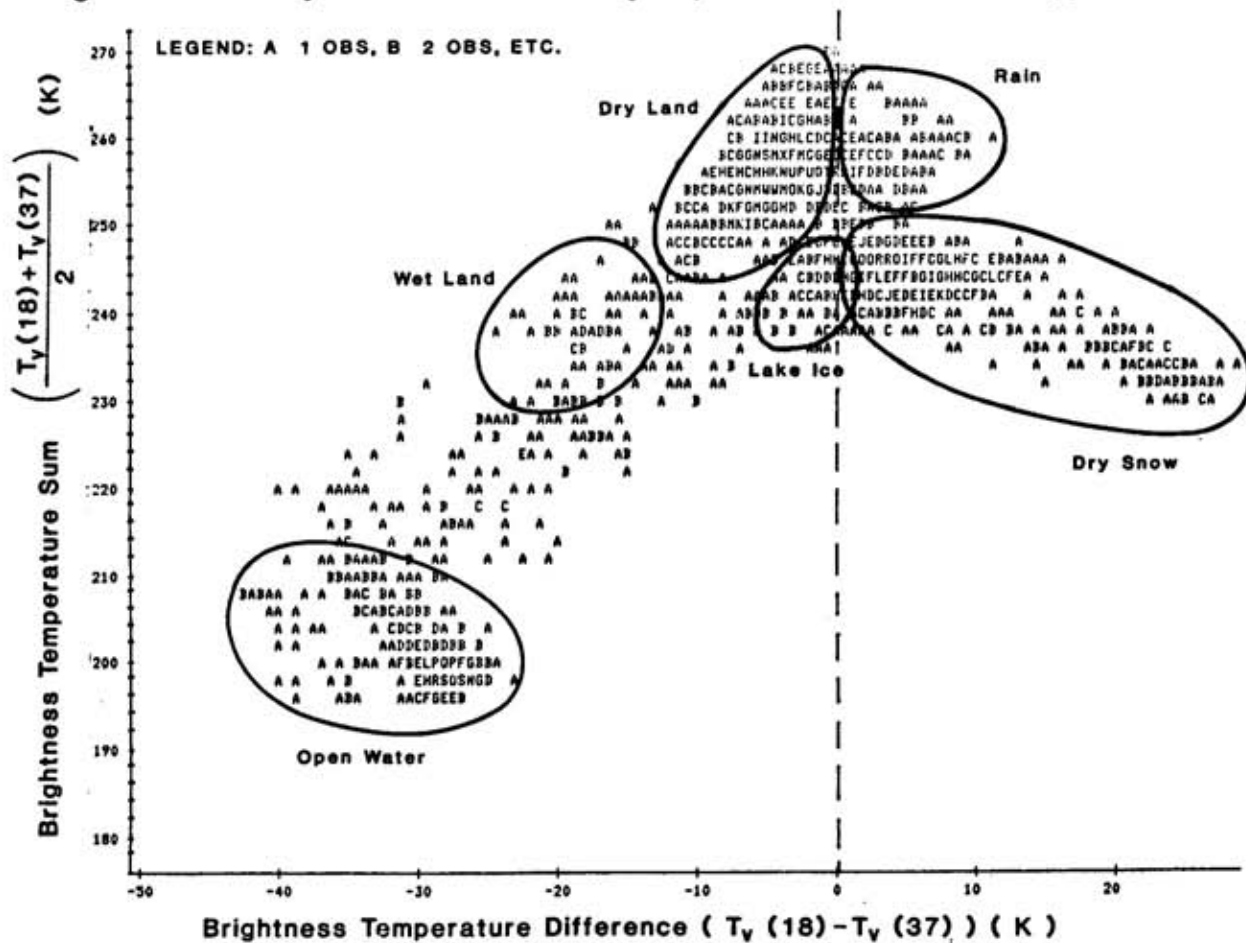


Fig. 2. Scatter plot of the average brightness temperature versus the brightness temperature difference using the 18 and 37 GHz vertically polarized SMMR channels for latitudes between 25° and 60°N on January 20, 1979.

The algorithm shown in Figure 2 has been applied to SMMR data to form a classification image (Ferraro et al., 1985). Each geophysical parameter is classified by requiring the brightness temperature measurements to lie within one of the six clusters. To simplify the designation, the clusters are represented as four point polygons, each having a specific color assigned to the pixels. Undefined pixels are indicated as white pixels. For a given color the intensity is defined by the magnitude of the brightness temperature "difference", i.e., dark intensities represent small differences, bright intensities large differences. These intensity variations yield insight to various features, such as snow depth, soil moisture content or rain intensity.

This paper presents a method using the 18 and 37 GHz vertically polarized brightness temperatures from the Nimbus-7 SMMR to classify six different geophysical parameters (dry snow, sea ice, dry land, flooded land, precipitation, and open water). The use of multichannel techniques is necessary because several surface and atmospheric features cannot be separated by single channel measurements. Finally, a technique of this type is quite attractive for producing maps, of geophysical parameters on an operational basis, which can be used as a screening tool to produce accurate quantitative algorithms.

References

- Ferraro, R.R.; Grody, N.C.; Kogut, J.A. (1985) Classification of geophysical parameters using passive microwave satellite measurements. (In: International Geoscience and Remote Sensing Symposium (IGARSS' 85), Amherst Massachusetts, 7-9 October, Proceedings, p.919-924.)
- Foster, J.L.; Hall, D.K.; Chang, A.T.C. (1984) An overview of passive microwave snow research and results. Reviews of Geophysics and Space Physics, 22, p.195-207.
- Grody, N.C.. (1984) Precipitation monitoring over land from satellites using microwave radiometry. (In: International Geoscience and Remote Sensing Symposium (IGARSS' 84) Strasbourg, France, 27-30 August, Proceedings, p.417-423.)
- Hoffer, R.; Matzler, C. (1980) Investigations of snow parameters by radiometry in the 3 to 60 mm wavelength region. Journal of Geophysical Research, 85, p.453-460.
- Kunzi, K.F.; Patil, S.; Rott, H. (1984) Snow-cover parameters retrieved from Nimbus-7 Scanning Multichannel Microwave Radiometer (SMMR) data. Reviews of Geophysics and Space Physics, 22, p.452-467.

Kukla, G; Barry, R.G.; Hecht, A.; Wiesnet, D. eds. (1986) SNOW WATCH '85. Proceedings of the Workshop held 28-30 October 1985 at the University of Maryland, College Park, MD. Boulder, Colorado, World Data Center A for Glaciology (Snow and Ice), Glaciological Data, Report GD-18, p.193-203.

Remote Sensing of Snow Properties in Mountainous Terrain

Jeff Dozier
University of California
Santa Barbara, California, U.S.A.

Abstract

Spectral albedo measurements from satellite (e.g. Landsat Thematic Mapper) require that spacecraft upwelling radiances be corrected for atmospheric absorption and scattering and for local surface illumination. The lower boundary condition of the atmospheric radiative transfer model varies with incidence angle, and the satellite data must be co-registered to digital elevation data. Results from extensive radiative transfer calculations fortunately fall into some simple statistical relationships, whereby the optical grain size of the snow and the degradation of albedo resulting from contamination are estimated. One remaining problem is that inaccuracies in the elevation data make precise registration with satellite data hard to achieve.

Introduction

This paper addresses climate modeling on a smaller scale than that considered by most of the other papers in this volume. Over a watershed we often want to estimate the energy transferred into the snow pack, in order to compute water balances and estimate snow melt runoff.

Solution of the snow surface energy balance components at a well instrumented, possibly remote micrometeorological site is feasible (Figure 1). With data on incoming and outgoing radiation in solar and thermal wavelengths, low-level atmospheric profiles of air temperature, wind speed, and water vapor density, and temperature profiles in the top layers of the snow pack, it is possible to compute the amount of energy expended in melting snow, and thereby estimate the amount of water produced (Anderson, 1976).

$$\Delta Q = R + H + L_v E + G \quad (1)$$

Here R is the net radiation at the snow surface, H and $L_v E$ are sensible and latent heat fluxes, and G is the soil heat flux. If ΔQ is positive, either the temperature of the snow pack increases, or, if it is already at 0°C , a mass of snow $M = \Delta Q / L_f$ is melted. L_v and L_f are the latent heats of vaporization and fusion. Of the components in equation (1), the net radiation term R usually dominates, but the issue is complicated by spectral and angular variation in the snow albedo ρ .



Figure 1. Measurement of snow pack energy balance parameters at a remote site, by transmitting instrument output data to satellite. Station is located at an elevation of 3200 m in Emerald Lake Basin, Sequoia National Park, California.

At a particular time the net radiation is sum of the solar and thermal components integrated over wavelength λ . If we simplify and assume the diffuse irradiance field is isotropic, the net radiation is

$$R = \int_{\text{solar}} \left[\mu_0 [1 - \rho_s(\lambda, \mu_0)] E_s(\lambda) + [1 - \rho_d(\lambda)] E_d(\lambda) \right] d\lambda + \int_{\text{thermal}} \epsilon_d(\lambda) \left[E_d(\lambda) - \frac{2hc^2}{\lambda^5 (e^{hc/k\lambda T} - 1)} \right] d\lambda \quad (2)$$

The first term represents the absorbed solar irradiance, the second accounts for the longwave radiation balance. ρ_s and ρ_d are the direct and diffuse spectral albedoes. E_s and E_d are the direct and diffuse spectral irradiances; E_d exists both at solar and thermal wavelengths. ϵ_d is the spectral hemispherical emissivity, and the last expression in the second term accounts for the Planck emission by the surface at temperature T ; h is the Planck constant, k is the Boltzmann constant, and c is the speed of light.

Our problem in analysis of surface climate hydrologic purposes is to evaluate equation (2) over a melt season and over a drainage basin. In this paper we concentrate on the estimation of spectral albedo ρ from measurements of satellite radiance above the atmosphere. Spectral albedo measurements from satellite (e.g. Landsat Thematic Mapper) require that spacecraft upwelling radiances be corrected

for atmospheric absorption and scattering and for local surface illumination. The lower boundary condition of the atmospheric radiative transfer model used must vary with incidence angle, and the satellite data must be registered to digital elevation data. The results from extensive radiative transfer calculations fortunately fall into some simple statistical relationships, whereby the optical grain size of the snow and the degradation of albedo resulting from contamination can be estimated. One difficult remaining problem is that precise registration of satellite and elevation data is hard to achieve, mainly because of inaccuracies in the elevation data.

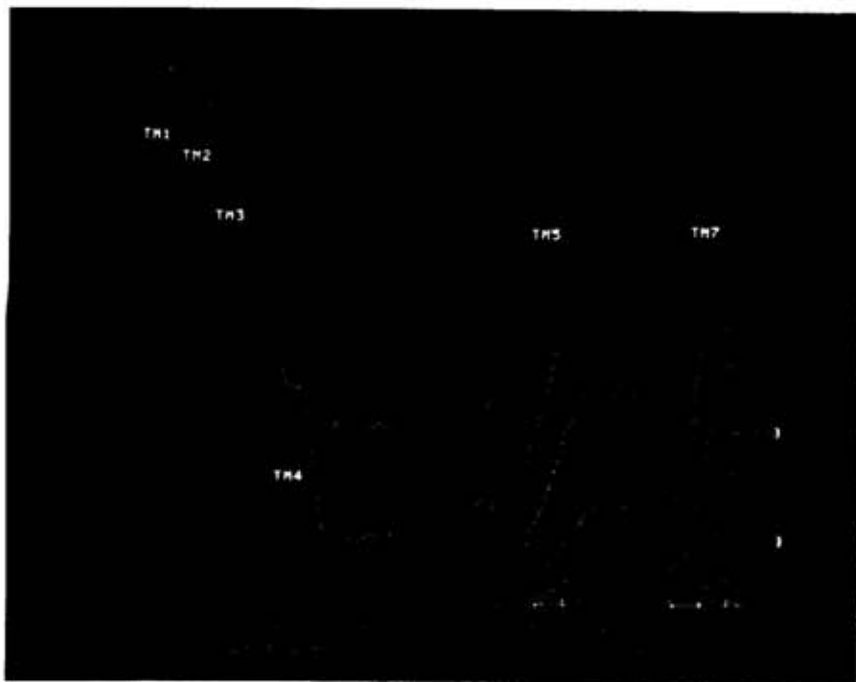


Figure 2. Snow reflectance in the Landsat Thematic Mapper bands, calculated for an illumination angle of 66° from a twostream approximation. Grain radii range from $50\ \mu\text{m}$, very fine new snow, to $2000\ \mu\text{m}$, coarse old melting or refrozen snow.

Landsat Thematic Mapper

The Thematic Mapper was first launched on July 16, 1982 aboard Landsat-4. The second instrument was launched on March 1, 1984 aboard Landsat-5. The satellite is at a nominal altitude of 705 km in a sun-synchronous orbit. Equator crossing time is between 09:30 at 10:00 local solar time, and the orbit period is 100 minutes. The repeat period is 16 days.

Table 1 specifies the wavelength bands of the TM. For the solar portion of the electromagnetic spectrum, the values of the "solar constant," exoterrestrial solar radiation at the mean earth-sun distance integrated over the wavelength bands, are also given. In the last column of the table the sensor saturation radiance is expressed as a percentage of the solar constant. If the product of the planetary reflectance and the cosine of the solar zenith angle exceeds this value, the sensor will saturate in this band.

Table 1. Landsat-5 Thematic Mapper Radiometric Characteristics

band	wavelength range (μm)		radiances ($\text{W m}^{-2} \mu\text{m}^{-1} \text{sr}^{-1}$)				
			$NE\Delta L$	L_{\min}	L_{\max}	L_{solar}	pct
TM1	0.45	0.52	0.63	-1.5	152.1	621	24
TM2	0.53	0.61	1.17	-2.8	296.8	540	55
TM3	0.62	0.69	0.80	-1.2	204.3	468	44
TM4	0.78	0.90	0.81	-1.5	206.2	320	64
TM5	1.57	1.78	0.108	-0.37	27.19	66.9	41
TM6	10.4	12.5	0.057	1.25	15.75	(thermal)	
TM7	2.10	2.35	0.057	-0.15	14.38	23.9	60

Snow Reflectance in TM Bands

In the visible wavelengths (TM bands 1 and 2 especially) snow reflectance is insensitive to grain size, but sensitive to modest amounts of absorbing impurities (Warren and Wiscombe, 1980). In the near-infrared (TM band 4) snow reflectance is insensitive to absorbing impurities but sensitive to grain size (Wiscombe and Warren, 1980). Figure 2 shows the spectral variation in reflectance of pure snow of various grain radii over the TM bands. We note that in TM4 the reflectance is sensitive enough to grain radius to allow estimate of the "optical grain size" from reflectance measurements. For albedo estimates from remote sensing, our aim is to estimate the important physical parameters, absorbing impurities and grain size, from spectral measurements in suitable wavelength bands. The spectral albedo or band-integrated albedo can be calculated. The scheme should fit the parameterization under development by Marshall and Warren (this volume).

In TM5 reflectance is sensitive to grain size only for very small radii. For most snow reflectance in this band will be near zero. Both ice and water clouds, however, will be appreciably brighter than snow, allowing for snow/cloud discrimination (Figure 3). Thermal data (TM6, Figure 4) cannot be used for snow/cloud discrimination, because in mountainous areas the overlying clouds may be colder or warmer than the snow.

Some details still need to be solved. In the radiative transfer approach (e.g. Wiscombe and Warren, 1980; Choudhury and Chang, 1981) snow reflectance is modeled as an ensemble of spheres. In reality snow grains may not be spherical (Figure 5). While it is possible to calculate the radius or distribution of radii of equivalent spheres, by choosing sizes that cause the radiative transfer calculations to fit the measurements, the question of how these equivalent sphere radii compare to the physical sizes and shapes of the grains is still unanswered. We are currently trying to resolve this issue, by measuring the spectral bidirectional reflectance-distribution function (BRDF) of snow at wavelengths from 0.3–3.0 μm . At the same time we are using the plane-section method (Perla, 1982; Perla and Dozier, 1984) to measure such grain properties as specific volume, specific surface area, mean intersection length, etc. Li's (1982) model can be used to compute the radiative transfer solution to the BRDF for a specified distribution of spherical radii.

Planetary Reflectance (Above the Atmosphere)

The satellite measures upwelling radiance L^\uparrow above the earth's atmosphere. We define "planetary reflectance" ρ_p as

$$\rho_p = \frac{L^\uparrow}{\mu_0 S_0} \quad (3)$$

πS_0 is the exoterrestrial solar irradiance ($\text{W m}^{-2} \mu\text{m}^{-1}$), incident at angle $\cos^{-1}\mu_0$. A simplified "two-stream" atmospheric model (Meador and Weaver, 1980) is defined by the following pair of differential

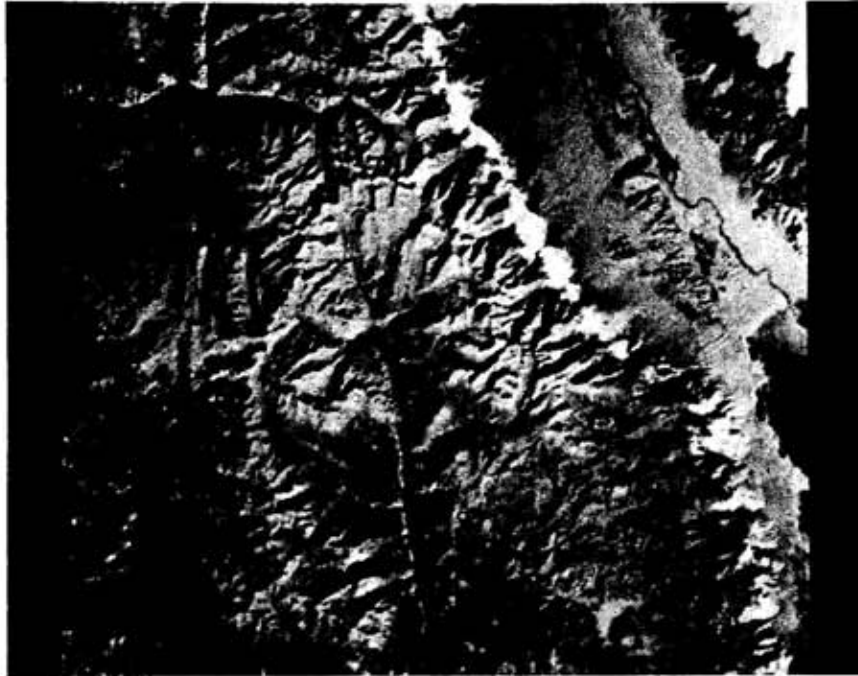


Figure 3. Snow/cloud discrimination with TM band 5. The area is the southern Sierra Nevada, with the Kern (south-flowing) and Kings (west-flowing) River basins shown. The clouds along the east side of the Sierra Nevada and over the White Mountains (northwest corner) are clearly visible. Date is December 10, 1982.

equations:

$$\frac{dL^{\uparrow}}{d\tau} = \gamma_1 L^{\uparrow} - \gamma_2 L^{\downarrow} - \bar{\omega} S_0 \gamma_3 e^{-\tau/\mu_0} \quad (4)$$

$$\frac{dL^{\downarrow}}{d\tau} = \gamma_2 L^{\uparrow} - \gamma_1 L^{\downarrow} + \bar{\omega} S_0 \gamma_4 e^{-\tau/\mu_0} \quad (5)$$

The atmospheric layer is considered homogeneous if the γ -values are independent of optical depth τ . The choice of the γ -values is determined by the particular approximation to the scattering phase function and the radiation intensity distribution. One constraint is that $\gamma_3 + \gamma_4 = 1$, because of energy conservation. Meador and Weaver (1980) give expressions for 7 different twostream approximations.

For a single-layer atmosphere, the solution to equations (4) and (5) depends on the boundary conditions. The usual top boundary condition in atmospheric radiative transfer problems is that there is no diffuse irradiance at the top, i.e. $L^{\downarrow} = 0$. At the bottom, however, the situation is not so simple. We must allow for rugged terrain, such that the local illumination angle $\cos^{-1}\mu_s$ on a slope S is not the same as $\cos^{-1}\mu_0$. Moreover, part of the incident diffuse irradiance comes from reflection from adjacent terrain. For some points, for example bottoms of valleys, the contribution from this source may be large, much larger than the diffuse irradiance on an unobstructed horizontal surface.

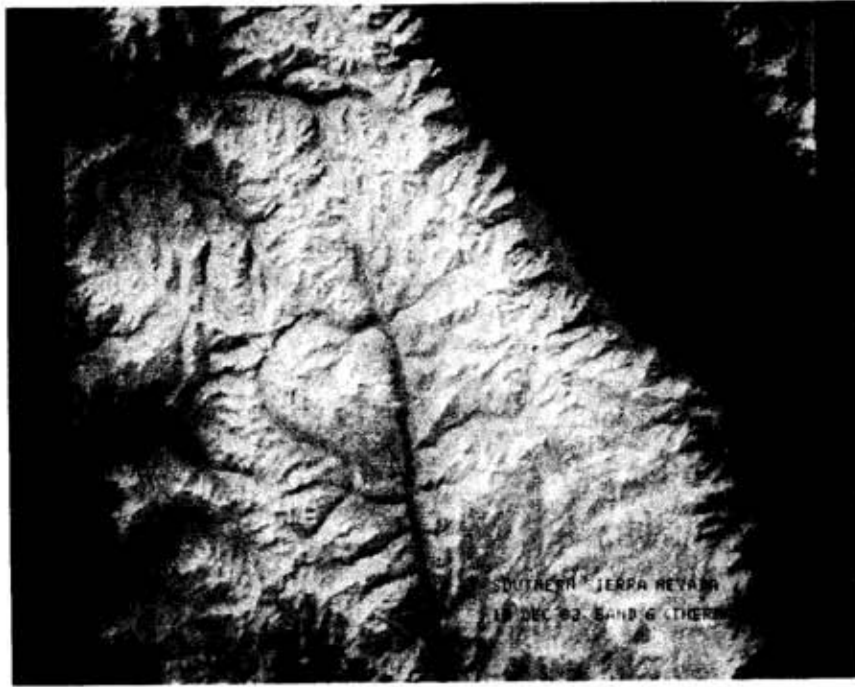


Figure 4. Snow/cloud discrimination is not feasible with TM band 6, the thermal band, because the snow is not necessarily colder than the clouds. This is the same area shown in Figure 3. The coldest areas are the brightest white. Warmest areas are dark.

We define two “view factors” to account for the effect of adjacent terrain. V_d , the view factor for diffuse irradiance, is the portion of the overlying hemisphere that is obscured by terrain, weighted for the cosine of the angle of any radiation reflected or emitted from adjacent slopes toward the slope whose radiation balance we want to calculate. Thus for an unobstructed horizontal point, $V_d = 0$, and $V_d < 1$ always. In typical mountainous areas in the Sierra Nevada, we have found that the largest values of V_d may exceed 0.4. It is computed from digital elevation data as follows. For each point in the elevation grid we calculate the angle to the horizon for some set of azimuths (typically 8–16) that cover the full circle of directions. For each azimuth ϕ , H_ϕ is the horizon angle, measured from horizontal. (Some authors measure this angle from zenith. Beware!) For the point in question, S is the slope and E is the exposure. We assume for generality that the local configuration can be approximated as a bowl surrounding the point, with sides uniformly sloping to the horizon in each direction.

$$V_d = \int_{2\pi} [\cos S \sin H_\phi + \sin S \cos H_\phi \cos(\phi - E)]^2 d\phi \quad (6)$$

The view factor V_s for direct irradiance is similar to V_d , except that the integrand for each direction ϕ must be weighted by the cosine of the illumination angle on the slope to the horizon, i.e. by $[\mu_0 \cos H_\phi - \sin \theta_0 \sin H_\phi \cos(\phi_0 - \phi)]$, where this term is set to zero if it is negative. $\theta_0 = \cos^{-1} \mu_0$ is the solar zenith angle, and ϕ_0 is the solar azimuth.

The optical depth of the atmosphere is τ_0 . The lower boundary condition for a surface with direct albedo $\rho_s(\mu_s)$ and diffuse albedo ρ_d is the sum of several terms:

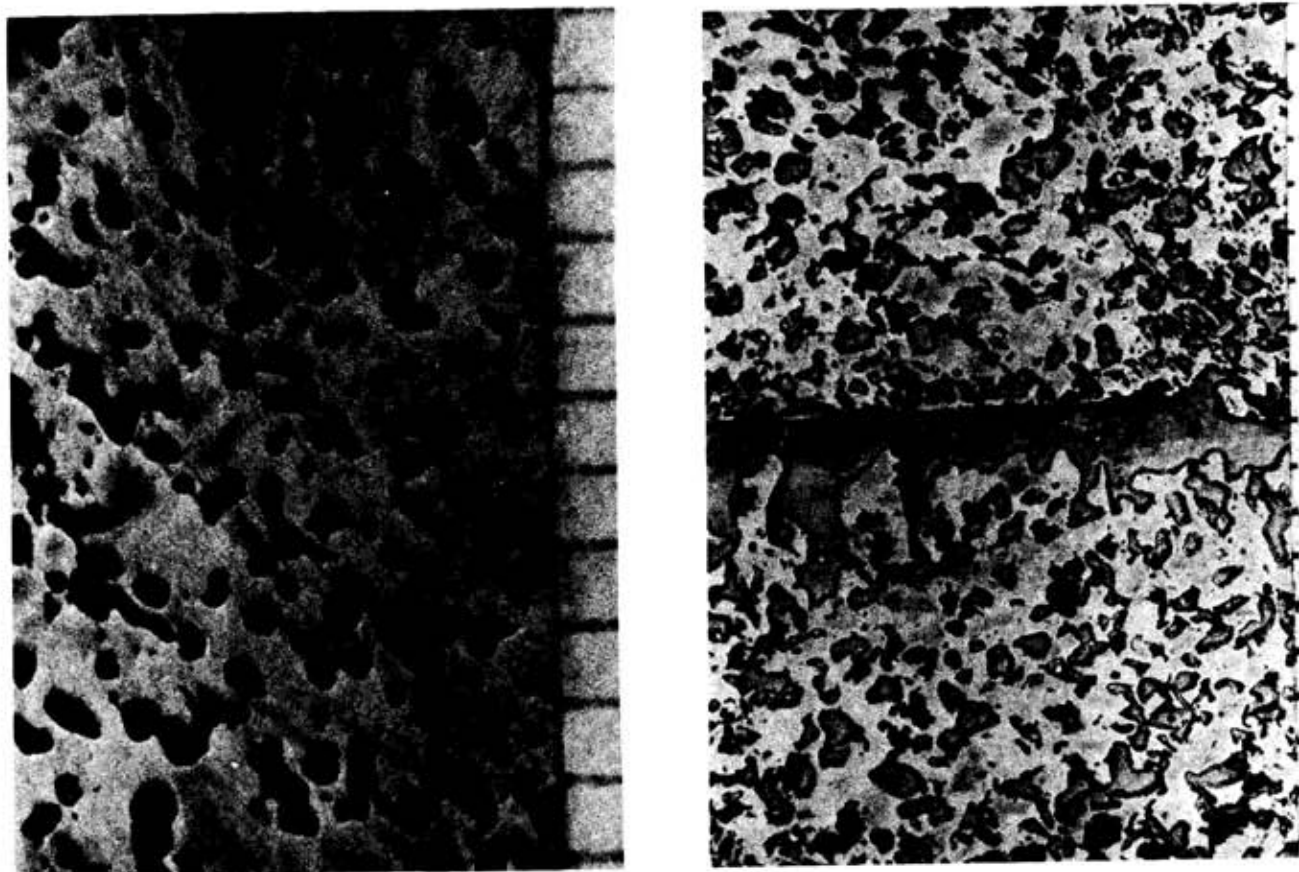


Figure 5. Plane sections of snow. In the left section, from snow kept at -5°C for 6 months, the grains are relatively spherical, but in the right section, from old kinetic growth metamorphism followed by formation of a sun crust, the grains are mostly concave. Grid spacing on edges is 1 mm.

reflected direct irradiance	$\rho_s(\mu_s)\mu_s S_0 e^{-\tau_0/\mu_0}$
reflected diffuse irradiance	$\rho_d(1-V_d)L^1(\tau_0)$
direct irradiance on adjacent slopes that is reflected toward point	$\rho_d\rho_s(\mu_0)V_s S_0 e^{-\tau/\mu_0}$
diffuse irradiance on adjacent slopes that is reflected toward point	$\rho_d^2 V_d L^1(\tau_0)$

The sum of the right hand terms above must be multiplied by $\cos S$ to find the mean upwelling radiance projected on a horizontal plane. Therefore the lower boundary condition is, after algebraic rearrangement:

$$L^1(\tau_0) = \cos S [S_0 e^{-\tau_0/\mu_0} \eta_s + L^1(\tau_0) \eta_d] \quad (7)$$

where

$$\eta_s = \rho_d \rho_s (\mu_0) V_s + \rho_s (\mu_s) \mu_s$$

$$\eta_d = \rho_d [1 - (1 - \rho_d) V_d]$$

Simplified bottom boundary conditions can be implemented by modifying some of the above terms. If the surface is Lambertian, set $\rho_s = \rho_d = \rho$; then $\eta_s = \rho(\rho V_s + \mu_s)$. If the surface is flat, set $\mu_s = \mu_0$ and $\cos S = 1$. If the surface is unobstructed by surrounding terrain, set $V_s = V_d = 0$; then $\eta_s = \rho_s (\mu_s) \mu_s$ and $\eta_d = \rho_d$.

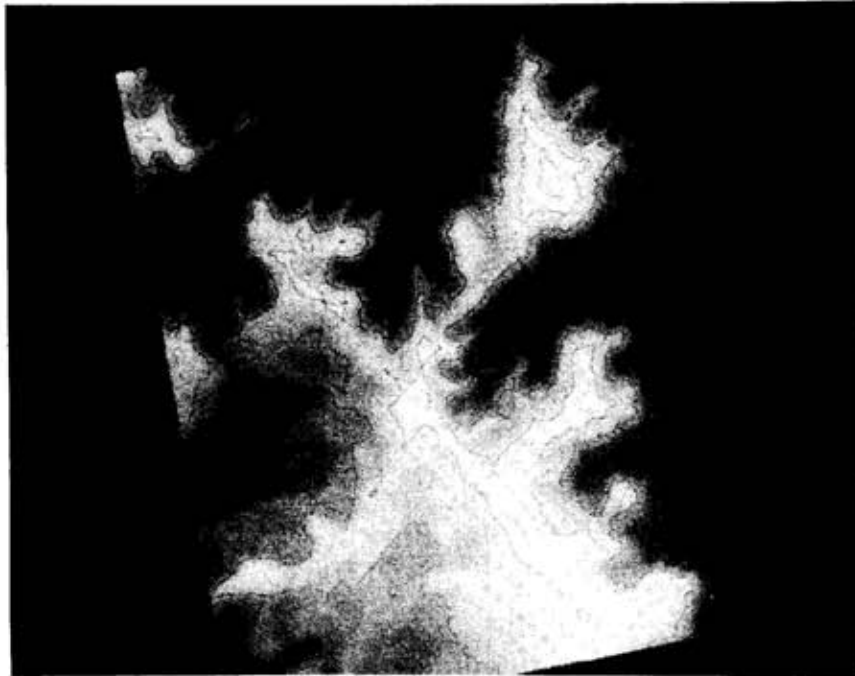


Figure 6. Digital elevation image of the 7.5×7.5 min Mt. Tom quadrangle, in the southern Sierra Nevada.

Snow Properties from Planetary Reflectance

Planetary reflectance can be measured from satellite. Can we therefore infer snow properties from satellite data? In the previous section, we described how planetary reflectance is a function of six variables:

slope	S	(known)
solar zenith cosine	μ_0	(known)
local illumination cosine	μ_s	(known)
atmospheric optical depth	τ_0	(unknown)
surface direct reflectance	ρ_s	(unknown)
surface diffuse reflectance	ρ_d	(unknown)

The values of ρ_s and ρ_d are connected, in that each can be inferred from the optical grain radius and amount of absorbing impurities in the snow. Similarly, the optical depths in various wavelengths are functions of the water vapor and aerosol contents of the atmosphere. Unfortunately for a given pixel ("picture element") the local values of S and therefore μ_s are not known. The spatial frequency at which elevation varies is low; therefore errors in digital elevation data or misregistration of the elevation grid to the satellite data do not cause severe errors if we want to know the elevation of a given pixel. Values of slope and exposure, however, vary at much higher spatial frequencies. Therefore errors in digital elevation data or misregistration of the elevation grid to the satellite data effectively eliminate the possibility of using information about local slope and local illumination angle for a given pixel. Figure 6 shows a digital elevation grid for the Mt. Tom 7.5x7.5 min quadrangle. Figure 7 shows a calculation of local values of μ_s computed from the data in Figure 6 and registered to a Thematic Mapper image. Division of the satellite radiance data by local values of μ_s leads to obvious misregistration effects, represented by the bright patches in Figure 7.



Figure 7. TM band 4 image divided by cosine of local illumination angle. The bright areas are due to misregistration with the elevation grid.

An alternative approach is statistical. We can use combinations of satellite spectral bands to estimate local values of reflectance, or of physical parameters that determine reflectance, without knowing local values for the illumination angle. This approach is similar to that used to determine sea surface temperatures from multispectral infrared measurements from the NOAA AVHRR (Deschamps and Phulpin, 1980; Bernstein, 1982; Strong and McClain, 1984).

The scheme then is to simulate planetary reflectance for a variety of atmospheric profiles, local illumination angles, local slopes, snow grain sizes, and amounts of absorbing impurities. Some radiances in the TM1 data are too low to be snow, even in the shadow. even in the shadows. Similarly, some of

the TM5 values are so high that the surface cannot be snow, even in full illumination. Examining the results further, we find that a linear combination of bands can be used to statistically fit the radiances to optical grain sizes (Figure 8).

$$\text{grain radius} = f \left(\frac{\text{TM3} - \text{TM4}}{\text{TM2}}, \frac{\text{TM2} - \text{TM4}}{\text{TM5}} \right) \quad (0q)$$

While the R^2 value of 0.75 is not high, the results are encouraging in that at least rough estimates of snow albedo are available from satellite, without requiring that the satellite images be registered to high-resolution digital elevation data.

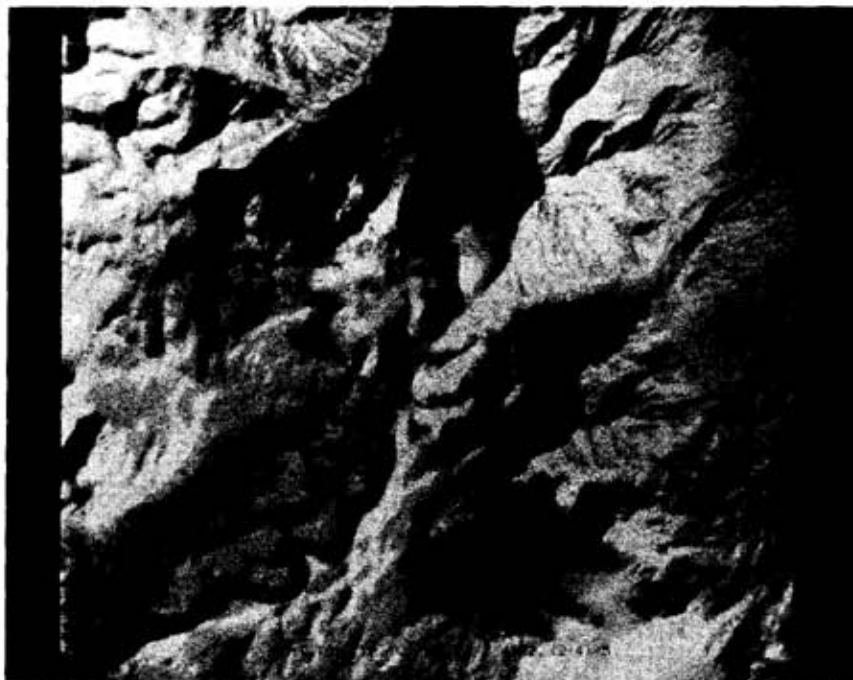


Figure 8. Linear combination of bands to estimate optical grain size of snow. Grain sizes in this image are clustered around $100\mu\text{m}$.

Conclusion

The Landsat Thematic Mapper has useful spectral bands for estimation of snow reflectance at fine spatial resolution over mountainous terrain. Even though the quality of the satellite data exceeds that of most available digital elevation data, the capabilities of the sensor can be used without requiring precise registration to the elevation grid.

References

Anderson, E. A., (1976) A point energy and mass balance model of a snow cover. NOAA Technical Report NWS 19, p. 1-150, Washington, DC.

- Bernstein, R. L., (1982) Sea surface temperature estimation using the NOAA 6 satellite Advanced Very High Resolution Radiometer. *Journal of Geophysical Research*, v. 87, p. 9455-9465.
- Choudhury, B. and Chang, A. T. C., (1981) On the angular variation of solar reflectance of snow. *Journal of Geophysical Research*, v. 86, p. 465-472.
- Deschamps, P. Y. and Phulpin, T., (1980) Atmospheric correction of infrared measurements of sea surface temperature using channels at 3.7, 11, and 12 μm . *Boundary-Layer Meteorology*, v. 18, p. 131-143.
- Li, Shusun, (1982) A model for the anisotropic reflectance of pure snow. M.A. Thesis, Discussion Paper 4, 61 p., Department of Geography, University of California, Santa Barbara, CA.
- Meador, W. E. and Weaver, W. R., (1980) Two-stream approximations to radiative transfer in planetary atmospheres: a unified description of existing methods and a new improvement. *Journal of the Atmospheric Sciences*, v. 37, p. 630-643.
- Perla, R., (1982) Preparation of section planes in snow specimens. *Journal of Glaciology*, v. 28, p. 199-204.
- Perla, R. and Dozier, J., (1984) Observations on snow structure. in *Proceedings, Sixth International Snow Science Workshop*, v. 28, p. 182-187, Mountain-Rescue, Aspen, CO.
- Strong, A. E. and McClain, E. P., (1984) Improved ocean surface temperatures from space – comparisons with drifting buoys. *Bulletin of the American Meteorological Society*, v. 65, p. 139-142.
- Thekaekara, M. P., (1970) The solar constant and the solar spectrum measured from a research aircraft. NASA TR-R-351, p. 139-142, NASA Goddard Space Flight Center, Greenbelt, MD.
- Warren, S. G. and Wiscombe, W. J., (1980) A model for the spectral albedo of snow, II, Snow containing atmospheric aerosols. *Journal of the Atmospheric Sciences*, v. 37, p. 2734-2745.
- Wiscombe, W. J. and Warren, S. G., (1980) A model for the spectral albedo of snow, I, Pure snow. *Journal of the Atmospheric Sciences*, v. 37, p. 2712-2733.

Kukla, G; Barry, R.G.; Hecht, A.; Wiesnet, D. eds. (1986) SNOW WATCH '85. Proceedings of the Workshop held 28-30 October 1985 at the University of Maryland, College Park, MD. Boulder, Colorado, World Data Center A for Glaciology (Snow and Ice), Glaciological Data, Report GD-18, p.205-206.

Remote Sensing of Snow Cover over the Carpathian Watersheds

Horia Grumazescu
Laboratory of Remote Sensing
Institute of Meteorology and Hydrology
Bucharest, Romania

Abstract

In 1980 the Institute of Meteorology and Hydrology started the surveillance and assessment of snow cover in the Carpathian basins using remote sensing techniques. The objective was to determine the seasonal water storage by obtaining timely input for snowmelt-runoff models.

The project activity was preceded by experimental research which was aimed at developing working procedures for the processing and interpretation of remote sensing data needed for hydrological assessment and forecasting. The development of the operational working techniques took into account the following:

- a) Complex morphometric, physiographic and hydrometeorologic conditions of the Carpathian watershed on a relatively small scale. The hydrologic regime is characterized by spring floods linked to snowmelt. This situation requires the use of large scale imagery which is provided by high resolution recorders such as airborne photogrammetric cameras and multispectral sensors. Repetitive measurements such as taken by MSS hand held recorders were also needed.
- b) Photographic products and magnetic tapes in the visible and thermal infrared bands are available from meteorological geostationary and polar-orbiting satellites and are received by a read-out station at the Institute. Data from the Landsat satellites in visible and near infrared bands and large scale black and white aerial photos are also

available. The heterogeneous character of the remotely sensed data as well as the large volume of information to be processed and interpreted in a relatively short time (as in the case of the operational charting of several Carpathian watersheds with relatively short snow melt periods) called for the use of efficient procedures for data processing and analysis with high speed and accuracy.

Two systems for digital processing of the remotely sensed data and for automated mapping of the hydrological targets have been developed and are currently in use. One is used for processing photographic satellite products and aerial recordings (SADFAS) and another for reprocessing the analog and digital data stored on magnetic tapes (SPID).

Emphasis has been given to the interactive procedures utilizing ground truth in hydrologic calibration of the reflectance levels recorded by the remote sensors.

At present, the operational snow cover assessment and surveillance is carried out on a routine basis and the resulting hydrologic information is transmitted to forecasting centers and to electric power stations in real time.

Kukla, G; Barry, R.G.; Hecht, A.; Wiesnet, D. eds. (1986) SNOW WATCH '85. Proceedings of the Workshop held 28-30 October 1985 at the University of Maryland, College Park, MD. Boulder, Colorado, World Data Center A for Glaciology (Snow and Ice), Glaciological Data, Report GD-18, p.207-214.

Effects of Snow Cover and Tropical Forcing on Mid-Latitude Monthly Mean Circulation

Alan Robock
James W. Tauss
Cooperative Institute for Climate Studies
Department of Meteorology
University of Maryland
College Park, Maryland, U.S.A.

ABSTRACT

The effect of anomalous snow cover on the monthly mean atmospheric circulation is studied, by incorporating such forcing into the simple, linear, steady-state climate model of Opsteegh and Mureau. Anomalous forcing fields of snow cover are created for three months (October, January and April) in the snow season of the winters of 1976 through 1982. Anomalous heating fields are also imposed based on observed tropical anomalies of outgoing longwave radiation. The monthly mean anomalous circulation patterns are calculated for each forcing separately and for the combined forcings. The outgoing longwave radiation has previously been shown to produce circulation that has small but positive correlations with the observed atmospheric circulation. In this study, correlation coefficients calculated for various regions in the Northern Hemisphere show that the addition of snow cover as a forcing mechanism does not produce better simulations of the monthly mean flow.

1. INTRODUCTION

The effect of anomalous snow cover has long been studied as having a pronounced influence on the temperature of the overlying atmosphere (Landsberg, et al., 1941; Namias, 1962; Wagner, 1973; Dewey, 1977; Yeh, et al., 1983; Foster, et.al., 1983). However, little if any literature has described the incorporation of such a forcing into a climate model to investigate the anomalous atmospheric response. It is the purpose of this paper to study the effects of such anomalous forcings when imposed on a monthly mean basic state using a simple, linear, steady-state climate model.

The model is described by Opsteegh and Mureau (1983). The

equations are linearized with respect to a fixed, zonally averaged basic state. The equations for the time-mean anomalous response to a time-mean forcing are then calculated. There are 15 levels in the vertical and the model equations are formulated in sigma coordinates. It is semi-spectral with gridpoints in the meridional direction and wave components (waves 1-6 in these experiments) in the zonal direction.

Since it is known that anomalous snow cover is not the only cause of monthly mean circulation anomalies and it has been suggested that anomalies of tropical atmospheric heating may produce anomalous mid-latitude circulation (e.g. Horel and Wallace, 1981), the model is forced with tropical heating alone, snow cover alone and tropical heating and snow cover together. If the results are good for snow cover alone, or if the tropical results are improved by including snow cover, then it can be concluded that this experiment suggests that snow cover is important. Preliminary results were presented by Robock and Tauss (1985). Essentially the same work is described by Robock and Tauss (1986).

2. RESULTS

Digitized NOAA satellite-derived snow cover data (Dewey and Heim, 1981) for 1967-1982 are used to create January, April and October snow climatology maps for the Northern Hemisphere. Because of some early data discrepancies over the Himalayas, the snow climatology for that region only covers the years 1976-1982. Subsequently, anomalous forcing fields are created for the period 1976-1982. To create 3-dimensional forcing fields, vertical profiles of diabatic heating are parameterized in terms of the anomalous heating.

Monthly anomalous Outgoing Longwave Radiation (OLR) fields in the tropics are created for the years 1976-1982 inclusive and used as a proxy for the anomalous monthly mean diabatic heating (Arkin, 1983). (No OLR data were available for 1978.) It is assumed that the profile of heating in the vertical has a maximum at 400 mb and gradually decreases toward the surface and the tropopause.

The first model runs contain "idealized" snow anomalies to examine anomalous response of the atmosphere. "Idealized" anomalies are created by removing climatologically present snow cover where it was found at least 50% to 100% of the time during the month (negative snow anomaly) or by adding snow cover to those areas exhibiting between 0% and 49% climatologically present snow cover (positive snow anomaly). A reasonable vertical profile of diabatic heat for a mid-latitude surface forcing such as this is selected to be $+1.0\text{C/day}$ for the negative (heat source) or positive (heat sink) anomaly at the lowest model level (967 mb).

The forcing field resulting from the idealized snow anomaly case was first imposed upon the January climatological basic state. The response was zonal in character. Strong surface high pressure was seen just downstream of the forcing with weaker low pressure upstream. At 300 mb a strong trough was seen just downstream of the forcing with weaker high pressure upstream. Similar responses were seen for April and October cases.

These results are similar in pattern to Egger (1977), who used sea surface temperature fields as anomalous surface forcing. Egger's model contained only two levels in the vertical. Since very similar patterns are obtained with both models, the increase in vertical resolution seemed to offer little additional information about the response.

The next series of experiments force the model with the actual observed snow anomalies for the month of January (both positive and negative). For these model runs, a vertical profile of $+2.0/+1.0/+0.5$ C/day in the three lowest model layers was used because it seemed to give a more realistic forcing. For January 1977, the observed positive height anomaly at 700 mb over Alaska and Northern Europe agrees with the model. The broad negative height anomaly observed over Siberia and the North Central Pacific also appears in the model response. However, other features are erroneous such as the model response of positive height anomaly over Northeast China, the model's southern displacement of the westerlies over Southern Europe and the lack of the observed trough over the Eastern United States.

For January 1978, the positive height anomaly in Western Canada, the broad negative height anomaly pattern stretching from Siberia through the Central North Pacific and the positive height anomaly over Northeast China is an erroneous model response and the high and low height anomaly centers are reversed over the Eastern United States and North Atlantic.

Because the model is linear, one expects the strongest forcings to produce the strongest responses. The years with the two largest snow cover anomalies of the years tested were January 1977 and 1978, which ranked 1st and 4th highest respectively across the Northern Hemisphere (Wiesnet and Matson, 1979). Still there are many regions where poor correlations between model response and observation appear to exist. This leads one to tentatively conclude that either the effect of extreme anomalous snow cover does not outweigh all the other causes of monthly mean circulation anomalies, or this model experiment does not adequately simulate this effect.

The model was also forced with tropical OLR anomalies alone and in combination with snow cover anomalies. Pattern Correlation Coefficients (PCC) are calculated over four separate regions. These are Northern Hemisphere (NH) (30 N - 90 N), North America only (NA), Eurasia only (EA), and North America and Eurasia (Northern Hemisphere land)(LAND). The partitioning in this

fashion is justified because anomalous snow cover is a regional phenomenon. Increasing correlation between model generated geopotential fields and observed geopotential fields should be seen over specific middle and high latitude regions downstream from the forcing rather than over the entire hemisphere.

PCC's are calculated for two model levels, 850 mb and 300 mb. These are shown in Tables 1 and 2. Because snow cover is an intense but shallow, low-level forcing, one should expect to see higher correlations with observed geopotential fields at the lower model level.

The results of the experiments calculating the correlation coefficients indicate that snow cover seems to have less influence on the atmospheric circulation than previously expected. Poor correlations were noted in general over all four regions when snow cover was the only forcing. However, in approximately 70% of the cases tested, good correlations existed between model generated and observed geopotential fields when OLR was the only forcing. No distinct pattern emerged with regard to improving the correlations when snow plus OLR were used as forcings. No appreciable change was detected between the 850 mb and 300 mb results although when good(bad) correlations existed at 850 mb for a particular month and region, good(bad) correlations also existed at 300 mb.

3. CONCLUSIONS

The expected higher correlations at 850 mb did not exist nor did the anticipated increase in correlation appear for specific land regions where snow cover would have a marked influence. This, in addition to the fact that little or no improvement occurred when snow forcing was added onto OLR forcing only, leads to the conclusion that the effect of snow cover is much less than previously thought and/or the many other variables not parameterized in this model are much stronger factors than snow cover.

Some of these factors associated with snow cover but not parameterized in the model include no change in albedo with latitude, no consideration of latent and sensible heat fluxes and no consideration of the effects of transients. Furthermore, enhanced baroclinicity and the associated vorticity forcing or dissipation to accompany the imposed diabatic heating are not included.

Future experiments will include the calculation of correlation coefficients at the surface to see if the effect of a very shallow forcing in the form of snow can be modelled.

TABLE 1. 850 mb Pattern Correlation Coefficients

<u>Month</u>			<u>Forcing</u>			<u>Region</u>			
Jan	Apr	Oct	Snow	Tropical	Tropical and Snow	NH	NA	EA	LAND
<u>1979</u>									
X			X			.05	-.23	-.15	-.11
X				X		.25	.45	-.14	.34
X					X	.21	.45	-.21	.12
	X		X			.07	.12	-.08	-.04
	X			X		.07	.46	.21	.27
	X				X	.10	.33	.00	.07
		X		X		-.02	-.43	.23	.02
		X			X	.14	.10	-.04	-.01
<u>1980</u>									
X				X		-.12	-.78	.04	-.29
X					X	-.02	-.21	.28	.13
	X			X		.29	.23	.21	.13
	X				X	.27	.26	.28	.17
		X		X		.23	.23	.42	.36
		X			X	.21	.28	.36	.32
<u>1981</u>									
X				X		.42	-.42	.13	-.17
	X			X		.30	.37	.53	.33
	X				X	.45	-.01	.40	.38
		X	X			.02	-.30	.27	.22
		X		X		-.16	.42	-.49	-.31
		X			X	.01	-.28	.26	.21
<u>1982</u>									
X			X			.05	.65	.27	.20
X				X		.38	.62	.49	.45
X					X	.21	.79	.40	.34
		X		X		.35	-.02	.31	.28
		X			X	-.04	.62	.23	.27

TABLE 2. 300 mb Pattern Correlation Coefficients

<u>Month</u>			<u>Forcing</u>			<u>Region</u>			
Jan	Apr	Oct	Snow	Tropical	Tropical and Snow	NH	NA	EA	LAND
<u>1979</u>									
X			X			-.30	-.68	-.53	-.53
X				X		.18	.38	.03	.20
X					X	.13	.25	-.13	.17
	X		X			.12	.16	-.18	-.11
	X			X		.23	.34	.07	.11
	X				X	.28	.36	.05	.10
		X		X		-.11	-.30	-.25	-.27
		X			X	.00	-.29	.02	-.11
<u>1980</u>									
X				X		.13	-.39	.41	.07
X					X	-.05	-.43	.46	.18
	X			X		.06	.19	.16	.12
	X				X	.38	.61	.38	.50
		X		X		.22	-.57	.69	.36
		X			X	.19	-.27	.39	.25
<u>1981</u>									
X				X		-.13	-.49	-.16	-.25
	X			X		.43	.60	.62	.52
	X				X	.50	.64	.59	.61
		X	X			.10	-.05	.20	.17
		X		X		-.30	-.33	-.39	-.29
		X			X	-.02	-.23	.13	.09
<u>1982</u>									
X			X			.14	.48	.34	.39
X				X		.39	.56	.16	.37
X					X	.45	.59	.31	.44
		X		X		.16	.04	.56	.40
		X			X	.10	.60	.58	.55

4. ACKNOWLEDGMENTS

This work was supported by NOAA grants NA81AA-H-00023 and NA84AA-H-00026 and NSF grant ATM-8213184. Computer time was provided by NASA/GLA.

5. REFERENCES

- Arkin, Phillip A., 1983: An examination of the southern oscillation in the upper tropospheric tropical and subtropical wind field. Ph. D. thesis, Department of Meteorology, University of Maryland.
- Dewey, Kenneth, 1977: Daily maximum and minimum temperature forecasts and the influence of snow cover. Mon. Weather Rev., 105, 1594-1596.
- Dewey, Kenneth and Richard Heim Jr., 1981: Satellite observations of variations in northern hemispheric snow cover. NOAA Tech Rep., NESS 87.
- Egger, J., 1977: On the linear theory of the atmospheric response to sea surface temperature anomalies. J. Atmos. Sci., 34, 603-614.
- Foster, James, Manfred Owe and Albert Rango, 1983: Snow cover and temperature relationships in North America and Eurasia. J. Clim. and App. Met., 22, 460-469.
- Horel, J.D. and J.M. Wallace, 1981: Planetary-scale circulations associated with the southern oscillation. Mon. Weather Rev., 109, 813-829.
- Landsberg, Helmut, G.P. Cressman and H.K. Saylor, 1941: The influence of a snow cover on air temperature. Proc. Central Snow Conference, 1, 45-48.
- Namias, Jerome, 1962: Influences of abnormal surface heat sources and sinks on atmospheric behavior. Proc. International Symposium on Numerical Weather Prediction., Tokyo, 615-627.
- Opsteegh, J.D. and Robert Mureau, 1984: Description of a 15-layer steady-state atmospheric model. Report SR-84-19, Department of Meteorology, University of Maryland, 25 pp.
- Robock, Alan and James W. Tauss, 1985: The effect of anomalous snow cover on the general circulation of the atmosphere using a simple climate model. Proc. Ninth Annual Climate Diagnostics Workshop, NOAA, 231-237.

- Robock, Alan and James W. Tauss, 1986: Effects of snow cover and tropical forcing on mid-latitude monthly mean circulation. Proc. WMO Workshop on the Diagnosis and Prediction of Monthly and Seasonal Atmospheric Variations Over the Globe, in press.
- Wagner, James, 1973: The influence of average snow depth on monthly mean temperature anomaly. Mon. Weather Rev., 101, 928-933.
- Wiesnet, Donald and Michael Matson, 1979: The satellite-derived northern hemispheric snow cover record for the winter of 1977-78. Mon. Weather Rev., 107, 928-933.
- Yeh, T.C., R.T. Wetherald and S. Manabe, 1983: A model study of the short-term climatic and hydrologic effects of sudden snow cover removal. Mon. Weather Rev., 111, 1013-1024.

Kukla, G; Barry, R.G.; Hecht, A.; Wiesnet, D. eds. (1986) SNOW WATCH '85. Proceedings of the Workshop held 28-30 October 1985 at the University of Maryland, College Park, MD. Boulder, Colorado, World Data Center A for Glaciology (Snow and Ice), Glaciological Data, Report GD-18, p.215-223.

Parameterization of Snow Albedo for Climate Models

Susan Marshall
Department of Geography
University of Colorado
Boulder, Colorado, U.S.A.

Stephen G. Warren
Department of Atmospheric Sciences
University of Washington
Seattle, Washington, U.S.A.

Abstract

General circulation models (GCMs) find that the response of climate to increases in CO₂ is enhanced by the snow-albedo-temperature feedback. The results are very sensitive to the assumed value of snow albedo. Snow albedo, however, is highly variable, and it is not calculated accurately in present-day GCMs. We would like to replace the current simple empirical parameterizations of snow albedo with a physically-based parameterization which is accurate yet efficient to compute.

Our approach is to develop simple functions which fit the spectrally-averaged results of a detailed theoretical model of the spectral albedo of snow which uses the delta-Eddington method for multiple scattering and Mie theory for single scattering. The spectrally-averaged snow albedo varies with snow grain size, solar zenith angle, snow cover thickness, underlying surface albedo (for thin snow), concentration of absorptive impurities in the snowpack, and cloud optical thickness (because clouds alter the solar spectrum at the surface). This method divides the solar spectrum into the two broad wavebands commonly used in climate models: visible and near-infrared.

General circulation models (GCMs) find that the response of climate to increases in CO₂ is enhanced by the snow-albedo-temperature feedback. The results are sensitive to the assumed value of snow albedo. Snow albedo, however, is highly variable, and it is not calculated accurately in present-day GCMs. Most GCMs assign a single value to the albedo of an optically-thick snow cover. These albedo values can range from 0.55 to 0.85, and generally remain constant with time until the snowpack decays to some critical depth, then decrease as a function of the snow depth until the albedo reaches the underlying surface albedo. Other GCMs allow the snow albedo to vary with solar zenith angle, snowpack thickness, age of the snow layer, and latitude. We would like to replace the current simple empirical parameterizations of snow albedo with a physically-based parameterization which is accurate yet efficient to compute.

Our approach is to develop simple functions which fit the spectrally-averaged results of a detailed theoretical model of the spectral albedo of snow which uses the delta-Eddington method for multiple scattering and Mie theory for single scattering (Wiscombe and Warren, 1980, Warren and Wiscombe, 1980, hereafter WWI and WWII, respectively). This method assumes a homogeneous snow-covered surface with no vegetation cover. The GCMs we surveyed (NCAR, GFDL, OSU, GISS, GLAS, LMD, UKMO, and ECMWF) break the solar spectrum into at most two parts. The break is either at $0.7 \mu\text{m}$ or $0.9 \mu\text{m}$ wavelength) with one exception at $0.78 \mu\text{m}$). We therefore also break the solar spectrum into two parts, "visible" and "near-infrared" (NIR). We will develop the parameterizations for the two regions split at $0.7 \mu\text{m}$. Then we expect that the functional forms we develop can also be used when the break is at $0.9 \mu\text{m}$, so we will need only to develop a second set of coefficients for those climate models which break the spectrum at $0.9 \mu\text{m}$. In all examples given here, the separation between "visible" and "near-infrared" is at $0.7 \mu\text{m}$.

The spectrally-averaged snow albedo varies directly with snow grain radius, r , effective solar zenith angle, θ , snow cover thickness, h (g cm^{-2}), underlying surface albedo (for thin snow), u_m , and concentration of absorptive impurities (especially soot) in the snow layer, s ; and indirectly with cloud cover. Figure 1 shows the effects of snow grain size and zenith angle on the spectral albedo of snow to be much greater in NIR wavelengths, while the effects of finite snow thickness and soot concentration on the spectral albedo are greater in the visible wavelengths. The similarity between the spectral signatures of grain size and zenith angle, and those of snowpack thickness and soot concentration, suggest that each pair of variables might be lumped together as one predictor.

The predictors of snow albedo will be effective grain size, r , effective zenith angle, θ , (which will depend on the diffuse direct ratio), impurity content, s , (as an effective soot content), and snowpack thickness, h (g cm^{-2}). In the NIR there will be an additional predictor, the atmospheric transmittance, t . This is needed because snow albedo varies greatly with wavelength, and the absorption of solar radiation by clouds is also wavelength-dependent. Clouds are more absorptive at the longer wavelengths (Figure 2), where snow albedo is also lower (Figure 1a), so increasing cloud optical thickness τ_c causes the NIR snow albedo to increase (table 1).

Changes in spectrally-integrated snow albedo due to differential atmospheric absorption (the visible albedo is insensitive to τ_c .) will also be caused by changes in water vapor optical depth, τ_w , and the atmospheric path ($\sec \theta_0$, where θ_0 is the solar zenith angle). We hypothesize that the effects c , w , and $\sec \theta_0$ can be lumped together, so that only one predictor, t , is needed. This will be desirable not just for simplifying the parameterization, but because not all GCMs compute τ_c , but they all obtain t .

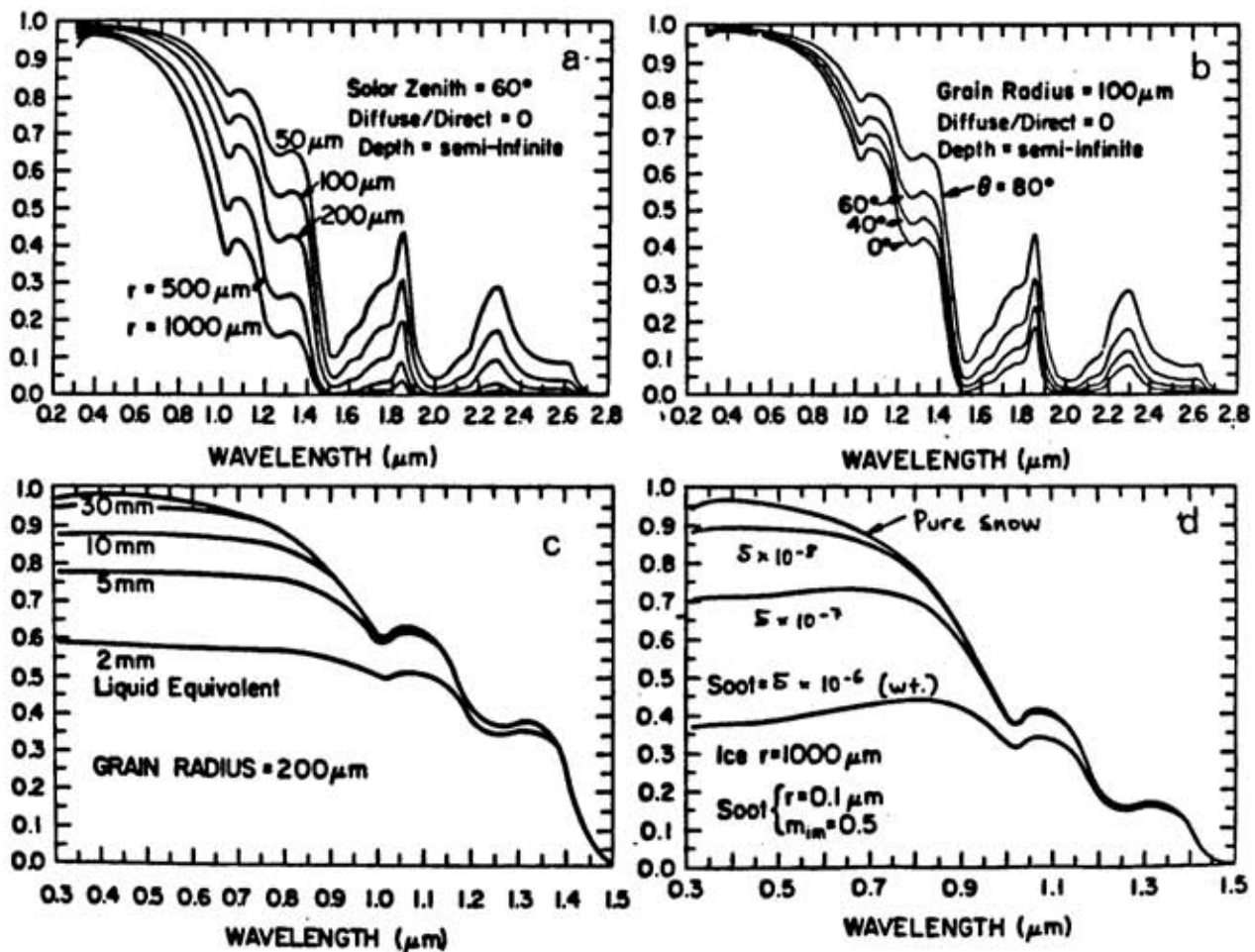


Fig. 1 Plots of the effects on the spectral albedo of snow of (a) snow grain size, (b) solar zentith angle, (c) snowpack thickness, and (d) contamination by soot (from WWI and WWII).

Table 1. Visible and near-infrared snow albedos for clear and cloudy Arctic sky conditions (using unusually thick cloud for Arctic; $\tau_c = 40$).

Spectral Interval (m)	Sky Condition	$\cos \theta_0$	Snow Albedo	Solar Downflux ($W m^{-2}$)
visible (0.3-0.7)	clear	0.40	0.98	226.5
visible (0.3-0.7)	cloud	0.40	0.97	171.7
infrared (0.7-3.0)	clear	0.40	0.64	195.3
infrared (0.7-3.0)	cloud	0.40	0.78	60.6

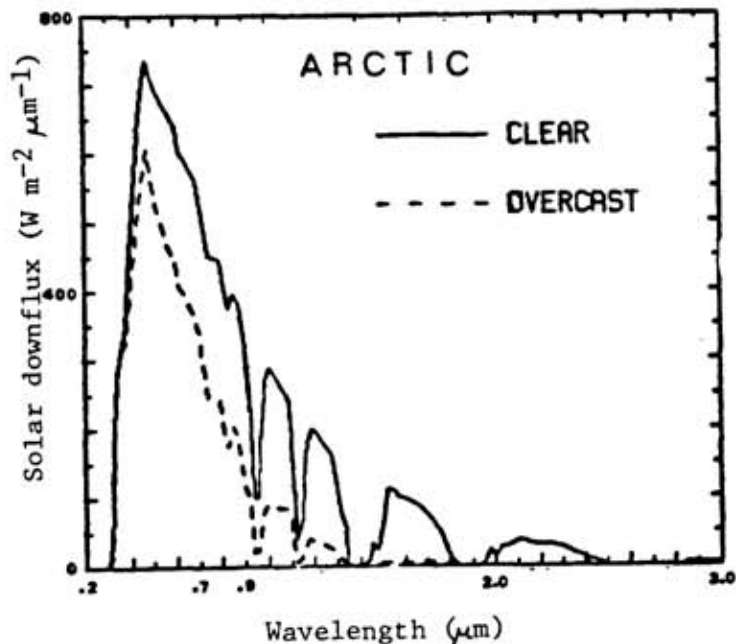


Fig. 2. Spectral distribution of incoming solar downflux ($\text{W m}^{-2} \mu\text{m}^{-1}$) for the Arctic summer under clear and cloudy (with an unusually thick cloud; optical thickness = 40) sky conditions. These are calculated using the ATRAD mode (Wiscombe *et al.*, 1984).

Table 2 shows the breakdown of the parameterization from (a) the final combination of visible and NIR albedos and downfluxes (F_{vis} , F_{nir}) into a single value of the snow albedo, to (d) the list of input values needed from the GCM to complete the parameterization. The parameterization will estimate the visible and NIR (clear-sky) snow albedos as functions of three main parameters: effective grain size, r , effective soot, s , and an effective zenith cosine, μ . The effect of cloud cover on the NIR snow albedo may be estimated using a value of the atmospheric transmittance, t .

The effective zenith cosine, μ , is a linear combination of the diffuse and direct-beam fractions of the solar irradiance and the diffuse and direct-beam zenith cosines (μ_d , μ_o). This relationship holds because the snow albedo is linear in μ for both the visible and NIR spectra. The fraction of insolation at the surface that is diffuse (d) will be parameterized, possibly as a combination of the atmospheric transmissivity and the direct-beam zenith angle. Because the spectral signatures of the grain radius and of the zenith angle are similar in their effect on the snow albedo, the two variables may be parameterized as one value, an effective grain size, r . Some properties of the albedo which may be useful are that it is nearly linear in $\cos \theta_o$, and that it is nearly linear in $r^{1/2}$ in the visible (Bohren and Barkstrom, 1974), but not in the NIR (WWI, figure 9).

The problem remains that snow grain size is difficult to predict, which is unfortunate since grain size is the most important variable controlling snow albedo. We will have to use observational data to develop a crude parameterization of grain size, probably in terms of the snow age and its temperature history, following the works of Anderson (1976).

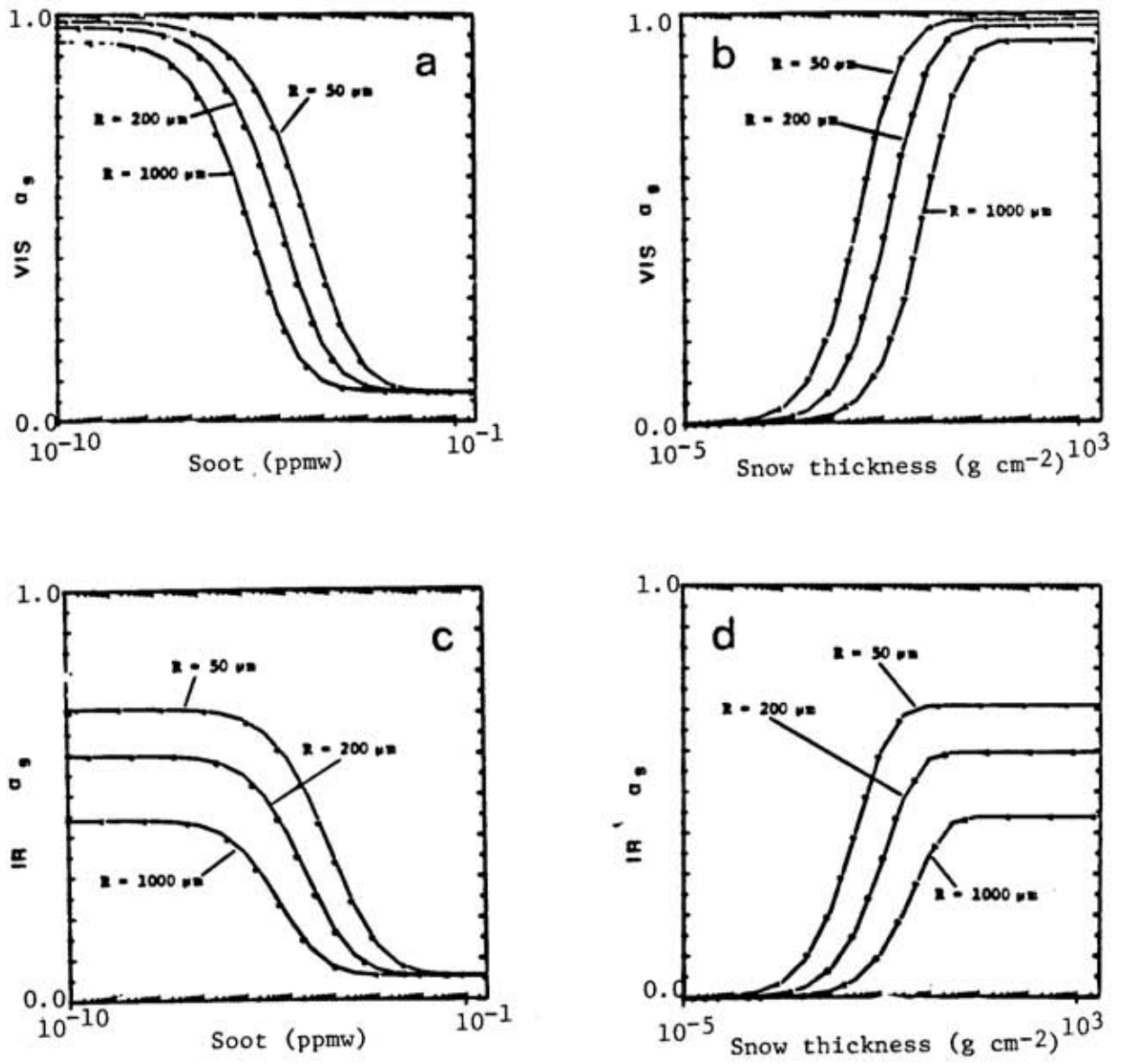


Fig. 3. Relationships between integrated snow albedo (α_s) and soot concentration in deep snow (a) and (c), and between integrated snow albedo and thickness of pure snow (b) and (d) for the visible and near-infrared wavebands, for three values of grain size, r .

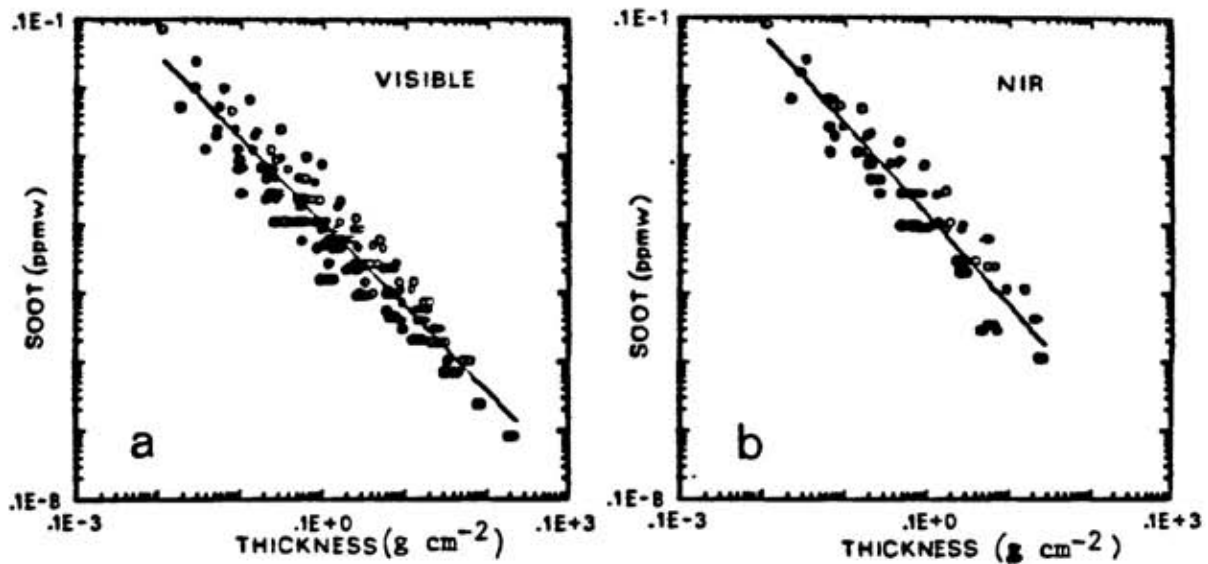


Fig. 4 A thin snowpack of pure snow has an albedo which can be mimicked by adding soot to a deep snowpack. These corresponding values of soot and thickness (for a variety of grain sizes and underlying albedos) are plotted as points here. The lines are least-squares fits, (a) visible (b) near-infrared.

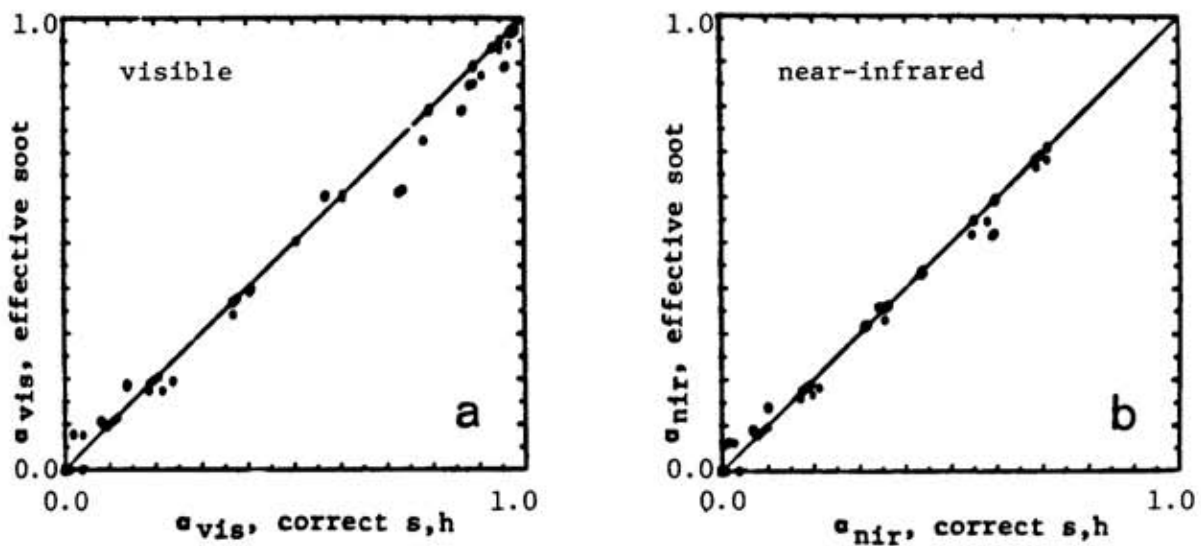


Fig. 5. Plots of integrated snow albedos using correct values of soot, s , and snow thickness, h , compared to integrated snow albedos using an "effective soot" calculation for (a) visible and (b) near-infrared integrations.

The final diagram (figure 6) outlines the structure we foresee for our parameterization. Task 1, the combination of snowpack thickness and concentration of soot into one parameter, an "effective soot", is now being completed. Task 2 involves the actual parameterization of the integrated snow albedos (visible and NIR) from given values of an effective grain radius, r , effective soot concentration, s , and effective zenith cosine, μ . The final task will then be to research methods by which the effective grain size can be estimated from data available to climate models. We are assuming that other steps not labelled as "tasks" will be relatively straight-forward.

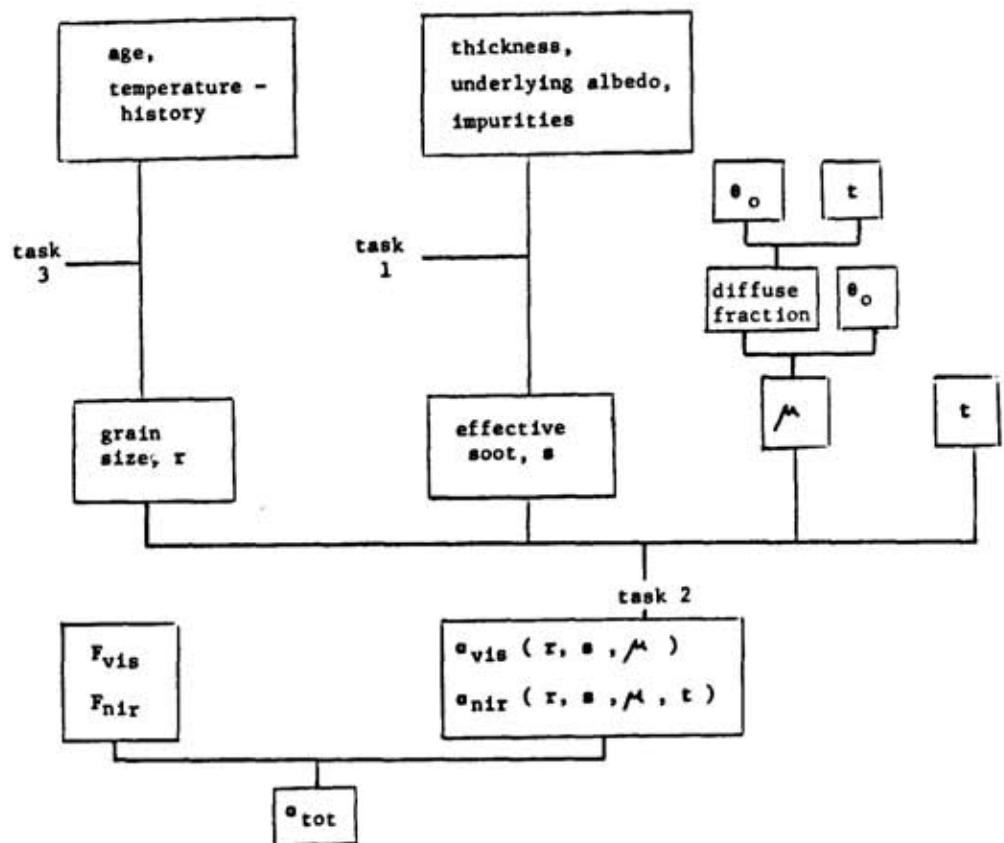


Fig. 6. Outline of research for parameterization of snow albedo.

This paper has presented completed work and outlined proposed tasks in the parameterization of snow surface albedo. Since much of this work is in the preliminary stages, the authors anticipate that changes will be made to the method as outlined at the workshop.

References

- Anderson, E.A. (1976) A Point Energy and Mass Balance Model of a Snow Cover. U.S. National Oceanic and Atmospheric Administration, Silver Spring, MD., NWS 19, 150p.
- Bohren, C.F.; Barkstrom, B.R. (1974) Theory of the optical properties of snow. Journal of Geophysical Research, v.79(30), p.4527-4535.
- Warren, S.G.; Wiscombe, W.J. (1980) A model for the spectral albedo of snow. II. Snow containing atmospheric aerosols. Journal of the Atmospheric Sciences, v.37, p.2734-2745.
- Wiscombe, W.J.; Warren, S.G. (1980) A model for the spectral albedo of snow. I. Pure snow. Journal of the Atmospheric Sciences, v.37, p.2712-2733.
- Wiscombe, W.J.; Welch, R.M.; Hall, W.D. (1984) The effects of very large drops on cloud absorption. Part I: Parcel models. Journal of the Atmospheric Sciences, v.41, p.1336-1355.

Acronyms

Atmospheric General Circulation Models

ECMWF	European Centre for Medium Range Weather Forecasting Bracknell, Berkshire, England.
GFDL	Geophysical Fluid Dynamics Laboratory Princeton, New Jersey
GISS	Goddard Institute for Space Studies New York, New York.
GLAS	Goddard Laboratory for Atmospheric Science Greenbelt, Maryland.
LMD	Laboratoire Meteorologie Dynamique Paris, France.
NCAR	National Center for Atmospheric Research Boulder, Colorado.
OSU	Oregon State University Corvallis, Oregon.
UKMO	United Kingdom Meteorological Office Bracknell, Berkshire, England

Kukla, G; Barry, R.G.; Hecht, A.; Wiesnet, D. eds. (1986) SNOW WATCH '85. Proceedings of the Workshop held 28-30 October 1985 at the University of Maryland, College Park, MD. Boulder, Colorado, World Data Center A for Glaciology (Snow and Ice), Glaciological Data, Report GD-18, p.225-240.

Modelling a Seasonal Snow Cover

E. M. Morris
Institute of Hydrology
Wallingford, Oxfordshire, U.K.

Abstract

This paper describes physics-based, distributed models for snow processes and their potential use in assessing the effects of climatic change produced by increased levels of CO₂ in the atmosphere. The conservation and constitutive equations for snow treated as a three phase, four component mixture are described and the simplifications made in the various current distributed models explained. One particular model, the SHE snow component, is used to estimate the sensitivity of predictions of snowmelt rate to variations in meteorological inputs using field data from a site in the Cairngorm Mountains of Scotland. This analysis indicates that, for the expected levels of climatic variation, the change in predicted snowmelt rates is of the same order as the uncertainty in these rates arising from uncertainty in one of the parameters of the model, the aerodynamic roughness length. However, field data suggests that it may well be possible to specify this parameter more precisely. Given that this can be achieved, the SHE snow routine, and other distributed models which use the aerodynamic roughness or an equivalent parameter, should form a useful component of general models for prediction of the effects of increased CO₂.

Introduction

The problem of describing the interaction between snow cover and the atmosphere concerns both hydrologists and climatologists. Both groups have developed general models which, for the purposes of discussion, may be described as consisting of two sub-models, for snow processes and for processes in the atmosphere, together with initial conditions, external

boundary conditions and equations describing transfers at the internal snow/atmosphere boundary. However, perhaps not surprisingly, the hydrologists have tended to simplify the atmospheric component of their models, and conversely climatologists have often used simplified snowmelt models. This paper describes some of the physics-based, distributed models for snow processes developed by hydrologists which might form a useful part of general models designed to allow the effect of changes in carbon dioxide levels in the atmosphere to be predicted.

In order to use a model to investigate the effects of hypothetical changes in inputs or system characteristics it is necessary to establish

- (i) that the model produces good predictions for the present situation
- (ii) that the parameters of the model can be specified a priori for conditions outside the range of those for which the model has been calibrated and
- (iii) that the uncertainty in model output is small compared to the effect of the hypothetical changes to be investigated.

The first criterion can be met by many relatively simple snowmelt models. Provided that output data are available for optimisation, indices linking snowmelt and meteorological data may be defined. The problem is that these parameters are found to be site and climate specific and therefore cannot be expected to fulfill the second criterion listed above. Physics-based models provide improved predictions for present day climates and, more importantly, use parameters which we can hope to define accurately for new situations without having to optimise the model. There are a series of such models now in use, ranging from the classic Anderson energy budget model (Anderson, 1968), which gives detailed equations for the snow/atmosphere boundary conditions but considers only average properties of the snow cover, to full distributed models (e.g. Morris, 1983) which give detailed predictions of the variation of properties such as temperature, density and water content within the snow.

One advantage of the full distributed physics-based models is that more accurate calculations of the mass and energy transport across the boundary between the snow and the atmosphere may be made. For example albedo, and hence the magnitude of radiative transfers, depends on the grain size, density and water content of the snow at the surface and within the snowcover. Turbulent transfer of sensible heat and evaporation both depend on the surface temperature and water vapour content. Comparison of the performance of various models using the same field data sets shows that distributed models provide the most accurate predictions provided that sufficient input data are available to run them correctly (Morris, 1982). Clearly the best chance of meeting the third criterion defined above is obtained by use of the most accurate model possible, since there are no restrictions on the range of hypothetical input data which may be provided for the model.

Mixture Theory

The basis of the distributed model is the concept that snow can be regarded as a mixture containing four constituents, ice, water, water vapour and dry air. Each volume element of snow is assumed to contain all four components dispersed within it. The first specific reference to the application of mixture theory to snow was made by Male et al. (1973). They made a dimensional analysis of the conservation equations for mass, momentum and energy in the snow, treated as a four-component mixture, and found 31 dimensionless groups, a telling indicator of the complexity of the problem. Male et al. concluded that "the development of general analytical, numerical or experimental models will prove impracticable" and suggested that field studies of situations involving a restricted number of parameters would prove to be the only tractable approach. Recently Kelly et al. (1986) have looked again at the general mixture theory problem in an attempt to define clearly the appropriate equations for a four-component analysis of snow processes and derive a hierarchy of simplified equations which may be used for particular cases. Since the distributed models used by other workers fit in as special cases of the general four-component case we begin with a brief outline of the general theory.

Let the subscripts i, w, v, a denote the components ice, water, water vapour and air respectively. The continuity equation for constituent k may be written

$$\frac{\partial}{\partial t} (\rho_k \theta_k) + \text{div} (\rho_k \theta_k \underline{v}_k) = \sum_j M_{kj} \quad (1)$$

where t is time, ρ_k is the intrinsic density of component k, θ_k the porosity (volume per unit volume of snow), \underline{v}_k the velocity and M_{kj} is the mass of component k produced per unit time per unit volume of snow by a phase change from component j. By definition, $M_{kj} = -M_{jk}$ and $M_{kj} = 0$. The porosities are related by the equation

$$\theta_i + \theta_w + \theta_v + \theta_a = 1 \quad (2)$$

and the density of the snow is defined as

$$\rho_s = \sum_j \rho_k \theta_k \quad (3)$$

The equations for conservation of momentum are

$$\rho_k \theta_k \frac{D}{Dt} (\underline{v}_k) = \text{div} \theta_k \underline{\sigma}_k + \rho_k \theta_k \underline{g} + \rho_s \underline{\beta}_k - \sum_j M_{kj} \underline{v}_k \quad (4)$$

where $\underline{\beta}_k$ are the interaction body forces acting on constituent k per unit mixture volume. By definition

$$\sum_k \underline{\beta}_k = 0. \quad (5)$$

$\underline{\sigma}_k$ are the intrinsic stresses for each component and gravity $\underline{g} = -g \underline{i}$ is assumed to be the only external body force. Note the term involving the momentum of the source/sink terms M_{kj} . It may be assumed that the interaction forces for the fluid components are given by the empirical

Darcy equations

$$\rho_s \underline{\beta}_k = \rho_k \text{grad } \theta_k - \rho_k \frac{\theta_k}{K_k} g (\theta_k \underline{v}_k - (1-\theta_1) \underline{v}_1) \quad (6)$$

where p_k is the intrinsic pressure and K_k is the hydraulic conductivity of fluid component k . Empirical equations are required to define K_k .

The derivation of the appropriate energy conservation equation, which is not at all straightforward, has been discussed in detail by Kelly et al. (1986). With the assumption that for all components, including the solid phase, the specific internal energy is a function solely of intrinsic density and temperature they derive the equation

$$\sum_k \rho_k \theta_k (c_p)_k \left(\frac{\partial T}{\partial t} + \underline{v}_k \cdot \text{grad } T \right) = \kappa \nabla^2 T + S_R + \sum_{k,j} M_{kj} L_{kj} + Q \quad (7)$$

where T is the temperature of the mixture, $(c_p)_k$ is the specific heat at constant pressure of component k , κ is the thermal conductivity of ice, L_{jk} is the latent heat produced by transformation of unit mass of component k to component j , S_R are sources of radiant energy and Q represents the stress working terms.

A series of constitutive equations are required to complete the model. Given that the air and water vapour behave as perfect gases we may begin by writing two equations of state

$$p_k = \rho_k \frac{R}{M_k} T \quad k = v, a \quad (8)$$

where M_k is the molecular weight of component k and R is the gas constant. An empirical equation for the diffusion of water vapour in air may be added to these

$$\underline{v}_v - \underline{v}_a = - \frac{D}{\rho_v \theta_v} \frac{\partial}{\partial z} (\rho_v \theta_v) \quad (9)$$

where D is the diffusivity. The relation between the water content and water pressure in the snow may be described by the characteristic equation

$$\theta_w = \frac{(1-\theta_i)}{\psi_a} \left(p_w - \frac{(p_a \theta_a + p_v \theta_v)}{(\theta_a + \theta_v)} \right)^\alpha \quad (10)$$

where ψ_a the air entry potential and α the pore size index are constants. A further equation should describe the motion of the ice matrix under the applied stress either in terms of the compressibility of the snow (e.g. Navarre, 1975) or by setting $y_i = 0$.

For the remaining two equations required to complete the model there is a choice of strategy. The snow can be regarded as a mixture in thermodynamic equilibrium, with the proportions of each component determined by equilibrium equations derived by minimising the Gibbs function of the mixture for a given bulk temperature and pressure. Alternatively, rate equations for the source/sink terms may be defined. In this case, which may well be a more realistic model of physical processes in snow, the mixture is not necessarily in thermodynamic equilibrium.

The boundary conditions to be applied at the upper and lower boundaries of the snow have been discussed by many authors. The precise equations used depend on the level of input data available for a particular application. Given the usual output from an automatic weather station the mass and energy flux at the snow/atmosphere interface can be calculated so long as the albedo and aerodynamic roughness length of the snow cover are known. Thus these quantities commonly appear as parameters in physics-based models. However, it is worth pointing out that both albedo and aerodynamic roughness can be measured in the field so they are not necessarily unknown for all applications.

Simplified forms of the equations

So far no working model of snow processes using the four-component equations has been produced. In this section the simplified equations

which form the basis of current models are described. We begin with the assumptions which allow the momentum equation (4) to be simplified to the familiar Darcy flow equations. These are

(i) that the stresses $\underline{\sigma}_k$ are purely hydrostatic so that $\underline{\sigma}_k = -p_k \underline{I}$

(ii) that the inertia terms on the l.h.s. of the momentum equation are negligible and

(iii) that the ice matrix is static so that $\underline{v}_i = 0$.

Then equations (4) and (6) reduce to

$$\theta_k \underline{v}_k + \frac{K_k}{\rho_k \theta_k g} \sum_j M_{kj} \underline{v}_k = \frac{-K_k}{\rho_k g} (\text{grad}(p_k) + \rho_k g \underline{I}) \quad (11)$$

which is recognisable as the Darcy flow equation with an extra term involving the source/sink terms M_{kj} . This extra term is negligible for normal values of M_{kj} .

If it is assumed that the ice and water phases are incompressible and the air and water vapour behave as perfect gases the term Q in the energy conservation equation may be written

$$Q = \sum_k p_k \frac{D\theta_k}{Dt} + \sum_{k=v,a} \theta_k \frac{Dp_k}{Dt} + \sum_k \theta_k (\underline{\sigma}_k + p_k \delta_{ij}) \frac{\partial (v_a)_i}{\partial x_j} \quad (12)$$

where the summation convention for repeated indices is used in the last term. Q is neglected in all current models. Some authors also neglect S_R but Navarre (1975), Colbeck (1979), Morris (1983) and Akan (1984) use empirical equations for radiation extinction in snow.

A major difference between distributed models arises in the choice of simplified thermodynamic equilibrium equations. Most authors make a distinction between two types of mixture; cold, dry snow, or ripe snow at the melting point T_0 .

For dry snow Sulakvelidze (1959), Yen (1962), Navarre (1975) and Obled and Rosse (1977) set

$$\theta_w = 0 \quad T < T_0 \quad (13)$$

Thus the mixture has only three components and only one thermodynamic equilibrium equation is required. The vapour pressure p_v is set equal to the saturated vapour pressure over ice which, following Yen (1962), is given by the empirical equation

$$p_s = (6.1 \cdot 10^2 \text{Pa}) \exp(8.57 \cdot 10^{-2} K^{-1} T) \quad (14)$$

Equation (9) is often replaced by an expression for the water vapour velocity

$$\underline{v}_v = \frac{D_{eff}}{\rho_v \theta_v} \frac{\partial}{\partial z} (\rho_v \theta_v) \quad (15)$$

D_{eff} is an effective diffusivity which varies with V_a .

For ripe snow with $\theta_w > 0$ the equation

$$T = T_0 \quad (16)$$

is used by Colbeck (1972) and Navarre (1975) as the second thermodynamic equilibrium equation. These authors also assume that the pressure of the moist air in the snow is constant. A new variable, the capillary tension

$$\Psi = p_w - \frac{(p_a \theta_a + p_v \theta_v)}{\theta_a + \theta_v} \quad (17)$$

is defined and equation (11) is simplified to

$$\theta_w \underline{v}_w = \frac{-K_w}{\rho_w g} (\text{grad}(\Psi) + \rho_w g \underline{I}) \quad (18)$$

In this "single-phase approximation" the terms M_{1v} , M_{ww} are considered to

be negligible and the model reduces to four equations (1), (10), (17), (18) for the four variables Ψ , θ_w , \underline{y}_w and M_{wi} .

Two authors, Morris (1983) and Akan (1984), have used a more complex thermodynamic equilibrium equation derived by Colbeck (1975). Colbeck derived the equation

$$T = (8.14 \cdot 10^{-7} \text{KN}^{-1} \text{m}^2) \Psi - (3.88 \cdot 10^{-7} \text{Km}) / d_i \quad (19)$$

by minimising the Gibbs function for a mixture of spherical ice grains of diameter d_i with a low water content so that all three phases are in contact (the "pendular" regime). Morris (1983) and Akan (1984) both assume that the terms M_{iv} , M_{wv} are negligible so their models are only valid for low temperature gradients in the snow.

Sensitivity analysis

To illustrate the potential of physics-based distributed models a sensitivity analysis has been carried out using the SHE snow process model, Morris (1983), and field data from a site in the Cairngorm mountains of Scotland. The site and the data have been described in detail by Morris (1983). Figure (1) shows the measured and predicted snow depths for a period of 297 hours in February/March 1979. The uncertainty in the predicted snow depth arises from the uncertainty in the measurements of initial snow density $\rho_s = 500\text{--}550 \text{ kg m}^{-3}$ and grain size $d_i = 1\text{--}2 \text{ mm}$. A constant aerodynamic roughness length of $z_o = 0.6 \text{ mm}$ and a fixed lower boundary temperature $T(0,t) = -0.4^\circ\text{C}$ have been used. The net long wave and short wave fluxes have been calculated from the measured net and incoming solar radiation using a fixed short-wave albedo of 0.9. A simple measure of variation in the model output is given by the normalised root mean square error function

$$F = \left\{ \frac{\sum_i (Z_i - Z_i')^2}{\sum_i (Z_i - \bar{Z})^2} \right\} \quad (20)$$

where \bar{Z} is the mean of the measured values of snow depth, Z_i , and Z_i' are

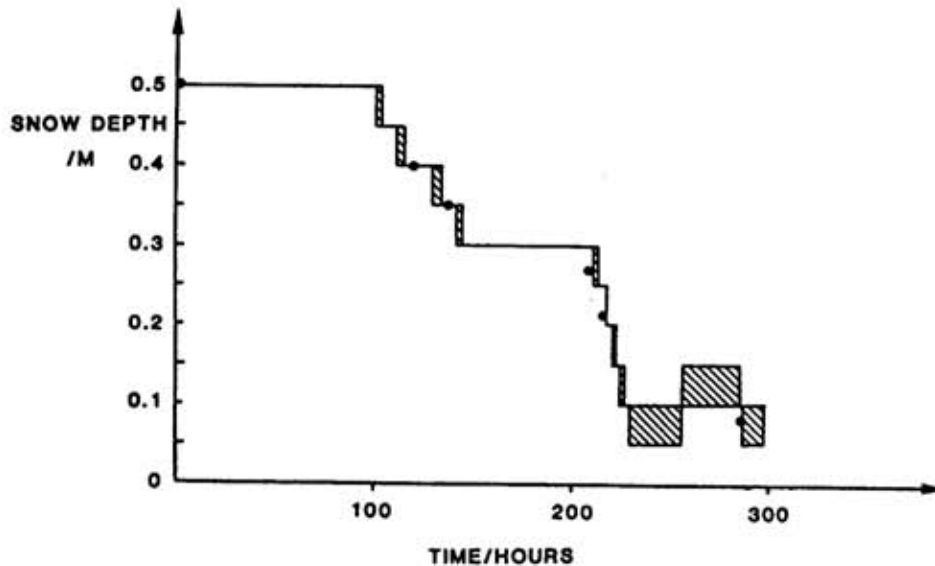


Fig.1 Measured \bullet and predicted $-$ snow depths for a site in the Cairngorm Mountains of Scotland. $t=0$ at 0800 hours on 21 February 1979. The shaded area shows the uncertainty in the predicted depths arising from uncertainty in the measured initial conditions.

predicted values. The r.m.s. error in the output for the predictions shown in Figure (1) ranges from $F = 0.162$ to $F = 0.223$.

The aerodynamic roughness length and lower boundary temperature, z_0 and $T(0,t)$, were not measured continuously throughout the experiment. They have therefore been treated as constant parameters in the model. Since they are in fact likely to have been variable, some uncertainty in the output will arise from uncertainty in these parameters. The effect of varying the lower boundary temperature within the range 0°C to -2°C is of the same order as the effect of measurement uncertainties in the initial conditions. F varies from 0.162 to 0.259. However, as shown in Figure (2), the effect of varying z_0 over the range of values from other field sites reported in the literature (Chamberlain, 1983), Harding et al. 1985) is significant. F reaches a value of 1.4 for the largest value reported,

$z_0 = 10$ mm. These results illustrate the importance of the correct determination of turbulent transfers at the snow/atmosphere interface. Clearly for the SHE model an expression specifying z_0 more precisely, presumably in terms of the physical characteristics of the surface snow and the meteorological conditions, would remove a major source of uncertainty in the output.

Chamberlain (1983) has shown that roughness lengths for blowing snow are related to friction velocities by Charnock's equation for the roughness length of the sea. This suggests that it may be possible to relate z_0 to measured wind speed. The value of $z_0 = 0.6$ mm which produces the best predictions (minimum value of F) for the Cairngorm data is given by

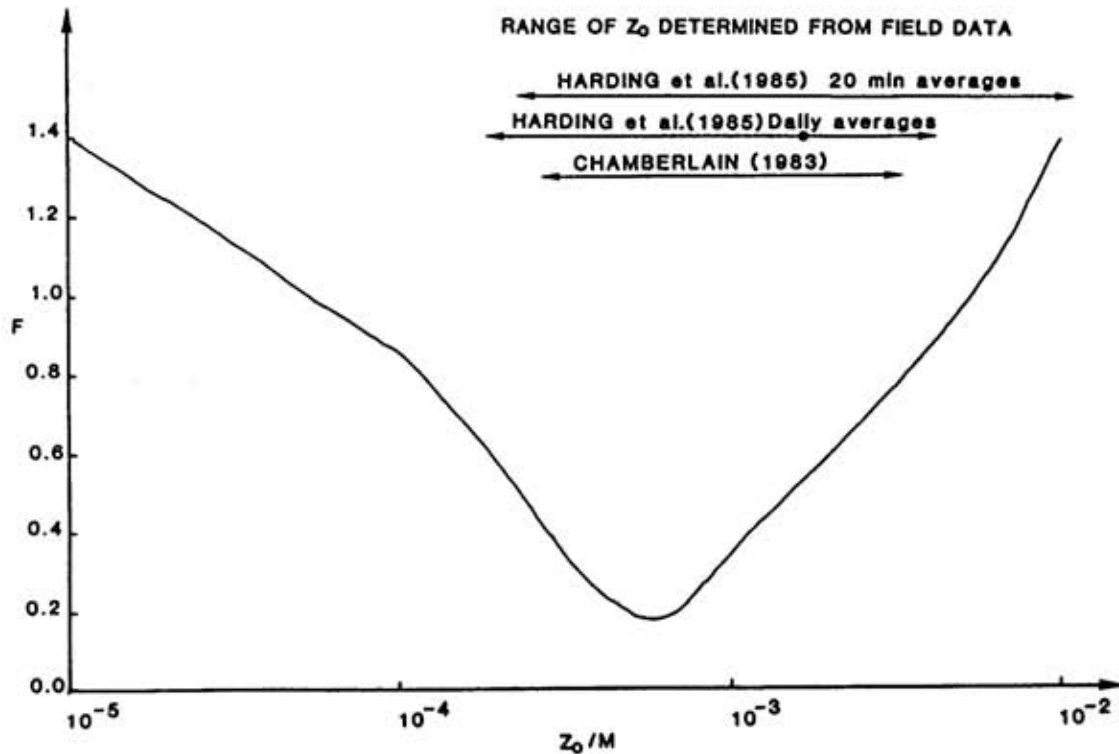


Fig.2 Variation of the r.m.s. error function, F , with aerodynamic roughness z_0 .

Charnock's equation using a wind velocity of 11.5 m s^{-1} at 1.2 m and a logarithmic wind velocity profile. Measured hourly average values of wind velocity at an anemometer height of 1.2 m at the Cairngorm site varied from 0.2 m s^{-1} to 11.8 m s^{-1} over the experimental period. Given that the best effective value for z_0 over the whole period is likely to be biased towards the value associated with the highest winds when most turbulent transfer takes place it appears that Charnock's equation would give a good a priori estimate of aerodynamic roughness for the Cairngorm data. Clearly this possibility needs further investigation.

In an experiment over stable, melting snow Harding et al. (1985) found that values of z_0 averaged over 20 minute intervals varied from $2.5 \cdot 10^{-4} \text{ m}$ to 10^{-2} m and daily average values lay between $2 \cdot 10^{-4} \text{ m}$ and $3.9 \cdot 10^{-3} \text{ m}$ with an average value over the 15 day experimental period of $1.7 \cdot 10^{-3} \text{ m}$. This is a

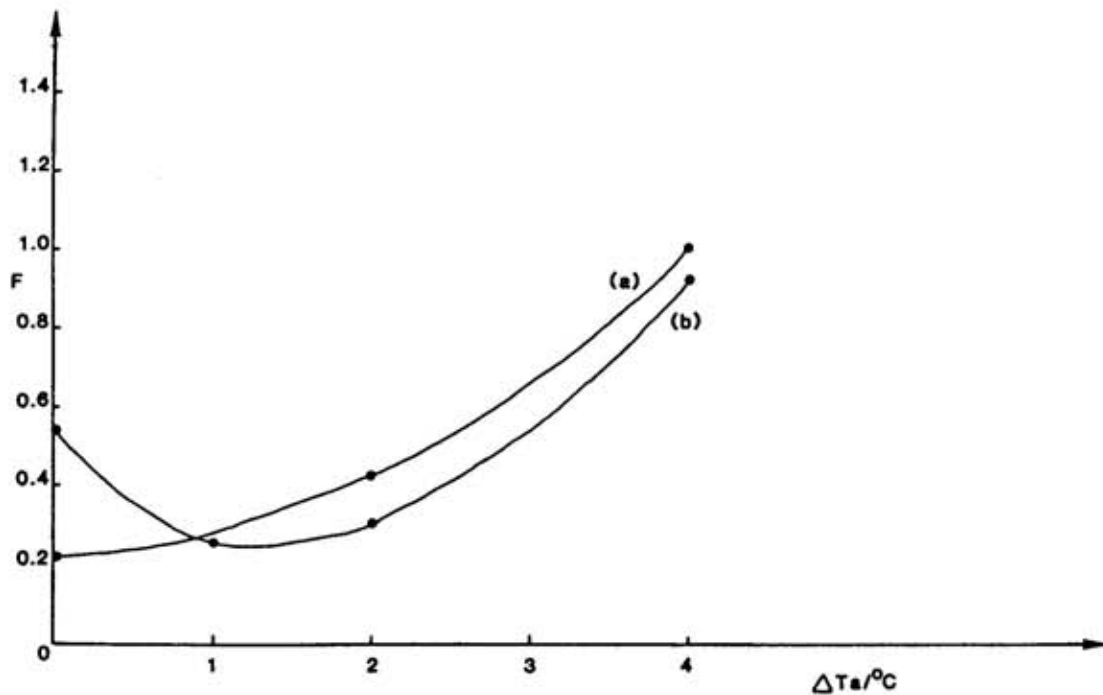


Fig.3 Variation of F with increase of air temperature ΔT_a and associated change in net long wave radiation (a) incoming solar radiation unchanged (b) incoming solar radiation reduced by 50%.

wide spread of values for one site but evidence was found that the value of z_0 could be related to the ageing of the snow surface with low values occurring after snowfalls. Thus there is reason to hope that further research will allow z_0 values to be specified more precisely.

The effect of a change in input data is demonstrated in Figure (3). Curve (a) shows the variation in F for an increase of ΔT in the hourly air temperature values input to the model. It is supposed that the net long-wave radiation is given by a temperature dependent equation

$$L_{\text{net}} = \sigma (\epsilon_a (T_a)^4 - \epsilon_s (T(Z,t))^4) \quad (21)$$

and the albedo is allowed to vary according to the grain size and water content of the surface snow

$$\alpha = \frac{0.02 \text{ m}^{\frac{1}{2}}}{d_1(Z,t)^{\frac{1}{2}}} - 0.09 \theta_w(Z,t) \quad (22)$$

This simple empirical equation could undoubtedly be improved but is sufficient for the purpose of this sensitivity analysis. All other meteorological inputs are held unchanged. Curve (b) shows the variation of F if, in addition to the changes which produce curve (a), the solar radiation input is reduced by 50% as a consequence of increased cloudiness. These curves give a crude idea of the magnitude of the change in output which would be produced at this site by the level of climatic variation we might expect to be produced by increased CO_2 in the atmosphere. The increase in air temperature produces increased melting from turbulent transfer of sensible heat whereas the increased cloudiness reduces melting from solar radiation. This is why curve (b) has a minimum.

Obviously these results can only be an estimate of the response at this site, since a properly coupled general model for the atmosphere and snow has not been used. However, they serve to reveal the existence of a problem which will almost certainly also arise with a general model. The effect of the hypothetical change in climate is to change the melt rate of the snowcover and hence raise the value of F . The maximum value of $F \approx 1$ is of the same order as the maximum value produced by uncertainty in z_0 as shown in Figure (2). Thus, unless some method of specifying z_0 more precisely is established criterion (iii) of the introduction cannot be fulfilled. This problem is not restricted to distributed models which use the aerodynamic roughness to calculate turbulent transfers. All models have to specify the energy flux at the upper snow boundary using one or more parameters and these, like z_0 , can only be known to a certain precision. For any snow model, it is necessary to establish the true uncertainty in the output before confident predictions about the effect of hypothetical changes in climate can be made.

References

- Akan, A.D. (1984) Simulation of runoff from snow-covered hillslopes. Water Resources Research Vol.20 no.6 p.707-713.
- Anderson, E.A. (1968) Development and testing of snow pack energy balance equations. Water Resources Research Vol.4 no.1 p.19-39.
- Chamberlain, A.C. (1983) Roughness length of sea, sand and snow. Boundary Layer Meteorology Vol.25 no.4 p.405-410.
- Colbeck, S.C. (1972) A theory of water percolation in snow. Journal of Glaciology Vol.11 no.63 p.369-385.
- Colbeck, S.C. (1975) Grain and bond growth in wet snow. In: Snow Mechanics. International Association of Hydrological Sciences Publication 114 p.51-61.

- Colbeck, S.C. (1979) Effect of radiation penetration on snowmelt runoff hydrographs. U.S. Army Cold Regions Research and Engineering Laboratory Report 76-11, Hanover, N.H.
- Harding, R.J., Calder, I.R., Moore, C.J. and Morris, E.M. (1985) A comparison of techniques for the estimation of snow melt and evaporation from a snow surface. Institute of Hydrology, Wallingford, 27pp.
- Kelly, R.J., Morland, L.W. and Morris, E.M. (1986) A mixture model for melting snow. In Press. Proceedings of the 2nd International Assembly of the International Association of Scientific Hydrology, Budapest, 1986.
- Male, D.H., Norum, D.E. and Besant, R.W. (1973) A dimensional analysis of heat and mass transfer in a snowpack. International Association of Hydrological Sciences Publication 107 (Banff Symposium 1972 - The role of snow and ice in hydrology) Vol.1 p.258-290.
- Morris, E.M. (1982) Sensitivity of the European Hydrological System snow models. In: Hydrological aspects of alpine and high mountain areas. International Association of Hydrological Sciences Publication 138 p.221-231.
- Morris, E.M. (1983) Modelling the flow of mass and energy within a snowpack for hydrological forecasting. Annals of Glaciology Vol.4 p.198-203.
- Navarre, J.P. (1975) Modele unidimensionnel d'evolution de la neige deposee. Neiges et Avalanches (Grenoble), No.11, p.109-27.
- Obled, C. and Rosse, B. (1977) Mathematical models of a melting snowpack at an index plot. Journal of Hydrology Vol.32 no.1/2 p.139-163.

Sulakvelidze, G.K. (1959) Thermoconductivity equation for porous media containing saturated vapour, water and ice. Bulletin of the Academy of Sciences of the USSR. Geophysics Series Vol.2 p.284-287.

Yen, Y.C. (1962) Effective thermal conductivity of ventilated snow. Journal of Geophysical Research Vol.67 p.1091-1098.

Kukla, G; Barry, R.G.; Hecht, A.; Wiesnet, D. eds. (1986) SNOW WATCH '85. Proceedings of the Workshop held 28-30 October 1985 at the University of Maryland, College Park, MD. Boulder, Colorado, World Data Center A for Glaciology (Snow and Ice), Glaciological Data, Report GD-18, p.241-248.

Characteristics of Seasonal Snow Cover as Simulated by GFDL Climate Models

Anthony J. Broccoli
Geophysical Fluid Dynamics Laboratory
National Oceanic and Atmospheric Administration
Princeton, New Jersey, U.S.A.

Abstract

Two climate simulations were performed using an atmospheric general circulation model developed at the Geophysical Fluid Dynamics Laboratory. The model employed for these simulations uses the spectral method, in which the horizontal distributions of atmospheric variables are represented by a limited number of spherical harmonics. In this study, the seasonally-varying distribution of insolation at the top of the atmosphere was prescribed, along with the climatological distributions of sea surface temperature and sea ice. The snow cover distributions produced in these simulations were compared with satellite observations. Both versions of the model generate snow cover very similar in extent to the observed snow cover.

A number of studies have suggested that the feedback mechanism involving snow cover, albedo, and temperature is an important factor in climatic change (e.g., Schneider and Dickinson, 1974). Thus, it is reasonable that the realistic treatment of snow cover may be quite important in studies of CO₂-induced climate change using mathematical models of the earth's climate. The most sophisticated of these models, the general circulation models (GCMs), are capable of simulating snow cover and its interactions with the atmospheric circulation. In such models, the proper representation of the snow-albedo-temperature feedback mechanism requires reasonable agreement between the simulated snow cover and reality. This study compares the area and distribution of Northern Hemisphere snow cover produced by a GCM with observational data from satellites.

The GCM used in this study was developed by S. Manabe and his collaborators at the Geophysical Fluid Dynamics Laboratory and is similar to that described by Manabe et al. (1979) and Manabe and Hahn (1981). The model is global with realistic geography and topography. Insolation at the top of the atmosphere is prescribed as a function of season, but no diurnal variation is included. Seasonally-varying sea surface temperature and sea ice cover are prescribed based on climatological data from Reynolds (1982), Walsh (1978), Zwally et al. (1983), and Alexander and Mobley (1976). Cloudiness is fixed and depends only on latitude and height. The model uses a hydrologic budget to predict soil moisture based on rainfall, snowmelt, evaporation, and runoff, and computes snow cover based on snowfall, snowmelt, and sublimation.

For its dynamical computations, the model uses the spectral method, in which the horizontal distribution of atmospheric variables is represented by a limited number of spherical harmonics. The model's horizontal resolution is

determined by the number of spherical harmonics retained. This study uses GCMs with two different horizontal resolutions; the low resolution version is truncated at wavenumber 15 (corresponding grid size: 4.5° latitude x 7.5° longitude) and the high resolution version at wavenumber 30 (2.25° latitude x 3.75° longitude). Nine finite-difference levels, extending from the surface to approximately 25 mb, are used to represent the vertical distribution of the atmospheric variables.

Both models are started from an initial state consisting of a dry, isothermal atmosphere at rest. A relatively short period of integration is required for the models to reach a quasi-equilibrium climate, since the sea surface temperature distribution is prescribed. The models are further integrated to provide data for analysis. This analysis period is nine model years for the low resolution model and only one year for the high resolution version due to its greater computational requirements.

The most comprehensive set of observations of Northern Hemisphere snow cover available for comparison with the model is the NOAA satellite-derived snow cover data base (Matson and Wiesnet, 1981). A climatology of the seasonal variation of Northern Hemisphere snow cover area based on this data set has been published by Dewey and Heim (1981), and monthly maps of mean Northern Hemisphere snow cover have been constructed by Robock (1980). Both of these studies will be used as sources of observed snow cover data to which the model snow cover distributions can be compared.

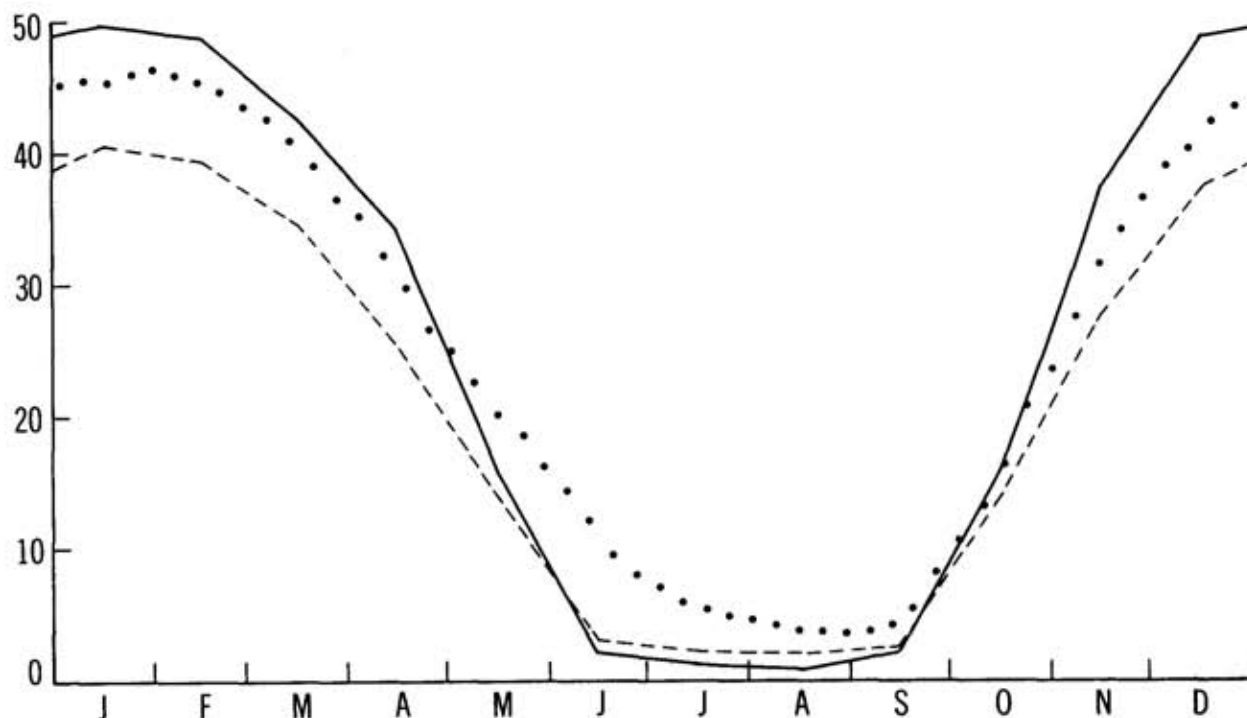


Figure 1. Areal coverage of Northern Hemisphere snow cover (10^6 km^2) from the low resolution (solid line) and high resolution climate simulations. The observed snow cover area from the climatology of Dewey and Heim (1981) is indicated by the solid circles.

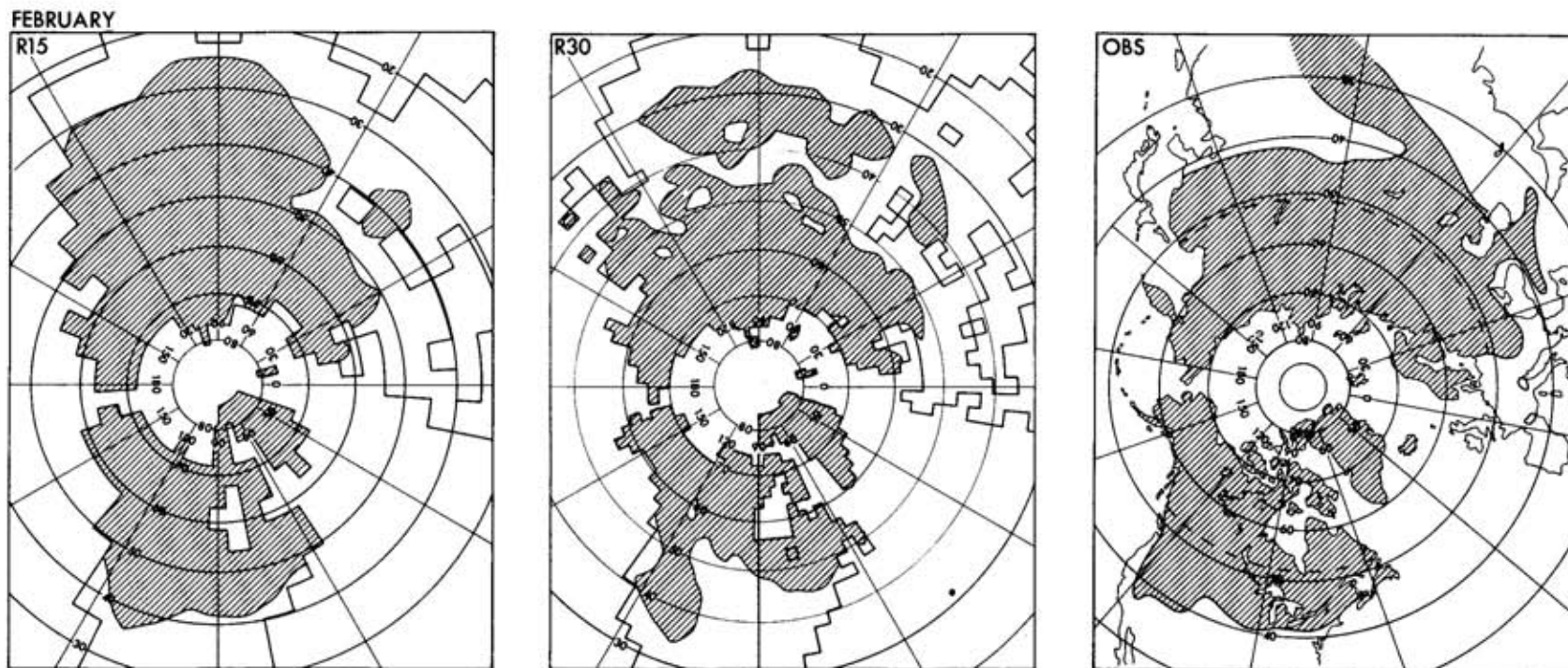


Figure 2. February mean snow cover: (left) low resolution model; (center) high resolution model; (right) observed. Hatched areas represent mean snow cover water equivalent of 1 cm or more from the climate model simulations and the observed mean snow cover based on the analysis by Robock (1980).

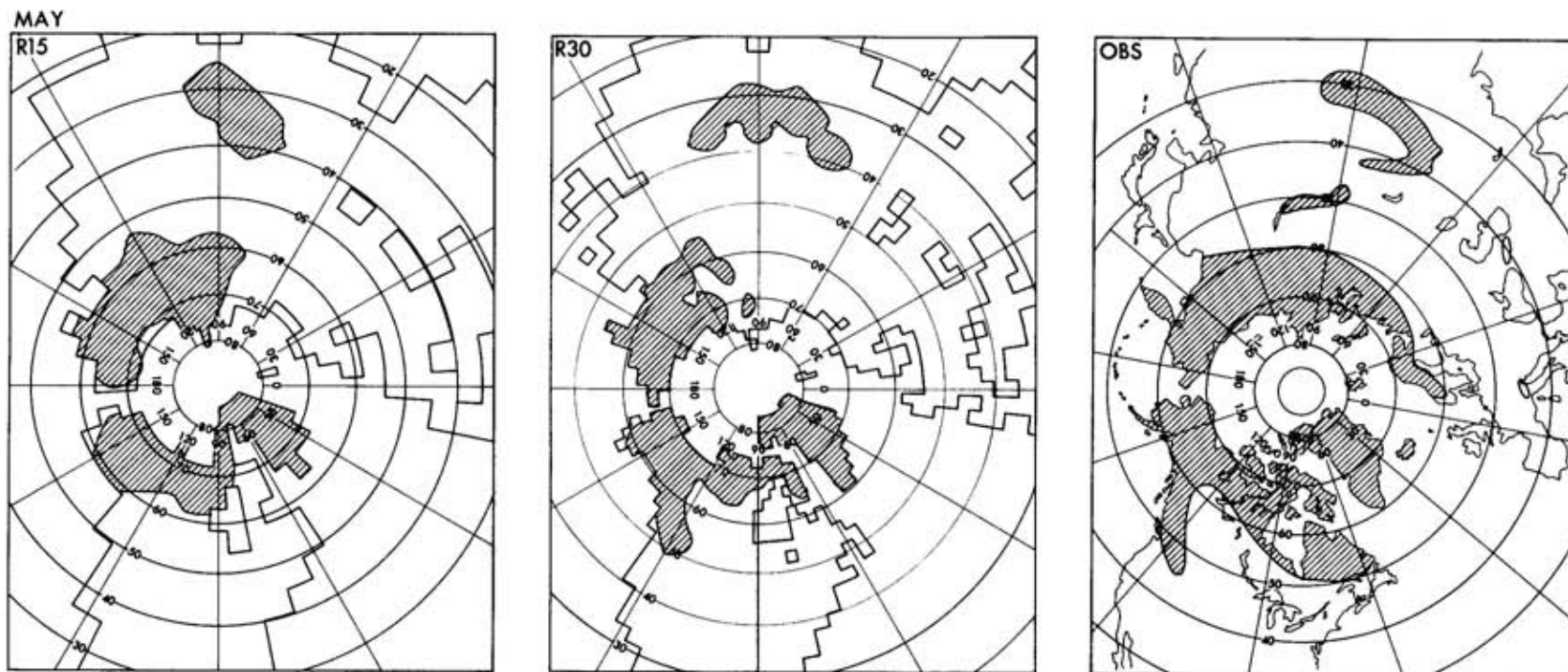


Figure 3. As in Figure 2 except for May.

The seasonal variation of snow cover area produced by both models is compared with observed data in Fig. 1. A model gridpoint is considered to be snow-covered if the water equivalent of the snow on the ground averages at least 1 cm. Both the high and low resolution versions of the model simulate a seasonal variation quite similar to that observed. The low resolution model overestimates snow cover from November through April and underestimates it from May through September. In contrast, the high resolution model systematically underestimates snow cover area in practically all seasons. In comparing the two resolutions with each other, the low resolution model has more snow cover in all but summer. Both versions produce a spring retreat of snow cover that is too rapid.

The comparison of the geographical distributions of snow cover produced by each of the GCMs with observations is made at two different times during the seasonal cycle. February is representative of the seasonal maximum of snow cover, and May illustrates the spring retreat phase of the seasonal cycle. Maps of snow cover from both resolution models are compared with the observed snow cover maps of Robock (1980) in Figs. 2 and 3.

During February, the low resolution model simulates snow cover which is slightly too extensive, while the high resolution version has snow cover area well below that observed. Over North America, the low resolution simulation is very close to reality, with the snowline at approximately 40°N. In the

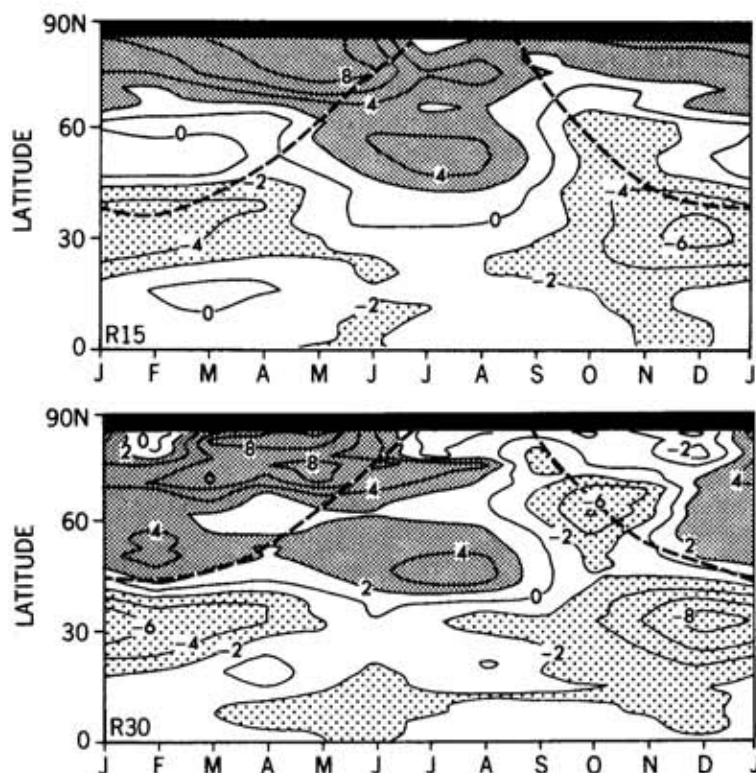


Figure 4. Latitude-time distribution of the difference between the climate model and observed zonal mean surface air temperature ($^{\circ}\text{C}$): (top) low resolution model; (bottom) high resolution model. The observed data are taken from the climatology of Crutcher and Meserve (1970). The dashed lines represent the approximate southern limit of snow cover from each model simulation.

high resolution model too little snow covers the eastern two-thirds of the continent. In western and central Europe both models are very similar to the observed snow cover, while a slight deficit of snow cover can be noted from eastern Europe to the Caspian Sea region south of 50°N. In Asia an excessive amount of snow covers China between 30-42°N in the low resolution model. This excess snow cover is the primary reason for the model's overestimation of winter snow cover area. In the high resolution simulation, only a slight excess of snow occurs in western China. The more patchy appearance of the snow cover in the high resolution model results from the short averaging period as compared with the low resolution case (one February versus nine Februaries).

Turning to the May maps (Fig. 3), both models can be seen to underestimate snow cover in the spring retreat season. In North America, the area east of Hudson Bay is free of snow in the model simulations in contrast to the snow cover observed in this area. In both models snow cover is also absent from much of high latitude Eurasia from Scandinavia along the coasts of the Barents and Kara Seas, while observations show this area to be snow covered. Better agreement occurs along the Arctic coast of Siberia east of 90°E.

In a model as complicated as a GCM, it can be difficult to ascertain the causes of a particular deficiency in the model's climate simulation because of the complex interactions that take place. In the case of snow cover, sorting out cause and effect can be particularly difficult. Its existence depends on factors such as temperature, precipitation, and solar radiation, but once present snow cover can influence each of these factors. Despite this difficulty, the strong association between temperature and snow cover may allow some insight to be gained into the systematic errors in the simulation of snow cover by studying the temperatures simulated by the model.

Figure 4 is a latitude-time plot of the difference between the simulated and observed zonal mean surface air temperature over land. The observed temperatures are taken from the Northern Hemisphere climatology of Crutcher and Meserve (1970). Both models have a similar error pattern, with temperatures too warm at high latitudes and too cold in middle latitudes. In the high resolution model, the region of excessive warmth extends farther south than it does in the low resolution version. This is consistent with the differences in the snow cover simulated by the two models.

An approximate southern limit of snow cover (excluding regions of elevated terrain) is indicated on each latitude-time plot by the heavy dashed line. During the spring retreat of snow cover, both models are too warm at the latitudes near the mean snow boundary. This is consistent with the too rapid retreat of the snow cover in both models. During the autumn expansion of snow cover, the snow boundary occupies latitudes at which the models' temperatures are close to or slightly cooler than observed. Although cause and effect cannot be distinguished, the consistent behavior of temperature and snow cover suggests that the models treat the interaction between these climatic variables in a reasonably realistic manner.

In summary, both models are quite successful in reproducing the seasonal variation of snow cover area, with the low resolution version producing more

snow than the high resolution model. In both model simulations, the spring retreat of snow cover occurs too rapidly. Errors in the simulation of surface air temperature are consistent with those involving snow cover.

Future efforts to validate climate models should continue to consider snow cover by virtue of its importance in the climate system. The availability of the NOAA satellite-derived snow cover data set in digital form should allow more detailed comparisons of observed snow cover frequency and variability with model simulations.

Acknowledgments

I am indebted to Suki Manabe for making his climate model available for this study and providing advice and encouragement. He and Tom Delworth contributed a number of useful suggestions that improved this manuscript. Many thanks to Joyce Kennedy for typing the camera-ready copy, and to John Conner and Phil Tunison and his staff for preparing the illustrations.

References

- Alexander, R.C., Mobley, R.L. (1976) Monthly average sea-surface temperature and ice-pack limits on a 1° global grid. Monthly Weather Review, v.104(2), p.143-148.
- Crutcher, H.L.; Meserve, J.M. (1970) Selected level heights, temperatures, and dew points for the Northern Hemisphere. U.S. Naval Weather Service, Report NAVAIR 50-IC-52.
- Dewey, K.F.; Heim, R., Jr. (1981) Satellite observations of variations in Northern Hemisphere snow cover. U.S. Department of Commerce, NOAA Technical Report NESS 87.
- Manabe, S.; Hahn, D.G. (1981) Simulation of atmospheric variability. Monthly Weather Review, v.109(11), p.2260-2286.
- Manabe, S.; Hahn, D.G.; Holloway, J.L., Jr. (1979) Climate simulations with GFDL spectral models: effect of spectral truncation. (In: Gates, W.L. ed. Report of the JOC Study Conference on Climate Models: Performance, Intercomparison and Sensitivity Studies. World Meteorological Organization, GARP Publication Series No. 22, p.41-94.
- Matson, M.; Wiesnet, D.R. (1981) New data base for climate studies. Nature, v.289, p. 451-456.
- Reynolds, R.W. (1982) A monthly averaged climatology of sea surface temperature. U.S. Department of Commerce. NOAA Technical Report NWS 31.
- Robock, A. (1980) The seasonal cycle of snow cover, sea ice and surface albedo. Monthly Weather Review, v.103(3), p.267-285.
- Schneider, S.H.; Dickinson, R.E. (1974) Climate modeling. Reviews of Geophysics and Space Physics, v.12(3), p.447-493.

- Walsh, J.E. (1978) A data set on Northern Hemisphere sea ice extent, 1953-76. World Data Center A for Glaciology (Snow and Ice). Glaciological Data, Report GD-2, p. 49-51.
- Zwally, H.M.; Comiso, J.C.; Parkinson, C.L.; Campbell, W.J.; Carsey, F.D.; Gloersen, P. (1983) Antarctic sea ice 1973-1976: satellite passive microwave observations. National Aeronautics and Space Administration, SP-459.

Kukla, G; Barry, R.G.; Hecht, A.; Wiesnet, D. eds. (1986) SNOW WATCH '85. Proceedings of the Workshop held 28-30 October 1985 at the University of Maryland, College Park, MD. Boulder, Colorado, World Data Center A for Glaciology (Snow and Ice), Glaciological Data, Report GD-18, p.249-270.

**CO_2 -Induced Changes in Seasonal Snow Cover Simulated
By The OSU Coupled Atmosphere-Ocean General Circulation Model**

Michael E. Schlesinger
Department of Atmospheric Sciences
and
Climatic Research Institute
Oregon State University
Corvallis, Oregon USA

1. Introduction

If the Earth's atmosphere were composed of only its two major constituents, nitrogen (N_2 , 78% by volume) and oxygen (O_2 , 21%), the Earth's surface temperature would be close to the $-18^\circ C$ radiative-equilibrium value necessary to balance the approximately $240 W m^{-2}$ of solar radiation absorbed by the surface-atmosphere system. The fact that the Earth's surface temperature is a life-supporting $15^\circ C$ is a consequence of the greenhouse effect of the atmosphere's minor constituents, mainly water vapor (H_2O , 0.2%) and carbon dioxide (CO_2 , 0.03%). Measurements taken at Mauna Loa, Hawaii show that the CO_2 concentration has increased from 316 ppmv in 1959 to 342 ppmv in 1983 (Elliott *et al.*, 1985), an 8% increase in 24 years. A variety of direct CO_2 measurements and indirect reconstructions indicate that the pre-industrial CO_2 concentration during the period 1800 to 1850 was 270 ± 10 ppmv (WMO, 1983). A study by Rotty (1983) reports that the CO_2 concentration increased from 1860 to 1973 due to the nearly constant 4.6%/yr growth in the consumption of fossil fuels (gas, oil, coal), and has continued to increase since 1973 due to the diminished 2.3%/yr growth in fossil fuel consumption. A probabilistic scenario analysis of the future usage of fossil fuels predicts about an 80% chance that the CO_2 concentration will reach twice the pre-industrial value by 2100 (Nordhaus and Yohe, 1983). Computer simulations of the climate change induced by a doubling of the CO_2 concentration have been made with a hierarchy of mathematical climate models and give a warming of 1.3 to $4.2^\circ C$ in the global-mean surface air temperature (Schlesinger and

Mitchell, 1985). Since such a global warming represents about 25 to 100% of that which is estimated to have occurred during the transition from the last ice age to the present interglacial (Gates, 1976a, b; Imbrie and Imbrie, 1979), there is considerable interest in the identification of a CO₂-induced climatic change, and in the potential impacts of such a change on the spectrum of human endeavors.

One aspect of a CO₂-induced change in climate is the change in the amount of snow on the Earth's surface. It can be argued that the amount of snow will decrease in response to the increase in temperature induced by increased amounts of CO₂ in the Earth's atmosphere. On the other hand, it can also be argued that the snow amount will increase as a result of there being more water vapor available to form snow in the warmer, CO₂-enriched atmosphere. The actual change in the snow cover induced by increased CO₂ is of potential importance because of the four roles that snow cover can play. First, changes in snow cover can influence the surface albedo to produce a feedback. Decreased snow cover would lower the surface albedo, produce more absorption of solar energy, and enhance the warming. Increased snow cover would raise the surface albedo, produce less absorption of solar energy and diminish the warming. Thus, insofar as the CO₂-induced warming is concerned, decreased snow cover produces a positive feedback and increased snow cover produces a negative feedback. Second, CO₂-induced changes in snow cover can have a significant impact on the surface hydrology. Two of the three most recent simulations of 2xCO₂-induced climate change performed with atmospheric general circulation models (AGCMs) coupled to prescribed-depth oceanic mixed layer models have shown a considerable desiccation of the soil in the mid-latitude agriculturally-productive areas in the Northern Hemisphere (see Schlesinger and Mitchell, 1985). This summer drying occurred in part due to the earlier spring melting of the seasonal snowpack in the CO₂-enriched world. Third, CO₂-induced changes in the Antarctic and Greenland snowpacks can change the equilibria of the corresponding ice sheets and surrounding ice shelves which could potentially affect sea level. Fourth, and lastly, changes in the rate of snow accumulation induced by increased CO₂ can be monitored to serve as one of the "fingerprint" quantities in a strategy to detect CO₂-induced climate change.

Because of these potentially important roles of changes in snow cover in CO₂-induced climate change, we report here results of two simulations performed with the Oregon State University (OSU) atmospheric general circulation model coupled to the OSU oceanic general circulation model. As these simulations differed only in their prescribed constant CO₂ concentrations, their differences can be interpreted as the climate change induced by increased CO₂. Selected results from these simulations have been presented and interpreted by Schlesinger et al. (1985) to obtain an estimate of the thermal response time of the atmosphere, ocean and sea ice components of the climate system. Here we shall focus attention on the simulated CO₂-induced changes in the surface snow cover and surface air temperatures.

In the following we briefly describe in section 2 the coupled atmosphere/ocean general circulation model and the two simulations. Selected results from the simulations are then presented in section 3. Finally,

conclusions regarding the importance of CO₂-induced changes in snow cover are described in section 4.

2. Description of the Model and Simulations

The atmospheric component of the coupled model is basically the same as the atmospheric general circulation model described by Schlesinger and Gates (1980, 1981), and documented by Ghan et al. (1982). This is a two-layer primitive equation GCM formulated using normalized pressure (sigma, σ) as the vertical coordinate, with the top at 200 mb and surface orography as resolved by a 4 degree by 5 degree latitude-longitude grid. The model predicts the atmospheric velocity (wind), temperature, surface pressure and water vapor, the surface temperature, snow mass, soil water and clouds, and includes both the diurnal and seasonal variations of solar radiation.

The oceanic component of the coupled model is basically the same as that described by Han (1984a, b). This is a six-layer primitive equation model of the world ocean that includes realistic lateral and bottom topography as resolved by the 4 degree by 5 degree latitude-longitude grid. In distinction from the oceanic GCM described by Han (1984a, b), however, the model version used in the present coupled simulation has been extended to include the Arctic Ocean. The model predicts the oceanic velocity (current), temperature and salinity (under the constraint of a prescribed surface concentration), and the formation and melting of sea ice.

The vertical structure of the coupled model is shown in Fig. 1 along with the primary quantities predicted during the course of a simulation. Here u and v are the horizontal components of the wind or current, T the temperature, q the atmospheric water vapor mixing ratio, s the oceanic salinity, and $\dot{\sigma}$ and w the atmospheric and oceanic vertical velocities, respectively. The surface boundary condition for the atmosphere is $\dot{\sigma} = 0$ at $\sigma = 1$, while that for the ocean is $w = 0$ at $z = 0$. At the ocean bottom the condition $w = \vec{V} \cdot \nabla h$ is imposed where \vec{V} is the horizontal velocity and h is the ocean depth, while $\dot{\sigma} = 0$ at the top of the model atmosphere at $\sigma = 0$ (200 mb). Figure 2 shows the horizontal resolution of the model and the orographies of the continental surface and depths of layers 1-3, 4-5 and 6 of the ocean model.

The coupling of the atmospheric and oceanic models is synchronous, that is, both component models simulate the same period of time. The atmospheric model is integrated forward in time one hour subject to the sea-surface temperature and sea ice thickness fields predicted by the oceanic model, and the latter is integrated forward in time one hour subject to the net surface heat flux and surface wind stress fields calculated by the atmospheric model.

Two 20-year simulations have been performed with the coupled atmosphere-ocean model that differ only in their prescribed CO₂ concentrations. In the "reference" or "1xCO₂" simulation the CO₂ concentration was taken to be constant in space and time and equal to 326 ppmv. In the "experiment" or "2xCO₂" simulation the concentration was doubled to 652 ppmv. Each simulation was started from the same initial condition. For the

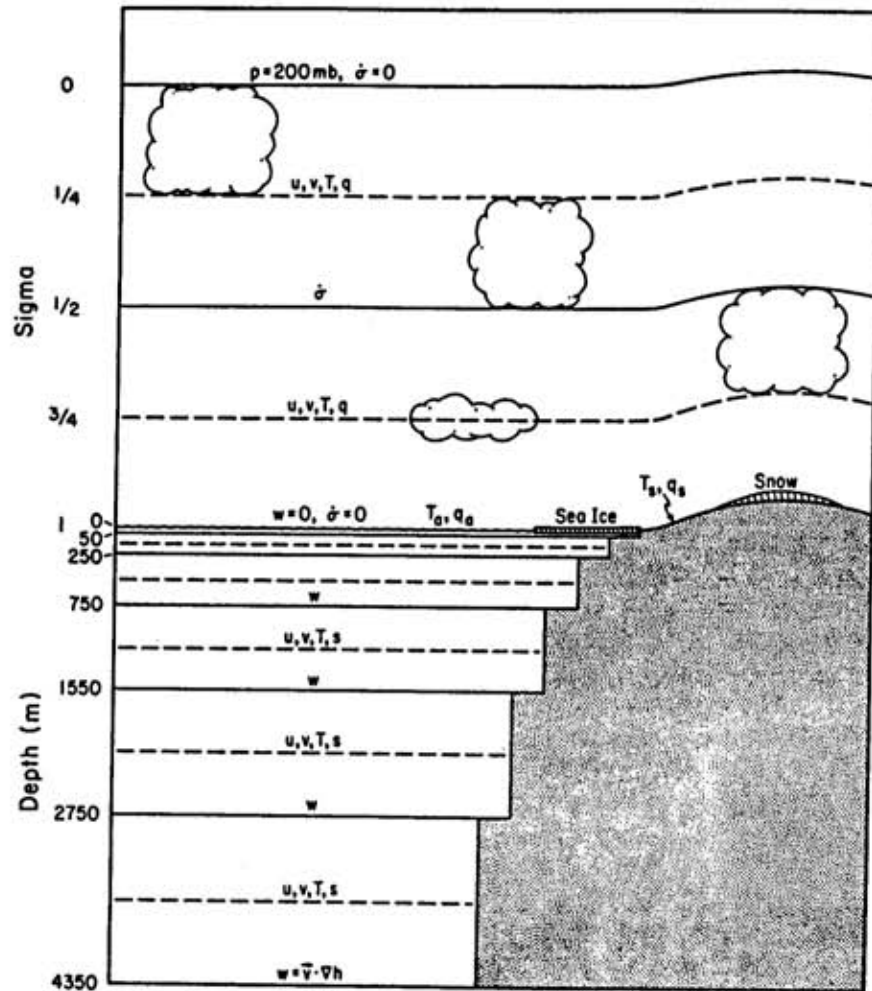


Fig. 1. The vertical structure of the coupled model, together with the primary dependent variables and boundary conditions in the atmosphere and ocean. The atmospheric GCM uses normalized pressure (sigma, $\sigma = (p - p_t)/(p_s - p_t)$, where p is pressure, p_t the 200 mb pressure of the top of the model, and p_s the variable surface pressure) as vertical coordinate and determines the horizontal velocity components u and v , the temperature T , and the water vapor mixing ratio q at two tropospheric levels $\sigma = 1/4$ ($p \sim 396$ mb) and $\sigma = 3/4$ ($p \sim 788$ mb), the vertical velocity $\dot{\sigma}$ at $\sigma = 1/2$ ($p \sim 592$ mb), the temperature T_a and water vapor mixing ratio q_a of the surface air, the temperature T_s of the earth's non-water surfaces, the soil water q_s , the snow mass, and the cloudiness. The z -coordinate oceanic GCM determines the horizontal velocity components u and v , the temperature T and the salinity s at six levels intermediate to those at which the oceanic vertical velocity w is determined. The boundary condition $\dot{\sigma} = 0$ is imposed at the model top and at the earth's surface, while the conditions $w = 0$ and $w = \vec{v} \cdot \nabla h$ are imposed at the ocean surface and ocean bottom, respectively, where \vec{v} is the horizontal velocity and h is the ocean depth.

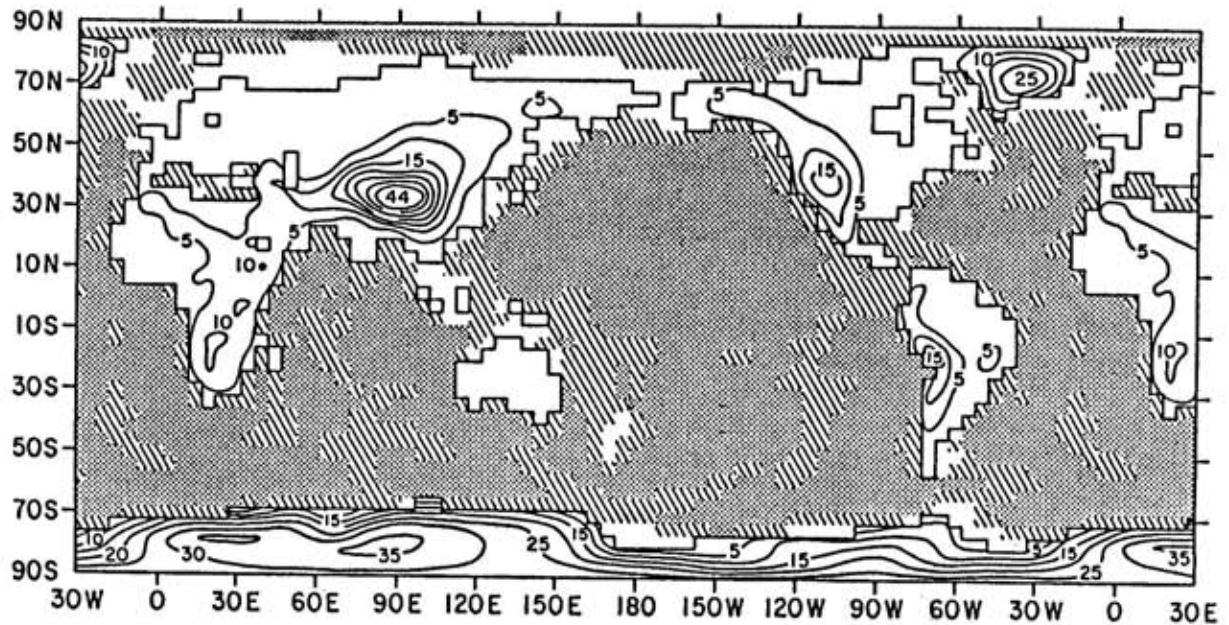


Fig. 2. The global domain of the coupled model, showing the continental outline and orography (in 10^2 m), and the oceanic depth resolved by the model's 4 degree by 5 degree latitude-longitude grid. Here the unshaded oceanic area is less than 750 m depth, the hatched area is between 750 m and 2750 m depth, and the shaded area is between 2750 m and 4350 m depth.

atmospheric component of the model the initial conditions were taken as those on 1 November of year 1 of a 10-year atmospheric GCM integration that was itself initialized from an earlier model simulation. For the oceanic component of the model the initial conditions were taken as those on 1 November of year 9 of an 11-year oceanic GCM integration with prescribed monthly atmospheric forcing that was itself initialized from an earlier 25-year simulation¹ with annually-averaged atmospheric forcing with initial conditions from the observed ocean climatology of Levitus (1982). In the following we shall identify the starting time for both the 1xCO₂ and 2xCO₂ simulations as 1 November of year 0. In this chronology each 20-year simulation terminates at the end of 31 October of year 20.

3. Results

In this section we present surface air temperature and snow cover results from the 1xCO₂ and 2xCO₂ simulations and their 2xCO₂-1xCO₂ differences. First, we present the temporal evolution of the global mean temperature and hemispheric snow cover areas. Second, we display the annual cycles averaged over the last five years of the simulations for the 2xCO₂-1xCO₂ differences in the zonal mean temperature and snow amount. Next, we exhibit the 5-year average geographical distributions of the 2xCO₂-1xCO₂ differences in temperature and snow amount for December-January-February (DJF) and June-July-August (JJA). Finally, we show plots for these seasons for each hemisphere of the 2xCO₂-1xCO₂ snow amount differences for each grid point versus the altitude of the grid point.

a. Temporal evolution of the 1xCO₂ and 2xCO₂ simulations

The top panel of Fig. 3 shows the temporal evolution of the global mean surface air temperature during the 20-year 1xCO₂ and 2xCO₂ simulations, together with the observed normal annual cycle. This panel shows that although the temperature of the 1xCO₂ simulation was initially colder than the observed temperature throughout the entire annual cycle, the 1xCO₂ simulation warmed with time such that there is relatively good agreement with the observed temperatures during at least the last five simulated years. The top panel of Fig. 3 also shows a similar warming with time of the 2xCO₂ simulation such that it is warmer than the 1xCO₂ simulation throughout virtually each annual cycle during the last five simulated years.

The temporal evolution of the difference between the global mean surface air temperatures for the 1xCO₂ and 2xCO₂ simulations is shown in the bottom panel of Fig. 3, together with the 12-month running mean superposed. This panel shows an initially rapid warming of the surface air temperature induced by the doubled CO₂ concentration, followed by a more gradual warming to a value of about 1.5°C averaged over the last five years of the simulations. Using a one-dimensional model to represent the evolution of the global mean warming of the atmosphere and ocean, Schlesinger et al. (1985) have estimated

¹ This was erroneously stated to be a 40-year simulation in Schlesinger et al. (1985).

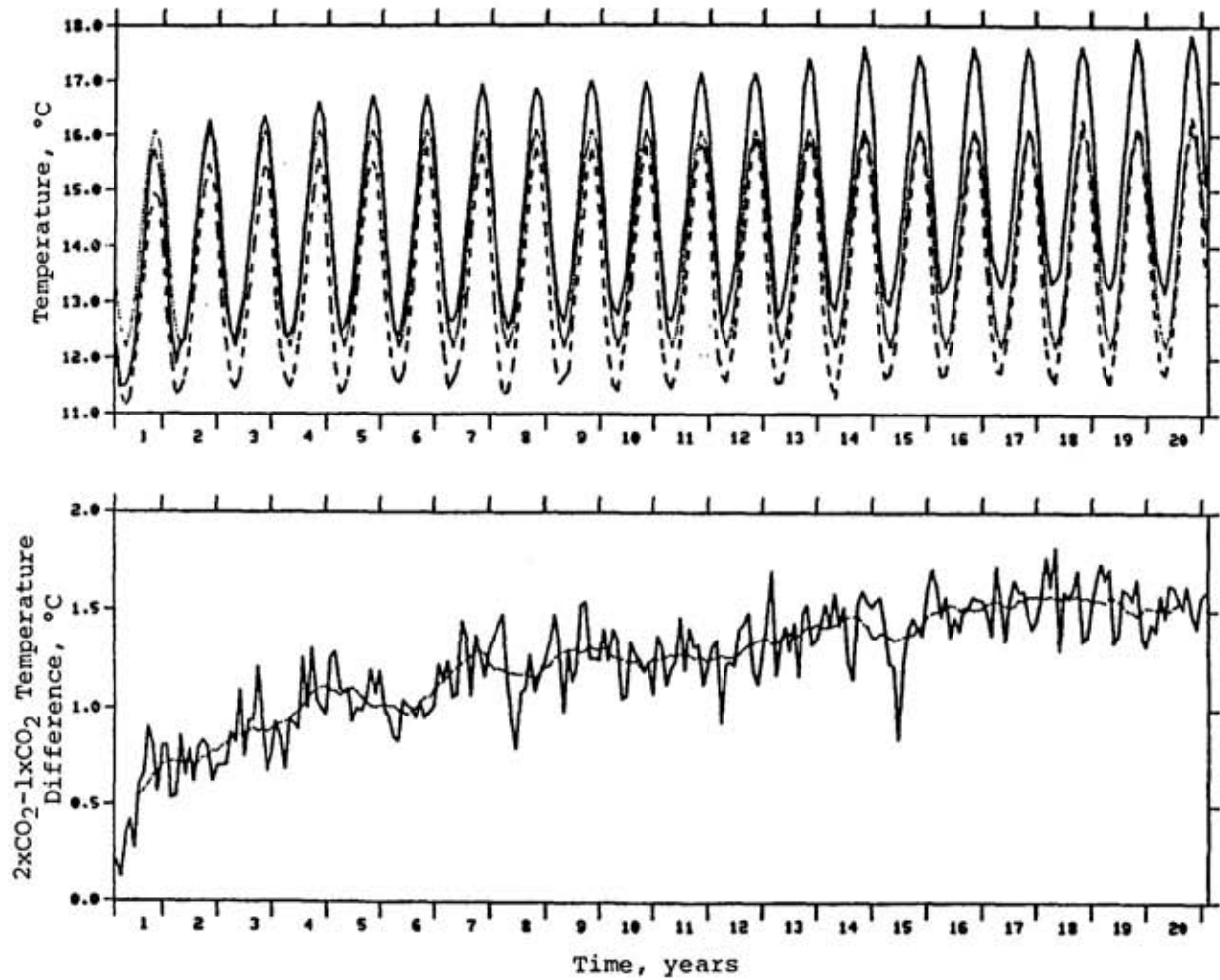


Fig. 3. The global mean surface air temperature (above) as simulated for 1xCO₂ (dashed line) and 2xCO₂ (solid line), and as observed (dotted line, from Jenne, 1975), and the 2xCO₂-1xCO₂ surface air temperature difference (below) with the 12-month running mean superposed (broken line).

that the asymptotic equilibrium warming of the surface air temperature is 2.8°C, and that the characteristic e-folding time required for the atmosphere and upper ocean to reach 63% of their equilibrium warming is about 50 to 75 years. This long thermal response time is a result of the downward transport of the CO₂-induced surface warming into the interior of the ocean by the oceanic general circulation.

The top panel of Fig. 4 depicts the evolution of the northern hemisphere snow area for the 1xCO₂ and 2xCO₂ simulations, together with the observed northern hemisphere snow area obtained by satellite observations from November 1966 through December 1980 (Dewey and Heim, 1981). This panel shows that the model simulates the observed minimum snow area quite well, but simulates its occurrence in July rather than in August each year. The model also simulates the maximum snow area about one month earlier than is observed (February) in 11 of the 20 years, and overestimates its magnitude by almost 30x10⁶ km² every year. However, this overestimate by the model of the winter snow area is not surprising because a model grid area is included in the total snow area if it has any non-zero snow cover, regardless of how small, while the satellite-observed snow area includes only those areas whose snow cover is larger than some unknown threshold value. Thus, to validate the surface snow cover simulated by GCMs, it is imperative that the snow-cover threshold of the satellite observations be documented.

The top panel of Fig. 4 also shows that the northern hemisphere snow area in the 2xCO₂ simulation evolves such that there is less snow cover throughout most of the annual cycle than there is in the 1xCO₂ simulation. This is more clearly shown by the 2xCO₂-1xCO₂ snow area differences presented in the lower panel of Fig. 4. Averaged over the last five years of the simulation, the northern hemisphere snow area is 4.8x10⁶ km² smaller in the 2xCO₂ simulation than in the 1xCO₂ simulation. However, the minimum and maximum northern hemisphere snow areas in the 2xCO₂ simulation occur at about the same time of the year as their counterparts in the 1xCO₂ simulation.

The top panel of Fig. 5 shows the evolution of the southern hemisphere snow area for the 1xCO₂ and 2xCO₂ simulations, together with two crude estimates for the observed southern hemisphere snow area. The smaller estimate (solid horizontal line) is simply the area of Antarctica, and thus presumes that there is negligible snow on the southern hemisphere sea ice (and elsewhere in the Southern Hemisphere). The larger estimate (dotted line) presumes that the southern hemisphere sea ice is everywhere covered by snow; thus, this estimate is taken as the area of Antarctica plus the area of the southern hemisphere sea ice as reported by Zwally *et al.* (1983) based on 9-years of satellite microwave observations. This panel shows that the southern hemisphere snow areas in the 1xCO₂ and 2xCO₂ simulations decrease with time from values that are about 5x10⁶ km² larger in the annual mean than the larger estimate of the observed area (due to an overestimate of the southern hemisphere sea ice by the oceanic general circulation model during its 34-year "spinup" integration), to values that are somewhat larger in the annual mean than the smaller estimate of the observed area. This decrease in the simulated southern hemisphere snow area with time is due to the decrease in the southern hemisphere sea ice area with time in both the 1xCO₂ and 2xCO₂

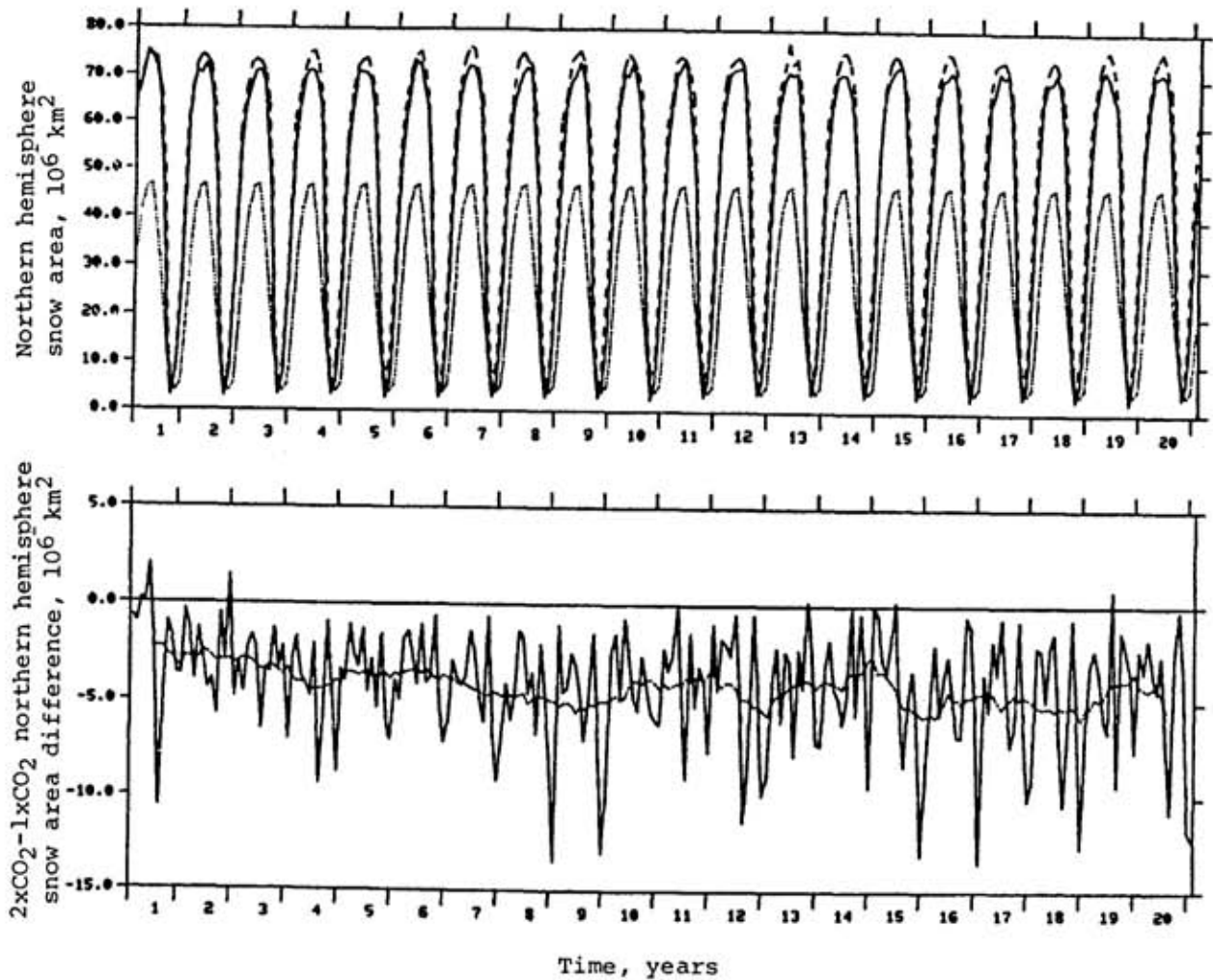


Fig. 4. The northern hemisphere snow area (above) as simulated for 1xCO₂ (dashed line) and 2xCO₂ (solid line), and as observed (dotted line, from Dewey and Heim, 1981), and the 2xCO₂-1xCO₂ northern hemisphere snow area difference (below) with the 12-month running mean superposed (broken line).

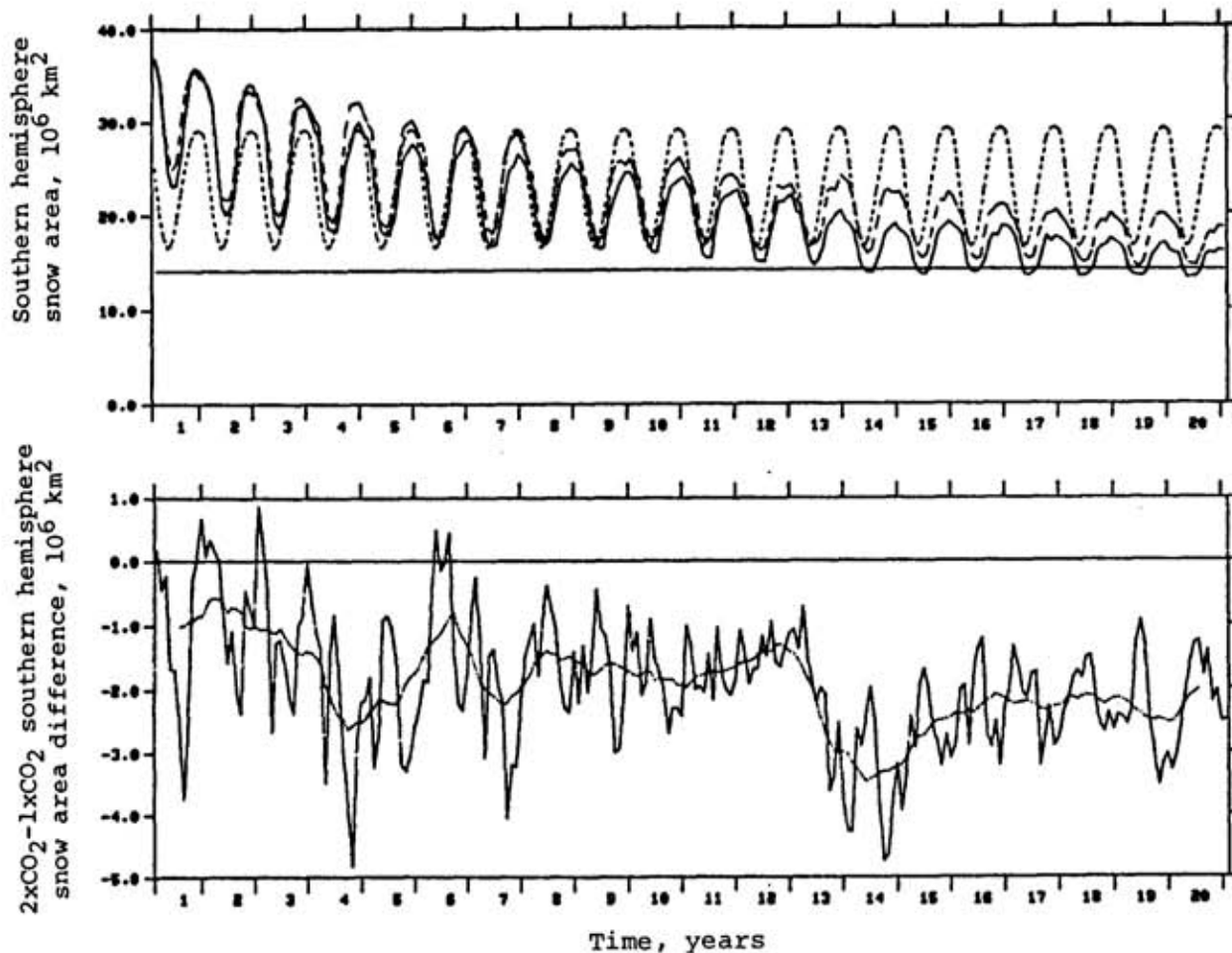


Fig. 5. The southern hemisphere snow area (above) as simulated for $1xCO_2$ (dashed line) and $2xCO_2$ (solid line), and the $2xCO_2-1xCO_2$ southern hemisphere snow area difference (below) with the 12-month running mean superposed (broken line). Two crude estimates of the observed southern hemisphere snow area are presented in the upper panel. The smaller estimate (solid horizontal line) is equal to the area of Antarctica, and the larger estimate (dotted line) is equal to the area of Antarctica plus the southern hemisphere sea ice area from Zwally *et al.* (1983).

simulations. The southern hemisphere snow area decreases more rapidly with time in the 2xCO₂ simulation than in the 1xCO₂ simulation. This is shown more clearly in the bottom panel of Fig. 5 wherein the evolution of the 2xCO₂-1xCO₂ differences in southern hemisphere snow area is presented. Averaged over the last five years of the simulations, the CO₂-induced decrease in the snow area of the Southern Hemisphere is 2.2x10⁶ km, or about half the decrease in the snow area of the Northern Hemisphere.

Although the estimate by Schlesinger *et al.* (1985) of the characteristic response time of the climate system indicates that the 1xCO₂ and 2xCO₂ simulations are not in equilibrium after only 20 years' integration, Figs. 3-5 show that the 2xCO₂-1xCO₂ differences in the global mean surface air temperature and hemispheric snow areas are at least not changing rapidly during the last five years of the simulations. It is therefore of interest to examine the seasonal and geographical characteristics of the CO₂-induced changes in these quantities during the five-year time period extending over years 16 to 20 of the simulations. Accordingly, in the following we present these CO₂-induced climate change characteristics based on averages taken over the last five years of the standard and doubled CO₂ simulations.

b. Five-year averaged CO₂-induced climatic changes

The five-year averaged CO₂-induced changes in selected global and hemispheric quantities are presented in Table 1. This table shows that the surface air temperature warmed somewhat more in the Northern Hemisphere than in the Southern Hemisphere, most likely as a result of their being more land in the boreal hemisphere than in the austral hemisphere. Table 1 also shows that the sea ice area decreased about equally in both hemispheres as a result of the CO₂ doubling. The decrease in snow area of the Southern Hemisphere is

Table 1. 2xCO₂-1xCO₂ Differences in Selected Annual-Mean Global and Hemispheric Mean and Total Quantities for Years 16-20.

<u>Quantity</u>	<u>Global Mean</u>	<u>N. Hemis. Mean</u>	<u>S. Hemis. Mean</u>
Surface Air Temperature (°C)	1.54	1.74	1.34
Snow Area (10 ⁶ km ²)	-7.04	-4.82	-2.21
Snow Mass (g cm ⁻²)	-0.34	-1.05	0.37
Snowfall (10 ⁻² g cm ⁻² day ⁻¹)	-0.14	-0.17	-0.11
Snowmelt (10 ⁻² g cm ⁻² day ⁻¹)	-0.05	-0.07	-0.04
Sea Ice Area (10 ⁶ km ²)	-3.86	-1.89	-1.97
Sea Ice Thickness (cm)	-2.56	-4.84	-0.87

^a These are total, not mean, quantities.

only somewhat larger than the decrease in southern hemisphere sea ice area, while the decrease in the northern hemisphere snow area is more than twice the decrease in the sea ice area of the Southern Hemisphere. This shows that the decrease in snow area in the Southern Hemisphere occurs primarily as a result of the decrease in the sea ice area, while the decrease in northern hemisphere snow area occurs over the northern hemisphere continents as well as a result of the decrease in sea ice extent in the Northern Hemisphere. Table 1 further shows that the average snow mass decreases in the Northern Hemisphere, but increases in the Southern Hemisphere. From the preceding, it is apparent that this increased southern hemisphere snow mass must occur over Antarctica. On the other hand, the average sea ice thickness decreases in both hemispheres. Finally, Table 1 shows that both the average snowfall and snowmelt decrease in both hemispheres as a result of the CO₂ increase, with the decreases in the Northern Hemisphere being about 60% larger than those in the Southern Hemisphere.

The annual cycle of the 2xCO₂-1xCO₂ zonal mean surface air temperature differences averaged over the last five years of the simulations is presented in Fig. 6. This figure shows that the CO₂-induced warming is small in the tropics throughout the year with a seasonal variation of less than 1°C. The seasonal variation of the warming is larger in the polar regions with maximum values of about 5°C and 3°C in the Northern and Southern Hemispheres, respectively. In the polar regions of both hemispheres the CO₂-induced warming is smaller in summer than in winter. In the Arctic the warming is maximum in fall and occurs at 78°N latitude, while in the Antarctic the warming is maximum in summer and occurs at 68°S latitude. These features of the annual cycle of CO₂-induced zonal mean surface air temperature changes are qualitatively similar to those obtained by the three most recent atmospheric GCM/mixed layer ocean model simulations of the equilibrium climate change resulting from a CO₂ doubling (Schlesinger and Mitchell, 1985). In these simulations, as well as in the present coupled atmosphere-ocean GCM simulation, the maximum high latitude warming occurs where the sea ice has retreated poleward in the 2xCO₂ simulation relative to that in the 1xCO₂ simulation.

Fig. 7 presents the annual cycle of the 2xCO₂-1xCO₂ zonal mean snow mass differences. Here it is seen that the snow mass in the Northern Hemisphere decreased at latitudes north of about 30°N virtually throughout the year, with a maximum decrease of 10 g cm⁻² centered near 70°N. This decrease in the northern hemisphere snow mass was already seen in Table 1 in terms of the annual mean value. A decrease in the southern hemisphere zonal mean snow mass is also exhibited in Fig. 7, but only equatorward of about 68°S latitude. Poleward of this latitude the snow mass increases with maximum values of 10 g cm⁻² centered near 74°S and 15 g cm⁻² over the interior of Antarctica. It is this increase in the snow mass over Antarctica throughout the year that gives rise to the increase in the annual mean southern hemisphere snow mass that was already noted in Table 1.

The geographical distributions of the CO₂-induced changes in the surface air temperature averaged over the last five years of the simulations are presented in Fig. 8 for December-January-February (DJF) and June-July-August (JJA). This figure shows that there is an increase in the surface air

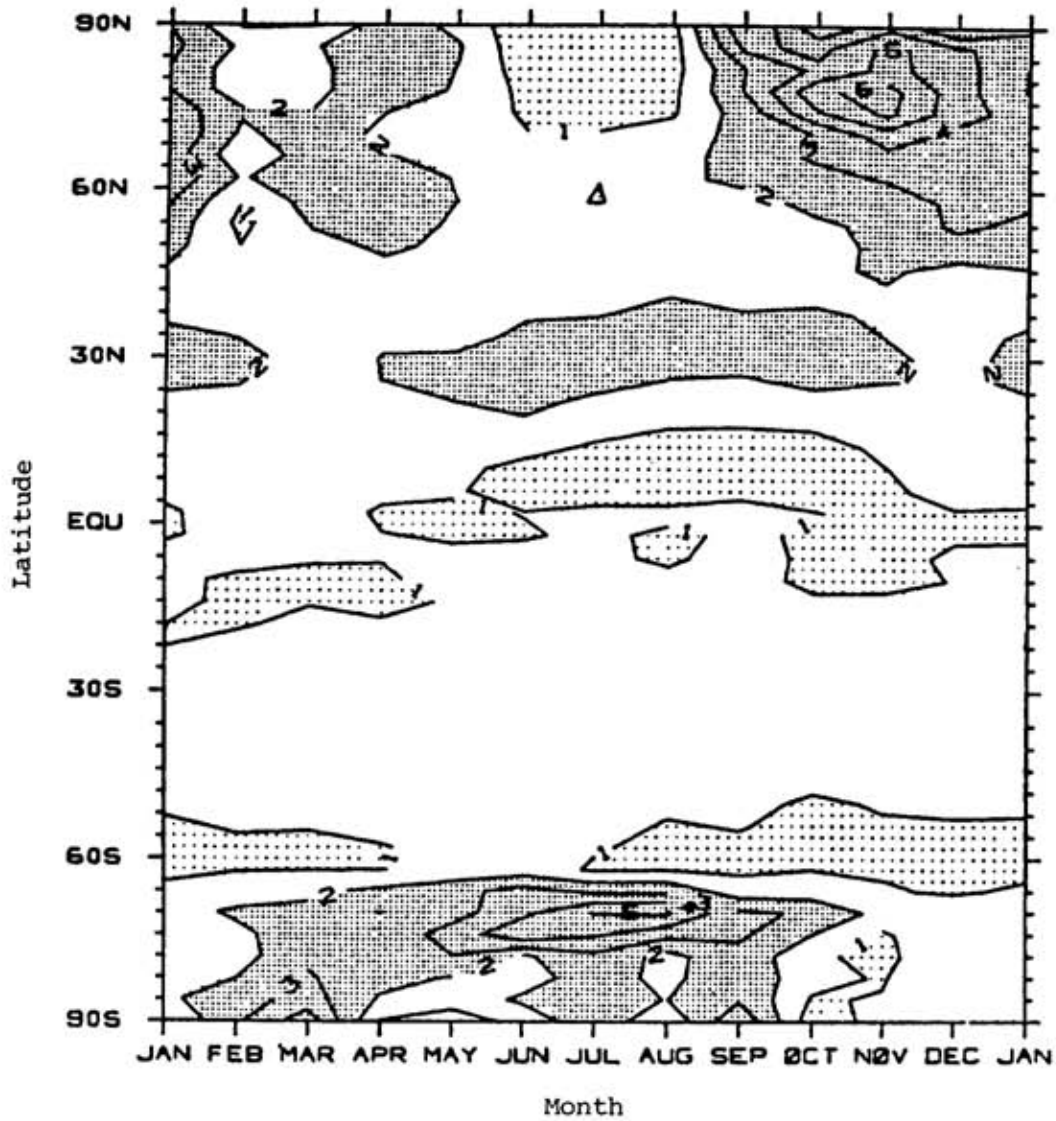


Fig. 6. The annual cycle averaged over the last five years of the simulations of the $2xCO_2 - 1xCO_2$ zonal-mean surface air temperature differences ($^{\circ}C$) as a function of latitude. Light stipple shows warming less than $1^{\circ}C$ and heavy stipple shows warming greater than $2^{\circ}C$.

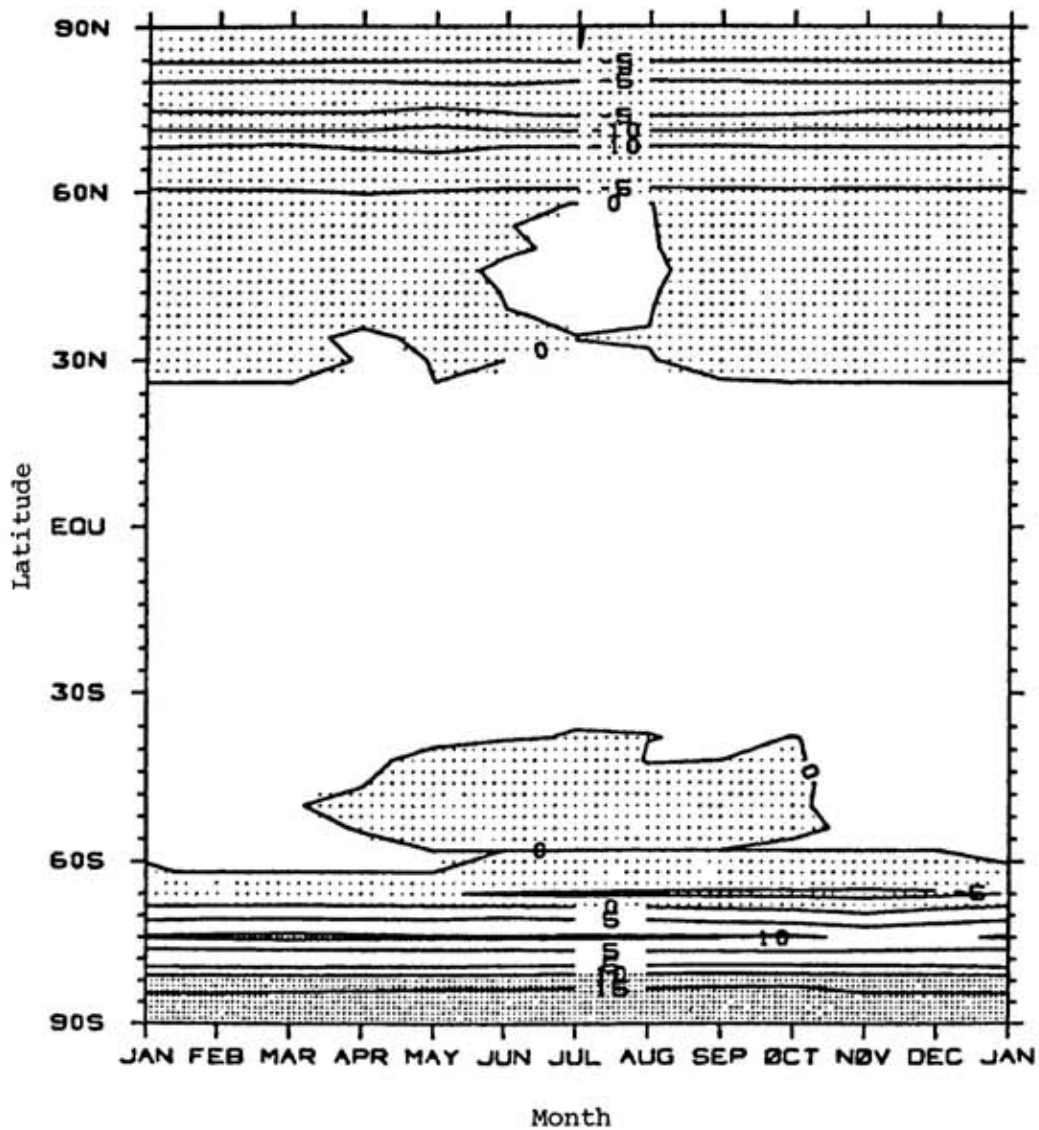


Fig. 7. The annual cycle averaged over the last five years of the simulations of the $2xCO_2-1xCO_2$ zonal-mean snow amount difference ($g\ cm^{-2}$) as a function of latitude. The zonal means exclude the open ocean. Light stipple shows decreases in snow amount, and heavy stipple shows increases greater than $10\ g\ cm^{-2}$.

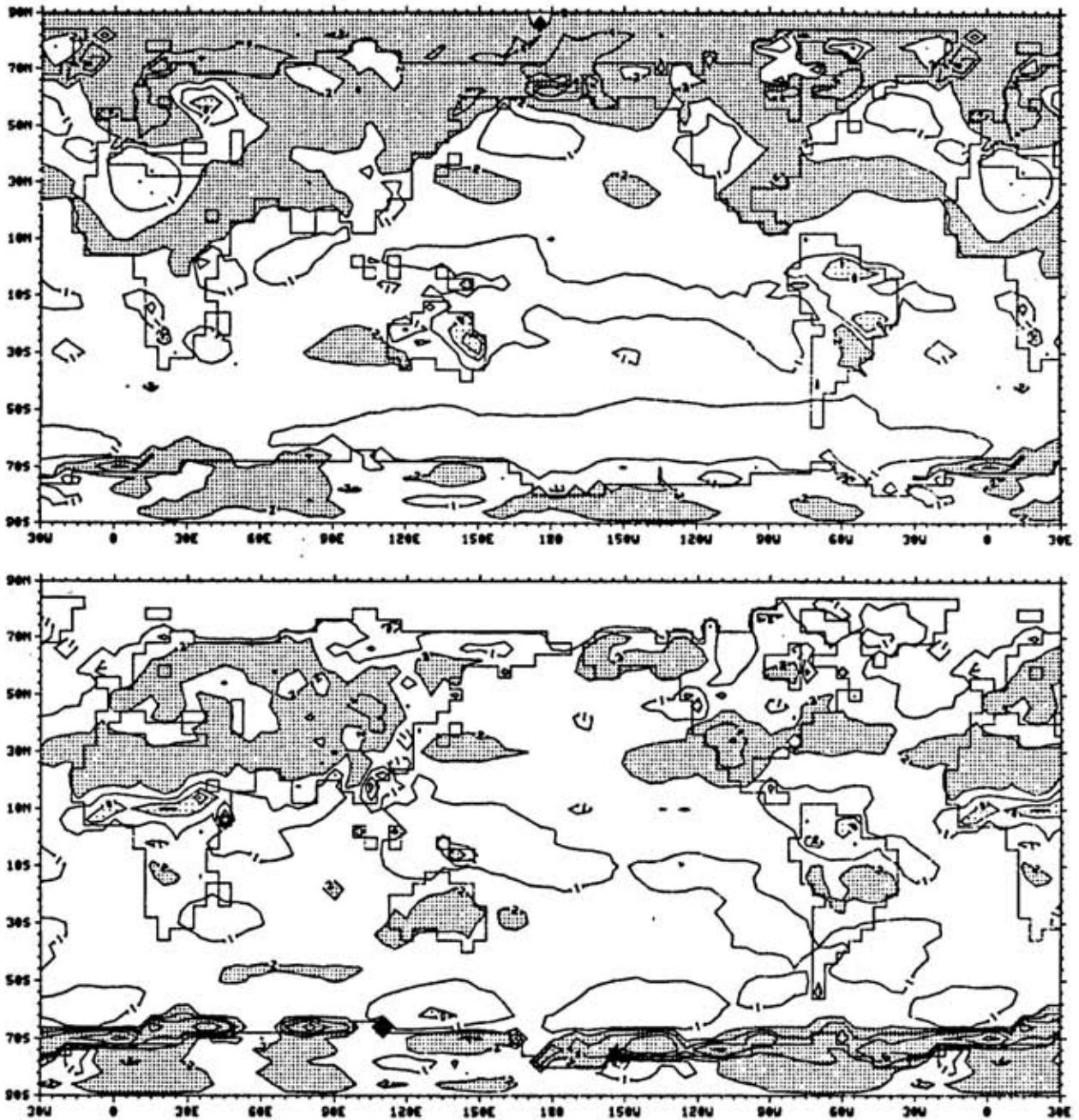


Fig. 8. The geographical distribution of the $2xCO_2 - 1xCO_2$ surface air temperature differences ($^{\circ}C$) for December-January-February (DJF, above) and June-July-August (JJA, below) as averaged over the last five years of the simulations. Light stipple shows cooling and heavy stipple shows warming greater than $2^{\circ}C$. Contours shown are $-1, 0, 1, 2, 4$ and $6^{\circ}C$, and also $-2, 10$ and $18^{\circ}C$ (below).

temperature almost everywhere, with warming larger than 2°C over most of the continents and less than 2°C over most of the ocean. The oceanic warming is less than 1°C over much of the equatorial region during both seasons, and is less than 1°C around the periphery of Antarctica in DJF and in the Arctic during JJA. On the other hand, warming in excess of 4°C is found around the periphery of Antarctica in JJA and near the northern boundaries of northern hemisphere continents in DJF. As previously noted, these regions of maximum warming are associated with the decrease in sea ice in the 2xCO₂ simulation relative to the 1xCO₂ simulation. In general, the qualitative features of the CO₂-induced surface air temperature simulated by the coupled atmosphere-ocean general circulation model are similar to the features simulated for a CO₂ doubling by the three most recent atmospheric GCM/mixed layer ocean models (Schlesinger and Mitchell, 1985).

Figure 9 presents the geographical distributions of the change in snow mass averaged over years 16-20 of the 1xCO₂ and 2xCO₂ simulations for both DJF and JJA. This figure shows that, in contrast to the surface air temperature, the snow mass decreases and increases over large geographical areas during both seasons. In particular, the snow mass increases in the interiors of Greenland and Antarctica during both winter and summer. The increased snow mass over Antarctica was already noted in the zonal mean snow mass change (Fig. 7) and for the entire Southern Hemisphere (Table 1).

It is of interest to examine the relationship between the elevation of a geographical location and the sign of its CO₂-induced snow mass change. This is done in Figs. 10 and 11 for the Northern and Southern Hemispheres, respectively. In the Northern Hemisphere (Fig. 10) in winter there is no relation between the altitude of a location and the sign of its snow mass change. In summer, however, locations with altitudes below about 1500 m predominantly have decreases in their snow mass, while higher-altitude locations have increases as well as decreases in their snow mass. As previously noted, these increases in snow mass occur over the Greenland interior. In the Southern Hemisphere (Fig. 11), increases in the snow mass predominate during both seasons and occur only at locations with altitudes larger than about 400 m. These high-altitude regions are located in the Antarctic interior as shown in Fig. 9.

4.0 Summary and Conclusions

Two 20-year simulations have been performed with the OSU coupled atmosphere/ocean general circulation model that differ only in their CO₂ concentrations, one a 1xCO₂ simulation with 326 ppmv CO₂, and the second a 2xCO₂ simulation with 652 ppmv CO₂. Although neither simulation attained its equilibrium during its 20-year period, it is useful to compare the simulated CO₂-induced changes in the seasonal snow cover.

Averages taken over the last five years of the 1xCO₂ and 2xCO₂ simulations show that there is a CO₂-induced increase in the annual mean surface air temperature in both hemispheres and a decrease in the snow area in each hemisphere. Although the snow mass decreases in the Northern Hemisphere, it increases in the Southern Hemisphere. Poleward of 30°N and equatorward of

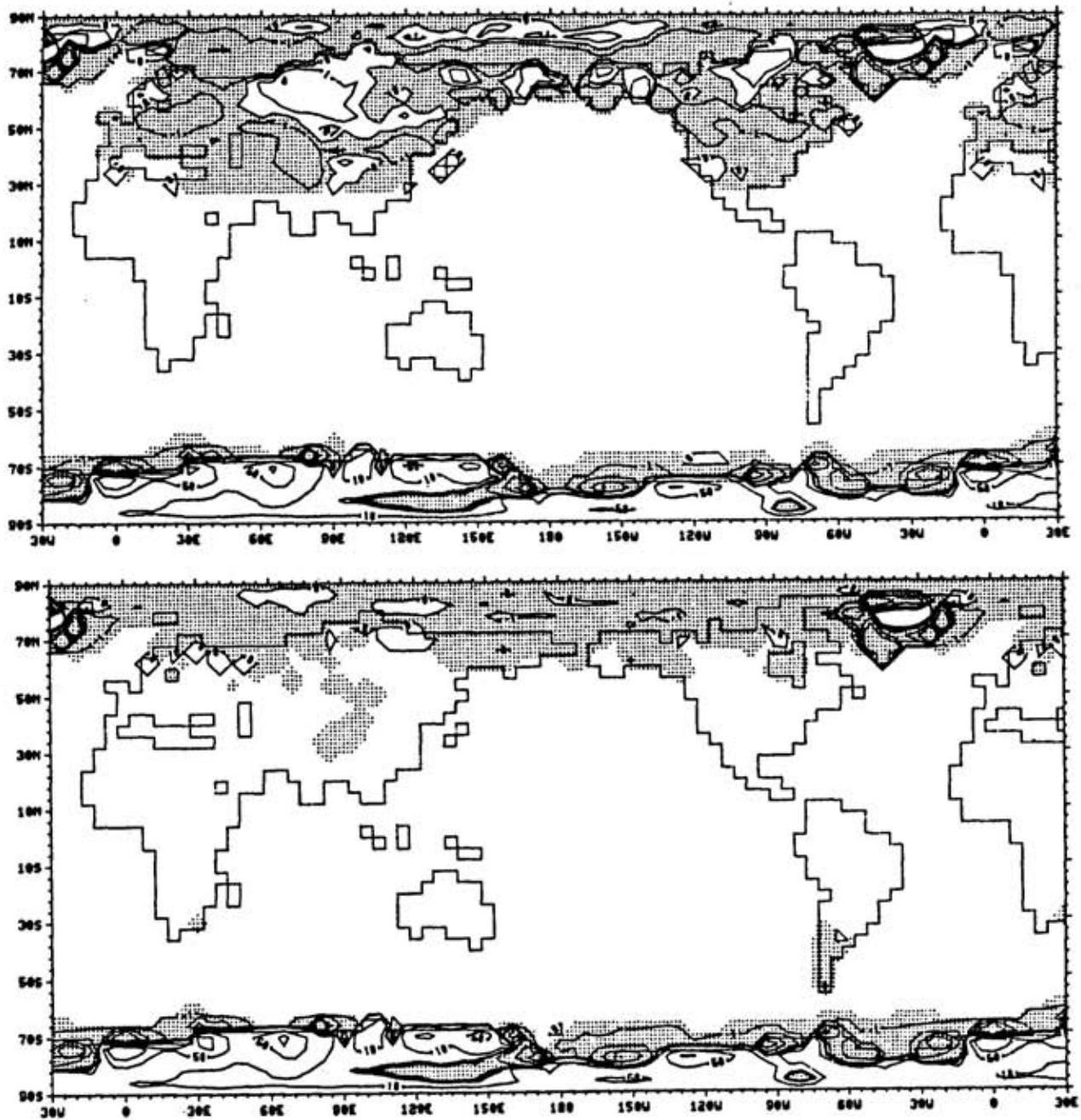


Fig. 9. The geographical distribution of the $2xCO_2 - 1xCO_2$ snow amount differences ($g\ cm^{-2}$) for DJF (above) and JJA (below) as averaged over the last five years of the simulation. Stipple shows decreases in the snow amount. Contours shown are 0, ± 1 , ± 10 , ± 50 and $\pm 100\ g\ cm^{-2}$.

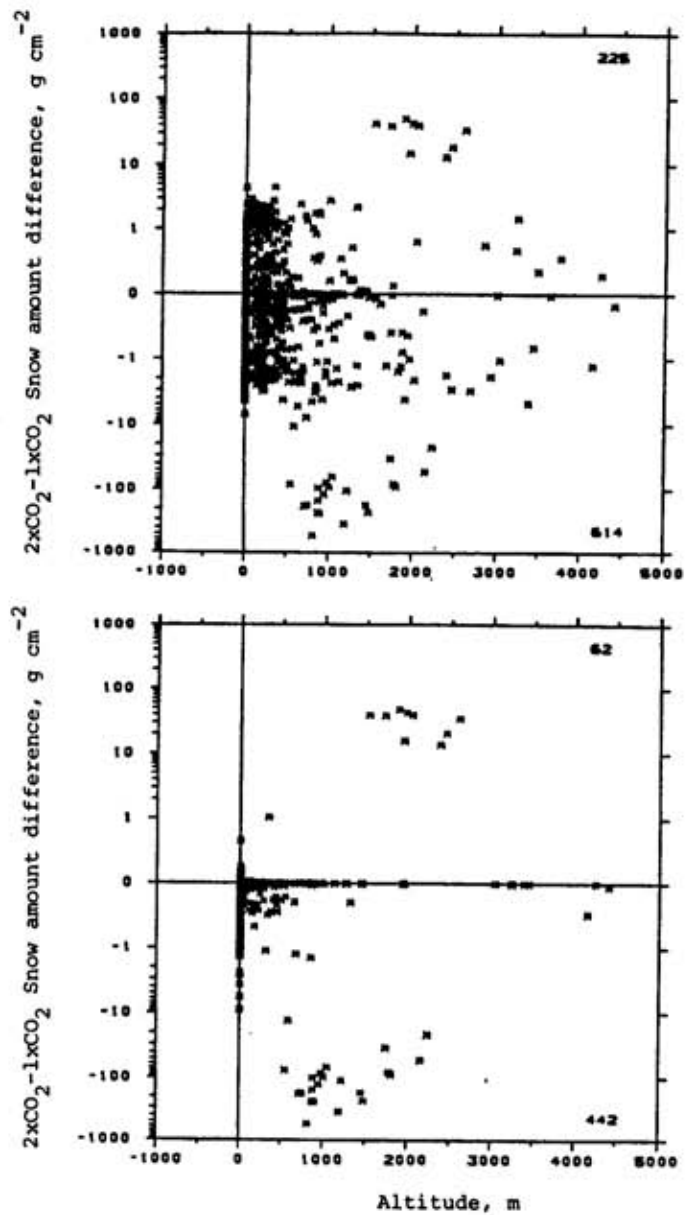


Fig. 10. The $2xCO_2 - 1xCO_2$ snow amount difference for each grid point in the Northern Hemisphere versus the altitude of the grid point for DJF (above) and JJA (below). The grid points where the snow amount was zero for both the $1xCO_2$ and $2xCO_2$ simulations are not shown. The number of grid points where the snow amount increased and decreased are displayed in the upper and lower halves of each panel, respectively.

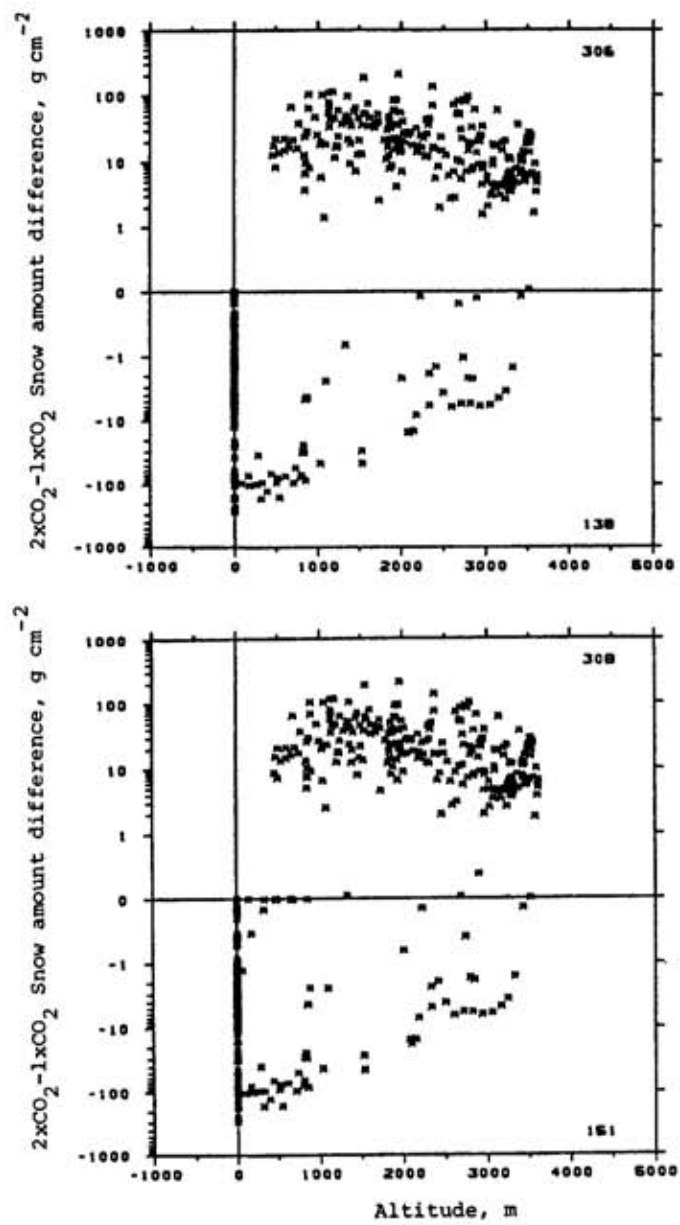


Fig. 11. As in Fig. 10, except for the Southern Hemisphere.

68°S the snow mass decreases virtually throughout the year in response to the CO₂ doubling, while the snow mass increases poleward of 68°S latitude throughout the year. In contrast to the CO₂-induced global warming of the surface air temperature, the snow mass both decreases and increases over large geographical areas during both December-January-February and June-July-August. In winter there is no relation between the snow mass change in the Northern Hemisphere and surface elevation. In summer, northern hemisphere locations below 1500 m elevation predominantly have snow mass decreases, while higher-altitude surfaces have both increases and decreases. The increases in northern hemisphere snow mass occur over the Greenland interior in both summer and winter. This simulated increase in the Greenland snow accumulation rate for a warmer climate is consistent with the decrease in the snow accumulation rate reconstructed at Dye, Greenland for the colder climate of the last ice age (Dahl-Jensen and Johnson, 1986). In the Southern Hemisphere, the snow mass increases during summer and winter in the interior of Antarctica above the 400 m level and decreases around the Antarctic coastline.

The simulated CO₂-induced snow mass increase in the interiors of Antarctica and Greenland suggests that the monitoring of the snow accumulation rates in these locations might be of use in the identification of the projected climatic change, and in the attribution of this change to the increasing concentration of CO₂ and other trace gases. Furthermore, it is likely that the simulated CO₂-induced changes in the Antarctic and Greenland snowpacks can change the equilibria of the corresponding ice sheets and surrounding ice shelves which could potentially affect sea level. This possibility should be investigated through the use of suitable glaciological models for Greenland and Antarctica.

ACKNOWLEDGEMENTS

I would like to thank Dean Vickers for programming assistance and Dee Dee Reynolds for typing the manuscript. This research was supported by the National Science Foundation and the U.S. Department of Energy under grants ATM 8205992 and ATM 8511889.

REFERENCES

- Dahl-Jensen, D., and S.J. Johnson, 1986: Paleotemperatures still exist in the Greenland ice sheet. *Nature*, 320, 250-252.
- Dewey, K.F., and R.H. Heim, 1981: Satellite observations of variations in northern hemisphere seasonal snow cover. NOAA Technical Report NESS 87, 83 pp.
- Elliott, W.P., L. Machta and C.D. Keeling, 1985: An estimate of the biotic contribution to the atmospheric CO₂ increase based on direct measurements at Mauna Loa Observatory. *J. Geophys. Res.*, 90, 3741-3746.
- Gates, W.L., 1976a: Modeling the ice-age climate. *Science*, 191, 1138-1144.
- Gates, W.L., 1976b: The numerical simulation of ice-age climate with a global general circulation model. *J. Atmos. Sci.*, 33, 1844-1873.
- Ghan, S.J., J.W. Lingaas, M.E. Schlesinger, R.L. Mobley and W.L. Gates, 1982: A documentation of the OSU two-level atmospheric general circulation model. Report No. 35, Climatic Research Institute, Oregon State University, Corvallis, 395 pp.
- Han, Y.-J., 1984a: A numerical world ocean general circulation model, Part I. Basic design and barotropic experiment. *Dyn. Atmos. Oceans*, 8, 107-140.
- Han, Y.-J., 1984b: A numerical world ocean general circulation model, Part II. A baroclinic experiment. *Dyn. Atmos. Oceans*, 8, 141-172.
- Imbrie, J., and K.P. Imbrie, 1979: *Ice Ages, Solving the Mystery*. Enslow Publishers, Short Hills, NJ, 224 pp.
- Jenne, R.L., 1975: Data sets for meteorological research. NCAR-TN/IA-111, National Center for Atmospheric Research, Boulder, CO, 194 pp.
- Levitus, S., 1982: Climatological Atlas of the World Ocean, NOAA Professional Paper No. 13, U.S. Government Printing Office, Washington, D.C., 173 pp.
- Nordhaus, W.D., and G.W. Yohe, 1983: Future paths of energy and carbon dioxide emissions. In *Changing Climate*, National Academy of Sciences, Washington, D.C., 87-153.
- Rotty, R.M., 1983: Distribution of and changes in industrial carbon dioxide production. *J. Geophys. Res.*, 88, 1301-1308.
- Schlesinger, M.E., and W.L. Gates, 1980: The January and July performance of the OSU two-level atmospheric general circulation model. *J. Atmos. Sci.*, 37, 1914-1943.

- Schlesinger, M.E., and W.L. Gates, 1981: Preliminary analysis of the mean annual cycle and interannual variability simulated by the OSU two-level atmospheric general circulation model. Report No. 23, Climatic Research Institute, Oregon State University, Corvallis, 47 pp.
- Schlesinger, M.E., W.L. Gates and Y.-J. Han, 1985: The role of the ocean in CO₂-induced climate warming: Preliminary results from the OSU coupled atmosphere-ocean GCM. In *Coupled Ocean-Atmosphere Models*, J.C.J. Nihoul, Ed., Elsevier, Amsterdam, 447-478.
- Schlesinger, M.E., and J.F.B. Mitchell, 1985: Model projections of equilibrium climate response to increased CO₂. In *The Potential Climatic Effects of Increasing Carbon Dioxide*, M.C. MacCracken and F.M. Luther, Eds., U.S. Department of Energy (in press).
- WMO, 1983: Report of the WMO (CAS) Meeting of Experts on the CO₂ Concentrations from Pre-Industrial Times to I.G.Y. World Climate Programme, WCP-53, WMO/ICSU, Geneva, 34 pp.
- Zwally, H.J., J.C. Comiso, C.L. Parkinson, W.J. Campbell, F.D. Carsey and P. Gloersen, 1983: Antarctic sea ice cover 1973-1976 from satellite passive microwave observations. NASA SP-459, National Aeronautics and Space Administration, Washington, D.C., 170 pp.

ACRONYMS AND ABBREVIATIONS

AES	-	Atmospheric Environment Service (Canada)
AMSU	-	Advanced Microwave Sounding Unit
AVHRR	-	Advanced Resolution Radiometer
CFM	-	Community Forecast Model (NCAR)
CMB	-	Composite Minimum Brightness
CROP	-	Weekly Weather and Crop Bulletin (U.S.)
CRREL	-	Cold Regions Research and Engineering Laboratory (U.S.)
DMSP	-	Defense Meteorological Satellite Program (U.S.)
EISLF	-	Snow and Avalanche Research Institute (Switzerland)
GCM	-	General Circulation Models
GOES	-	Geostationary satellites
GTS	-	Global Telecommunications System
JIC	-	Joint Ice Center (U.S.)
JPL	-	Jet Propulsion Laboratory
N-ROSS	-	Naval - Remote Ocean Sensing Satellite
NASA	-	National Aeronautics and Space Administration (U.S.)
NCAR	-	National Center for Atmospheric Research
NESDIS	-	National Environmental Satellite, Data, and Information Service (U.S.)
NIR	-	Near-infrared
nm	-	Nautical mile
NMC	-	National Meteorological Center (U.S.)
NOAA	-	National Oceanic and Atmospheric Administration (U.S.)
NSIDC	-	National Snow and Ice Data Center
NWS	-	National Weather Service (U.S.)
OLR	-	Outgoing Longwave Radiation
PODS	-	Pilot Ocean Data System
RCM	-	Radiative - convective model
SAB	-	Satellite Analysis Branch (U.S.)
SCS	-	Soil Conservation Service
SMA	-	Switzerland Meteorological Agency
SMHI	-	Swedish Meteorological and Hydrological Institute
SMMR	-	Scanning Multichannel Microwave Radiometer
SNOTEL	-	Snow telemetry network (U.S.)
SSM/I	-	Special Sensor Microwave imager
SST	-	Sea surface temperature
TM	-	Thematic Mapper
USAFGWC	-	U.S. Air Force Global Weather Central
USDA	-	U.S. Department of Agriculture
USFS	-	U.S. Forest Service
VHRR	-	Very High Resolution Radiometer
WCP	-	World Climate Programme (WMO)
WMO	-	World Meteorological Organization
WRB	-	Water Resources Branch (Canada)

NOTES

Meetings

International Association of Hydrological Sciences (IAHS) at the XIX General Assembly of the International Union of Geodesy and Geophysics:

In response to an invitation from the Canadian National Committee for the International Union of Geodesy and Geophysics and sponsored by the National Research Council of Canada, the International Union of Geodesy and Geophysics (IUGG) will hold the XIX General Assembly in Vancouver, British Columbia, Canada, from 9-22 August 1987.

The principal aim of the IAHS General Assembly is to promote the advancement of the hydrological sciences, to review the newest developments in a few selected fields and also to outline new directions for future research. In identifying the main themes for the XIX General Assembly an attempt was made to select interdisciplinary topics which will ensure the cross-fertilization of the work and ideas of the different Commissions of the Association. The main themes include:

- a) Climate/hydrology interactions with emphasis on the effects of climate change;
- b) Transport and movement of pollutants in surface and sub-surface hydrological systems;
- c) Snow and ice studies;
- d) Environmentally sound methods of water management including sediment studies.

The Assembly will be held on the campus of the University of British Columbia. Lecture halls and meeting rooms will be available on campus for symposia, workshops and business meetings.

Symposia and Workshops of particular interest to the snow and ice community include:

S1: Large Scale Effects of Seasonal Snow Cover. Convenor: Dr. B.E. Goodison, Canadian Climate Center, Atmospheric Environment Service.

Objective: To focus on the developing state of knowledge and research techniques related to snow/climate interactions in both polar and mid-latitude regions, snowmelt effects in major (>2500km²) river basins and appropriate methods for acquiring data pertinent to large-scale effects of seasonal snow cover.

S3: The Influence of Climate Changes and Climatic Variability on Hydrological Regime and Water Resources. Convenor: Prof. S.I. Solomon, Department of Civil Engineering, University of Waterloo, Waterloo, Ontario.

Objective: To focus on the influence of climate changes and variability on hydrological processes and water resource systems and to define better these changes using developing research techniques, hydrological proxy data and time series analysis.

S5: The Physical Basis of Ice Sheet Modelling. Convenor: Dr. E.D. Waddington, Geophysics Program AK-50, University of Washington.

Objective: To focus on a complete description of ice sheet physics (rheology, boundary conditions, and interactions with the atmosphere, oceans, and mantle) in a form suitable for ice sheet models, and to bring together a body of data of sufficient size and quality to both calibrate and test increasingly complex ice sheet models.

W5: River Ice. Convenor: Dr. K.S. Davar, Department of Civil Engineering, University of New Brunswick, Fredericton, N.B., Canada.

Objective: To assess recent progress in approaching problems of river ice and especially focus on the important subject of ice jams and regional flooding.

IAHS Symposia. Any scientist wishing to present a paper or poster at an IAHS symposium should send an extended abstract in English or French (300-500 words) to the symposium Principal Convenor and a copy to:

Dr. G.J. Young
Inland Waters Directorate
Environment Canada
Ottawa, Ontario
Canada K1A 0E7
Telephone: (819) 997-1487
Telex: 053-3188 Env HQ Hull

by 15 May 1986. Authors will be notified of acceptance/rejection by 15 August 1986 and will be given instructions on preparing papers at that time. Deadline for receipt of full papers including a short abstract preferably in English and French (maximum 200 words) will be 30 November 1986. All IAHS Symposia will be pre-published and available at the Assembly.

Fifth International Conference on Permafrost, Trondheim, Norway, 2-5 August 1988.

The importance of cold regions is growing and thus the interest in the cold regions science and engineering. It is necessary to give scientists and engineers an opportunity to meet regularly in order to report on progress made and to get impulses for further work.

The V International Conference on Permafrost is an important tool to reach this goal. The Conference will take place in Trondheim, Norway, 2-5 August 1988. The arrangement will be under auspices of the Norwegian Committee on Permafrost and organized by the Norwegian Institute of Technology.

The first four International Conference on Permafrost were held at Purdue University, USA (1963), Yatutsk, USSR (1973), Edmonton, Canada (1978) and Fairbanks, Alaska (1983).

Tentative Items: The Conference Themes will be separated into permafrost science and permafrost engineering, and will deal with the following items:

SCIENCE

Thermal aspects
Physics and chemistry
of frozen ground
Hydrology
Geocryology, past and present
Regional permafrost
Ecology of natural and
disturbed areas

ENGINEERING

Site investigations and
terrain analyses
Geothermal considerations
Geotechnical properties
Geotechnical engineering
Petroleum engineering
Municipal engineering
Mining engineering

If you are interested in being added to the mailing list for bulletins of the V International Conference on Permafrost, send your request to:

V International Conference on Permafrost (VICOP)
Norwegian Road Research Laboratory
P.O. Box 6390 Etterstad
N-0604 OSLO 6
Norway
Telephone: + 47 2 466960 Telex: 71238 sregN

Recent Publications of WDC/NSIDC Staff Include:

- Barry, R.G.; Crane, R.G.; Weaver, R.L.; Anderson, M.A. (1984) Sea-ice and snow-cover data availability, needs and problems. Annals of Glaciology, 45, p.9-15.
- Barry, R.G.; Brennan, A.M. (1984) World Data Center-A for Glaciology Antarctic-related activities, 1983-1984. Antarctic Journal of the United States, V. 19(5), p.245-246.
- Barry, R.G. (1985) Snow and ice data. (In: HEcht, A.D., Paleoclimate Analysis and Modeling, New York, Wiley, p.259-290.
- Barry, R.G.; Brennan, A.M. (1985) World Data Center-A for Glaciology: functions and services. Antarctic Journal of the United States, v.20(1), p.14-16.
- Weaver, R.L.; Barry, R.G. (1985) Cryospheric Data Management System for Special Sensor Microwave Imager DMSP Data. (In: Oceans '85 Conference Record, proceedings of the conference held November 12-14, 1985, San Diego, CA, p.411-415.)

GLACIOLOGICAL DATA SERIES

Glaciological Data, which supercedes Glaciological Notes, is published by the World Data Center-A for Glaciology (Snow and Ice) several times per year. It contains bibliographies, inventories, and survey reports relating to snow and ice data, specially prepared by the Center, as well as invited articles and brief, unsolicited statements on data sets, data collection and storage, methodology, and terminology in glaciology. Contributions are edited, but not refereed or copyrighted. There is a \$5 shelf stock charge for back copies.

Scientific Editor: Roger G. Barry

Technical Editor: Ann M. Brennan

The following issues have been published to date:

- GD- 1, Avalanches, 1977
- GD- 2, Parts 1 and 2, Arctic Sea Ice, 1978
- GD- 3, World Data Center Activities, 1978
- GD- 4, Parts 1 and 2, Glaciological Field Stations, 1979, Out of Print
- GD- 5, Workshop on Snow Cover and Sea Ice Data, 1979
- GD- 6, Snow Cover, 1979
- GD- 7, Inventory of Snow Cover and Sea Ice Data, 1979
- GD- 8, Ice Cores, 1980, Out of Print
- GD- 9, Great Lakes Ice, 1980, Out of Print
- GD-10, Glaciology in China, 1981
- GD-11, Snow Watch 1980, 1981
- GD-12, Glacial Hydrology, 1982
- GD-13, Workshop Proceedings: Radio Glaciology; Ice Sheet Modeling, 1982
- GD-14, Permafrost Bibliography, 1978-1982, 1983
- GD-15, Workshop on Antarctic Climate Data, 1984
- GD-16, Soviet Avalanche Research; Avalanche Bibliography Update; 1977-1983, November 1984
- GD-17, Marginal Ice Zone Bibliography, July 1985
- GD-18, Snow Watch '85, April 1986

Contributions or correspondence should be addressed to:

World Data Center-A for Glaciology (Snow and Ice)
CIRES, Box 449
University of Colorado
Boulder, Colorado 80309
U.S.A.

Telephone (303) 492-5171; FTS 320-5311